DOE/MC/11089--3108

DE92 041344

Pressurized Fluidized-Bed Hydroretorting of Eastern Oil Shales

Topical Report, Beneficiation

By
M.J. Roberts
F.S. Lau
M.C. Mensinger
C.W. Schultz
R.K. Mehta
W.E. Lamont
S.H. Chiang
R. Venkatadri
M. Misra

May 1992

Work Performed Under Contract No.: DE-AC21-87MC11089

For
U.S. Department of Energy
Office of Fossil Energy
Morgantown Energy Technology Center
Morgantown, West Virginia

By
Institute of Gas Technology
Chicago, Illinois

DISCLAIMER

DOE/MC/11089-3108

Pressurized Fluidized-Bed Hydroretorting of Eastern Oil Shales

Topical Report, Beneficiation

By
M.J. Roberts
F.S. Lau
M.C. Mensinger
C.W. Schultz
R.K. Mehta
W.E. Lamont
S.H. Chiang
R. Venkatadri
M. Misra

Work Performed Under Contract No.: DE-AC21-87MC11089

For
U.S. Department of Energy
Office of Fossil Energy
Morgantown Energy Technology Center
P.O. Box 880
Morgantown, West Virginia 26507-0880

By
Institute of Gas Technology
IIT Center, 3424 S. State Street
Chicago, Illinois 60616

May 1992

EXECUTIVE SUMMARY

The Mineral Resources Institute at the University of Alabama, along with investigators from the University of Pittsburgh and the University of Nevada-Reno, have conducted a research program on the beneficiation of Eastern oil shales. The program was supported by a contract from the Department of Energy (DE-AC21-87MC11089) through a subcontract from the Institute of Gas Technology (S1-14063).

The objective of the research program was to evaluate and adapt those new and emerging technologies that have the potential to improve the economics of recovering oil from Eastern oil shales. The technologies evaluated in this program can be grouped into three areas: fine grinding, kerogen/mineral matter separation, and waste treatment and disposal.

Four subtasks were defined in the area of fine grinding. They were as follows: Ultrasonic Grinding, Pressure Cycle Comminution, Stirred Ball Mill Grinding, and Grinding Circuit Optimization. The planned ultrasonic grinding research was terminated when the company that had contracted to do the research failed.

Pressure cycle comminution is a novel process in which rock is confined in a fluid-filled vessel, the fluid is pressurized, then subjected to a near-instantaneous pressure release. The rapid pressure release creates a tensile force (high internal pressure) on the rock. Under the proper conditions this tensile force can be great enough to cause shattering of the rock. Researchers at the University of Nevada-Reno evaluated the applicability of this process to Eastern oil shales.

A microcomputer-based digital control strategy was developed to control pressure rise time, hold time, and pressure release time. Extensive testing under controlled conditions indicated that --

1. Surface energy modifiers increase the amount of fines generated when grinding shale at comparable energy use

2. Multiple pressure release cycles have a positive effect on oil shale breakage

3. The pressure cycle technology cannot be used as a stand alone method for the ultimate fine grinding of oil shale

4. The technology may be advantageous as a precursor to conventional grinding technology.

Stirred ball milling is a well-developed technology for specialty applications that is beginning to find application in mineral processing. Evaluation of this technology was performed by the University of Alabama research team. Research was conducted using a 4-liter Netzsch mill equipped with a "John option" agitator and instrumented to provide constant digital power draw readout.

Operating variables evaluated in the investigation of stirred ball mill grinding included feed size, pulp density (feed percent solids), feed rate,

media size, percent of mill volume occupied by media (percent filling), and rotor speed. Tests were performed in a continuous mode on both Alabama and Indiana oil shales. The size distribution of the mill produced was monitored with a SILAS model/715 Granulometer.

The results showed that the mill was most efficient at 80% to 90% media filling with pulp densities of approximately 50%. Within the range of test conditions, finer sized media required less energy per ton of shale ground to any specific size than did coarser-sized media. Slow rotor speeds generally resulted in lower energy consumption and media wear, but also reduced the mill capacity.

Detailed analyses of test data showed that stirred ball milling follows Charles law and the concept of self-preserving size distributions. It was also shown that stirred ball mills require less energy per ton at a given size product than do conventional tumbling ball mills.

Research performed in grinding circuit optimization led to major reductions in the energy consumed in grinding. The key to energy reduction was in eliminating material from the circuit at the earliest possible time. It was found that half of the output of the primary ball mill could be screened out so as to bypass the first stage of stirred ball milling. Rougher flotation proved to be successful in producing a "throw away" tailing. Sizing of the rougher flotation concentrate resulted in further reduction in the amount of feed to the second (final) stage of stirred ball milling. Thus, an integrated circuit combining conventional grinding, fine screening, stirred ball milling, and rougher column flotation results in a net grinding energy consumption of 48.86 kWh/t of raw feed.

Three technologies for effecting a separation of kerogen from its associated mineral matter were evaluated: column flotation, the air-sparged hydrocyclone, and the LICADO process. Column flotation proved to be the most effective means of making the kerogen/mineral matter separation.

Column flotation tests were performed in a continuous or equilibrium mode. An initial screening of operating variables showed that air flow rate was a dominant factor with low rates yielding high concentrate grades and high rates resulting in high kerogen recoveries. In summary, the research established that the preferred conditions for column flotation were as follows: low pulp interface level with high feed point addition, 45 ppm frother concentration, 3% to 5% solids, and a feed rate of 12.5 g/min. Increased solids in the feed were generally detrimental to the flotation response, but that effect could be overcome by increased column height or by increased residence time.

Flotation concentrates containing 40 gal/ton (167 L/metric ton) with oil recoveries of 95% could be achieved in one stage of column flotation on an Alabama shale that had been ground to 10 μm. Comparable, but less favorable, results were obtained with shale samples from Indiana, Michigan, and Kentucky. Samples from Tennessee and Ohio responded least favorably, possibly due to weathering effects on the samples.

Rougher flotation tests performed in conjunction with the grinding research revealed that an effective separation could be made at a grind of

23 μm. Over 97% of the kerogen was recovered in a concentrate containing 20+ gal/ton (83 L/metric ton).

The air-sparged hydrocyclone proved to be ineffective in making a kerogen/mineral matter separation. Tests over a wide range of operating pressures, air flow rates, pedestal diameters, and fuel oil additions revealed no tendency to selectively float the kerogen.

The LICADO process was evaluated by the University of Pittsburgh research team. Their research showed that the process has potential for beneficiating oil shales but may require further development to be commercially competitive.

Tests of finely ground samples showed that it is possible to make concentrates containing as much as three times the oil content of the raw shale at oil recoveries of 90%. Unlike coal, oil shales do require surfactant addition for satisfactory separation. An alcohol, 1-Octanol, proved to be effective.

An investigation of waste treatment and disposal was conducted at the University of Alabama. Both liquid (water) and solid (tailings) wastes were investigated. Analysis of wastewaters produced in the beneficiation of the six shales included in this program showed that the metal content of the water was directly dependent upon the shale source. Beneficiation of Alabama shales, for example, resulted in highly acid waters (pH 4.3); yet, Ohio shales yielded water containing anomalous levels of cadmium and chromium.

Ion exchange and sulfide precipitation both proved to be effective in removing dissolved ions from tailing water. Sulfide precipitation is particularly interesting because it increases the potential for recovering metals as a by-product of oil shale operations.

Pozzolanic tests on oil shale tailings revealed that they do not have pozzolanic properties and cannot be added to concrete. It is known, however, that raw shale and combusted shale can be used in the production of Portland cement.

Although this program has resulted in substantial advances in the art of oil shale beneficiation, further work is recommended. Further reduction in grinding energy consumption may be achieved through an investigation of alternative grinding media. Grinding research must also focus on the auxiliary operations of fine screening and hydrocyclone sizing.

Column flotation has proven to be a very successful separation technology. Further work must be done to determine the long-term effects of recycled water use and to select the most efficient commercially available columns.

No problems are expected in the disposal of oil shale tailings. It is assumed that the tailings will be placed in a sealed pond and the water recycled to the plant as is the normal practice. It may be advantageous, however, to conduct further research on the recovery of metals as by-products and to assess the market for tailings as an ingredient in cement making.

TABLE OF CONTENTS

TABLE OF CONTENTS, Cont.

TABLE OF CONTENTS, Cont.

TABLE OF CONTENTS, Cont.

LIST OF FIGURES

LIST OF FIGURES, Cont.

LIST OF FIGURES, Cont.

LIST OF FIGURES, Cont.

LIST OF FIGURES, Cont.

LIST OF FIGURES, Cont.

LIST OF TABLES

LIST OF TABLES, Cont.

LIST OF TABLES, Cont.

61WP/61090t4-tc/RPP

OIL SHALE BENEFICIATION RESEARCH

INTRODUCTION

Research at the University of Alabama (UA) (Hanna, 1981) established the technical feasibility of beneficiating Eastern (Devonian) oil shales. This work showed that a combination of fine grinding and froth flotation could produce concentrates containing ~25 gal/ton (~104 L/metric ton) from raw shales containing ~12 gal/ton (~50.1 L/metric ton). Subsequent research sponsored by the Department of Energy (Contract No. DE-AC21-87MC11089) established that a synergistic economic effect is realized when the beneficiation technology developed at the UA is used to provide feedstock for the hydroretorting technology developed by the Institute of Gas Technology (IGT). The use of concentrated feedstocks reduced the size (and hence cost) of the high-pressure hydrogen retorts required to produce a unit volume of oil by an amount more than sufficient to pay for the cost of beneficiation (Johnson and Riley, 1988).

SUBTASK 4.1. GRINDING STUDIES

Grinding is by far the most energy intensive and the least efficient unit operation in mineral beneficiation. Up to 99% of the energy consumed in grinding the mineral ores is expended in the movement of machinery, the generation of noise and heat, and undesirable by-products, leaving less than 1% of the applied energy available for size reduction (Herbst, 1981). The low energy utilization efficiency in grinding operations indicates an enormous potential for improvement.

There are several reasons for conducting grinding research on Eastern oil shales:

1. Comminution (fine grinding) is the highest-cost unit operation in the beneficiation of oil shale.

2. The recovery of oil and the grade of kerogen in the concentrate largely depends on the method and rate of power input to grind the shale; a high-grade concentrate obtained by flotation requires grinding the shale to less than 10 μm (Fahlstrom, 1979).

3. The comminution characteristics of Eastern oil shales are not known; therefore, it is necessary to establish the scientific base of understanding concerning their comminution behavior.

Little attention has been given to fine grinding of oil shale, possibly due to the limited research interest in oil shale processing by physical beneficiation (Fahlstrom, 1979; Lamont and Hanna, 1983; Misra et al., 1983). Moreover, these studies are restricted to conventional devices (ball mills) with no report of correlation between size reduction and expended energy except a few (Misra et al., 1983; Misra and Hilleke, 1987) in stirred ball mills, where the energy requirements for ultra-fine grinding of Kentucky and Chattanooga shale were determined.

The objectives of this task were to evaluate three advanced grinding technologies and to optimize the overall grinding operation. The advanced technologies were: ultrasonic grinding, pressure cycle comminution, and, stirred ball mill grinding.

Subtask 4.1.1. Ultrasonic Grinding

This subtask was subcontracted to Energy and Minerals Research Company which had developed an ultrasonic grinding technology. This technology was presumed to promote intergranular rather than transgranular fracture, thereby promoting liberation at the coarsest possible size. Prior testing on coal had shown considerable promise. Energy and Mineral Research Company declared bankruptcy shortly after the contract was awarded and no work was performed.

Subtask 4.1.2. Pressure Cycle Comminution

Introduction

The power requirement for the comminution of ores is on the order of 32 billion kWh per year in the United States, which corresponds to 2% of the

total electrical energy (Herbst, 1981; DOE, 1978; Lawrison, 1974). Mineral processing industries rely on conventional tumbling mills for size reduction. Although tumbling mills are the most important comminution devices, they are energy intensive and inefficient. In a tumbling mill operation, only 0.6% of the energy is used for grinding, the rest is wasted. Table 4-1 shows the typical distribution of energy for a comminution operation (DOE, 1978; Lawrison, 1974).

Table 4-1. TUMBLING MILL ENERGY CONSUMPTION

	Percent
Bolt Friction	4.3
Gear Losses	8.0
Heat Losses From Drum	6.4
Heat Absorbed by Air Circulation	31.0
Heat Absorbed by Product & Steel	47.6
Unaccounted Energy	2.1
Product Reduction	0.6

In recent years a significant amount of research has been directed to reduce the energy demand for comminution by increasing the efficiency and/or by utilizing process control strategies. Progress has been substantial in the areas of process control and simulation, liberation analysis and the study of large ball mills (Austin et al., 1989; Herbst, 1984; Report TR89-90). However it should be emphasized that research in the area of new grinding processes is limited.

Objective

The objective of this research program was to develop an energy-efficient comminution technology for oil shale grinding involving pressure cycle comminution (Misra et al., 1990; Rao et al., 1990; Rehbinder and Kalinkosvasky, 1937). The approach involves hydraulically developing and propagating microcracks along the grain boundaries where the applied energy can initiate the fracture with minimum energy.

Background

Recent studies have shown that oil shale can be ground to an extremely fine size at a moderate energy input if stirred ball mill grinding techniques are used. Previous work on oil shale grinding are given in Table 4-2 (Misra and Hilleke, 1987). Conventional ball mill grinding of oil shale to 80% finer than 20 μm requires a specific energy input in the range of 47 to 72 kWh/ton depending on the types of oil shale used. In contrast, the energy for grinding oil shale to 80% passing 20 μm in a stirred ball mill is about 26 kWh/ton. Stirred ball milling can reduce the energy demand by at least 50% compared to conventional ball-mill grinding. Nevertheless, the energy requirement for ultra-fine grinding is still high.

Table 4-2. ENERGY-SIZE REDUCTION RELATIONSHIP FOR DIFFERENT OIL SHALES

Oil Shale	Mill Type	Energy Input, kWh/ton
Colorado (Mahogany Zone)	Rod-Ball Mill	25-45
Michigan (Antrim)	Ball Mill	46
Colorado (Anvil Point)	Ball Mill	72
Kentucky (Ohio)	Ball Mill	46
Kentucky (Ohio)	High Speed Stirred Ball Mill	16

Process Description

The novel pressure-cycle comminution technique uses instantaneous pressure fluctuation and rapid depressurization to shatter the ore. The process involves three major steps (Misra et al., 1990; Rao et al., 1990).

1. Loading a liquid filled vessel with oil shale.

2. Pressurizing the fluid slowly according to a predetermined rate.

3. Releasing the confined fluid suddenly.

Initially, pieces of oil shale saturated with air at one atmosphere are immersed in the fluid in a reservoir and are penetrated by the fluid as it is pressurized. The fluid is forced into the micro-cavities of the ore pieces and also creates additional fractures and micro-cracks depending on the local stress. In this way, the internal pressure increases until it is the same as the external pressure. The sudden release of the confining pressure results in very high stress gradients in all regimes of the specimen (that is, the stress differential between the inside and outside), causing the material to fracture into small particles. For effective fracturing, it is important that the specimen be saturated with the fluid and that the de-pressurization be very rapid so that the differential stress will cause the micro-cracks to fracture the particle. The external stress leads to differential strain between mineral grains.

Theoretical Considerations

The flow of fluid inside an ore specimen can be approximated by analogy to the general equation of heat flow in a solid sphere as follows:

$$\left\{\frac{(d^2T)}{dx^2} + \frac{(d^2T)}{dy^2} + \frac{(d^2T)}{dz^2} + \frac{1(d^3q)}{K\ dt^3}\right\} = \left\{\frac{1}{\alpha}\frac{dT}{dt}\right\} \qquad (1)$$

where --

t = time

T = temperature

q = heat generated per unit volume

α = thermal diffusivity [thermal conductivity/(specific heat X material density)]

Assuming a uniform sphere with α constant and that the pressure is analogous to temperature, the above heat conduction equation can be approximated to --

$$\left\{\frac{1}{\alpha_o}\frac{dP}{dt}\right\} = \left\{\frac{(d^2P)}{dr^2} + 2\frac{dP}{(rdr)}\right\} \qquad (2)$$

where --

P = pressure

r = radius of the specimen

α_o = is the fluid diffusivity and is given by,

$$\left\{\frac{1}{\alpha_o}\right\} = \left\{\frac{\mu}{k}\left[\beta_e - \beta_s + \eta(\beta_f - \beta_s)\right]\right\} \qquad (3)$$

where --

μ = water viscosity

k = the material permeability

η = material porosity

β_e = effective ore compressibility

β_s = solid compressibility of the ore

β_f = water compressibility

The normalized solution is,

$$\frac{P}{P_o} = 1 + 2\frac{r_o}{(\pi r)}\sum_{n=1}^{\infty}\frac{[(-1)^{(n+1)}]}{n}\sin\frac{(\eta\,\pi\,r)}{r_o}\,e^{(-\beta t\eta^2)} \qquad (4)$$

Where, $\beta = \frac{(\pi^2)}{(r_o \alpha_o)}$, the normalized time constant.

P_o = the applied pressure

P = the required pressure at radius r at time t.

From these equations, for a given average ore size with known porosity, permeability, and compressibility, it is possible to predict the pressure required at the center of the ore and thus the pressure rise and hold times to shatter the ore.

Experimental Procedure

Experimental Setup

The laboratory setup (Figure 4-1) is composed of a pressure vessel, a computer-controlled positive displacement fluid reservoir, and transducers and sensors along with a very fast acting dump valve. The experimental reactor assembly was built by Terra Tek, Inc. (Salt Lake City). A small motor/adapter combination controlled by the computer is used to open and close the valve on command. The setup includes a wattmeter with which the A/D converter can automatically record the total power consumed in each test, including the losses in the power consumed in each test, losses in the electric motors and the pump. The pressure vessel is a cylindrical stainless steel chamber 6 inches in diameter and 6 inches in height (15.2 cm in diameter and 15.2 cm in height). Actuation of the valve is controlled by the computer. The fast-acting dumping valve was manufactured by the NordBerg Company. Extensive research and development was directed towards the development of the automatic control. The experimental setup is divided into two main categories; mechanical hardware and electrical hardware. The system is designed to be operated either in manual or automatic control mode.

Results and Discussion

The experimental results presented in this report are divided into two main parts. One part deals with control strategy development and the other part deals with the pressure cycle comminution study. As this is a rapid pressure release system, most of the research efforts were directed towards controller development.

Controller Design

In high-performance hydraulic systems, it is necessary to have an accurate representation of the systems input-output relationship or transfer function. In the case of this high pressure comminution system, as the process is very slow, typically in the 100's of seconds, the transfer function could be easily determined by measuring the input-output response. Also, since the high pressure chamber is already connected to the process with electric motor, water lines, A/D converters, etc. an easy way to find its transfer function would be to measure the output response for a known output. Using the computer network analyzer, the system response for the open loop transfer [Gc(s)] was measured for a step input as shown in Figure 4-2.

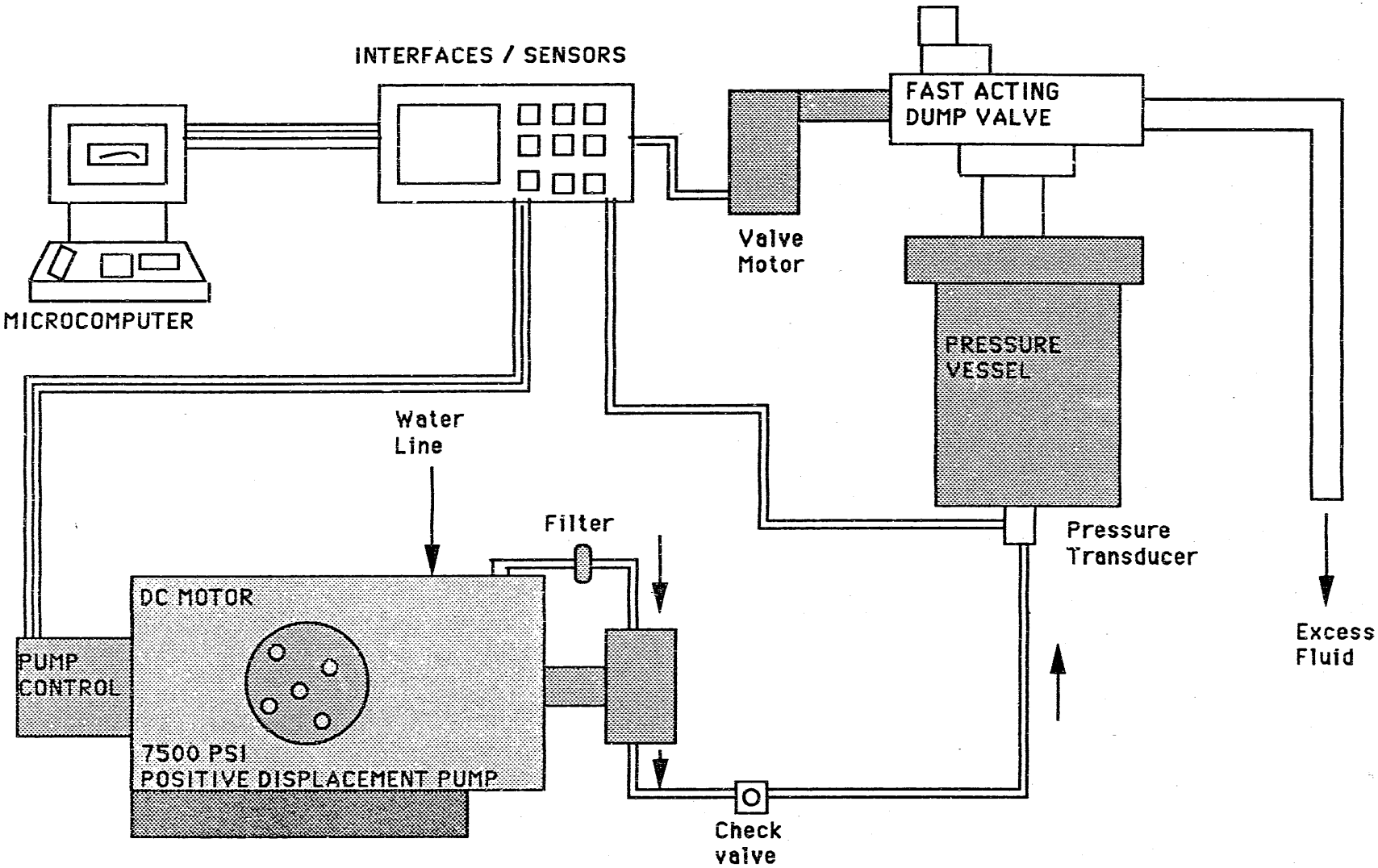

Figure 4-1. SCHEMATIC DRAWING OF LABORATORY PROTOTYPE EXPERIMENTAL SETUP

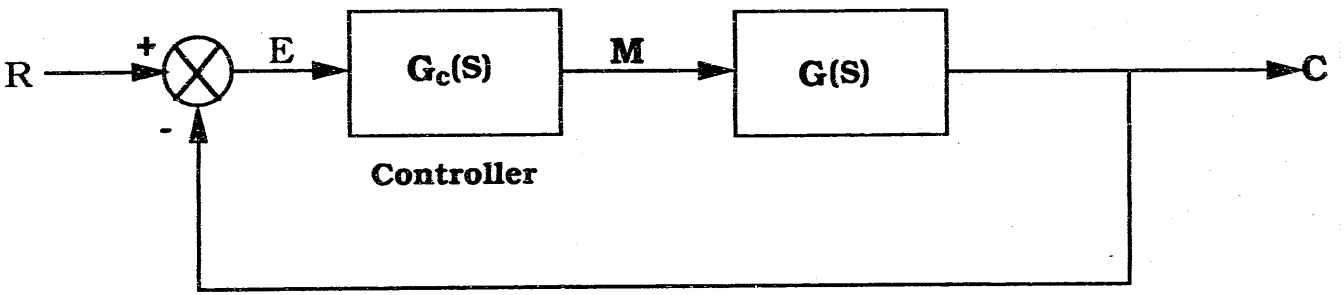

Figure 4-2. BLOCK DIAGRAM OF THE CONTROL SYSTEM LOOP

The following assumptions were made.

1. The 12-bit A/D converter used is calibrated to accurately represent the 0 to 100% speed and stroke of the motor.

2. The motor speed is linear over the range of interest.

The input to the system at 50% stroke and 50% speed is given by:

$$X(t) = 2048*2048u(t) \tag{5}$$

$$X(s) = \frac{4194304}{s} \tag{6}$$

The response was plotted and was fit to a linear curve given by:

$$Y(s) = \frac{26.1324}{s^2} \tag{7}$$

It can be easily seen from Misra et al. (1989) that the transfer function of the system is a first order integrator. With a sampling time of 1 s, the z transform of the system with zero-order hold is given by,

$$G(z) = \frac{6.2304 \times 10^{-4}}{z-1} \tag{8}$$

An important factor in designing the compensator for this system, is that the A/D converter provides data about the last response of the system. Also, because the sample rate is slow, the response time in this kind of a physical system will have an inherent delay. As the system is a first order integrator and from Equation 4 one can see that for successful comminution, input pressure rise should be exponential or parabolic, hence forcing the controller to have more zeros than poles so as to have a finite steady state error. A control algorithm, determined by trial and error, for the system that will provide a good control of the pressure rise time into the comminution system is given by,

$$C(1) = C(-1) + 25e(0) - 37.5e(-1) + 17.2e(-2) - 2.34e(-3) \tag{9}$$

where --

C(1) is the next output of the compensator

C(-1) is the last output of the compensator

e(0) is the difference between the current and the desired pressure

e(-1) is the error at the last sample

e(-2) is the error at two samples away

e(-3) is the error at three samples away

The transfer function of the compensator for the pressure rise is given by

$$G_c(z) = \frac{25 - 37.5\, z^{-1} + 17.2\, z^{-2} - 2.34\, z^{-3}}{1 - z^{-1}} \qquad (10)$$

However, once the peak value of the pressure has been reached, the transfer function of the compensator to hold the pressure at this peak value is given by

$$G_c(z) = \frac{25 - 37.5\, z^{-1} + 17.2\, z^{-2} - 2.34\, z^{-3}}{2(1 - z^{-1})} \qquad (11)$$

As mentioned above, the values for the compensator were obtained by trial and error and were found to work very well even with different kinds of inputs, such as ramp, parabolic, etc. Figure 4-3 shows actual pressure rise curve and the error associated with the ramp and parabolic inputs. Except at the start, the error is within 8% for both the ramp and parabolic inputs.

Pressure cycle comminution is an emerging potentially energy efficient concept in grinding. Several interrelated variables control the operation and comminution steps. The variables are divided into two groups:

1. Process variables
   - Saturation pressure
   - Pressure rise time
   - Hold time
   - Pressure release time
   - Energy requirements

2. Ore Characteristics
   - Size (nominal diameter)
   - Permeability
   - Porosity
   - Hardness

Process Control

A typical plot of computer-controlled pressure rise time, hold time and pressure release time is given in Figure 4-4. The first section of the curve is the rate of pressurization from atmospheric pressure to the desired value. The second section is the hold time at the peak pressure. The third section of the curve is the pressure release from the maximum pressure to atmospheric. The pressure release time is a critical aspect of the pressure release comminution. Faster pressure release will allow rapid breakage. The release time is limited by the modified dump valve used in the system. However, calculations showed that the release time is sufficiently fast to develop fluid expansion inside the rock (at 5000 psi external pressure) and thus to shatter the particles. The process control has been developed in such a way that multiple pressure rise and pressure release experiments can be done on command. A typical plot for multiple cycles with calculated energy required to achieve pressure size is given in Figure 4-5.

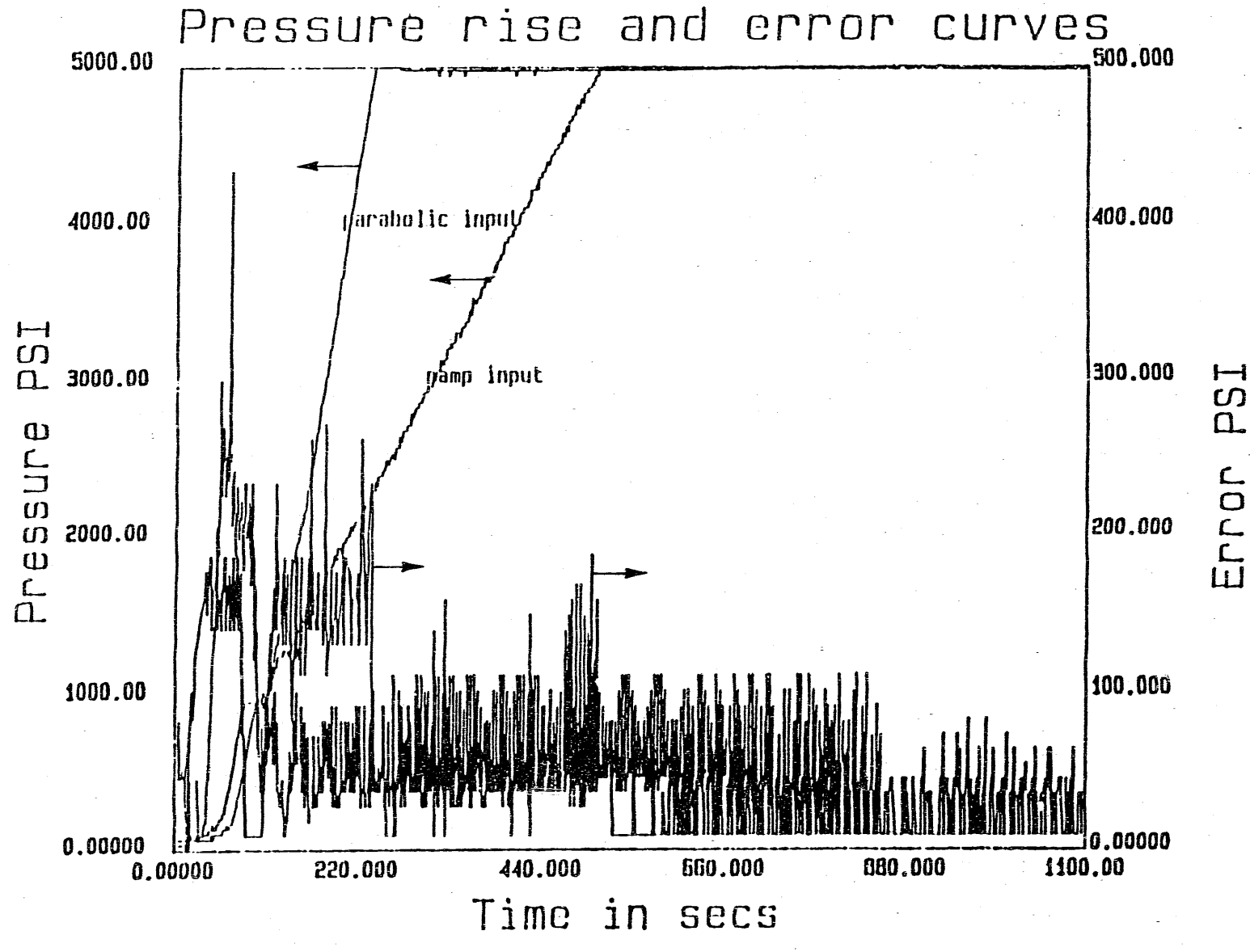

Figure 4-3. ACTUAL PRESSURE RISE AND ERROR CURVE

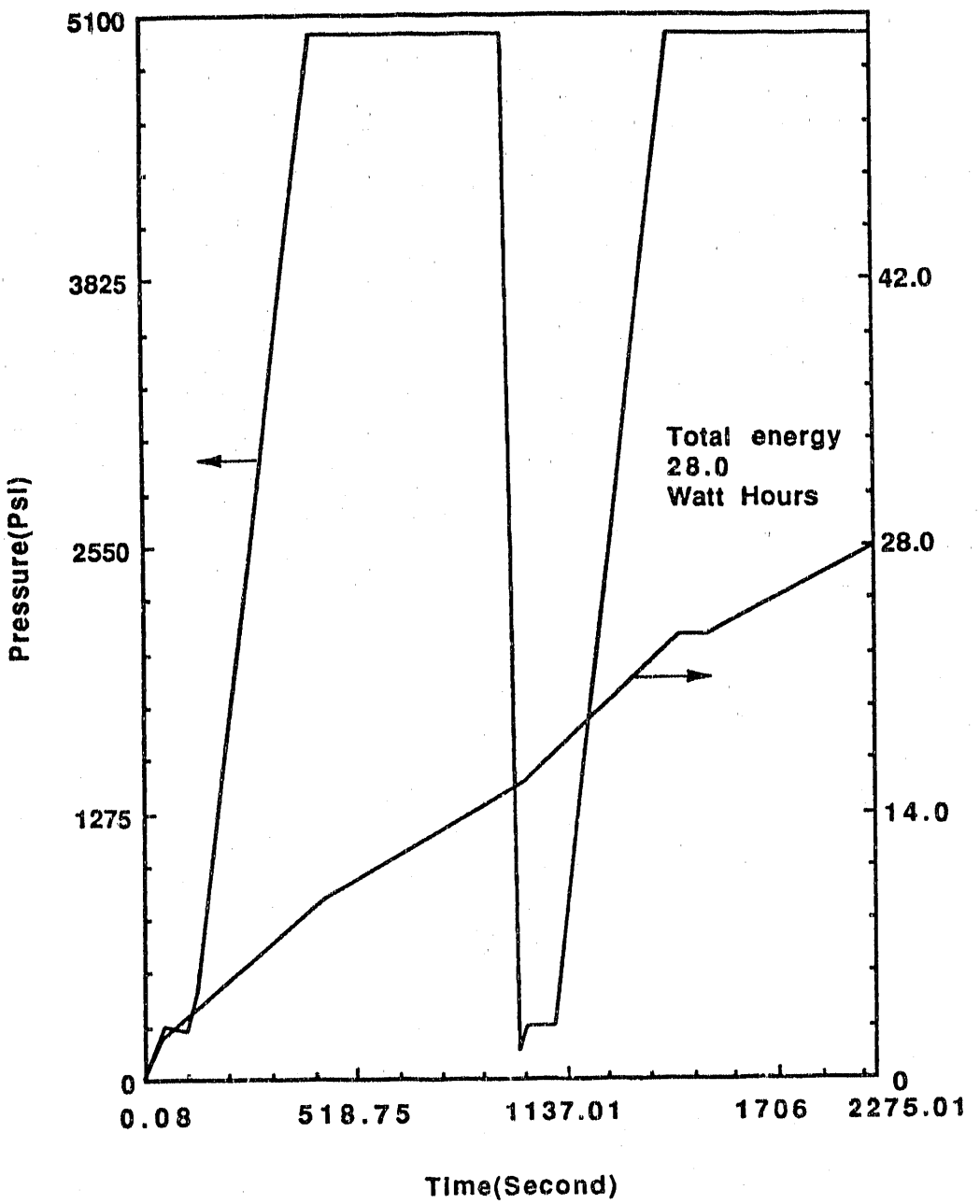

Figure 4-4. STEPS IN PRESSURIZATION WAVE FORMS

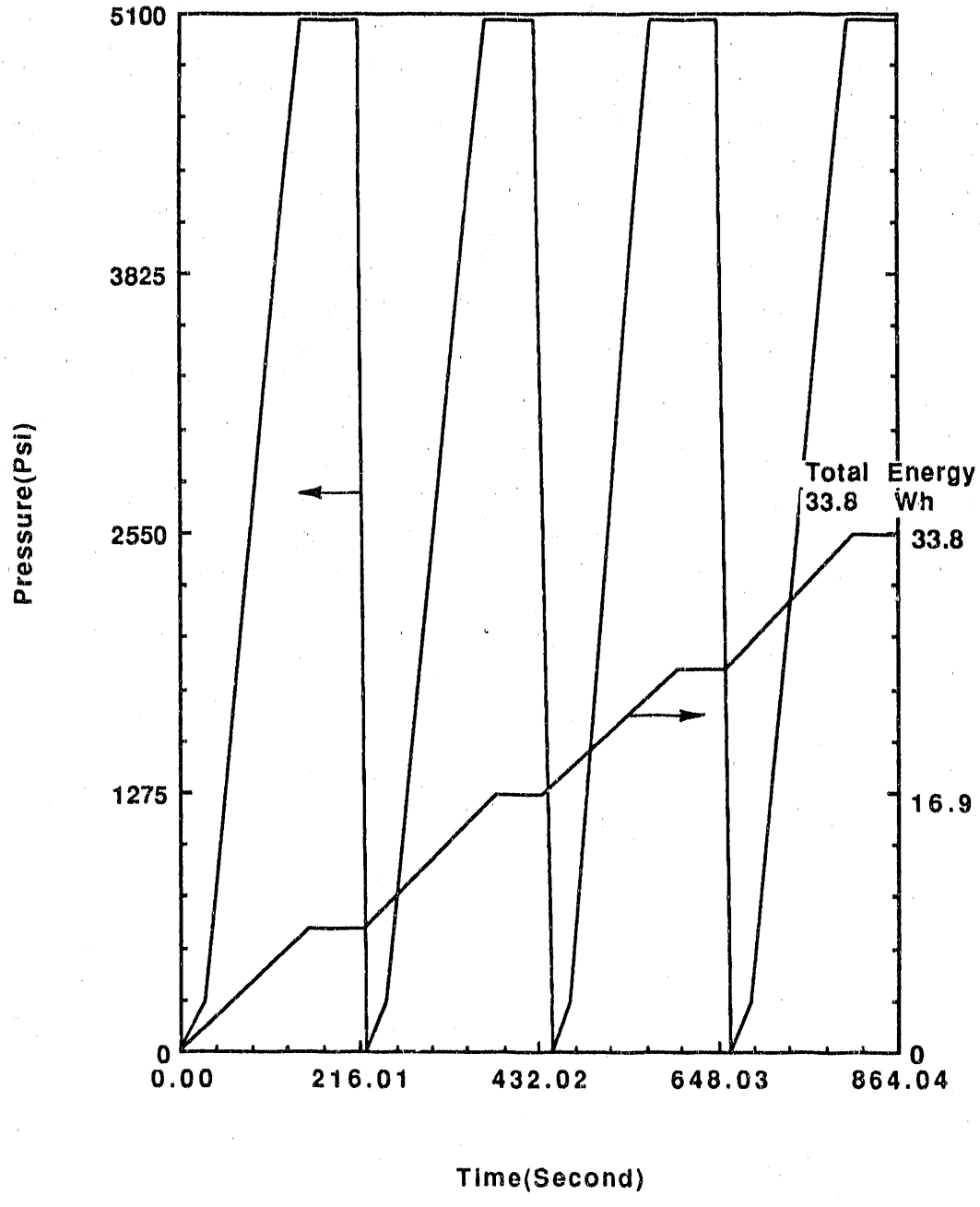

Figure 4-5. TYPICAL MULTIPLE PRESSURE CYCLE PLOT GENERATED BY COMPUTER

The confined pressure within the rock can be increased by increasing the applied pressure. The nature or wave form by which pressure is increased determines the extent of penetration of invading fluids into rock. Three different wave forms, linear, exponential and parabolic, were tested. The nature of these wave forms is given in Figures 4-6 through 4-8. The results indicate that the exponential and parabolic pressure rise techniques were more effective than the linear pressure rise. This is probably due to the low permeability and porosity of Eastern oil shales. Table 4-3 illustrates the energy required to achieve desired pressure in the reactor starting at ambient pressure (calculations are based on 50% stroke and 50% speed).

Experiments With Oil Shale

As described in the experimental section, most of the tests were conducted with Indiana shale. Selected tests were conducted with Alabama shale. Experiments were conducted as a function of the following variables:

1. Particle size
2. Saturation pressure
3. Hold time
4. Pressure rise time
5. Pressure cycle
6. Fluid compositions (surface energy modifiers, surfactants)
7. Gas phase compositions (Air and Carbon Dioxide).

Effect of Particle Size

Many experiments were conducted with different particle size, pressure rise time, saturation time, saturation pressure and pressure release time. The results showed that a saturation pressure of 5000 psi (34.6 MPa) (or more), hold time of 600 s, and minimum pressure release time of 15 to 20 ms are required to develop some breakage in the shale. It was noticed that due to the pressure release several layers of shale were removed from the surface and no catastrophic breakage was noticed. The surfacial breakage was due to the inherent laminar structure of shale material and low permeability. In each case, at optimum condition (exponential and/or parabolic pressure rise, 5000 psi peak pressure, 600 s hold time, 15 ms release time, one cycle) about 1% to 2% material was removed from the shale. For particle sizes below 1 mm, no significant breakage was noticed. The effect of pressure cycle was rather pronounced on coarse size materials.

Coarse sized Indiana and Alabama oil shales having narrow size range of 30 X 16 mm were used in all the tests. After pressure treatment, oil shale samples were ground under a standard condition in a tumbling mill. Grinding of the wet materials (immediately after removing from the pressure reactor) showed improved grindability. A material mass balance experiment showed that less than 0.5% of the fines generated during the pressure release experiments

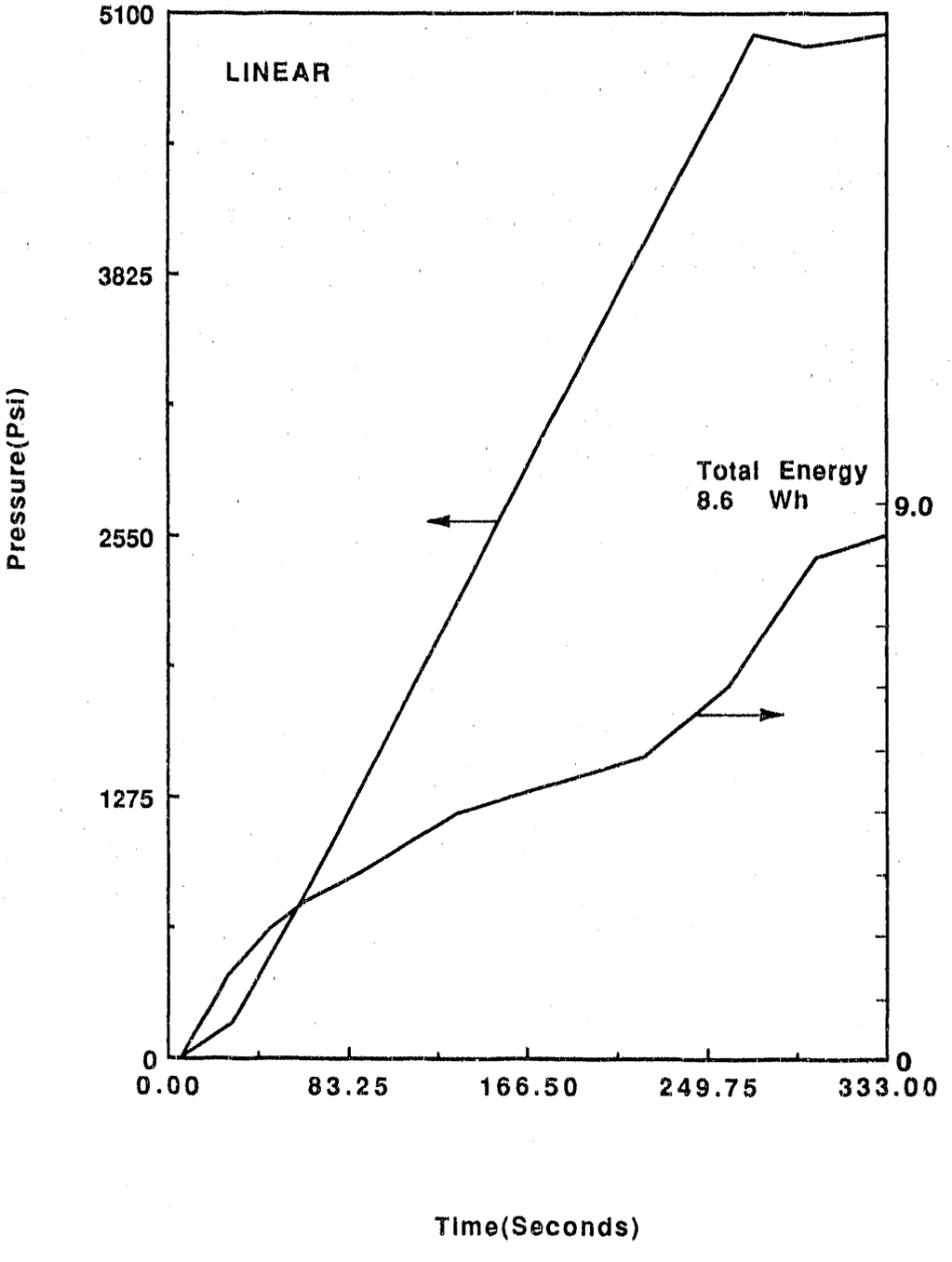

Figure 4-6. LINEAR PRESSURE RISE CURVE

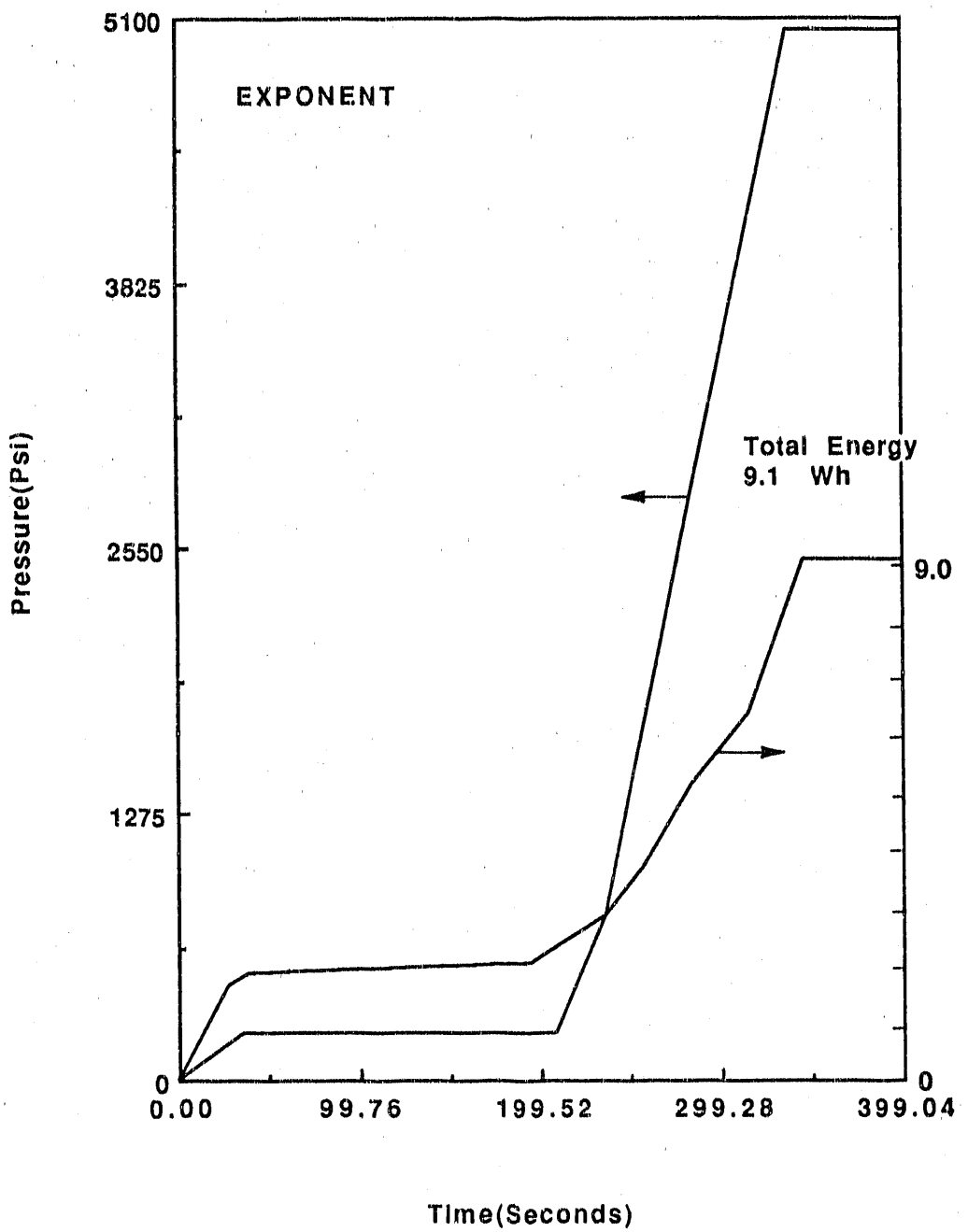

Figure 4-7. EXPONENT PRESSURE RISE CURVE

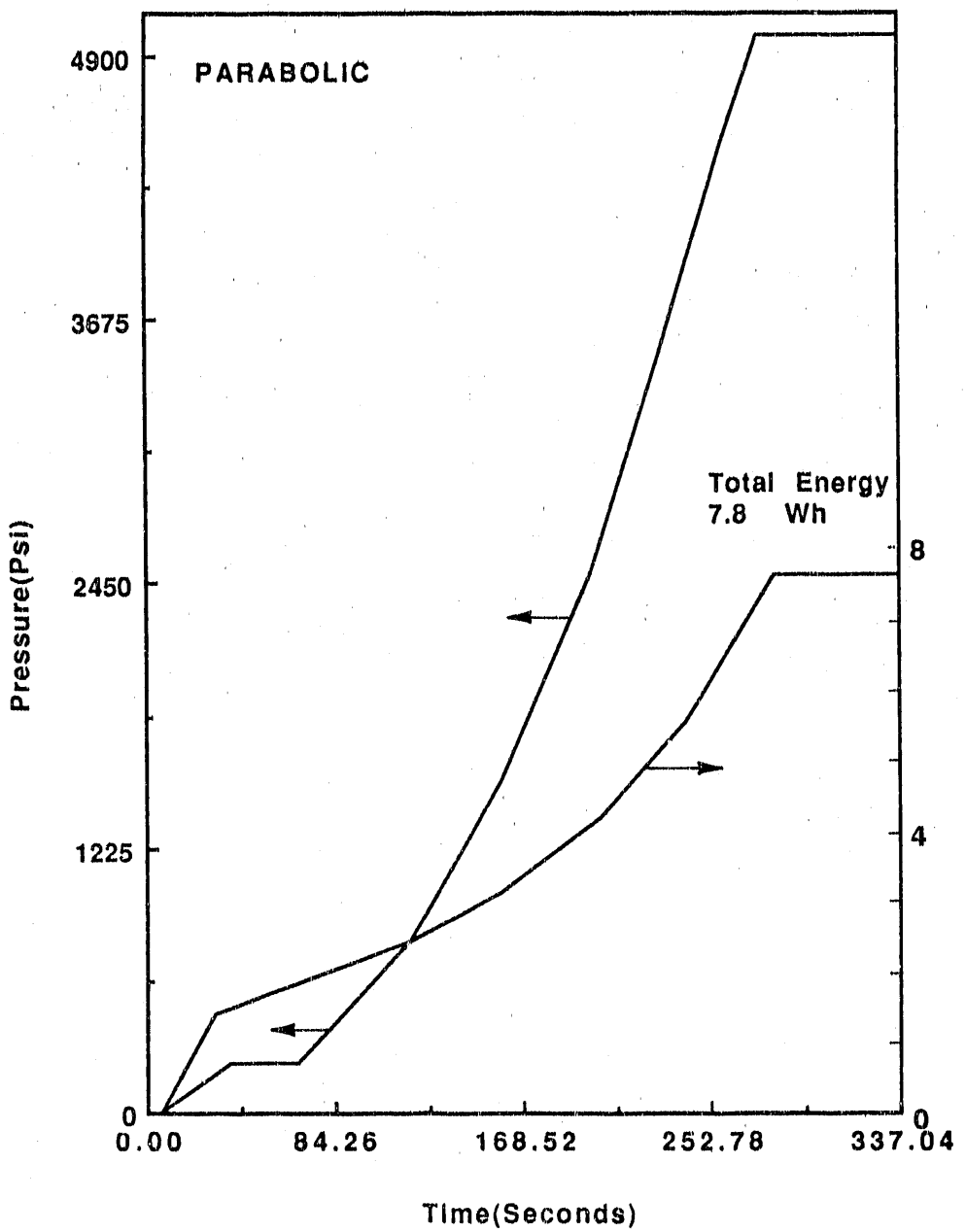

Figure 4-8. PARABOLIC PRESSURE RISE CURVE

Table 4-3. ENERGY REQUIRED TO ACHIEVE DESIRED PEAK PRESSURE (Exponential, Oil Shale 1 kg)

Peak Pressure, psi	Time, s	Energy Requirements, watt-h
5000	250	7.14
4000	200	5.69
3000	180	4.43
2000	135	3.29

are entrapped in the valve assembly and less than 1% released along with the discharged water.

Effect of Pressure Cycles

The effect of several pressure cycles on the breakage of Indiana shale is given in Table 4-4. As described before, due to the inherent nature of Eastern oil shale, surfacial (or layered) breakage was noticed. To quantify the effect of pressure cycle on the surfacial breakage, standard grinding tests with treated shale were conducted. The fine materials produced during pressure cycle experiments were removed by wet screening prior to each grinding test. The size analysis of the crushed products was conducted using a conventional screening technique. After 5 pressure cycles, the amount of -1.7-mm materials produced was 14.2% as compared to 5.73% without pressure cycle treatment. Similarly, the fines produced in multiple cycles increased from 0% to 4.3%. The increase in the number of pressure cycles has a positive effect on fines production.

Table 4-4. EFFECT OF PRESSURE CYCLE ON OIL SHALE COMMINUTION (30 X 16 mm Feed Size, 5000 psig, 500 s Exponential Rise Time and 600 s Hold Time)

	Cumulative Percent Passing				
		Pressurized			
Product Size, mm	No Pressure	Cycle 1	Cycle 2	Cycle 3	Cycle 5
-30	100	100	100	100	100
-16	72.83	77.81	83.69	88.23	92.23
-8	16.8	18.23	23.50	30.21	36.41
-3.5	6.97	8.30	11.12	14.21	18.5
-1.7	5.73	6.43	9.46	11.23	14.21
Fines (-38 µm removed before griding)	0	<1	<1	2.30	4.3

Effect of Surface Energy Modifiers

In the early thirties it was suggested by Rehbinder that certain chemicals can reduce the cohesive force which holds the discrete particles together (Rehbinder and Kalinkosvasky, 1937; Austin et al, 1984). This phenomenon is referred as the Rehbinder effect. The Rehbinder effect reduces

the surface binding energy due to the adsorption of surface active agents at the cracks and in flaws (Figure 4-9). There are two kinds of Rehbinder effects, "the external effect" and "internal effect." As far as grinding is concerned the "external effect" is insignificant. The "internal effect," which arises due to the penetration and adsorption of additives at the cracks, is responsible for the decrease in surface energy and the cohesive force. Some of the chemicals that can be used as ore softeners are chlorides of sodium and aluminum. Tests showed that these reagents have some effect on the breakage, however, the effect was not significant (Klimpel et al., 1978). This is not surprising because the mill dynamics, fluctuations and the solution chemistry in the grinding mill can mask the effect of these reagents. If these additives are allowed to penetrate the ore through the cracks and micro-cavities, the surface binding energy can be decreased. A series of tests were conducted with selected surface energy modifiers. The effect of surface energy modifiers during the pressure cycle comminution is given in Figure 4-10. Oil shale samples were pretreated with sodium chloride solution for 24 hours. After 24 hours, the shale was transferred into the pressure reactor. The reactor pressure was increased in an exponential wave form and was kept for 15 minutes at 4300 psi (29.7 MPa). The pressure cycle was repeated three times. It was noticed that pressure treatment and surface energy modifiers enhanced the grindability. A similar effect was noticed with aluminum chloride conditioning. It should be mentioned that the surface energy modifiers alone did not improve grindability.

In addition to selected inorganic hardness reducers, three different surfactants (anionic, cationic and nonionic) were used in the pretreatment experiments. In each case, oil shale particles of 30 X 16 mm were treated with 0.01 M surfactant solutions for 24 hours. After 24 hours, the treated oil shale was transferred along with the solution into the reactor. A parabolic pressure rise wave form was used. Oil shale particles were kept at a saturation pressure of 5000 psi for 600 seconds. After 600 seconds, the pressure was released. Oil shale particles were removed from the reactor and the fines (-400 mesh) were removed by washing on a 400-mesh screen. The wet particles were ground under a standard condition as described before. Experiments with the oil shale treated with surfactants without pressure treatment were conducted for comparison purposes. The results (Table 4-5) show that only the cationic surfactant (low molecular weight amine-hydrochloride) had some positive effect on the breakage of oil shale. It is recommended that future research should be continued in this promising area.

Effect of Gas Phase Composition

All the experiments were conducted with sized oil shale samples exposed to ambient pressure. A few experiments were conducted with CO_2 pressurization. It has been demonstrated that CO_2 has a specific interaction at the surface of coal (Miller and Misra, 1985). It was thought that pressurization of oil shale with CO_2 (as dry ice) in the reactor might improve the breakage kinetics. In this regard, shale particles (1 X 2 inch, Alabama shale) were mixed with dry ice (0.5 kg/kg oil shale) in the reactor and the pressure was increased to 4790 psi and the peak pressure was maintained for 600 s. However, the addition of CO_2 in the reactor created some problems during the depressurization time. Under normal circumstances the pressure release time is in the range of 15 to 20 ms. With the addition of CO_2 the pressure release time was rather slow and erratic. This phenomenon is probably due to the solubility of CO_2 in the fluid phase.

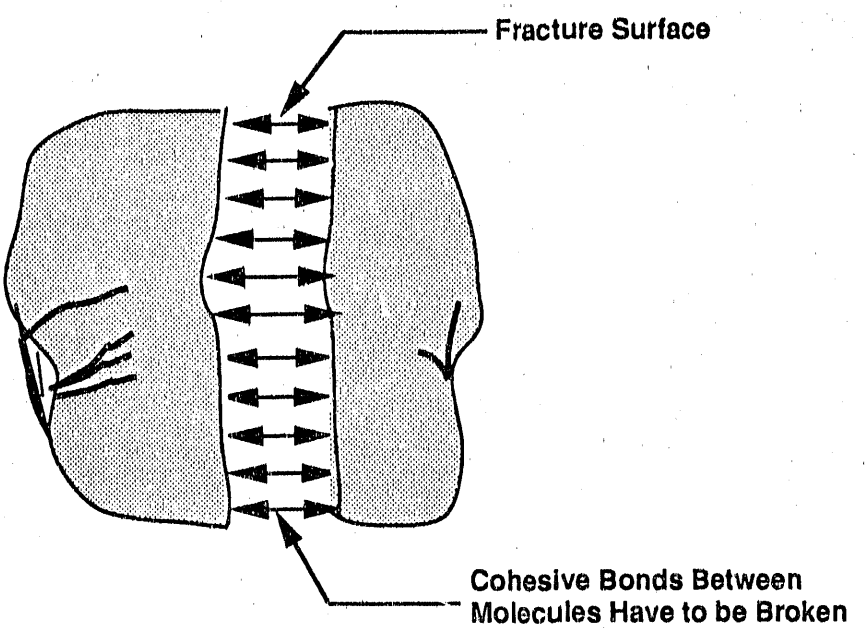

Figure 4-9. ILLUSTRATION OF BONDING ENERGY BETWEEN FRACTURE SURFACES

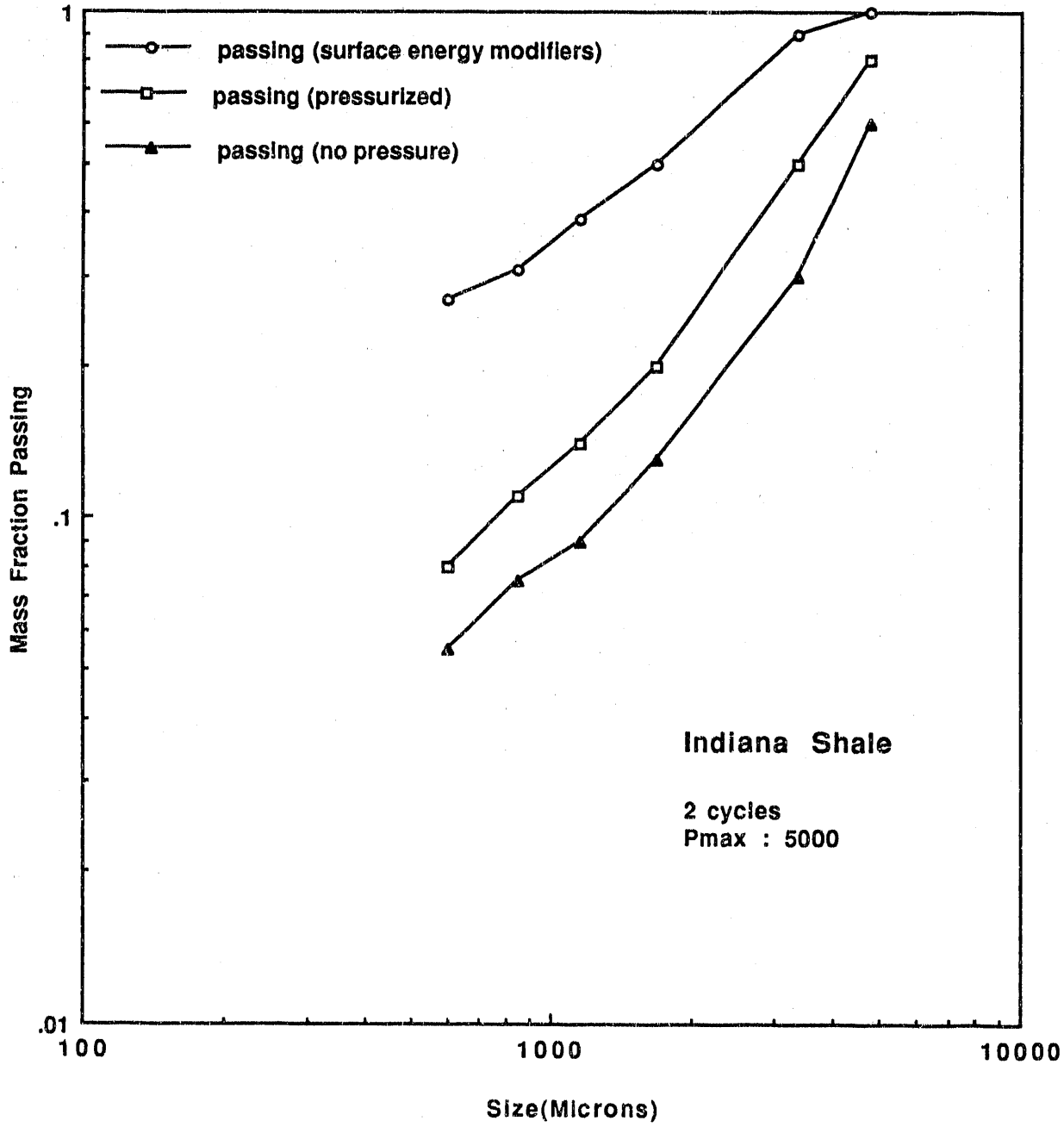

Figure 4-10. EFFECT OF SURFACE ENERGY MODIFIERS

Table 4-5. EFFECT OF SELECTED SURFACTANT ON THE PRESSURE CYCLE COMMINUTION OF OIL SHALE
(Condition: 0.001 M, 5000 psi, Hold Time 600 s)

Surfactants	Remarks
Anionic (Sodium Oleate)	No Positive Effect
Nonionic (Igepal 650)	No Positive Effect
Cationic (Amine)	Improved Grindability

Conclusions

Several process variables such as saturation pressure, pressure rise time, hold time and pressure release time control surfacial breakage and fracture of the oil shale. The critical part for the implementation of this emerging technology is largely dependent upon the process control strategy. A microcomputer-based digital control strategy has been developed to control the pressure rise time, hold time and pressure release time. Another aspect of this process is the implementation of convenient multiple pressure release cycle along with the incremental power requirement to achieve that operation.

The research conducted during the project period demonstrated that the pressure cycle technology cannot be used as a stand-alone method for the ultimate grinding of oil shale. This process can be used as a pretreatment (or pre-processing) strategy to create enough cracks and fracture in the ore so that subsequent size reduction can be accomplished. The addition of surface energy modifiers during the pressurization increased the grindability of oil shale significantly. Multiple pressure release cycles have a positive effect on breakage of oil shale. It is recommended that pressure cycle strategy be used as an adjunct to conventional milling operation.

Subtask 4.1.3. Stirred Ball Mill Grinding

Grinding tests on coal have indicated that the stirred ball mill offers an attractive alternative to conventional ball/rod mills for fine grinding to micron sizes. In contrast to conventional rod or ball mills, the stirred ball mill is reported to achieve particle size reduction of mineral materials in a more energy-efficient way. In conventional ball/rod mill grinding, much of the size reduction is obtained principally by impact crushing of the mineral particles. As a result, when grinding to extremely fine sizes, considerable energy is expended in the balls or rods impacting on each other. The stirred ball mill operates in a different fashion. The mineral material being processed is stirred with a charge of small steel or ceramic balls. During stirring, the mineral matter is trapped in the spaces between the balls, and is subjected to a combination of compressive and shear forces by the small balls. A comparison of the grinding action in conventional and stirred ball mills is shown in Figure 4-11. Estimates indicate that an energy savings of 80% (Stehr et al., 1985) or more can be achieved by grinding coal in the stirred ball mill to a size of about 5 μm.

Thus, fine grinding of oil shale in the stirred ball mill offers the opportunity to substantially reduce the cost of the fine grinding step prior to concentration by froth flotation. Realization of this opportunity is

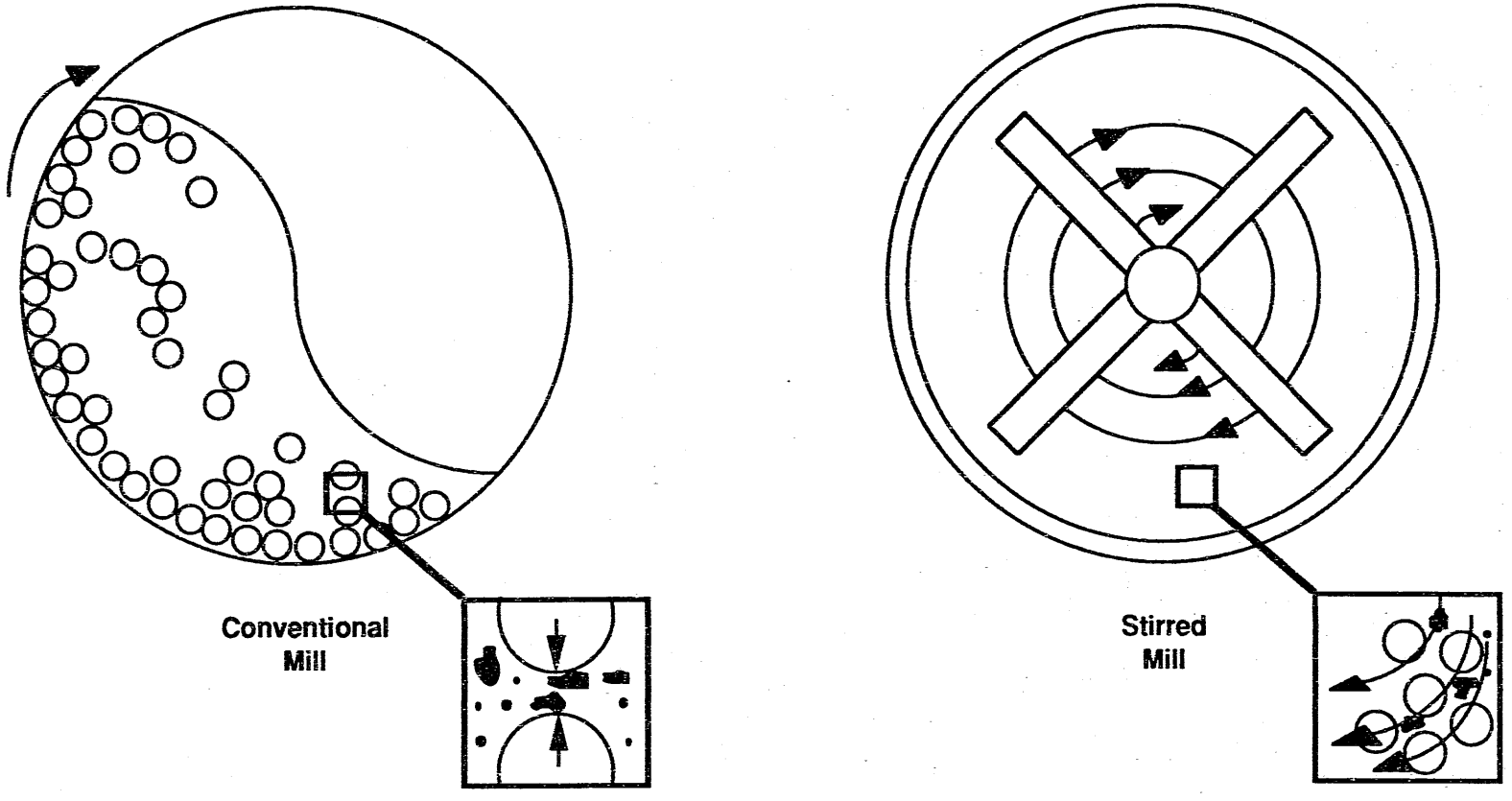

Figure 4-11. COMPARISON OF GRINDING ACTIONS IN CONVENTIONAL AND STIRRED BALL MILLS

important because effective flotation requires that the shale feed be ground to about 10 μm. The objective of this subtask was to obtain energy-size reduction data on Eastern oil shales and rougher flotation concentrates, and to determine the most efficient mill operating conditions.

Equipment

Stirred Ball Mill

An LME-4 Netzsch stirred ball mill was used in the John Option mode. This consisted of a stationary cylindrical vessel with a net volume of 2.48 liters attached to the drive unit. The stirrer shaft was furnished with 8 annular rows of 4 stirrer pins each. The grinding shell was equipped with the same type of pins which were radially fastened to the inner wall of the grinding chamber. Accordingly, stirrer pins plus stationary pins imbedded in the shell form a rotor-stator type of agitator. The grinding chamber was typically filled with small grinding media (1.1- to 3-mm diameter) to a media filling of 80% to 90% by volume. The ground suspension discharged through a screen that was sized to prevent grinding media from leaving the mill. This device was operated in continuous mode.

Particle Size Analyzer

The particle size analysis was carried out using Marco Scientific Model No. 715 Granulometer.

Experimental Procedure

Continuous grinding tests were carried out using Eastern oil shales of varying fineness. The feed stock to the Netzsch mill was prepared using a rod mill [11-inches long X 8.25 inches in diameter (27.9 cm long X 20.9 cm in diameter)] with 27 stainless steel rods [8.75 inch length X 0.6 inch diameter (22.2 cm long X 1.5 cm in diameter)] each weighing 402 grams. The amount of shale used was -4 mesh (1000 grams). The grinding was done at 40% solids for 30 minutes. The grinding done at these conditions gave a product which was approximately -100 mesh. Figure 4-12 shows the stirred ball mill grinding setup. The grinding was carried out using stainless steel media of 1.1-mm, 2-mm, and 3-mm diameter. The degree of media filling was varied between 80% to 90%, but in most cases kept at an intermediate value of 85%. The rotor speed was varied between 1200 to 2000 rpm. The slurry feed rate was varied between 100 to 1400 mL/min. Slurry percent solids was varied between 33% to 55%.

Raw Shale Grinding Studies

The Netzsch mill was operated at different speeds and the power draw of the mill was recorded. The data was used in plotting a calibration curve for tare power as shown in Figure 4-13. The linear regression resulting from the data is also shown in this figure.

Net power was calculated by subtracting the tare power from the total power observed at steady state. Tare power is calculated from the following equation:

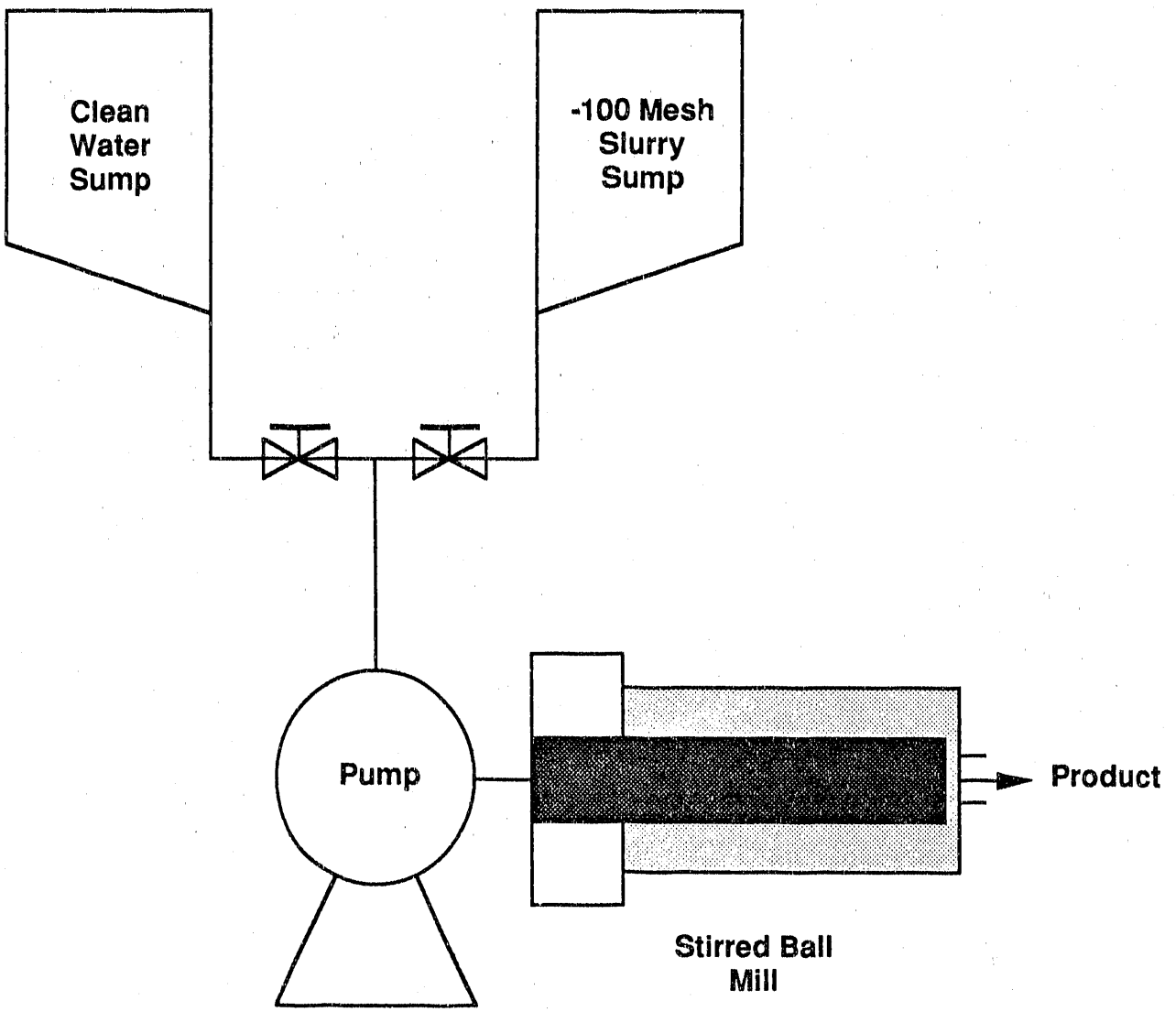

Figure 4-12. SCHEMATIC DIAGRAM OF THE NETZSCH LME-4 STIRRED BALL MILL SETUP FOR CONTINUOUS GRINDING

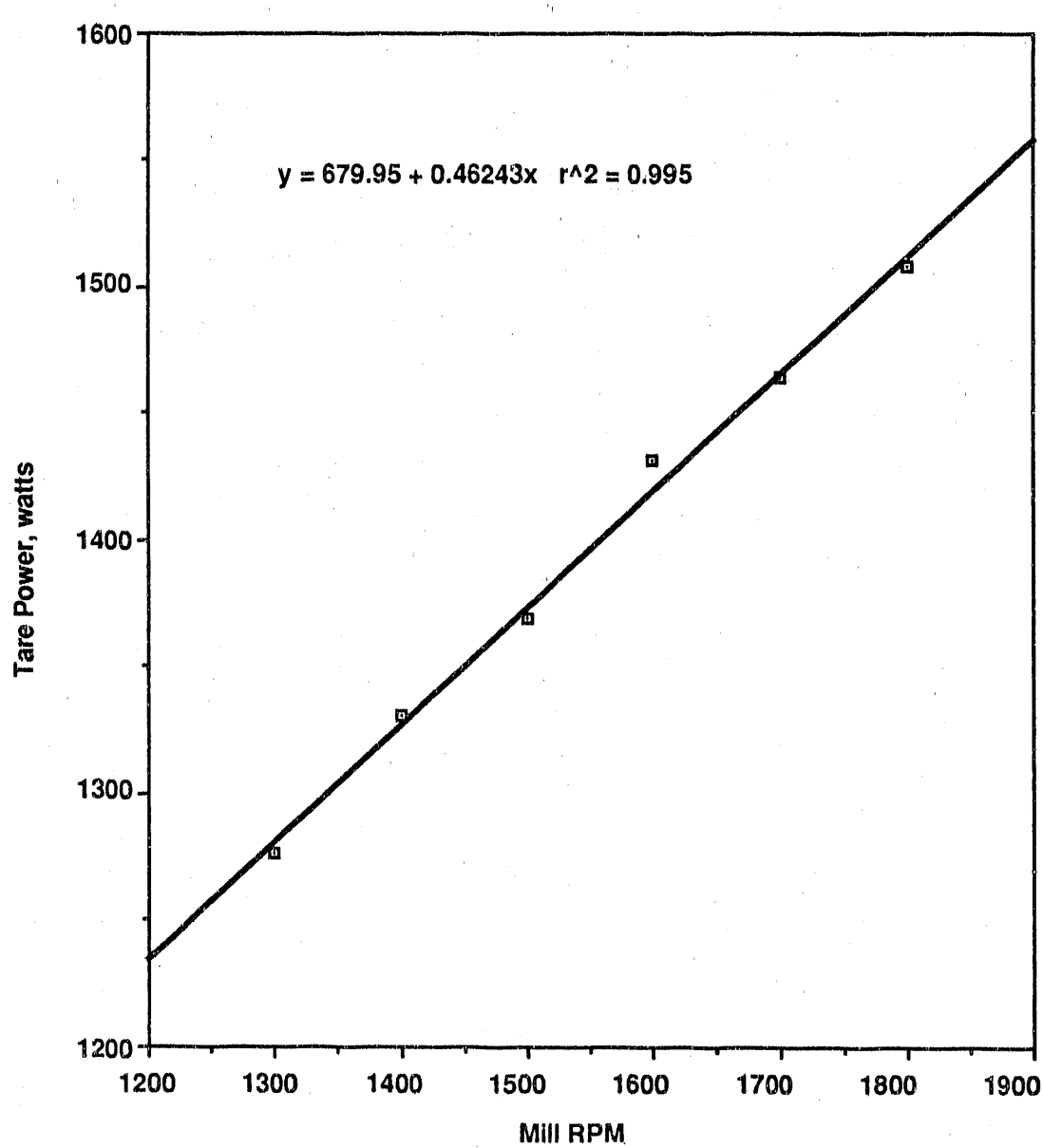

Figure 4-13. CALIBRATION CURVE OF THE TARE POWER FOR THE LME-4 NETZSCH MILL

$$\text{Tare Power (watts)} = 679.9525 + 0.4624*N \qquad (12)$$

Where N is rotor speed >1200; for N <1200, a value of tare power = 1235 watts was used.

Slurry density was calculated by assuming a raw shale density of 2.4 g/mL. The dry shale feed rate was calculated using the following equation:

$$\text{Feed rate (t/h)} = \text{slurry flow rate (mL/min)} \times \text{slurry density (g pulp/mL)}$$

$$\times \text{ fractional solids } \left(\frac{\text{g shale}}{\text{g pulp}}\right) \times \frac{60}{1 \times 10^6}$$

The first series of experiments were carried out with Indiana and Alabama shales. Both shale feeds were -100 mesh and tests were made by targeting a ground product having a d_{90} of 10 μm. Tables 4-6 and 4-7 list the energy-size reduction data obtained at different operating conditions. These results show that the energy requirements for producing micronized shale are quite high.

Table 4-6. CONTINUOUS GRINDING DATA USING 2-mm BEADS FOR INDIANA SHALE (-150 mesh: d_{90} = 51.0 and d_{50} = 15.4 μm) AT DIFFERENT OPERATING CONDITIONS

Rotor Speed, rpm	Media Filling, %	Solids, wt %	Feed Rate, mL/min	Net Power, watts	Specific Energy, kWh/t	Product, μm	
						d_{90}	d_{50}
1170	80	46	--	1316	--	18.9	6.3
1300	80	46	540	2069	101.4	14.8	5.2
1500	80	46	720	3026	110.8	15.8	5.6
1200	80	43	150	1505	295.1	13.9	4.9
1300	80	43	150	2009	393.7	11.1	4.0
1450	80	43	150	2929	574.3	10.5	3.7
1500	80	43	150	3211	629.6	8.1	3.2
1200	80	43	275	1505	160.1	15.4	5.4
1300	80	43	275	1919	204.1	12.9	4.5
1450	80	43	275	2699	287.1	11.5	4.0
1500	80	43	275	3086	328.3	11.4	3.9
1200	85	45	250	1645	180.8	13.9	4.9
1300	85	45	250	2099	230.5	11.7	4.2
1450	85	45	300	2879	264.1	10.9	3.8
1500	85	45	300	3226	296.0	10.8	3.9

The next series of tests were conducted using a coarser shale feed. Feedstock for these tests was prepared by grinding -10 mesh Indiana shale in a rod mill for 15 minutes to achieve -65 mesh feed. The stirred milling tests were conducted using 2-mm beads. Table 4-8 lists the energy-size reduction data for this series of tests. In these tests, energy requirements are also very high possibly because of three reasons: first, low percent solids, second, coarse feed size, and third because of lower media filling.

Table 4-7. CONTINUOUS GRINDING DATA USING 2-mm BEADS FOR ALABAMA SHALE (-100 mesh: d_{90} = 84.0 and d_{50} = 23.9 μm) AT DIFFERENT OPERATING CONDITIONS AT SLURRY DENSITY OF 45% SOLIDS

Rotor Speed, rpm	Media Filling, %	Feed Rate, mL/min	Net Power, watts	Specific Energy, kWh/t	Product, μm d_{90}	Product, μm d_{50}
1350	85[a]	240	2911	334.5	11.8	4.4
1400	85	275	3173	317.2	10.3	3.7
1450	85	275	3499	349.9	9.9	3.5
1500	85	275	3786	378.6	9.8	3.5
1550	85	275	4153	415.3	9.4	3.4
1600	85	275	4450	445.0	9.2	3.4
1350	83[b]	150	2246	408.2	11.6	4.1
1400	83	170	2473	398.7	11.1	4.0
1450	83	200	2829	387.5	10.6	3.7
1500	83	205	3026	403.5	10.5	3.7
1550	83	215	3243	415.8	10.4	3.6
1600	83	215	3590	460.2	10.1	3.5
1200	87[c]	300	1885	172.9	13.8	5.1
1300	87	300	2264	207.6	11.3	4.2
1400	87	300	2873	263.5	10.8	3.9
1500	87	300	3576	328.1	10.2	3.7
1550	87	300	3853	353.5	10.1	3.6
1600	87	300	4310	395.4	10.0	3.6
1600	87	200	4240	580.8	9.8	3.6
1600	87	450	4130	251.8	11.2	3.8
1600	87	120	4230	961.4	9.6	3.6

[a] Void Volume = 1265 cc.

[b] Void Volume = 1245 cc.

[c] Void Volume = 1180 cc.

Table 4-8. EXPERIMENTAL CONDITIONS AND RESULTS FOR THE LME-4 NETZSCH MILL* OPEN-CIRCUIT TESTS WITH INDIANA OIL SHALE FEED**

Test No.	Rotor Speed, rpm	Feed Rate, mL/min	New Power, watts	Specific Energy, kWh/t	Residence Time, min	Product, μm d_{90}	Product, μm d_{50}
1	1300	500	1895	160.6	2.5	15.5	5.7
2	1400	350	2648	320.5	3.6	12.0	4.6
3	1500	300	3554	502.1	4.2	10.7	4.0
4	1600	300	4757	671.9	4.?	10.2	3.8
5	1500	200	3783	801.6	6.3	10.5	4.3

* Mill charged with 2-mm beads at 81.7% loading, void volume = 1264 cc.

** Feed -65 mesh, 32% solids by weight having d_{90} = 96.0 and d_{50} = 25.4 μm.

In another series of experiments, coarse feed shale was ground at 85% media filling using higher slurry solids content (44% to 48%). These data are listed in Table 4-9. Again, the magnitude of energy requirements is high.

Table 4-9. EXPERIMENTAL CONDITIONS AND RESULTS FOR THE LME-4 NETZSCH MILL OPEN-CIRCUIT TESTS WITH INDIANA OIL SHALE FEED USING 2-mm BEADS AT 85% MEDIA FILLING

Test No.	Rotor Speed, rpm	Feed Rate, mL/min	Solids, wt %	Net Power, watts	Specific Energy, kWh/t	Feed, µm		Product, µm	
						d_{90}	d_{50}	d_{90}	d_{50}
1	1300	400	44.5	2449	169.6	198.4	62.1	11.7	4.3
2	1400	400	44.5	3123	216.2	198.4	62.1	11.3	4.2
3	1500	400	44.5	3773	261.3	198.4	62.1	10.9	3.9
4	1600	400	44.5	4600	318.6	198.4	62.1	10.6	3.7
5	1600	250	44.5	4610	510.9	198.4	62.1	9.1	3.4
6	1300	600	47.1	2268	97.0	96.4	16.9	14.3	5.2
7	1400	600	47.1	2973	127.1	96.4	16.9	13.5	4.9
8	1500	600	47.1	3796	162.4	96.4	16.9	12.5	4.6
9	1600	600	47.1	4830	206.6	96.4	16.9	11.9	4.3
10	1300	325	49.1	2358	175.8	205.5	81.8	11.5	4.2
11	1400	325	49.1	3117	232.4	205.5	81.8	11.0	3.9
12	1500	325	49.1	3856	287.5	205.5	81.8	10.7	3.8
13	1600	325	49.1	4760	354.9	205.5	81.8	10.4	3.7
14	1300	525	49.1	2179	100.5	205.5	81.8	13.7	4.8
15	1400	525	49.1	2793	128.9	295.5	81.8	12.6	4.6

In previous tests, energy requirements were found to be high. This result was attributed to the rotor speed. Therefore, it was thought that if the rpm could be kept low and other variables changed parametrically, then a reduced energy requirement may result.

Therefore, grinding tests were carried out using -65 mesh Indiana shale and -100 mesh Alabama shale at an agitator speed of 1130 rpm. The energy size reduction data are shown in Table 4-10. It was interesting to note that high slurry density and high mill feed rate at lower agitator rpm lead to lower energy requirements.

The tests conducted thus far were aimed at producing a product having d_{90} of 10 µm in one pass. The data indicate that this could be accomplished, but with relatively high energy requirements. Therefore, it was decided to determine the energy requirements to produce a product having d_{90} in the vicinity of 20 µm using 3-mm steel beads. A series of tests was conducted using Alabama shale at high slurry density (56% solids) and low agitator speed (1130 rpm) by varying feed rate in the range of 1000 to 2000 mL/min. Table 4-11 lists the energy-size reduction data obtained in these tests. A product having d_{90} of 20.1 µm required 83.6 kWh/t (Sample 1), whereas, a product having d_{90} of 25.3 required only 37.8 kWh/t (Sample 8). This reduction in specific energy gave an indication of a two step beneficiation route where shale could be ground to a product size of d_{90} = 25 µm suitable for rougher flotation and subsequently rougher flotation concentrate could be reground to achieve a feed having d_{90} = 10 µm suitable for cleaner flotation.

Table 4-10. EXPERIMENTAL CONDITIONS AND RESULTS FOR THE LME-4 NETZSCH MILL OPEN-CIRCUIT TESTS
(Rotor Speed = 1130 rpm, 85% Media Filling, 2-mm Steel Beads)

Shale Type	Feed Rate, mL/min	Net Power, watt	Specific Energy, kWh/t	Feed, μm		Product, μm	
				d_{90}	d_{50}	d_{90}	d_{50}
Indiana	375	4515	282.3	199.7	61.4	10.1	3.8
(50.25%	600	3945	154.2	199.7	61.4	12.1	4.7
solids)	800	3725	109.2	199.7	61.4	13.4	5.0
-65 mesh	1000	3565	83.6	199.7	61.4	13.9	5.1
	1100	3335	71.5	199.7	61.4	14.8	5.4
Alabama	500	3525	149.0	135.7	23.1	11.9	4.8
(53.81%	700	3305	100.4	135.7	23.1	13.3	5.1
solids)	800	3245	86.2	135.7	23.1	13.9	5.3
-100 mesh	1000	3215	68.3	135.7	23.1	15.6	5.9

Table 4-11. EXPERIMENTAL CONDITIONS AND RESULTS FOR THE LME-4 NETZSCH MILL OPEN-CIRCUIT TESTS FOR THE ALABAMA SHALE AT 55.9% SOLIDS
(Rotor Speed = 1130 rpm, 85% Media Filling, 3-mm Steel Beads)

Sample No.	Feed Rate, mL/min	Net Power, watts	Specific Energy, kWh/t	Feed, μm		Product, μm	
				d_{90}	d_{50}	d_{90}	d_{50}
1	1000	4166	83.6	115.7	27.6	20.1	6.9
2	1200	4015	67.1	115.7	27.6	21.4	7.4
3	1400	4001	57.3	115.7	27.6	22.4	7.7
4	1450	3905	54.0	115.7	27.6	22.5	7.8
5	1600	3895	48.8	115.7	27.6	23.3	8.1
6	1700	3875	45.7	115.7	27.6	23.5	8.2
7	1800	3845	42.8	115.7	27.6	24.1	8.6
8	2000	3765	37.8	115.7	27.6	25.3	8.8

In order to compare the energy efficiency of 2-mm beads with 3-mm beads, -65 mesh Alabama shale feed was ground separately with 2-mm and 3-mm beads at identical rotor speed (1140 rpm) and media filling (85%). The results of this comparative study are shown in Tables 4-12 and 4-13. True comparison of the efficiency of 2-mm and 3-mm beads in terms of energy saving and mill capacity can only be done at identical product size distributions. However, in the absence of such data, the comparison can be done at identical d_{90} and d_{50} product size.

Considering a comparison at identical d_{90} of 21.9 μm (compare Test 3 of Table 4-12 with Test 4 of Table 4-13), the specific energy is reduced from 62.2 to 40.0 kWh/t when using finer size media, also the mill capacity is increased by 41.6% (1700 mL/min as compared with 1200 mL/min). Similarly, considering a comparison at identical d_{50} of 7.5 μm (compare Test 2 of Table 4-12 and Test 2 of Table 4-13), the specific energy is reduced from 69.1 to 50.4 kWh/t when using finer size media and the mill capacity is increased by 18.2% (1300 mL/min as compared with 1100 mL/min).

Table 4-12. EXPERIMENTAL CONDITIONS AND RESULTS FOR THE LME-4 NETZSCH MILL OPEN-CIRCUIT TESTS FOR THE ALABAMA SHALE (Rotor Speed = 1140 rpm, 85% Media Filling, 3-mm Steel Beads, 52% Solids)

Sample No.	Feed Rate, mL/min	Net Power, watts	Specific Energy, kWh/t	Feed, μm		Product, μm	
				d_{90}	d_{50}	d_{90}	d_{50}
1	1000	3465	77.4	133.6	67.1	21.0	7.3
2	1100	3405	69.1	133.6	67.1	21.7	7.5
3	1200	3340	62.2	133.6	67.1	21.9	7.7
4	1200	3265	60.8	133.6	67.1	22.6	7.9
5	1750	3287	42.0	133.6	67.1	26.0	9.4
6	2500	3345	29.9	133.6	67.1	33.6	11.8

Table 4-13. EXPERIMENTAL CONDITIONS AND RESULTS FOR THE LME-4 NETZSCH MILL OPEN-CIRCUIT TESTS FOR THE ALABAMA SHALE (Rotor Speed = 1140 rpm, 85% Media Filling, 2-mm Steel Beads, 52% Solids)

Sample No.	Feed Rate, mL/min	Net Power, watts	Specific Energy, kWh/t	Feed, μm		Product, μm	
				d_{90}	d_{50}	d_{90}	d_{50}
1	1100	2945	59.8	133.6	67.1	17.5	6.7
2	1300	2935	50.4	133.6	67.1	20.0	7.5
3	1500	2905	42.4	133.6	67.1	21.2	8.0
4	1700	3045	40.0	133.6	67.1	21.9	8.3

The higher efficiency of 2-mm beads compared with 3-mm beads can also be demonstrated by utilizing Charles relationship. If one plots the size reduction data for Alabama shale as shown in Figure 4-14, for 2-mm beads and 3-mm beads, by using specific energy and product median values, it is clear that to produce a given product median size, 2-mm beads require less specific energy input than 3-mm beads. Another interesting feature of this plot is that stirred ball milling data can be normalized.

Up to this point the tests were conducted with a view to lowering energy requirements by keeping rotor speed at its lowest level. This is because the mill power draw is proportional to the third power of mill speed (Sepulveda, 1981). This results in lower energy consumption but also reduces the mill capacity. This is because, at lower agitator speed, mill throughput should be low enough to yield reasonable residence time for particle breakage. Alternatively, mill throughput can be increased, but agitator speed must be increased proportionately to offset the decrease in residence time.

In fine grinding, the objective is to minimize energy requirements by maintaining a high mill capacity for a specific product size. The critical task, therefore, is to determine the optimum combination of rotor speed and feed rate to achieve the objective. In order to determine which one, whether high or low rotor speed, will be more energy efficient, tests were conducted at high (1300) and low (1150) rpm. At high rpm (1300), the mill feed rate was

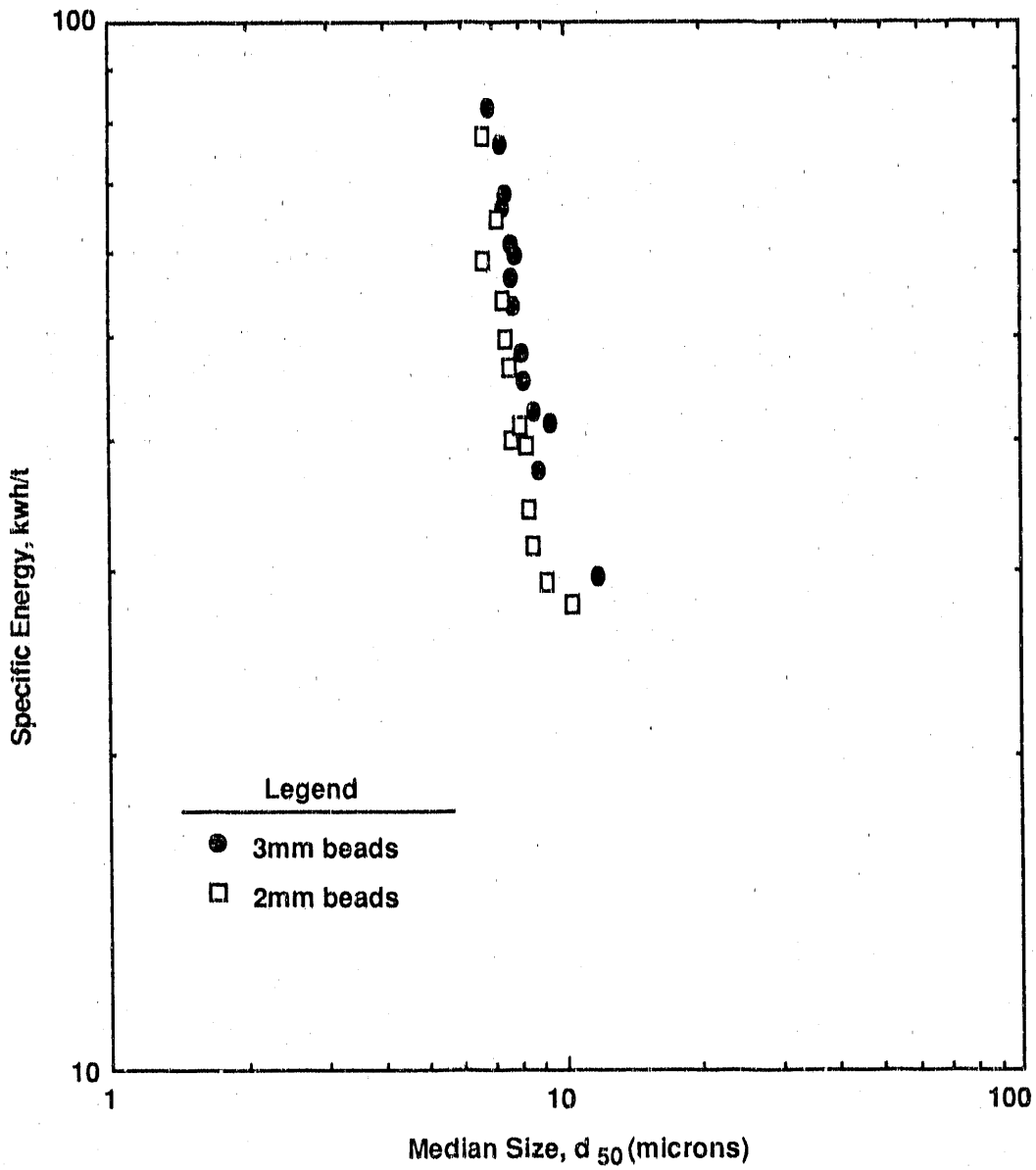

Figure 4-14. ENERGY SIZE REDUCTION RELATIONSHIP FOR STIRRED BALL MILLING OF ALABAMA SHALE DEMONSTRATING THE CONCEPT OF ENERGY NORMALIZABILITY

varied in the range of 1000 to 2100 mL/min. The results (Table 4-14) show that energy requirements at 1300 rpm can be reduced from 72.7 to 31.6 kWh/t by increasing feed rate from 1000 to 2100 mL/min maintaining the desired a product d_{90} (~20 μm).

Table 4-14. EXPERIMENTAL CONDITIONS AND RESULTS FOR THE LME-4 NETZSCH MILL OPEN-CIRCUIT TESTS FOR THE ALABAMA SHALE (85% Media Filling, 2-mm Beads, 52% Solids, d_{90} = 171.0 and d_{50} = 62.7 μm)

Sample No.	Rotor Speed, rpm	Feed Rate, mL/min	Net Power, watts	Specific Energy, kWh/t	Product, μm d_{90}	Product, μm d_{50}	Pressure bar
1	1150	2000	2535	28.3	27.2	10.4	0.5
2	1150	1800	2395	29.7	23.3	9.2	0.5
3	1300	1999	3479	77.7	16.8	6.7	0.7
4	1300	1200	3469	64.5	18.7	7.2	0.7
5	1300	1400	3399	54.2	19.7	7.4	0.6
6	1300	1600	3344	46.7	20.0	7.6	0.6
7	1300	1800	3219	39.9	20.4	7.7	0.6
8	1300	2000	3069	34.3	21.8	8.4	0.6
9	1300	2100	2969	31.6	21.9	8.5	0.5

At low rotor speed (1150 rpm) two experiments were performed (Tests 1 and 2), which indicate that at this rpm, a feed rate lower than 1800 mL/min had to be maintained to achieve the targeted product size, and it was likely that energy requirement would be higher than 31 to 56 kWh/t (on the basis of observed trend in specific energy values of Tests 1 and 2).

Rougher Concentrate Regrinding Studies

Alabama shale rougher flotation concentrate from column flotation tests was used to collect energy-size reduction data for regrinding in the range of d_{90} = 10 μm. The primary objective was to determine the efficiency of 2-mm beads versus 1.1-mm beads. The rougher concentrate measuring density of 2.14 g/mL, and having a d_{90} = 26.9 and d_{50} = 10.2 μm was ground at 85% media loading and 53% solids. The data are listed in Tables 4-15 and 4-16. By comparing the efficiency of 2-mm beads versus 1.1-mm beads, on the basis of equal throughput, specific energy input (~50 kWh/t), 1.1-mm beads are more energy efficient because they produce finer products (compare Test 3 of Table 4-15 with Test 1 of Table 4-16). Similarly, by comparing the efficiency at almost equal product size, 1.1-mm beads are superior to 2-mm beads in terms of lesser specific energy input and higher throughput (compare Test 1 of Table 4-15 with Test 3 of Table 4-16).

Grindability Comparison

The Charles equation (Charles, 1957) is an empirical relation often used to correlate energy input with some characteristic size of the particle distribution obtained by coarse grinding. For ultra-fine grinding, the median size (d_{50}) is an appropriate representative size because of the significant amount of fines present. For conventional or coarse grinding, the coarse end

Table 4-15. EXPERIMENTAL CONDITIONS AND REGRINDING RESULTS FOR THE LME-4 NETZSCH MILL OPEN-CIRCUIT TESTS FOR THE ALABAMA SHALE ROUGHER CONCENTRATE (2-mm Beads, 85% Media Loading, 53% Solids Having Shale Density of 2.14 g/mL, d_{90} = 26.9 and d_{50} = 10.2 μm)

Test No.	Rotor Speed, rpm	Feed Rate, mL/min	Net Power, watts	Specific Energy, kWh/t	Product, μm	
					d_{90}	d_{50}
1	1160	475	1675	79.6	12.6	5.1
2	1160	600	1725	64.9	13.4	5.4
3	1160	800	1775	50.1	14.1	5.6
4	1160	1000	2025	46.7	14.0	5.7
5	1300	1000	3149	71.1	13.1	5.3
6	1500	1000	4746	107.1	11.8	4.9

Table 4-16. EXPERIMENTAL CONDITIONS AND REGRINDING RESULTS FOR THE LME-4 NETZSCH MILL OPEN-CIRCUIT TESTS FOR THE ALABAMA SHALE ROUGHER CONCENTRATE (1.1-mm Beads, 85% Media Loading, 53% Solids Having Shale Density of 2.14 g/mL, d_{90} = 26.9 and d_{50} = 10.2 μm)

Test No.	Rotor Speed, rpm	Feed Rate, cc/min	Net Power, watts	Specific Energy, kWh/t	Product, μm	
					d_{90}	d_{50}
1	1160	800	1755	49.5	12.7	5.5
2	1300	600	2879	108.3	11.4	4.8
3	1300	1000	2689	60.7	12.5	5.2
4	1500	1000	4366	98.6	11.5	4.8

(d_{80}) is appropriate. If the representative size is taken to be the median size (d_{50}), the modified Charles equation is of the form:

$$\bar{E} = A(d_{50,p}^{-\gamma} - d_{50,f}^{-\gamma}) \qquad (13)$$

where --

$\bar{E}$ = Energy input to the mill (kWh/t)

A, γ = Constants

$d_{50,p}$ = 50% passing size or median size of the product (μm)

$d_{50,f}$ = 50% passing size or median size of the feed (μm)

For comparing the energy utilization among different oil shales, because these shales had a different feed size and the product size was not much finer than feed size, the approximation made in Equation 13, where $d_{50,f}^{-\gamma} << d_{50,p}^{-\gamma}$

is no longer valid. Hence Equation 13 was used in its original form. A logarithmic transformation of this equation yields:

$$\log \bar{E} = \log A + \log (d_{50,p}^{-\gamma} - d_{50,f}^{-\gamma}) \qquad (14)$$

If this form of the modified Charles equation is appropriate for a material-grinding device combination, then a plot of log $\bar{E}$ against log $(d_{50,p}^{-\gamma} - d_{50,f}^{-\gamma})$ should result in a straight line of slope 1. A major disadvantage of this technique is that it requires the determination of γ on a trial and error basis until the slope of line obtained becomes unity. However, for comparison purposes, an approximate estimate of γ was obtained by plotting $\bar{E}$ versus d_{50} on a log-log scale as shown in Figure 4-15. The estimates of γ for Alabama and Indiana shales were found to be 2.243 and 2.886, respectively. Using these values of γ, the data of $\bar{E}$ verses $(d_{50,p}^{-\gamma} - d_{50,f}^{-\gamma})$ was plotted on log-log scale. This plot is shown in Figure 4-16, where X denotes $(d_{50,p}^{-\gamma} - d_{50,f}^{-\gamma})$. The slope of these lines fitted through data points turned out to be close to 1.0, as they should if the empirical Charles relationship holds true for this material-grinding device combination.

Another interesting feature of this plot is the relative grindability of the shales in the particle size ranges finer than 150 μm. The curve on the left side of the plot is characteristic of a material which is harder to grind and the curve on the right is for material that is easier to grind. Therefore, resistance to grinding of the shales based on the Charles approach in the fine grinding regime was higher for the Indiana shale than the Alabama shale. Also, the size reduction energy input correlation is much better for the Indiana shale than the Alabama shale as shown by the correlation coefficients. This indicates that the breakage pattern of Alabama shale is relatively more complex.

Self-Similar and Self-Preserving Size Distributions

The size distribution of the comminuted products obtained at different operating conditions was used to obtain the median size (d_{50}). Using these d_{50} values, the distributions of the ground products were plotted as a function of modified dimensionless size (d/d_{50}) in Figure 4-17 and 4-18 to obtain the "characteristic curves" for Indiana and Alabama shales. The size distribution points, obtained with different conditions of the experiments, fall onto the same curve indicating that the characteristic curve remains constant with changes in the levels of the variables. This is in confirmation with the earlier observation reported for other materials (Kapur, 1972).

The self preserving nature of the characteristic curve implies that the size distribution of the comminuted product can be predicted if the following are known:

1. The shape of the characteristic curve

2. The d_{50} value of the ground shale for any set of conditions of the experiment.

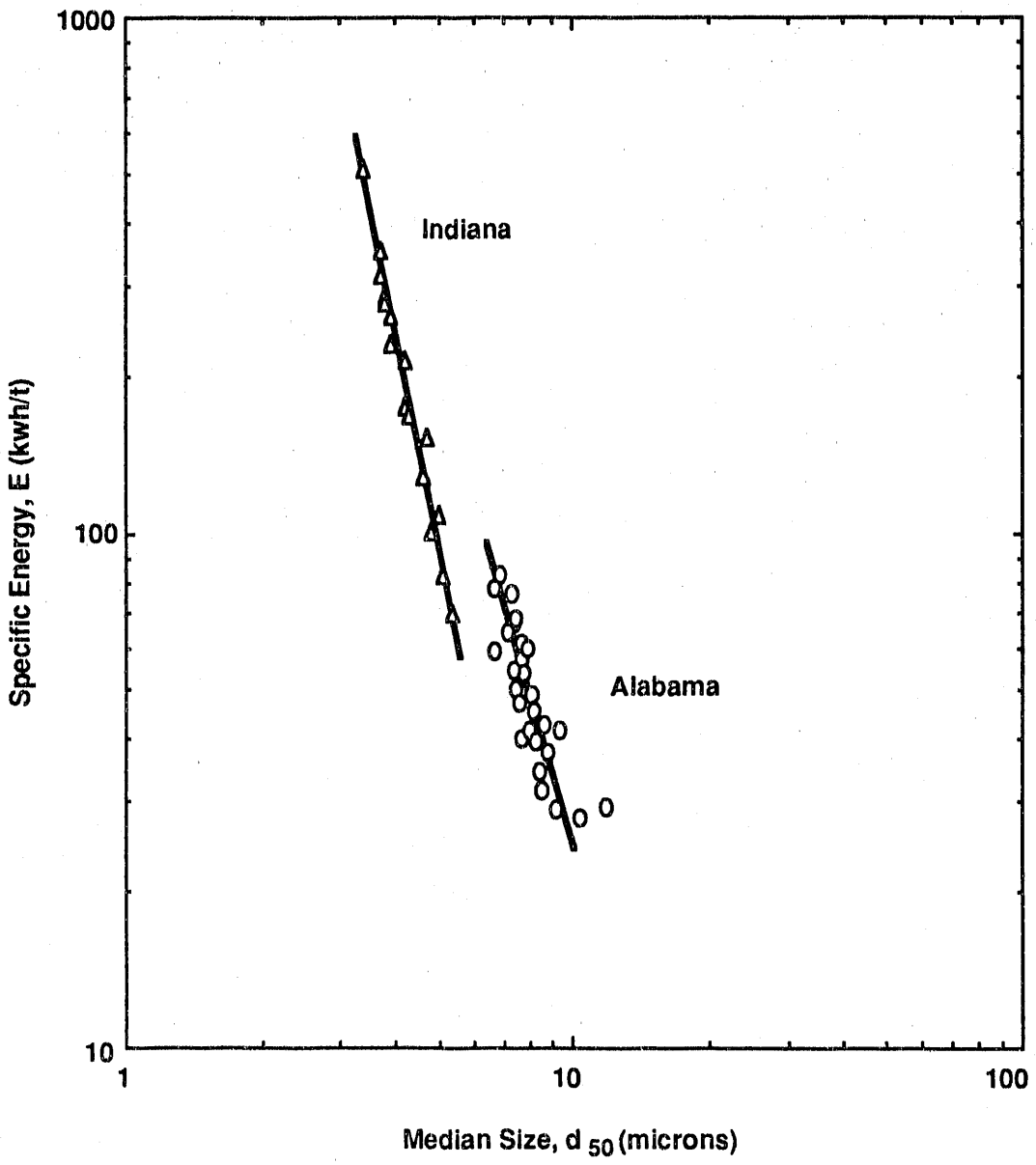

Figure 4-15. DIFFERENCE IN ENERGY-SIZE REDUCTION BEHAVIOR OF ALABAMA AND INDIANA SHALES IN STIRRED BALL MILLING

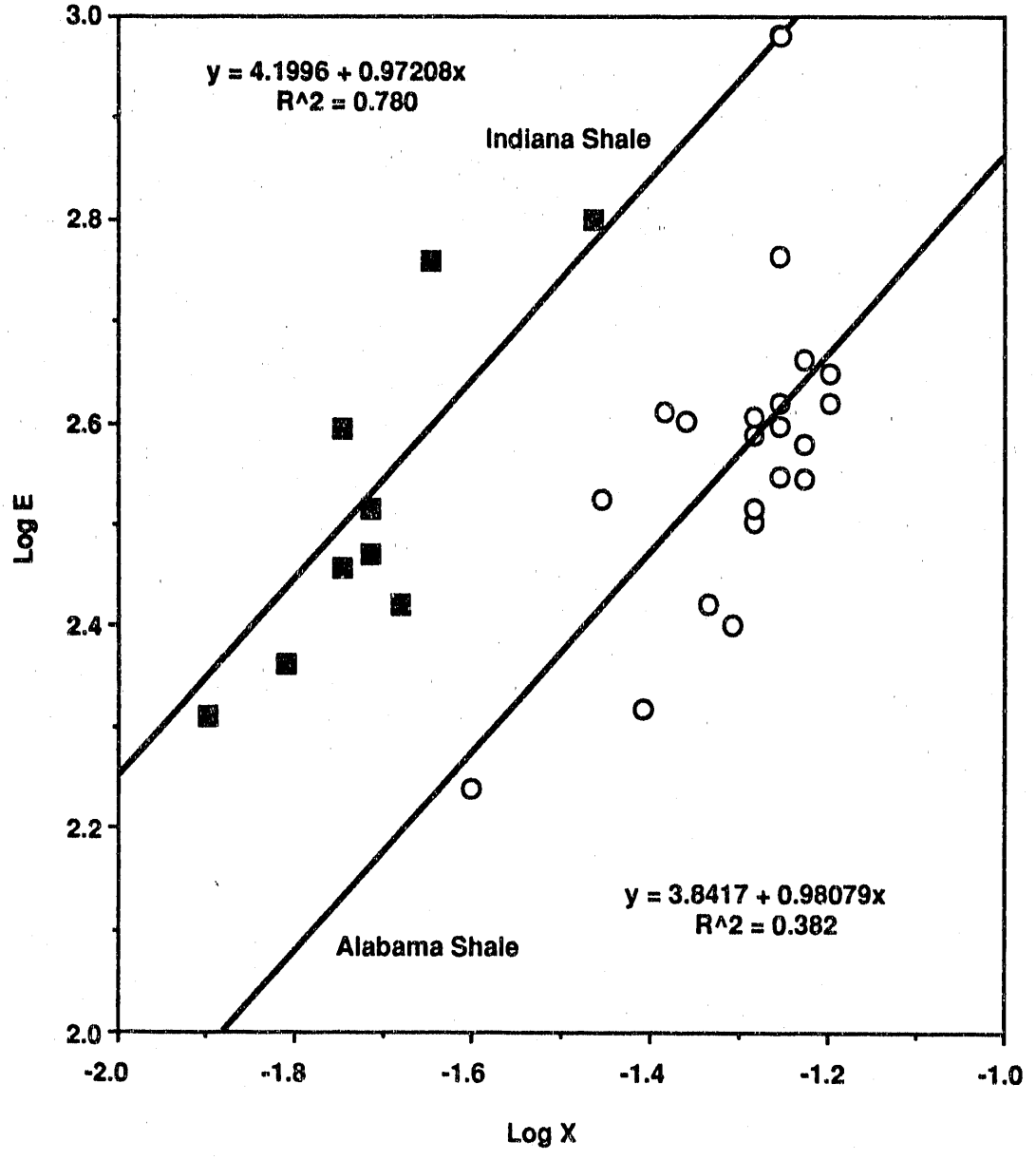

Figure 4-16. ENERGY-SIZE REDUCTION RELATIONSHIP (Charles Plot) IN THE ULTRA-FINE SIZE RANGE UNDER VARIOUS CONDITIONS

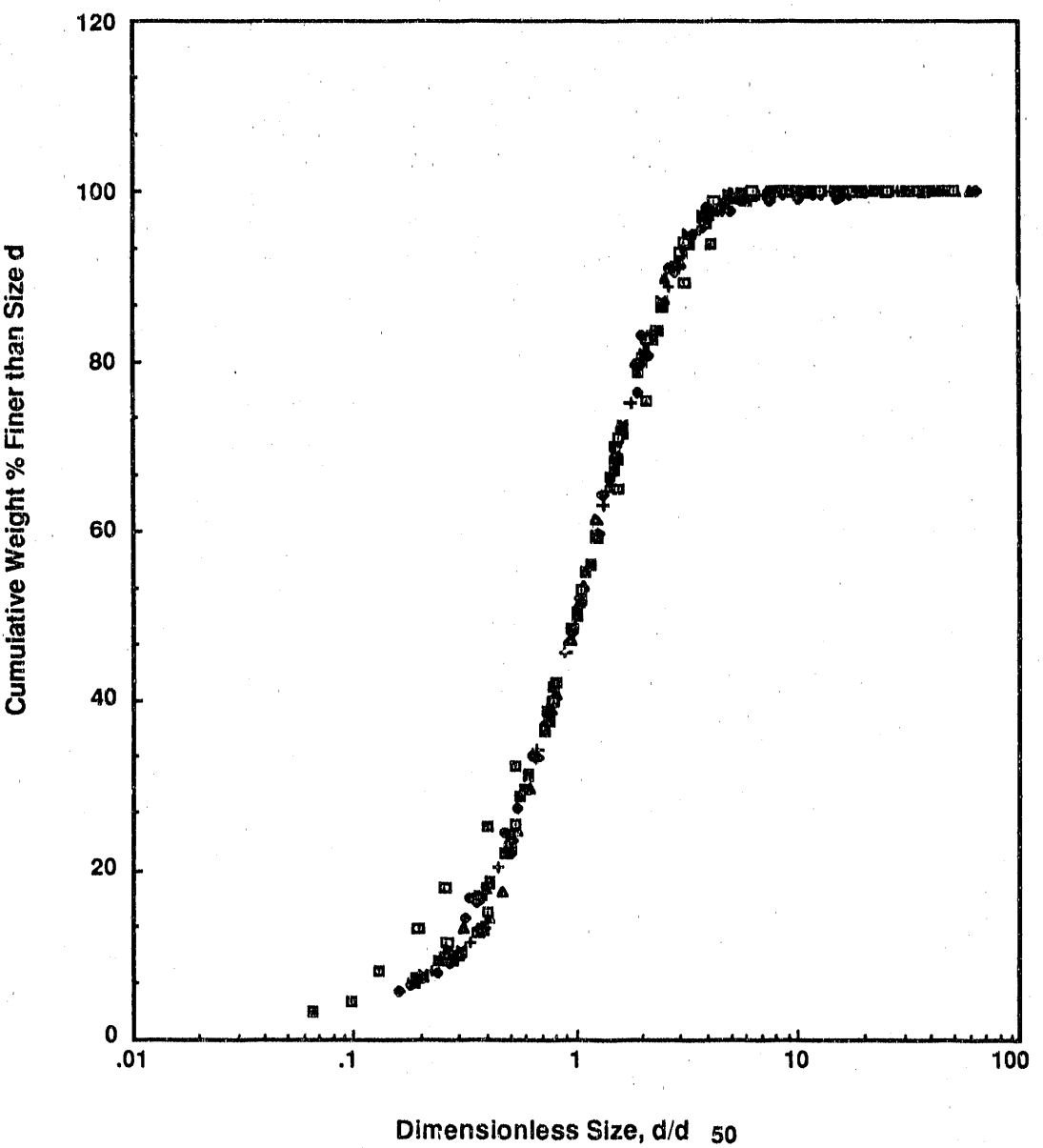

Figure 4-17. SELF-PRESERVING SIMILARITY SIZE SPECTRA OF THE INDIANA SHALE PARTICLES GROUND IN A LME-4 NETZSCH STIRRED MILL

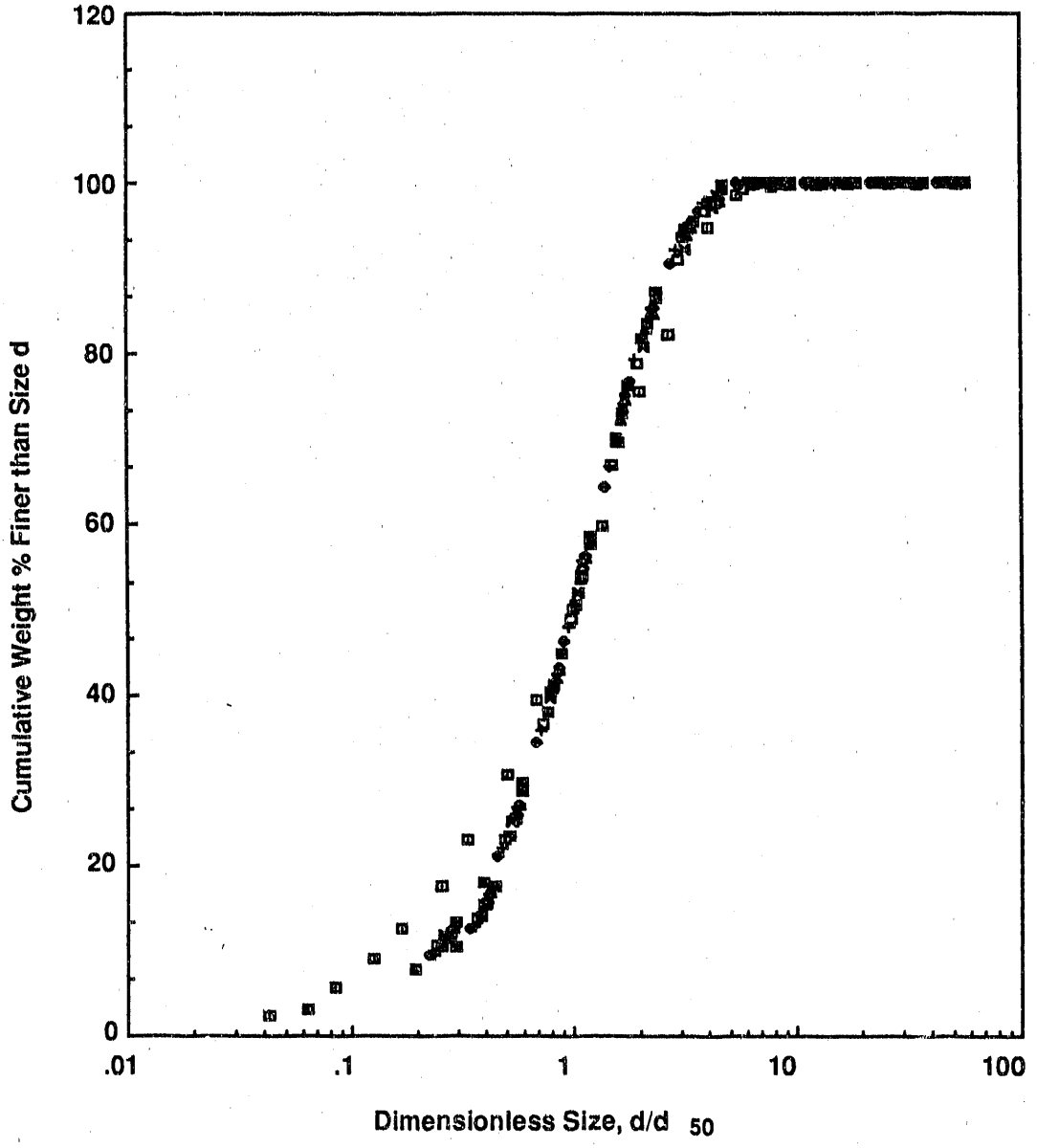

Figure 4-18. SELF-PRESERVING SIMILARITY SIZE SPECTRA OF THE ALABAMA SHALE PARTICLES GROUND IN A LME-4 NETZSCH STIRRED MILL

Quantification of the Characteristic Curve

The characteristic curve was quantified using the equations proposed for the reduced efficiency curves encountered in hydrocyclone classification. There have been many mathematical forms of equations used in quantifying the characteristic curve but two are quite extensively used (Lynch and Rao, 1975; Plitt, 1976).

The Lynch and Rao equation is given as --

$$F_3(d) = \frac{e^{\gamma x} - 1}{e^{\gamma x} + e^{\gamma} - 2} \qquad (15)$$

and the Plitt equation is given by --

$$F_3(d) = 1 - \exp[-0.613\ (d/d_{50})^m] \qquad (16)$$

When these equations are used for representing the characteristic curve, $F_3(d)$ represents the cumulative weight fraction of ground material passing size d, γ, and m are constants, and x represents dimensionless size (d/d_{90}). Of these two equations, Equation 15 requires an iterative procedure for the evaluation of the constant γ, whereas in Equation 16, the constant "m" can be evaluated directly after taking logarithms using the method of least squares. Hence, the Plitt equation was used in the present analysis for representing the characteristic curve.

The equation for the characteristic curve plotted in Figure 4-17 after the evaluation of the constant "m" was found as:

$$F_3(d) = 1 - \exp\ [-0.693\ (d/d_{50})^{1.0883}] \qquad (17)$$

Predicting the Particle Size Distribution of Comminuted Product

The self-similar particle size curve as described by Equation 17 and shown in Figure 4-17 in conjunction with the energy-size reduction relation as shown in Figure 4-16 are useful for predicting the entire size distribution of the ground product for a given expenditure of energy as follows:

1. Corresponding to the level of the specific energy input to the mill, obtain the median size of the comminuted product using the plot such as that in Figure 4-16

2. Substitute the value of d_{50} obtained in Equation 17 to yield entire particle size distribution.

In order to validate such approach, one grinding test was carried out with Indiana shale. The -100 mesh slurry feed, at 31% solids, was ground at 1400 rpm using a feed rate of 225 mL/min. The media loading was kept at 87%. The level of specific energy input was determined as 128 kWh/t.

Using the correlation mentioned in Figure 4-16, d_{50} was calculated as 4.183 μm as opposed to experimentally determined value of 4.2 μm. The

predicted size distribution based on this value of (d_{50} = 4.183) is plotted in Figure 4-19, along with the experimental data. The experimental and predicted d_{50} agreed well and an excellent agreement with regard to the upper part of the size distribution was present, however, there was a discrepancy in the finer portion of the size distribution. This may be due to the complex transport behavior of particulate phase in 1 to 3 μm range.

In the absence of a phenomenological model in the ultra-fine grinding regime, this approach for predicting the particle size distribution is of potential use for scale up and circuit simulation purposes.

Media Wear Studies

One of the principal factors contributing to the high cost of stirred ball milling is the consumption of grinding media. In the course of high energy density stirred ball milling, media wear is quite significant. Therefore, during fine grinding tests, the ground shale product was analyzed for media contamination. Figure 4-20 shows that the chromium content of Indiana shale ground product was as much as 3 to 4 times that of feed shale (0.029%). This plot also shows that the degree of contamination is directly related with grinding severity, that is, high media filling tends to give higher contamination. This chromium pick-up in the shale was due to wear of grinding beads. The data also show that the chromium content of the ground product was directly related to the specific energy consumption. Higher specific energy input to the mill resulted in increasingly severe wear of the beads which ultimately found its way into the product. The rate of media consumption in grinding was calculated from the increase in the chromium content of the shale. For example, if the chromium content of the ground product is 0.05% then the increase of 0.021% can be attributed to grinding. This in turn amounts to 0.21 kg of chromium per ton of shale ground. If the grinding media contains 20% chromium, then 1.05 kg of media have been consumed in grinding one metric ton of shale on the basis of chromium wear.

In another series of grinding tests (Table 4-8), the product was analyzed for Cr, Ni, Cu and Mn. The results (Table 4-17) again show an increased element uptake by shale with increased specific energy to the mill. Based on these test results, a media consumption of 1.46 kg/t of shale is expected. Tables 4-18 and 4-19 list another series of shale contamination and media consumption data corresponding to grinding tests mentioned in Table 4-9. Again, similar trends as observed previously are seen.

Based upon the data collected, it can be concluded that about 0.9 kg of media will be consumed in grinding one metric ton of Indiana shale.

Subtask 4.1.4. Grinding Circuit Optimization

Objective

The objectives of this task were to collect energy-size reduction data on Eastern shales by performing Bond locked cycle grindability tests, conduct conventional ball mill tests to verify the population balance model framework for scale-up design, conduct experiments on auxiliary unit operations, such as screening, and integrate grinding, sizing, and concentration devices to minimize total energy.

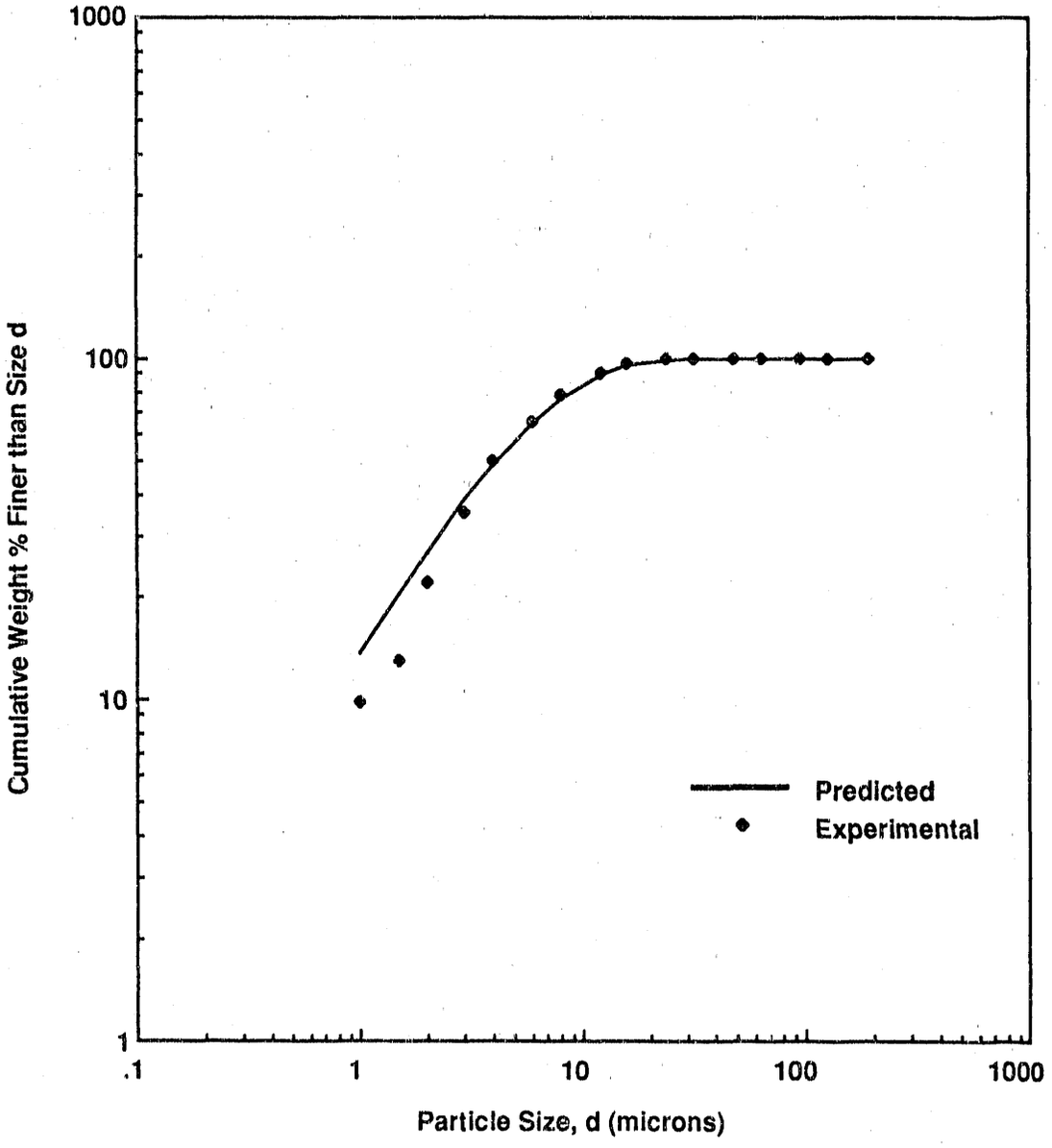

Figure 4-19. COMPARISON OF EXPERIMENTAL AND PREDICTED SIZE DISTRIBUTION USING SELF-SIMILARITY APPROACH FOR INDIANA SHALE

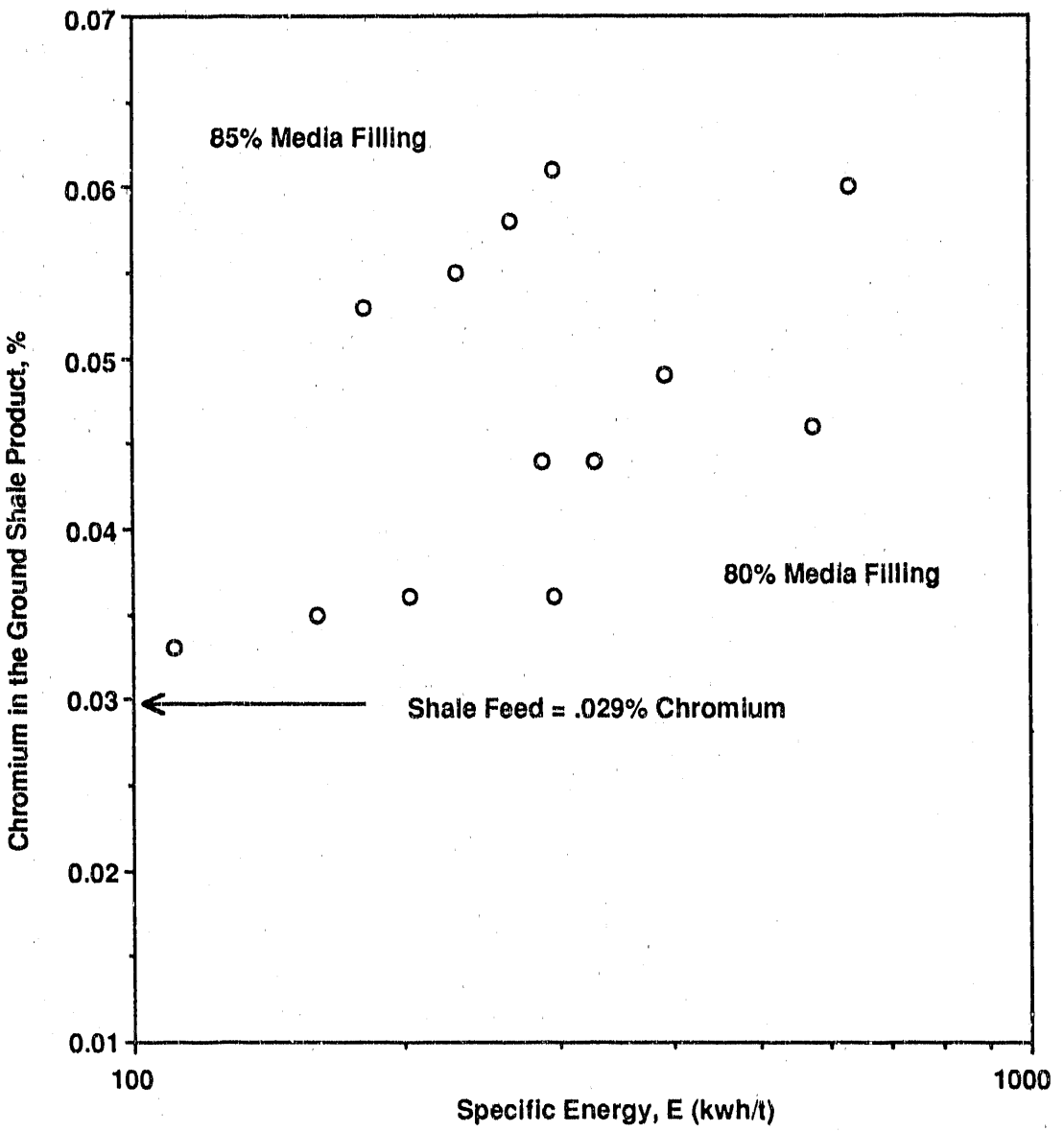

Figure 4-20. CHROMIUM ANALYSIS OF THE GROUND SHALE AS A FUNCTION OF SPECIFIC ENERGY FOR INDIANA SHALE FOR TWO MEDIA FILLINGS

Table 4-17. INDIANA SHALE CONTAMINATION AND MEDIA CONSUMPTION DATA FOR TESTS LISTED IN TABLE 4-8

Element Analyzed	Feed Shale, wt %	Product, wt % Tests					Characteristic Product, wt % Avg. of Test 4-5	kg of Element Uptake per Ton of Shale	Media Consumption, kg/ton
		1	2	3	4	5			
Chromium	0.0112	0.0257	0.0287	0.0352	0.0391	0.0420	0.0405	0.2929	1.46
Nickel	0.0150	0.0175	0.0200	0.0212	0.0199	0.0199	0.0199	0.0489	
Manganese	0.0207	0.0262	0.0262	0.0285	0.0286	0.0270	0.0278	0.0709	
Copper	0.0090	0.0100	0.0100	0.0105	0.0112	0.0110	0.0111	0.0209	

Table 4-18. INDIANA SHALE CONTAMINATION AND MEDIA CONSUMPTION DATA FOR TESTS 1-5 LISTED IN TABLE 4-9

Element Analyzed	Feed Shale, wt %	Product, wt % Tests					Characteristic Product, wt % Avg. of Test 4-5	kg of Element Uptake per Ton of Shale	Media Consumption, kg/ton
		1	2	3	4	5			
Chromium	0.009	0.020	0.022	0.024	0.027	0.032	0.032	0.2299	1.149
Nickel	0.013	0.017	0.017	0.018	0.017	0.018	0.018	0.0499	
Manganese	0.014	0.014	0.014	0.017	0.016	0.018	0.018	0.0399	
Copper	0.007	0.008	0.007	0.008	0.007	0.008	0.008	0.0099	

Table 4-19. INDIANA SHALE CONTAMINATION AND MEDIA CONSUMPTION DATA FOR TESTS 7-10 LISTED IN TABLE 4-9

Element Analyzed	Feed Shale, wt %	Product, wt % Tests 7	8	9	10	Characteristic Product, wt % Highest of Test 4-5	kg of Element Uptake per Ton of Shale	Media Consumption, kg/ton
Chromium	0.009	0.017	0.018	0.020	0.022	0.022	0.129	0.649
Nickel	0.012	0.015	0.015	0.015	0.015	0.015	0.030	
Manganese	0.014	0.015	0.015	0.016	0.015	0.016	0.020	
Copper	0.007	0.008	0.012	0.007	0.012	0.050		

Bond Grindability Tests

The concept of an energy-size correlation has led to a number of relationships that can be used in mill design. The best known of the energy-size relationships is that developed by Bond (1962), which can be expressed as:

$$\bar{E} = 10\ W_i\left(\frac{1}{X_p^{0.5}} - \frac{1}{X_f^{0.5}}\right) \qquad (18)$$

Where $\bar{E}$ is specific energy (kWh/t), X_p and X_f are the 80% passing sizes (μm) in the product and feed, respectively, and W_i is an empirical factor called the Work Index. Standard Bond locked cycle grinding tests were conducted to estimate work indices of Eastern oil shales.

Equipment

A Hazen-Quinn Package Grinding Unit was used to estimate the Bond work indices of Eastern shales. The grinding mill is 12 inches (30.5 cm) in inside diameter by 12 inches (30.5 cm) inside length with radiused corners to meet Bond specifications and for ease of cleanout. A large, easily detachable cover plate for discharge is provided. Also, a direct drive from 1/3 hp and 60 rpm gear motor provides required Bond grinding speed. The ball charge consisted of 285 balls weighing about 20.4 kg and distributed as follows:

Ball Diameter -- inch ---	No. of Balls
1-1/2	43
1-1/4	67
1	10
3/4	165

Procedure

The feed for these tests was crushed to -8 mesh. About 8 to 10 kg of each oil shale sample was prepared. These samples were split into 500- to 700-gram batches to facilitate addition and minimize particle segregation of the make-up fresh sample. The oil shale sample was packed to 700 cc volume using a vibrating table. The weight of this volume of sample was the initial ore charge to the mill and this weight was maintained throughout the test. For the first cycle, the mill was run for a certain number of mill revolutions (~75) to produce about 400 to 500 grams of finished product, that is, passing the test sieve (P_1 = 100 mesh). The oversize fraction was returned to the mill for the second cycle. This was built up to the original weight of ore charge by replacing the finished product removed with exactly the same weight of fresh sample. The unit weight of product produced per mill revolution was calculated. This number, the ore grindability for the cycle, was used to estimate the number of revolutions required for the next grinding cycle in order to produce a circulating load of 250%.

The locked cycle test was continued until steady state was reached. This condition was indicated by slight changes in grindability of the ore with

grinding cycles, or small fluctuations about a certain value. At this point, the weight of the finished product was close to that required for 250% circulating load. This condition required 6 to 8 grinding cycles.

After having reached equilibrium, the grindabilities for the last three cycles were averaged. Similarly, the finished product produced during the last three grinding cycles was combined, mixed, and sampled for screen analysis. The average value was taken as the standard Bond ore grindability to calculate the work index (W_i) in kWh/t computed using the following empirical equation (Yap, Sepulveda and Jauregui, 1981).

$$W_i = \frac{44.5}{(P_1^{0.23})(G_{bp}^{0.82})} \left[\frac{10}{(P^{0.5})} - \frac{10}{(F^{0.5})}\right]^{-1} \qquad (19)$$

where --

P_1 = the sieve opening at which the test was made in microns [for these tests this was 150 µm (100 mesh)]

G_{bp} = Bond's standard ball mill grindability, net grams of ball mill product passing sieve size P_1 produced per revolution

P = Product, 80% passing size (µm)

F = Feed, 80% passing size (µm)

According to Bond's Third Theory, the work input is proportional to the new crack tip length produced in particle breakage and equals the work represented by the product minus that represented by the feed. For particles of similar shape, the crack tip length is equivalent to the square root of one-half the surface area and the new crack length is proportional to $[1/(P^{0.5}) - 1/(F^{0.5})]$; where P and F are particles diameter of product and feed, respectively.

Therefore, the work input is given by,

$$W = W_i \left[\frac{10}{(P^{0.5})} - \frac{10}{(F^{0.5})}\right] \qquad (20)$$

where --

W = the energy input to the mill (kWh/t)

W_i = work index as determined by Equation 18

P and F = defined previously in Equation 18

Dry and Wet Ball Milling Tests

A more complete analysis of grinding systems can be obtained by considering the process to be analogous to a chemical reaction in which large particles react in the mill to produce a set of smaller particles. For such

systems, it is convenient to describe the process in terms of the kinetic models of grinding which involve two fundamental parameters of the breakage process, S_j (selection function) and b_{ij} (breakage function). This analysis is carried out by collecting energy-size reduction data in a laboratory tumbling mill. Also, this analysis has the capability of describing the breakage pattern of shales.

Conventional Tumbling Ball Mill

The dry grinding tests performed initially were carried out in a 10-inch (25.4 cm) diameter by 11.5-inch (29.2 cm) length stainless batch mill at the Comminution Center, University of Utah. This mill has been used extensively for grinding studies in the past and is described in detail elsewhere (Mehta, 1987). These tests were performed externally, because MRI was in the process of setting up its own grinding mill. The tests performed at the later time for comparison purposes were carried out using the MRI ball mill set up as shown in Figure 4-21. This mill is a stainless steel batch ball mill 8.25 inches in diameter and 9 inches long with 8 square lifters (0.25 inch in height) and equipped with a variable-speed drive and DAS-16F data acquisition system for current measurement drawn during the grinding for the purpose of measuring power draw.

Conventional Dry Ball Milling Tests Using 10 Inch Mill

The University of Utah mill is equipped with a Graham variable speed transmission coupled to a BLH torque sensor and a recorder to measure power draw directly from the drive shaft between the transmission and the mill. The specific energy input to the mill was computed from the measured net torque. The equation used is given below.

$$P = 1.18 \times 10^{-5}\ T \cdot N\ (kW) \qquad (21)$$

Where T is the net torque recorded by the sensor in in-lb and N is the number of revolutions per minute of the mill. The specific energy input ($\bar{E}$), in kWh/t to the mill is computed from the relationship:

$$\bar{E} = \frac{Pt}{H} \qquad (22)$$

Where t is the grinding time in hours and H is the mass hold-up in the mill in tons.

A stainless steel ball load of 30.5 kg was used, which corresponds to a 50% filling of the mill. The ball size distribution approximated that of an "equilibrium charge distribution" often used in laboratory tests for mill scale-up design. The distribution is listed in Table 4-20.

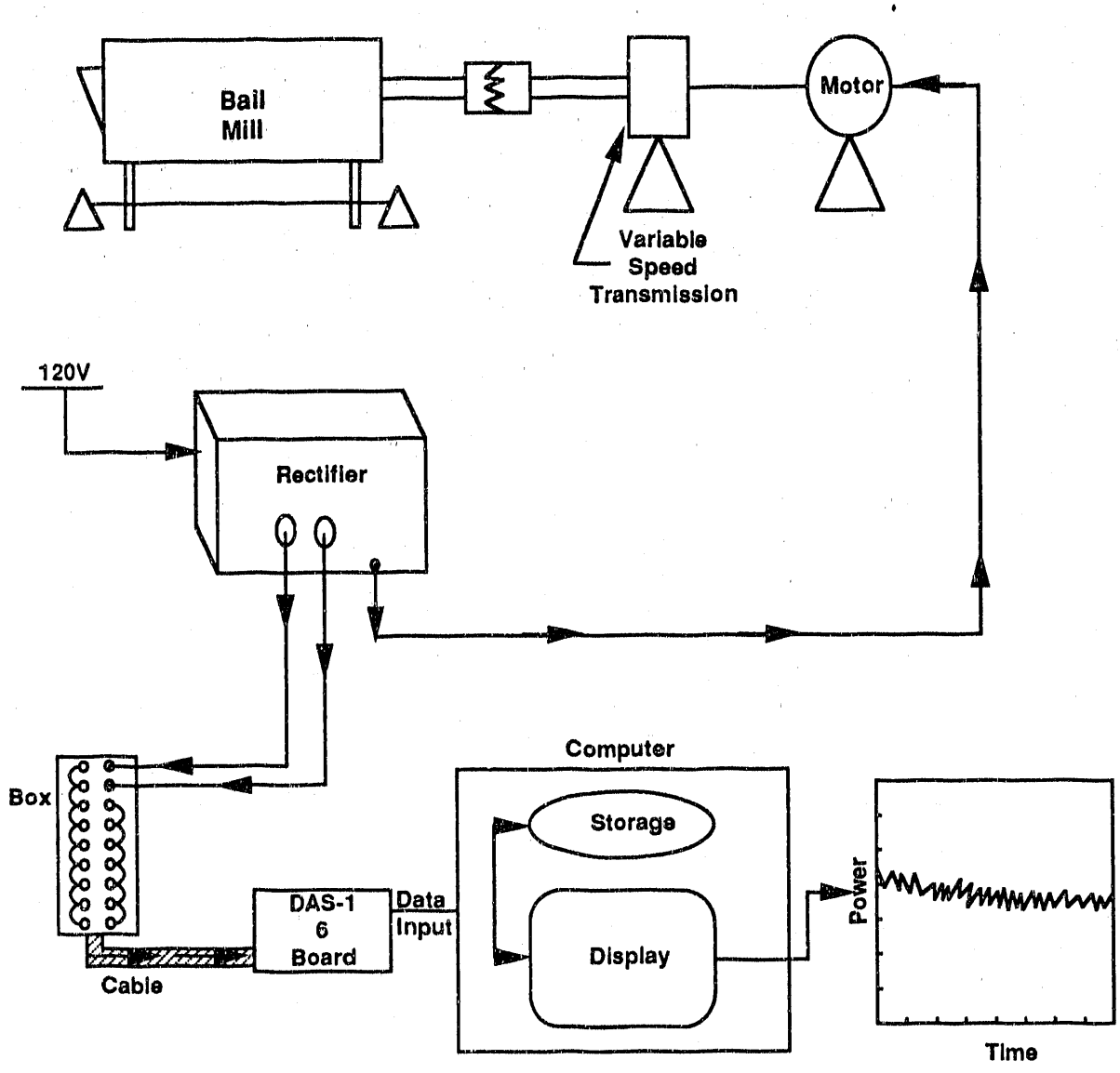

Figure 4-21. SCHEMATIC DIAGRAM OF THE 8.25-INCH X 9.0-INCH MRI MILL WITH VARIABLE SPEED TRANSMISSION AND REAL TIME DATA ACQUISITION SYSTEM USED FOR MONITORING THE POWER DRAFT

Table 4-20. BALL SIZE DISTRIBUTION USED FOR 10 INCH BALL MILL

Ball Diameter, inches	cm	Weight, %	Mass, kg
1-1/2	3.81	52.8	16.1
1	2.54	30.2	9.2
3/4	1.91	11.6	3.5
1/2	1.27	5.4	1.7

In all tests, the mill was loaded with about 3000 grams of -8 mesh shale, which corresponded to 100% filling of the interstices of the ball charge in the mill. The speed of the mill for all tests was kept at 70% of the critical speed (64 rpm). A dead torque value of 28 in-lb was taken into consideration to calculate net average torque. Batch test conditions are summarized in Table 4-21.

Table 4-21. BATCH GRINDING TEST CONDITIONS FOR 10-INCH BALL MILL

Shale Type	Feed Size, mesh	Mass Hold-Up, grams	Average Net Torque, in-lb	m-N	Grinding Time, minutes
Alabama	8 X 0	2990	96	10.8	2, 4, 8, 16
Kentucky	8 X 0	2997	100	11.3	2, 4, 8, 16
Ohio	8 X 0	2996	98	11.1	4, 8*
Tennessee	8 X 0	2989	100	11.3	2, 4, 8, 16
Michigan	8 X 0	3024	98	11.1	2, 4, 8, 16
Indiana	10 X 0	3000	96	10.8	2, 4, 8, 16

* Due to unavailability of sample, only two grinding tests were carried out.

After each grinding time, the ground product was wet screened through a 325 mesh sieve to remove very fine material, which may be occluded to the coarser particles. The -325 mesh material was filtered and its weight determined after drying. The +325 mesh product was dried, split to obtain a representative sample of about 150 to 200 grams, and screened using a Ro-tap testing sieve shaker for 20 minutes. The weight of the material retained on each sieve was determined using a Mettler balance. The size distribution of ground product was obtained by combining wet and dry screen data.

Conventional Dry and Wet Ball Milling Using MRI Ball Mill

Dry and wet grinding experiments were carried out using -10 mesh Alabama and Indiana shales. Wet grinding tests were conducted at 40% solids. The calculations of ball charge, material filling and mill speed were done using standard methods and are listed in Table 4-22. The tests were carried out for 2- and 4-minute periods.

Table 4-22. BATCH GRINDING TEST CONDITIONS FOR 8.25-INCH MILL

Mill Size = 8.25 Inch X 9 Inch (20.96 cm X 22.86 cm)
Ball Filling = 50%
Ball Load = 18.5 kg
Material Filling = 100%
Oil Shale Charge = 2.5 kg
Ball Size Distribution = 9.8 kg (1.5 Inch) (3.81 cm)
5.6 kg (1.0 Inch) (2.54 cm)
2.2 kg (.75 Inch) (1.91 cm)
0.9 kg (.50 Inch) (1.27 cm)
Mill Speed = 75% N_c = 77 rpm
Current Drawn With No Load = 1.2 amp
Current Drawn With Load = 1.85 amp

Results and Discussion

Bond Work Indexes

Estimates of specific energy values were calculated using Equation 20. The results of these calculations are listed in Table 4-23 along with Bond Work Indexes.

Table 4-23. BOND WORK INDEXES (W_i) AND COMPUTED SPECIFIC ENERGY ESTIMATES (W) FOR EASTERN OIL SHALES

Oil Shale Type	Bond Work Index* W_i, kWh/t	Specific Energy Input** W, kWh/t
Alabama	23.2	16.5
Kentucky	19.6	13.9
Ohio	15.6	11.1
Michigan	13.3	9.5
Tennessee	12.7	9.0

* Based on a theoretically infinite feed size to a product of 80% passing 100 µm.

** Based on a feed size of 80% passing 1200 µm to a product of 80% passing 100 µm.

The Bond Work Index is the comminution parameter that expresses the resistance of the material to crushing and grinding. Numerically, the work index is the energy required to reduce the material from theoretically infinite feed size to 80% passing 100 µm. Based on the experiments conducted in this study, it is concluded that the Alabama shale offers the most resistance to grind followed by Kentucky, Ohio, Michigan, and Tennessee. The Indiana shale was not used in this study because at the time of experimentation, a representative sample was unavailable.

Energy-Size Reduction Relationship in the Context of Empirical Approach

The Charles equation (as mentioned in Subtask 4.1.3) is an empirical relation often used to correlate energy input with some characteristic size of the distribution for coarse grinding. If the representative size is taken to be the 80% passing size then the modified Charles equation is of the form:

$$\bar{E} = A(d_{80,p}^{-\gamma} - d_{80,f}^{-\gamma}) \qquad (23)$$

Because these shales have different feed sizes and product size is not much finer than feed size, therefore, for the purpose of comparing the energy utilization among different oil shale, the approximation made to Equation 23, where $d_{80,f}^{-\gamma} \ll d_{80,p}^{-\gamma}$ is not valid. A logarithmic transformation of equation yields:

$$\log \bar{E} = \log A + \log (d_{80,p}^{-\gamma} - d_{80,f}^{-\gamma}) \qquad (24)$$

If this modified form of the Charles equation is appropriate for a material device combination then a plot of log $\bar{E}$ against log $(d_{80,p}^{-\gamma} - d_{80,f}^{-\gamma})$ should result in a straight line of slope one. A major disadvantage of this technique is that it requires the determination of γ on a trial and error basis until the slope of line obtained becomes unity. However, for the comparison purposes, an approximate estimate of γ was obtained by plotting $\bar{E}$ versus $d_{80,p}$ on a log-log scale. Using values of γ thus obtained, the data of $\bar{E}(d_{80,p}^{-\gamma} - d_{80,f}^{-\gamma})$ on log-log scale was plotted. This plot is shown in Figure 4-22. Interestingly, the slope of lines for all shales was equal to 0.71 to 0.73 except for Michigan (0.53). This may be due to the nature of Michigan shale sample (outcrop). Another interesting feature of this plot is the relative grindability of these shales. The curve on the far left side of the plot is characteristic of a material which is harder to grind and the resistance to grinding decreases from left to right. Therefore, the relative grindability of these shales based on Charles approach was:

Alabama > Indiana > Kentucky > Tennessee > Ohio > Michigan

Interestingly, this approach gave results that seem to correlate the hardness of these shales with their geological origins. As one moves from south to north, the shale grinds easier.

Energy-Size Reduction Relationship in the Context of Population Balance Approach

A very well known approach in the modeling area of comminution, known as population balance approach (Herbst, Grandy and Fuerstenau, 1973; Herbst and Fuerstenau, 1973) was used to describe the breakage characteristics of these shales. The advantages in using this approach are:

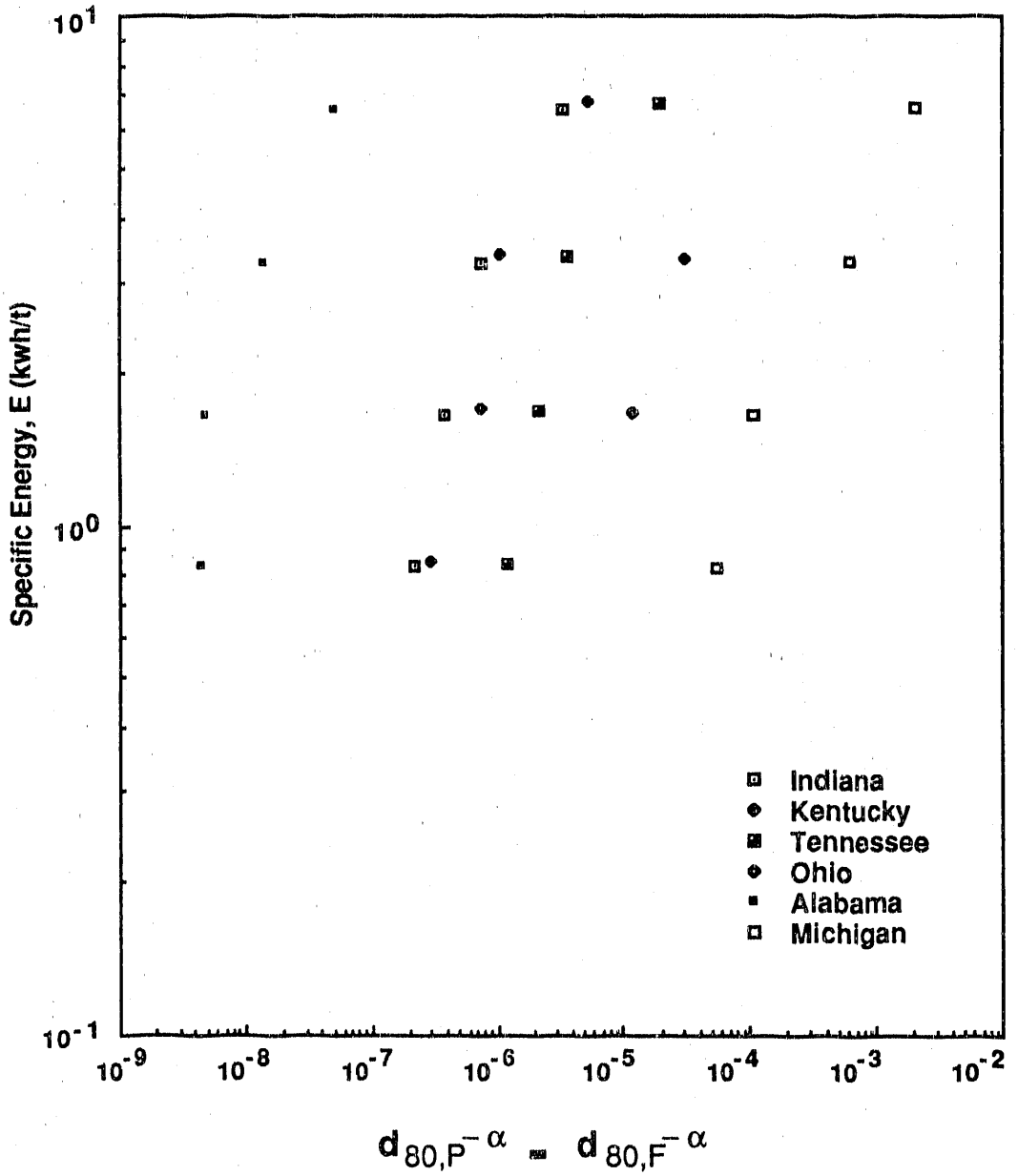

Figure 4-22. ENERGY-SIZE REDUCTION RELATIONSHIP (Charles Plot) FOR THE CONVENTIONAL DRY BALL MILLING OF EASTERN SHALES IN A 10-INCH MILL

1. This approach is based on first principles.

2. Instead of taking into account one characteristic particle size (d_{80} or d_{50}), complete particle size distribution is taken into consideration for breakage analysis, which is realistic.

3. Breakage behavior of different shales in terms of breakage distribution and breakage rate of different size particles can be estimated.

A detailed discussion of the population balance framework is given in Appendix A. A computer program MRIEST, based upon the principles mentioned above was used to estimate kinetic parameters from the batch grinding data. Figure 4-23 shows the estimated specific selection function S_i^E $(kWh/t)^{-1}$ versus particle size provided by MRIEST-fit and Figure 4-24 show the estimated cumulative breakage distribution function B_{ij} versus particle size.

Figure 4-23 shows that the specific selection function values for any shale are strongly dependent upon particle size. In other words, the shale particles of one type which are hardest to grind in coarse particle regime may change their comminution behavior in the fine particle regime. This is particularly true for the Indiana and Ohio shales. The distinct comminution features of these shales are more clearly exhibited in the fine particle range. Figure 4-24 shows that the breakage behavior of the Alabama shale is quite different from the other shales. The Alabama shale is the hardest to grind in terms of initial threshold energy value, but once the particles break, they yield the finest size distribution. The breakage distribution function values of the Kentucky and Ohio shales are comparable and similar values were observed for the Tennessee and Indiana shales. Table 4-24 lists the values of breakage parameters obtained from these estimation runs.

Comparison of Dry and Wet Grinding in the Context of PBM*

Dry and wet grinding tests on -10 mesh Alabama and Indiana shales were carried out using MRI ball mill. Dry grinding tests were conducted on each shale for 2 and 4 minutes. Wet grinding tests at 40% solids were conducted for one time period (4 minutes). The current drawn during dry and wet grinding remained the same. The data collected in these runs was treated by MRIEST. Figure 4-25 shows a plot of estimated specific selection functions, S_i^E versus geometric particle size for dry grinding of Alabama and Indiana shales. As can be seen from this plot, comminution behavior of these shales is highly dependent on particle size for example, in the coarse particle size range (1500 to 352 μm). Alabama shale particles are relatively harder to grind, whereas, as we go in the fine-size range (< 352 μm), Indiana shale particles are harder to grind. This type of information is very important and must be taken into consideration when comparing the comminution behavior of these shales. Figure 4-26 shows a plot of the cumulative breakage function (B_{ij}) versus particle size for dry grinding of these shales. The breakage distribution of Alabama shale is finer than Indiana shale. In comparing these shales in wet mode, Figure 4-27 shows a plot of S_i^E versus particle size. The Alabama is a little harder than Indiana for all particle sizes, however, the difference in S_i^E values is not much. Figure 4-28 shows a comparison of B_{ij}

* Population Balance Method.

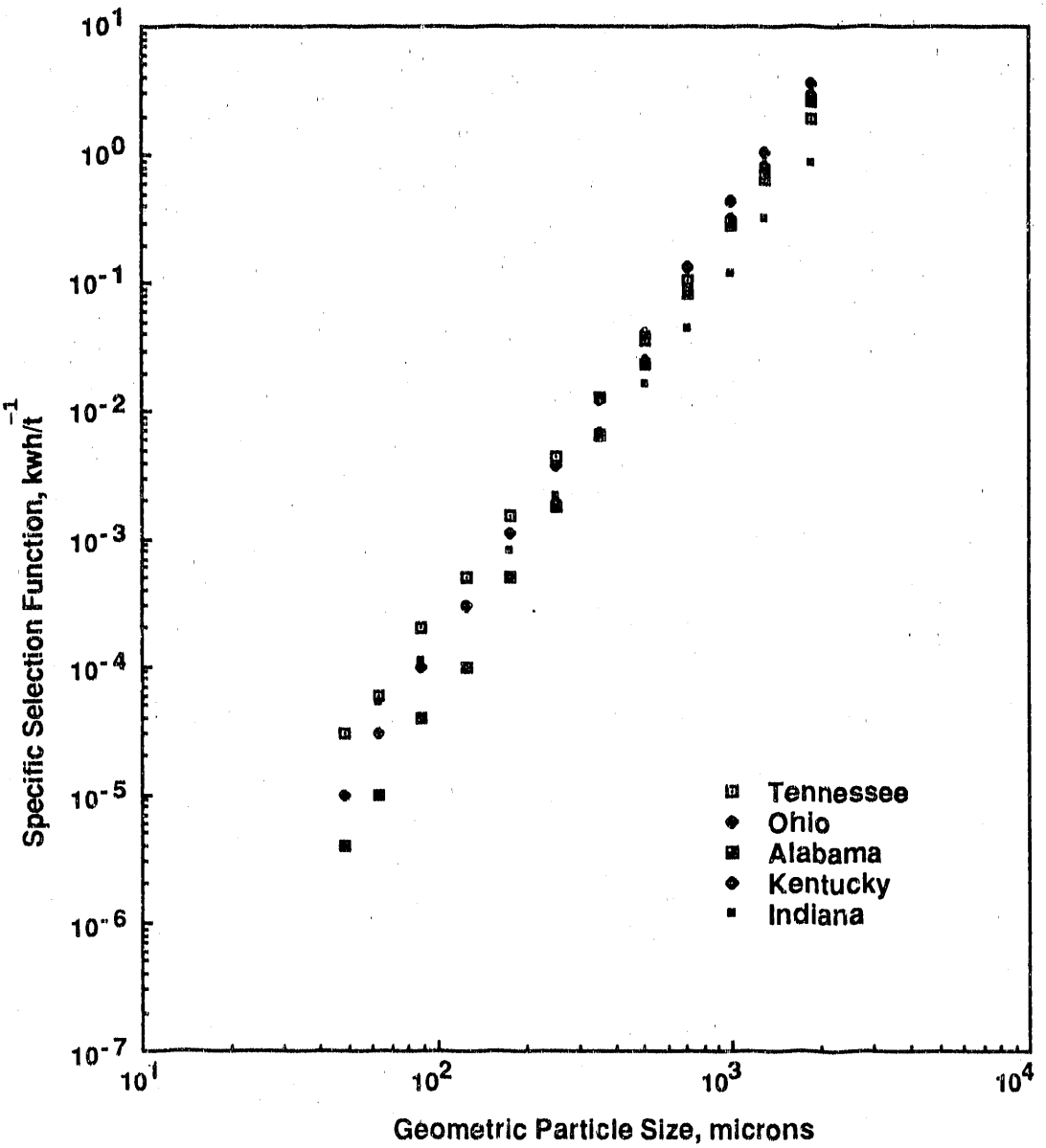

Figure 4-23. SPECIFIC SELECTION FUNCTIONS VERSUS GEOMETRIC PARTICLE SIZE PROVIDED BY MRIEST FIT FOR DRY GRINDING OF EASTERN SHALES WITH RAW FEED IN 10-INCH BALL MILL

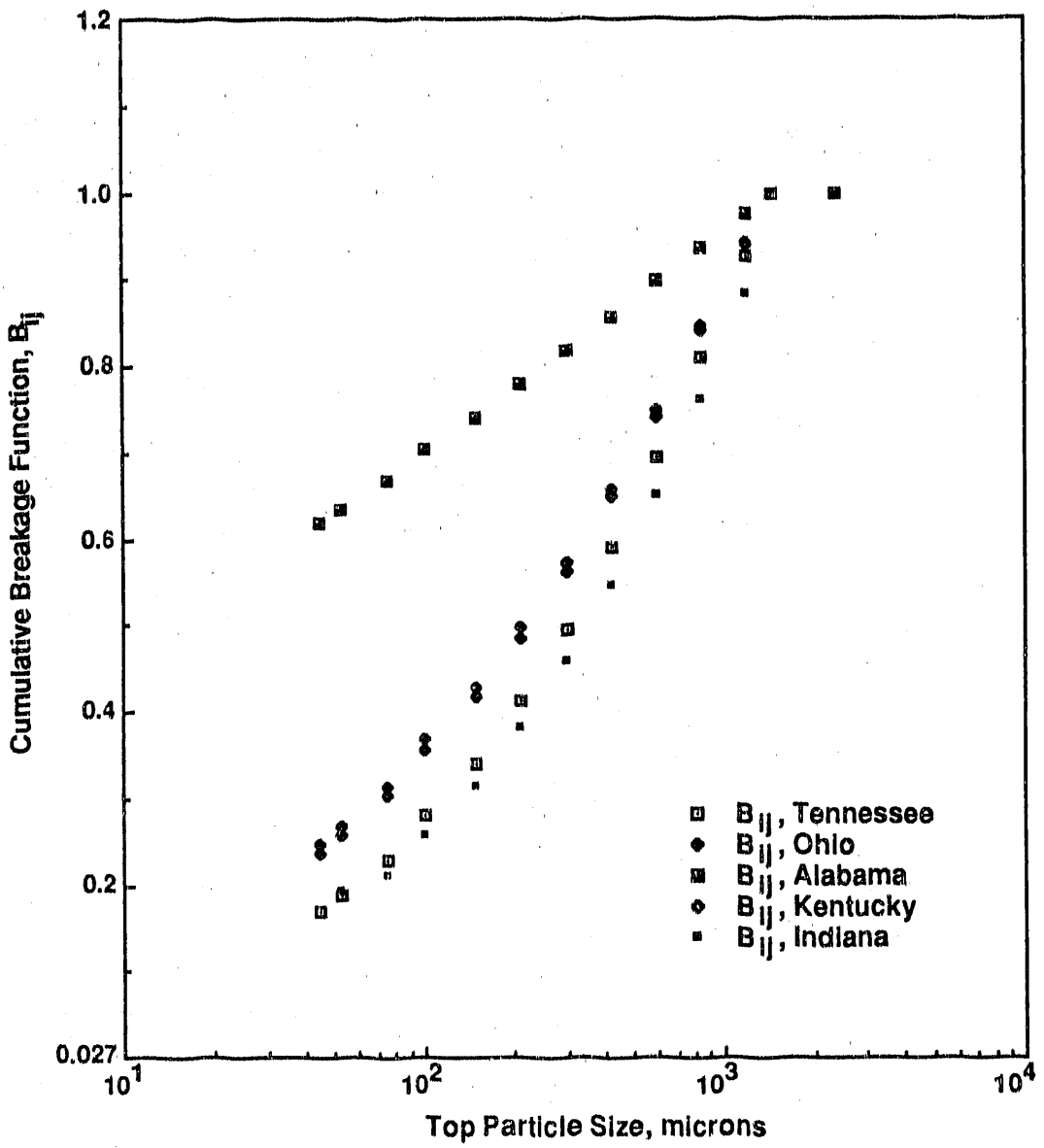

Figure 4-24. CUMULATIVE BREAKAGE FUNCTION VERSUS TOP PARTICLE SIZE PROVIDED BY MRIEST FIT FOR DRY GRINDING OF EASTERN SHALES WITH RAW FEED IN 10-INCH BALL MILL

Table 4-24. COMPARISON OF BREAKAGE PARAMETERS FOR DRY GRINDING OF EASTERN OIL SHALES USING 10-INCH MILL

Shale Type	S_i $(kWh/T)^{-1}$	ζ	β
Tennessee	1.8578	3.029	0.6249
Ohio	3.5090	3.4396	0.5092
Alabama	2.6257	3.6532	0.2022
Kentucky	2.9726	3.6876	0.5227
Indiana*	0.8493*	2.8730*	0.6248*

* Top particle size is 1700 μm.

values of these shales for wet grinding. Interestingly, their breakage distribution behavior is quite reversed to that of dry grinding (compare Figures 4-26 and 4-28). From these data, one may conclude that the presence of water not only enhances the grinding rate of each shale, as expected, but also alters the comminution behavior in terms of particle breakage.

Kinetic Approach to Wet Ball Milling Scale-Up

Most commercial ball mill scale-up procedures in the mineral industry have been based on the empirical Bond energy-size reduction equation, however, this procedure has several limitations (Herbst et al. 1982). The procedure does not allow the prediction of circuit size distributions. The principal drawback of the Bond approach to mill design results from its inability to account for 3 important sub-processes (breakage kinetics, particle transport and size classification). The Bond scale-up lumps the effect of these sub-processes into a single empirical equation (Herbst and Fuerstenau, 1980).

In recent years there have been considerable research efforts on the subject of phenomenological grinding models derived from population balance approach. This type of model is capable of predicting the size distribution in a tumbling mill as a function of time and mill position. In these models, the breakage process is characterized by two physically interpretable quantities (that is, selection function and breakage function). Selection function gives the fractional rate of breakage of particles in each size interval and breakage function gives the average size distribution of daughter fragments resulting from primary breakage of parent particles. By suitably defining the dependence of these two quantities on mill design and operating conditions, the behavior of each size fraction in the mill can be represented mathematically for grinding conditions of industrial importance (Herbst and Fuerstenau, 1980).

The research conducted in the last decade in this area confirms the validity of the scale-up procedure suggested by Herbst (1980) for the description of dry and wet ball milling (Herbst et al. 1983) of homogeneous materials (limestone and quartz) as well as heterogeneous minerals (complex molybdenite ore). In addition, these models have demonstrated the predictive capability of the performance of industrial-scale large diameter mills (Herbst, Lo and Rajamani, 1985).

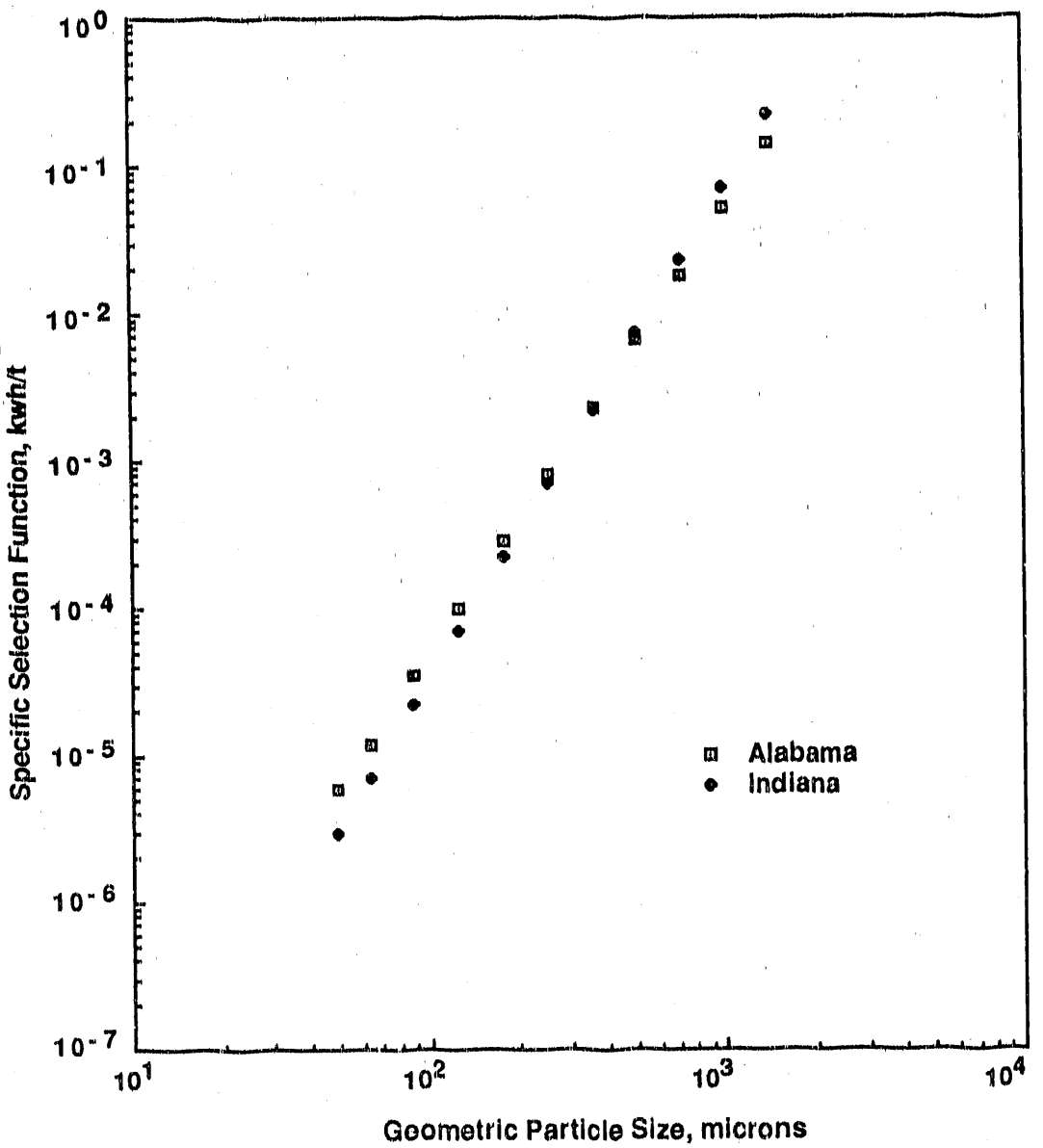

Figure 4-25. SPECIFIC SELECTION FUNCTIONS VERSUS GEOMETRIC PARTICLE SIZE PROVIDED BY MRIEST FIT FOR DRY GRINDING OF EASTERN SHALES WITH RAW FEED IN 8.25-INCH BALL MILL

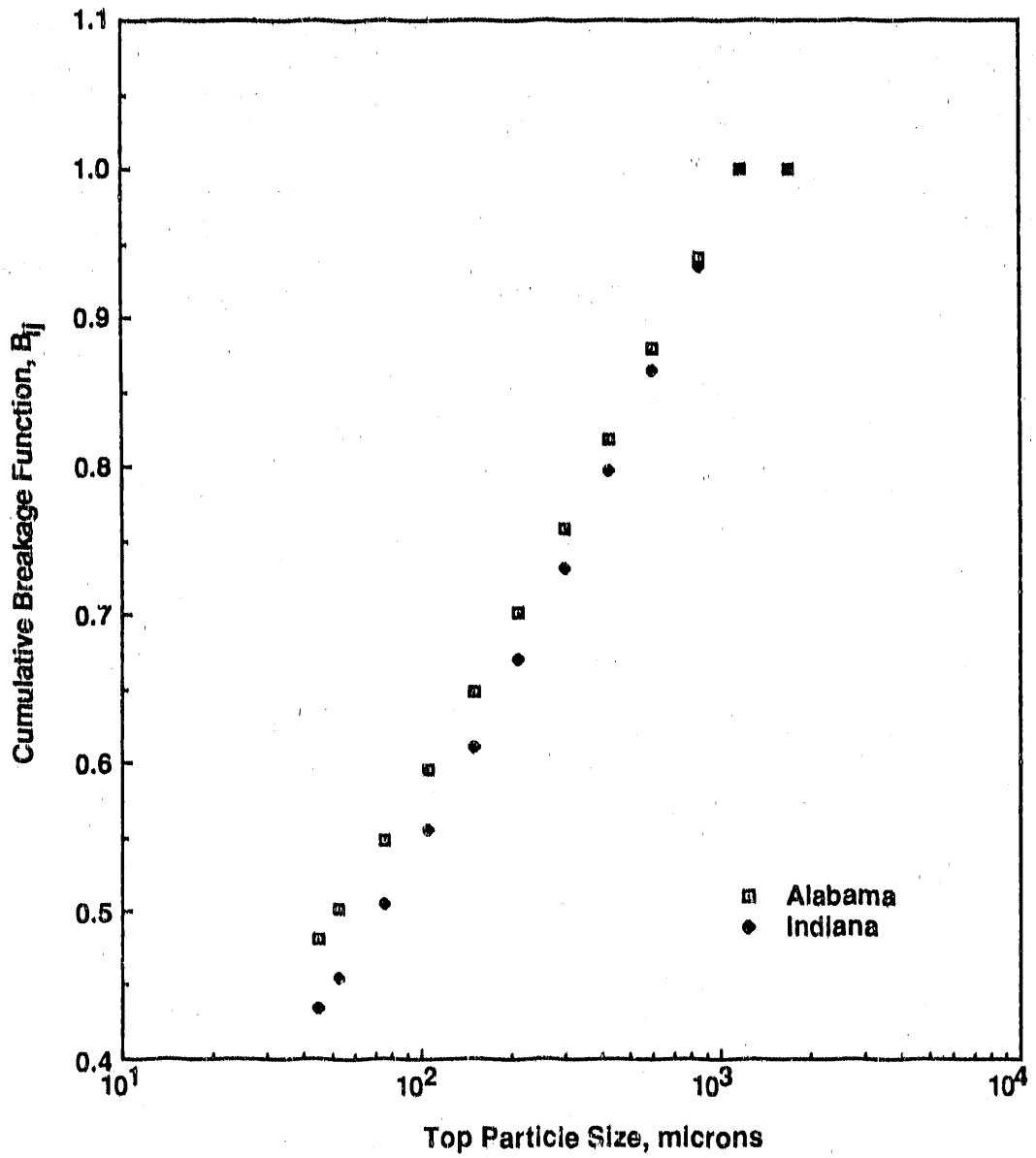

Figure 4-26. CUMULATIVE BREAKAGE FUNCTION VERSUS TOP PARTICLE SIZE PROVIDED BY MRIEST FIT FOR DRY GRINDING OF EASTERN SHALES WITH RAW FEED IN 8.25-INCH BALL MILL

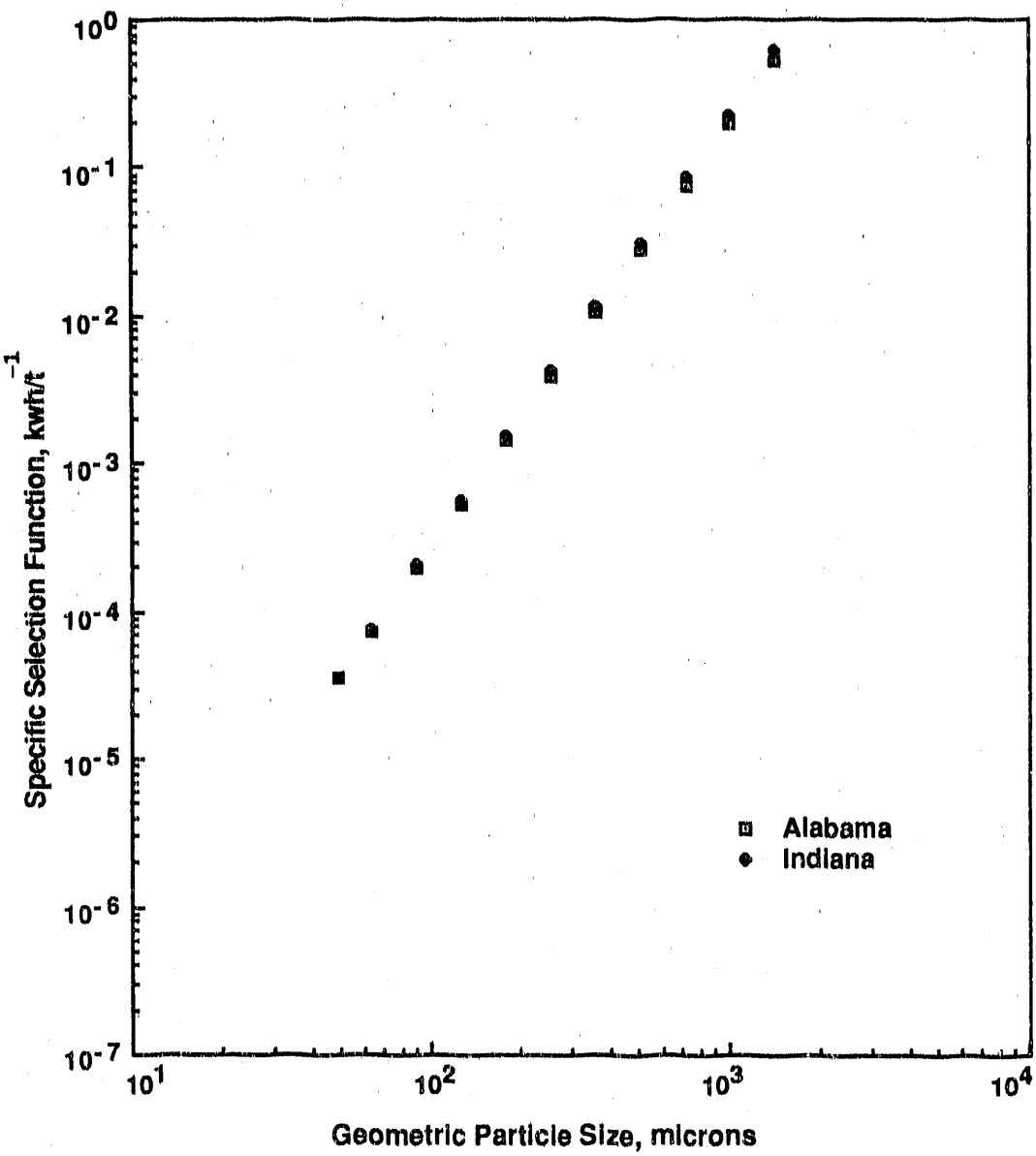

Figure 4-27. SPECIFIC SELECTION FUNCTIONS VERSUS GEOMETRIC PARTICLE SIZE PROVIDED BY MRIEST FIT FOR WET GRINDING OF EASTERN SHALES WITH RAW FEED IN 8.25-INCH BALL MILL

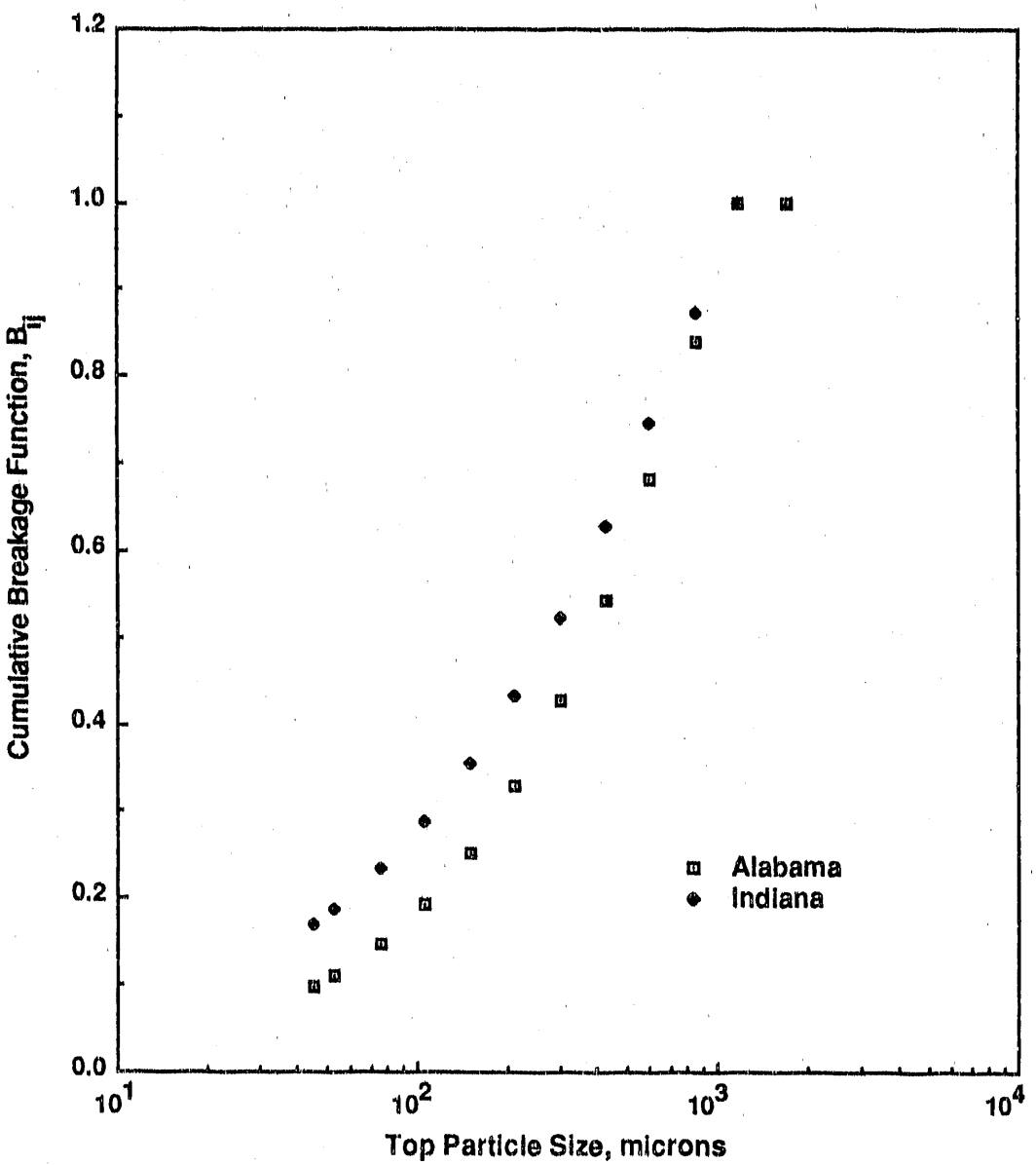

Figure 4-28. CUMULATIVE BREAKAGE FUNCTION VERSUS TOP PARTICLE SIZE PROVIDED BY MRIEST FIR FOR WET GRINDING OF EASTERN SHALES WITH RAW FEED IN AN 8.25-INCH BALL MILL

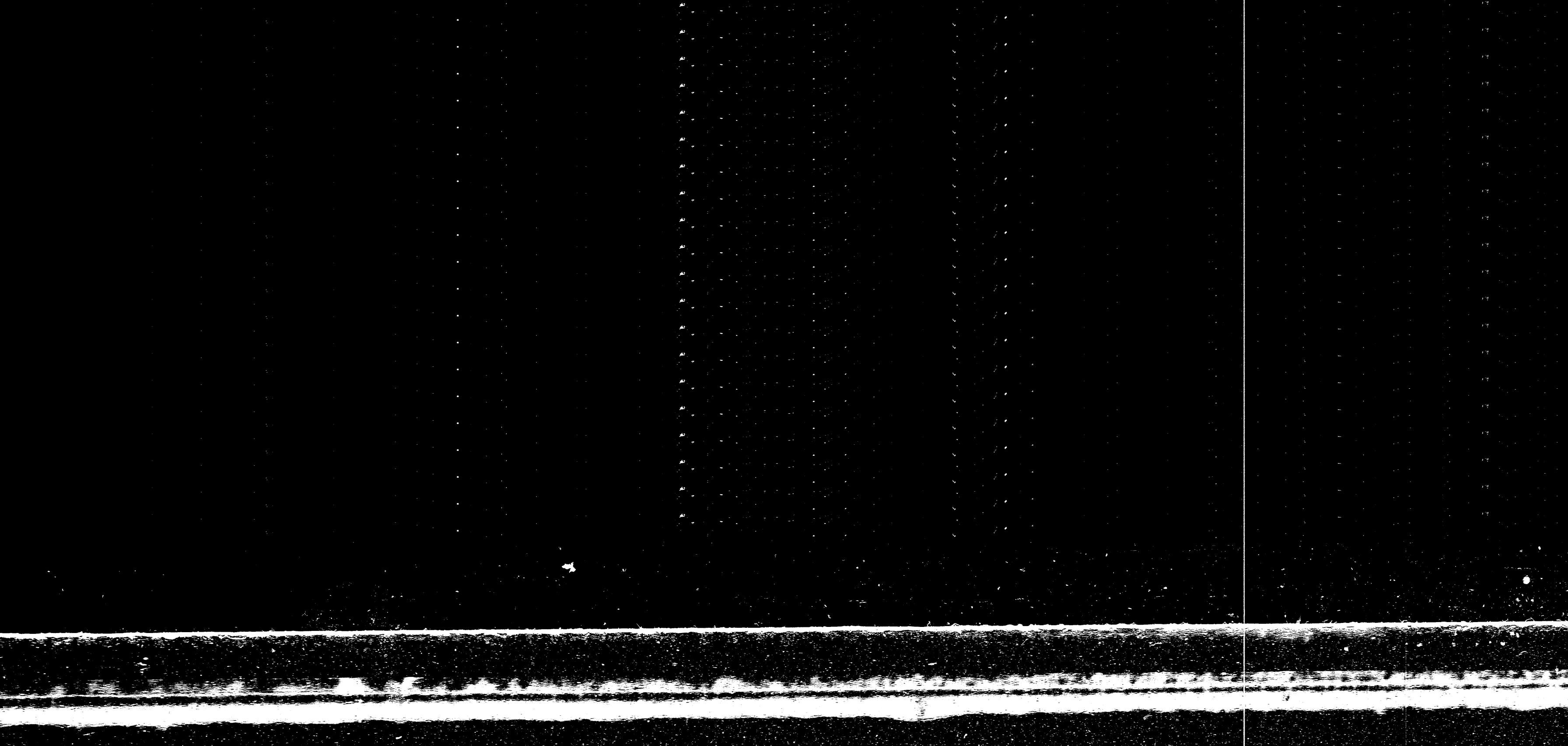

The objective of this section is to provide additional confirmation of the scale-up procedure referred to here as "similar fineness of grind" (Herbst et al. 1982) for the ball milling of Eastern oil shales.

Experimental Procedures

The data presented in this section are the results of dry and wet grinding tests performed in batch mill (8 inch X 9.25 inch) and a continuous wet grinding test in a [18 inch X 30 inch (45.7 X 76.2 cm)] Marcy rod mill operated in a ball mill mode. The ball size distributions used for two mills are given in Table 4-25. The mill speed for the batch mill and the continuous mill was kept at 75% N_c (77 rpm) and 81% N_c (50 rpm), respectively.

Table 4-25. BALL SIZE DISTRIBUTION USED FOR 8.25- AND 30-INCH MILLS

Ball Diameter, Inches	Percent by Weight	8.25 Inch Mill 50% Filling	30 Inch Mill 50% Filling
1-1/2	52.9	9.8	164.4
1	30.3	5.6	94.3
3/4	11.9	2.2	37.0
1/2	4.9	0.9	15.7
Total	100.0	18.5 kg	311.4 kg

Batch grinding tests were carried out with Indiana and Alabama oil shales having a specific gravity of 2.4 using monosize fraction (4 X 6 mesh) and -4 mesh raw feed. Continuous wet grinding test in open-circuit mode was carried out using -4 mesh Alabama shale at a feed rate of 780 lb/h for 2 hours to allow the mill to reach steady state before mill product was sampled for analysis.

Breakage Kinetics

Monosize fractions (4 X 6 mesh) of Alabama and Indiana shales were dry and wet ground (at 55% solids) in the batch mill under standard conditions for 2, 4, 8, and 16 minutes. The energy-size reduction data collected was analyzed by writing the first order disappearance kinetic equation in the energy normalized form using specific energy as a reduced time variable:

$$M_i(\bar{E}) = M_i(0)\exp\left(-S_i^E \bar{E}\right) \qquad (25)$$

Figure 4-29 is a disappearance plot for dry and wet ground Indiana shale. Interestingly, the specific selection function (S_i^E) for dry ground shale is higher [0.406 $(kWh/t)^{-1}$] than the wet ground shale [0.266 $(kWh/t)^{-1}$]. This indicates that wet grinding of this shale at such slurry density and given conditions is energy inefficient. Usually wet grinding of minerals is kinetically faster than dry grinding and this should be true for shale grinding too. Hence, data of Figure 4-29, if replotted on the time scale and specific rate of breakage (min^{-1}) were to be determined on a regression basis, then, as one would expect, S_i, wet to be higher (0.007) compared to S_i, dry (0.0056). From mill scale-up design considerations energy normalized

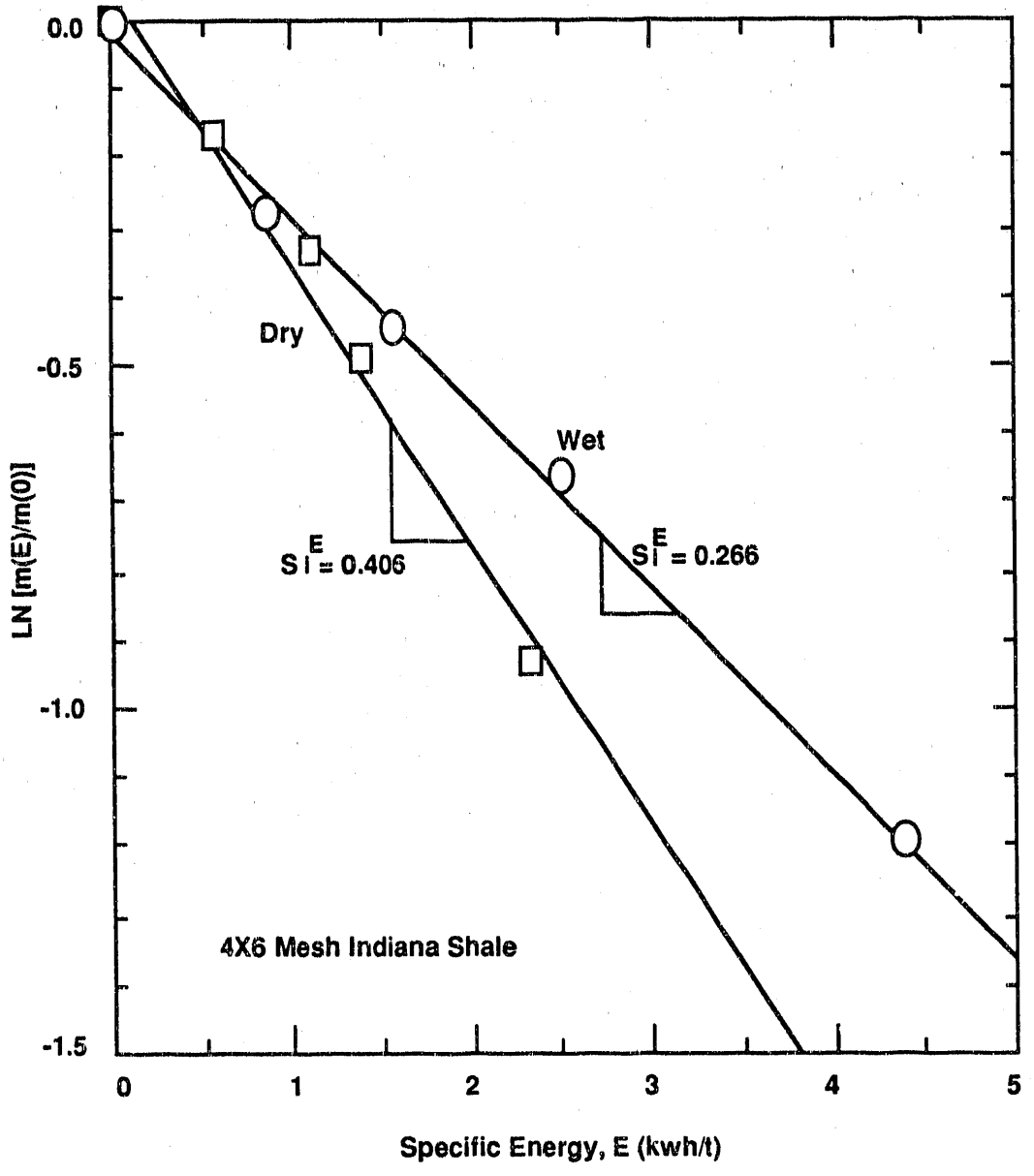

Figure 4-29. FIRST ORDER DISAPPEARANCE PLOT FOR DRY AND WET GRINDING OF INDIANA SHALE

selection function values are more relevant because as mentioned earlier, they are independent of mill design and operating conditions.

Figure 4-30 is a disappearance plot describing the breakage kinetics of Indiana and Alabama shale under similar conditions. This reveals that Alabama shale is harder to grind. In other words, the Alabama shale will require twice as much energy as the Indiana shale. This finding is consistent with the researchers in the oil shale beneficiation area (Lamont, 1990).

Estimation

Top size breakage kinetic data yielded a good starting estimate for specific selection function value. Estimation was carried out using energy-size distribution data obtained by grinding -4 mesh Alabama (1 and 4 min) and Indiana (4 min) shale at 50% solids. Estimated specific selection function values for Alabama and Indiana shale are plotted as a function of particle size in Figure 4-31. Note that specific selection function values are almost independent of particle size (smaller slope) for Indiana shale, whereas, they are highly dependent on particle size (higher slope) for Alabama shale. Also, the differences in specific energies required to comminute equal size Alabama and Indiana shale particle increases as particle size becomes finer.

Figure 4-32 is a plot of the estimated cumulative breakage function (B_{ij}) versus particle size (X_i). It is clear from this plot that the distribution of daughter fragments produced from primary breakage of parent particles is narrower for the Indiana shale and results in very small amount of fines.

The quality of estimation can be judged by comparing how well the experimental data is fitted. Figure 4-33 shows experimental and fitted size distribution data for Indiana shale. The fit is satisfactory except in the fine particle size range. This is due to the presence of small amounts of material in this size range. Another important feature of estimation, which can be used to judge the quality of estimation is simulation and prediction. Figure 4-34 shows a comparison of predicted and experimental size distribution data for Alabama shale.

Continuous Grinding

Having shown the utility of population balance model in predicting the response of a batch grinding system, this procedure must be able to predict the performance of a continuous grinding mill.

Steady state open-circuit predictions require residence time distribution (RTD) information in addition to breakage rate parameters. The RTD parameters (N, τ) were estimated using correlations available in the literature (Lo *et al.* 1988). These correlations have been successfully used in predicting large scale mill performance. In this study, the power draw of 8-inch mill predicted by Equation A-10 was identical to the experimentally measured value. Hence, power draw of large mill was not experimentally measured but a value calculated from the correlation was used. Figure 4-35 shows a similar fineness prediction for the open-circuit wet grinding of Alabama shale in 18 inch X 30 inch pilot scale Marcy Ball Mill using a -4 mesh feed at 780 lb/h. The experimental product size distribution is also shown in this

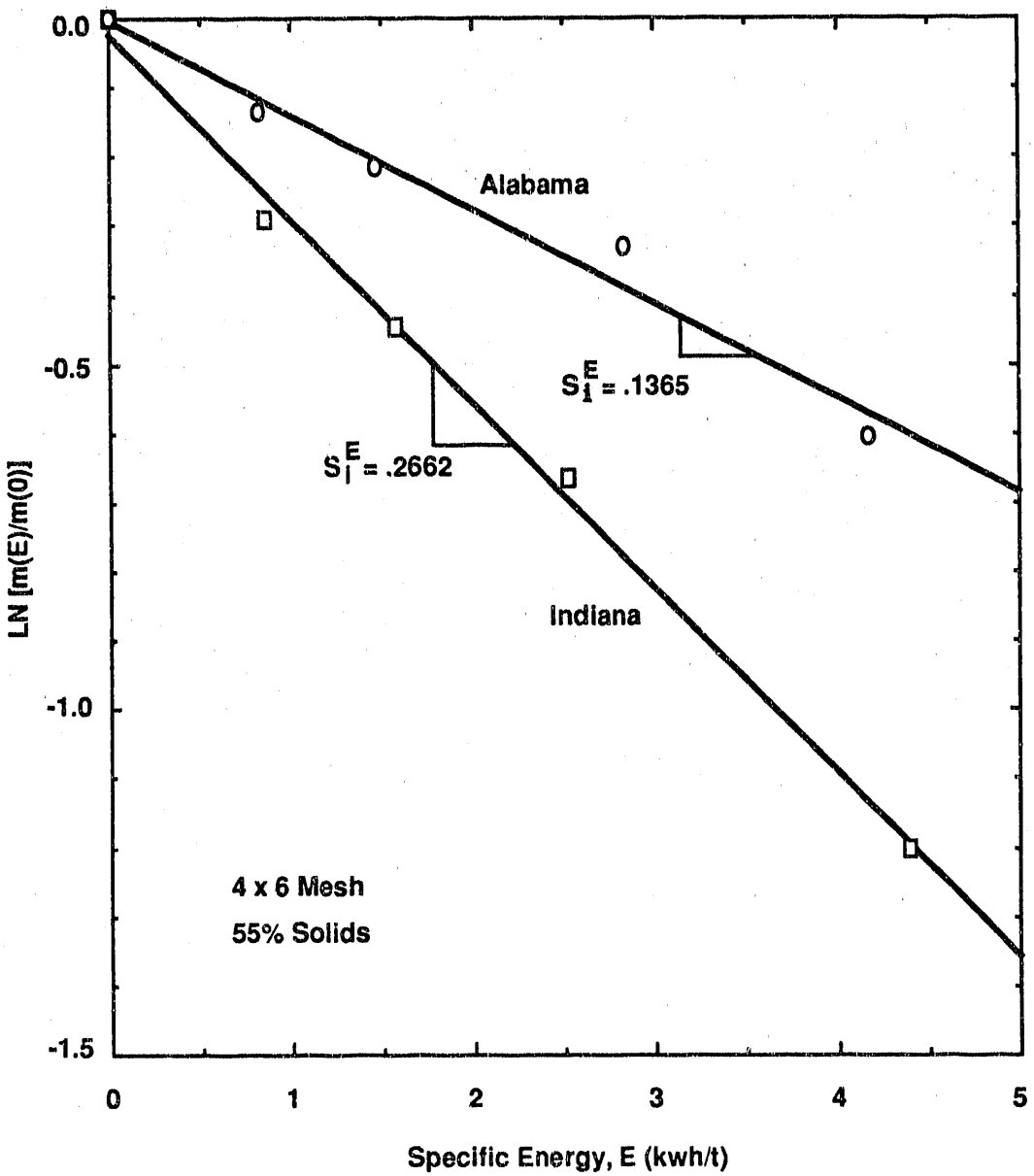

Figure 4-30. FIRST ORDER DISAPPEARANCE PLOT FOR WET GRINDING OF 4 X 6 MESH INDIANA AND ALABAMA SHALES IN CONVENTIONAL BALL MILLING

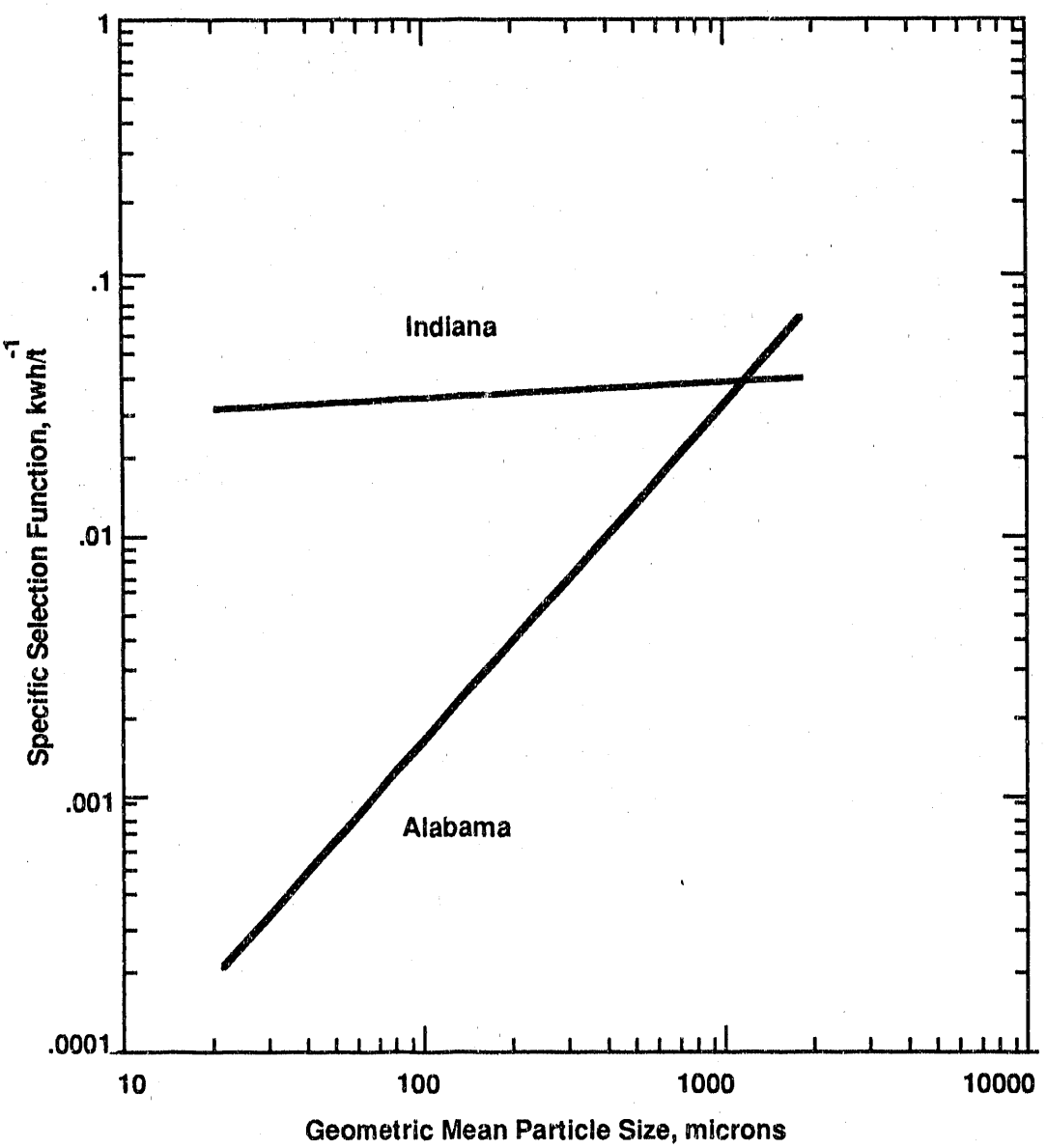

Figure 4-31. ESTIMATED SPECIFIC SELECTION FUNCTION VALUES FOR WET GRINDING OF INDIANA AND ALABAMA SHALES

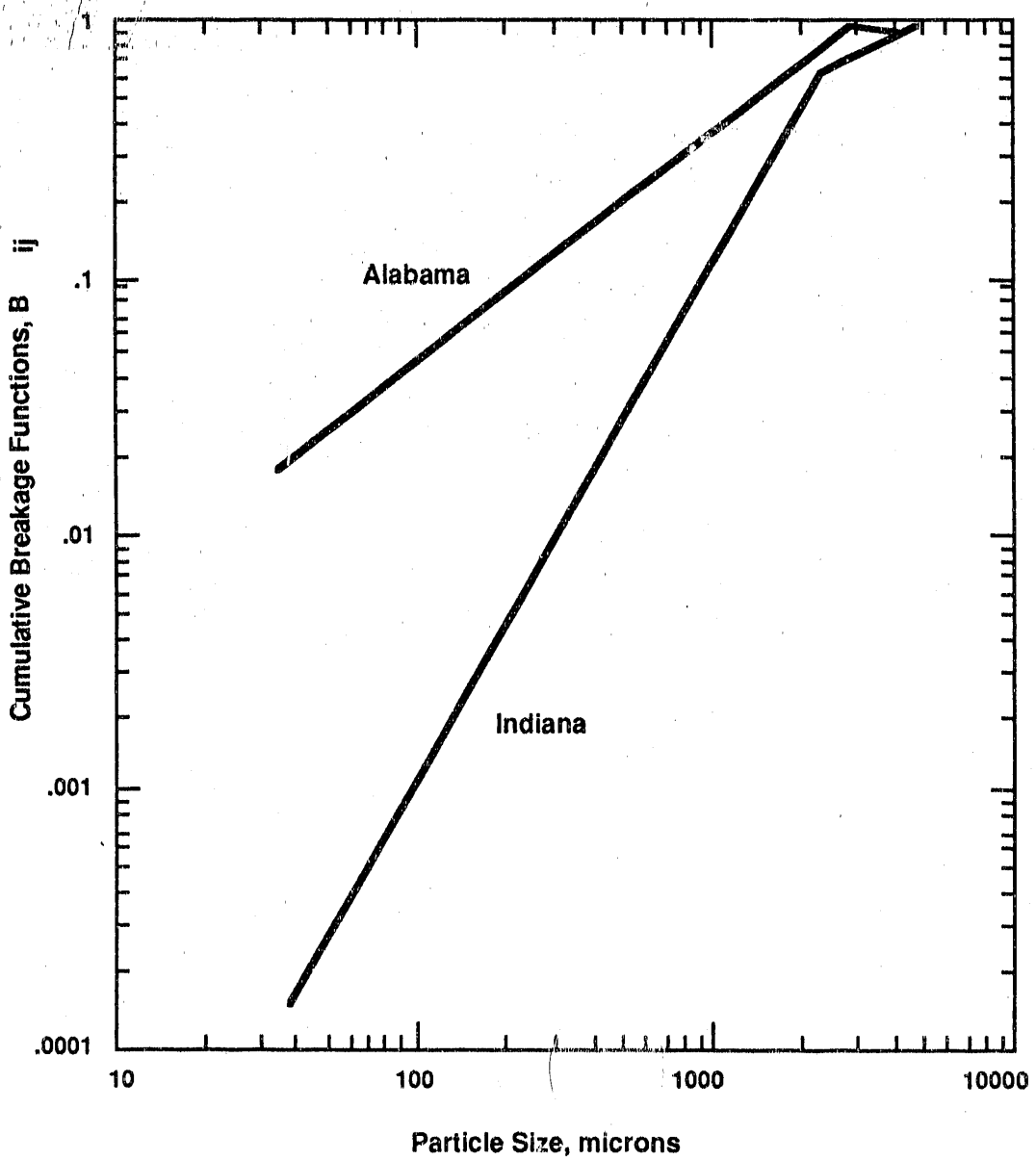

Figure 4-32. ESTIMATED B_{ij} VALUES FOR WET GRINDING OF INDIANA AND ALABAMA SHALES

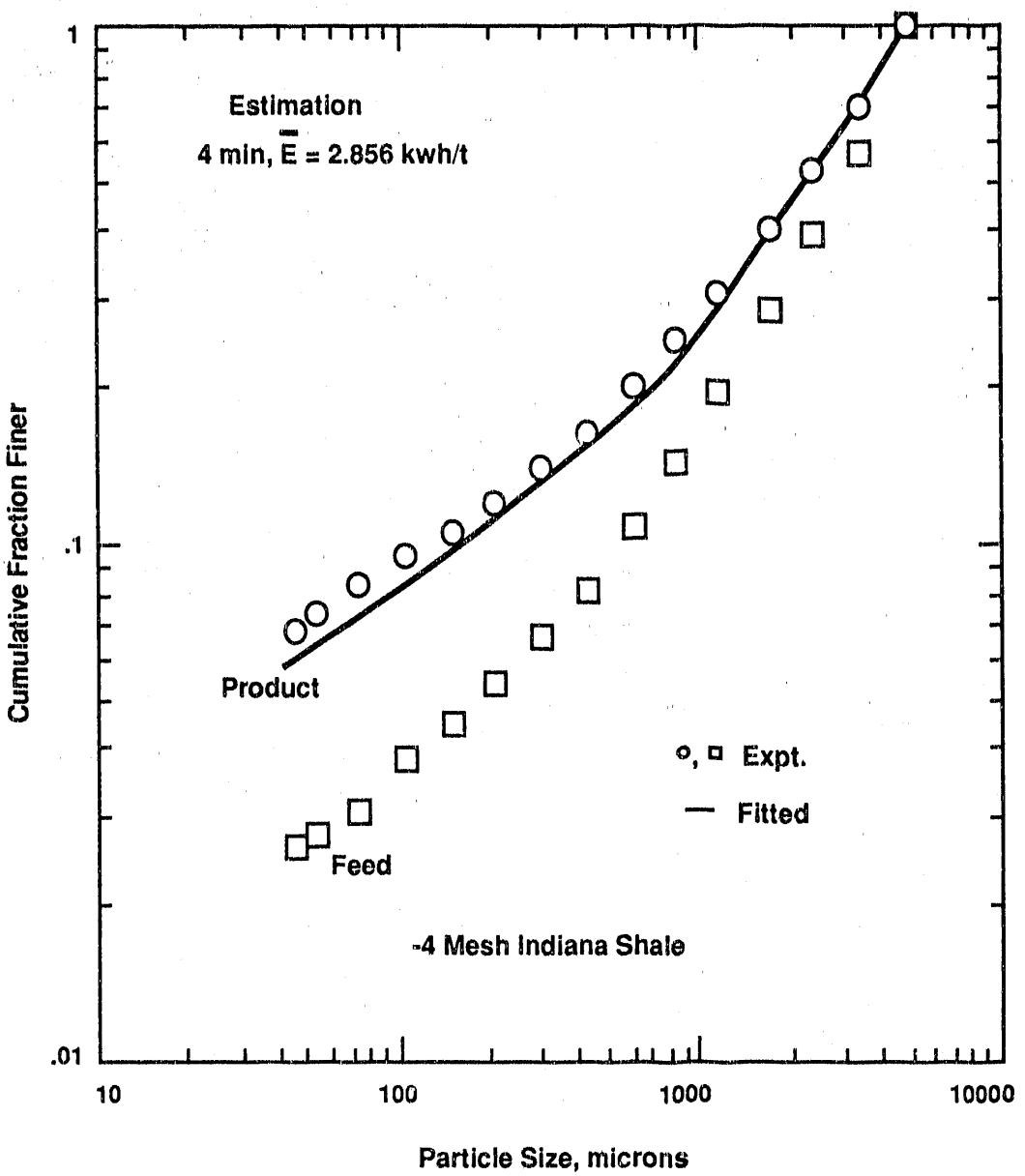

Figure 4-33. COMPARISON OF EXPERIMENTAL AND FITTED PARTICLE SIZE DISTRIBUTIONS FOR INDIANA SHALE

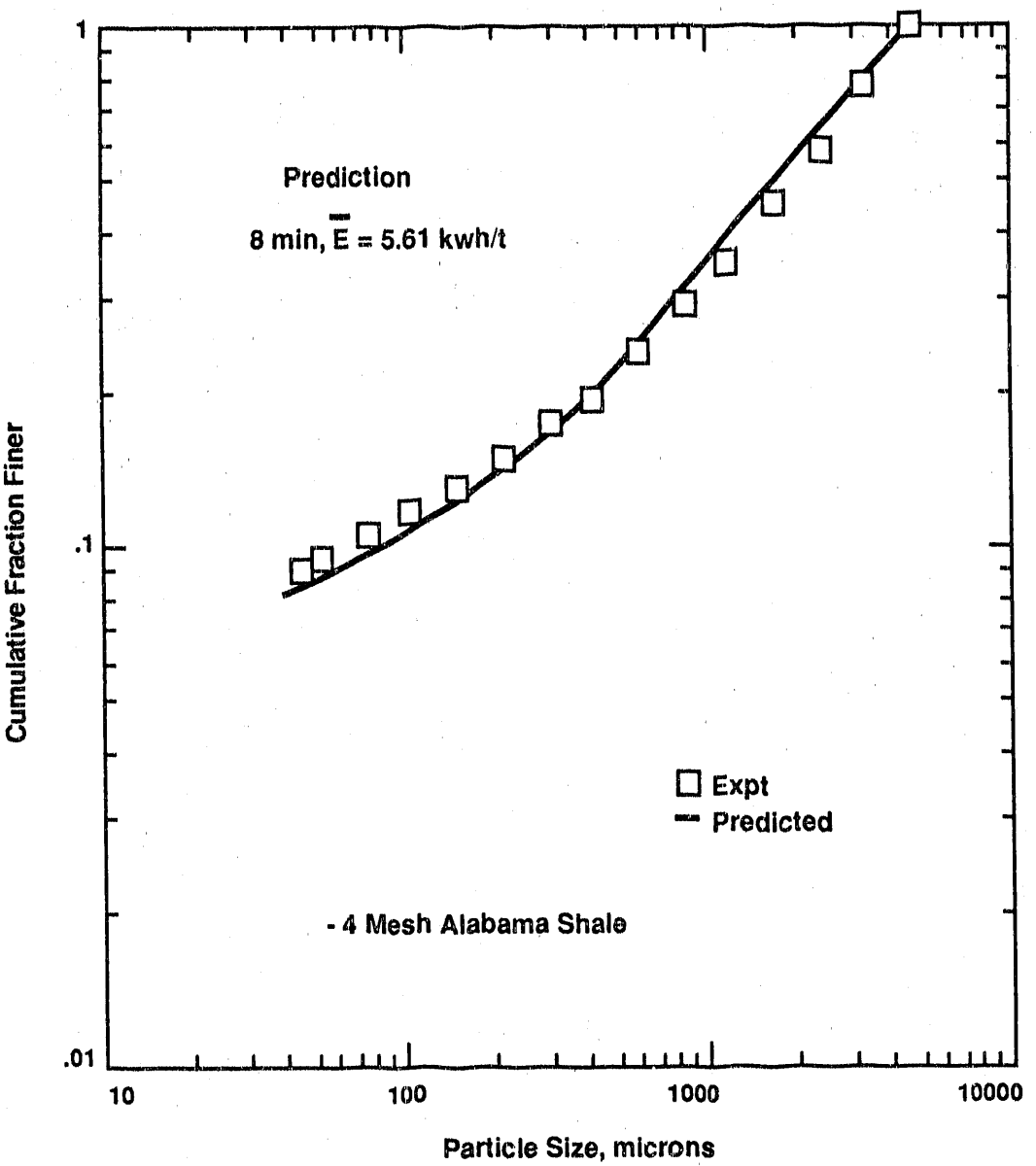

Figure 4-34. COMPARISON OF EXPERIMENTAL AND PREDICTED PARTICLE SIZE DISTRIBUTIONS FOR ALABAMA SHALE

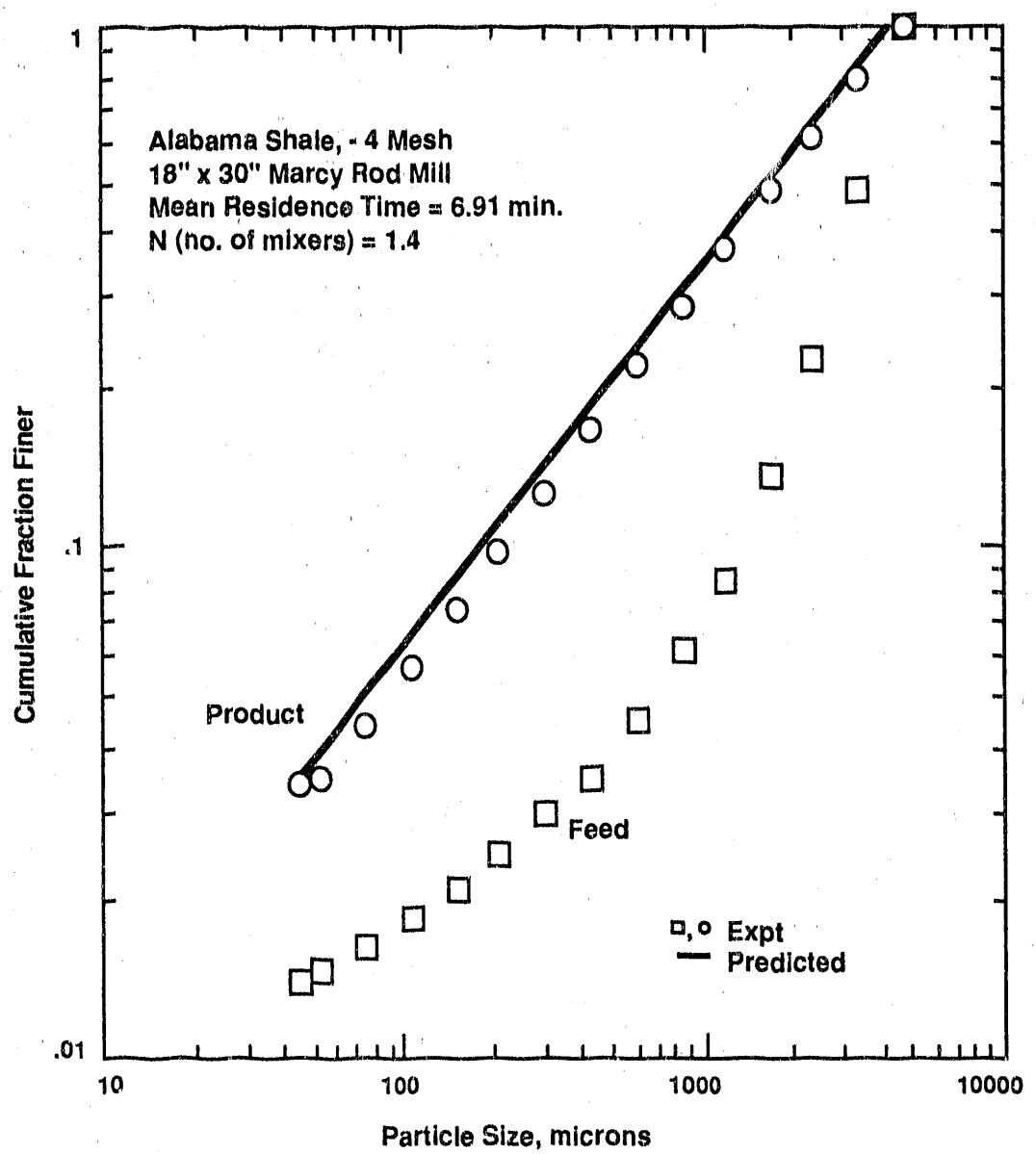

Figure 4-35. COMPARISON OF PREDICTED AND EXPERIMENTAL SIZE DISTRIBUTIONS FOR AN OPEN CIRCUIT CONTINUOUS GRINDING TEST (50% Solids)

plot. The kinetic approach is quite satisfactory in predicting the response of a large mill based upon the tests conducted in a small batch mill.

Integrated Circuit Optimization

An integrated oil shale beneficiation circuit involves three steps: grinding, sizing and concentration. Research on grinding and concentration was carried out in this project in separate subtasks. In order to avoid over-grinding in the stirred ball mill, the ball mill ground product must be screened to remove 25 μm material. This can be achieved by a sizing step, one of which is screening. Therefore, tests were conducted using a Derrick Screen incorporating 460 mesh screen cloth to demonstrate the feasibility of such sizing separation.

Derrick Screening Tests

These tests were conducted to remove material finer than 20 μm, which otherwise would result in over-grinding. There were two feed streams in the beneficiation circuit that needed screening: The first was the primary ball mill product (that is, feed to the stirred ball mill), and the second was the rougher concentrate to be used for regrinding in the secondary stirred ball milling step. A vibrating Derrick screen having slotted 400/460 mesh size screen cloth was used for screening tests. Since feed rates tested were low, the feeder was modified to cover the entire area of the screen. Tests were run for a predetermined time and samples of oversize and undersize were collected. The oversize samples were wet screened on a 270 mesh screen and analyzed in the same manner as the undersize sample.

Results

The -48 mesh feedstock for stirred ball mill tests contained material about 50% finer than 24 μm. A series of experiments were conducted to remove this fraction of material from the feed. In most cases, the screening efficiency at 24 μm was close to 85%. The data obtained in this series of tests are listed in Tables B-1 through B-4 (Appendix B). Figure 4-36 shows particle size distribution for feed, undersize and oversize, obtained for a typical test using the 460-mesh Derrick Screen.

Early column flotation tests led to the assumption that the beneficiation flow sheet might be of the form shown in Figure 4-37 (No. 1). This assumption reflects the observation that one stage of column flotation could replace several stages of conventional flotation. Also considered was the indication that initially satisfactory flotation could not be achieved at sizes coarser than about 10 μm.

Such a configuration is appealing because capital costs are minimized. In this flow sheet, optimization consists of defining the sizes at which the transition from conventional to stirred ball milling and between successive stages of stirred ball milling is made.

The inherent inefficiency of this flow sheet is that the entire feed stream passes through two stages of energy intensive stirred ball milling. The concept of removing finished (ground) material from the circuit at the earliest possible time is ignored.

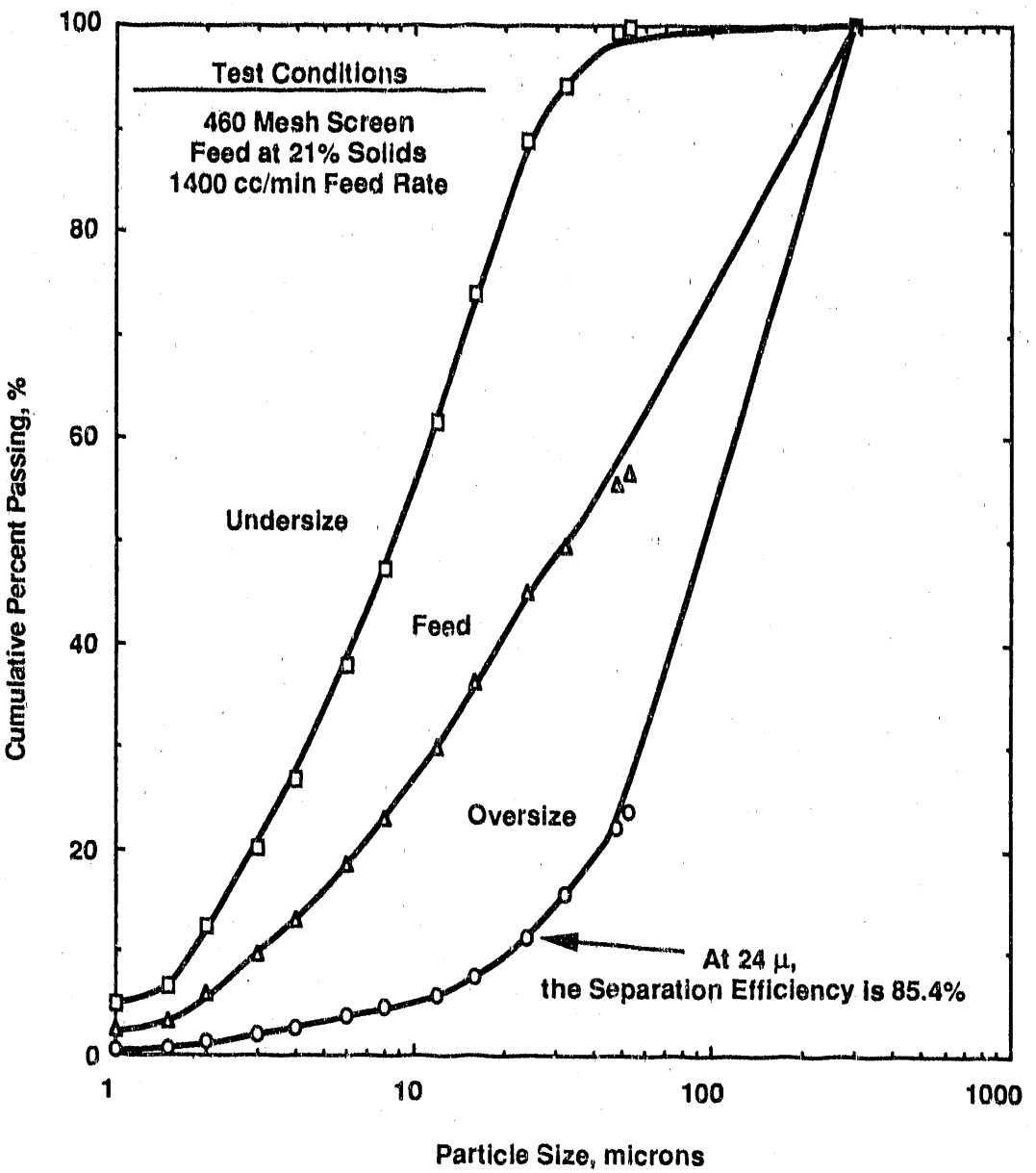

Figure 4-36. PARTICLE SIZE DISTRIBUTION FOR THE FEED AND PRODUCTS OF A 460-MESH DERRICK SCREEN SEPARATION

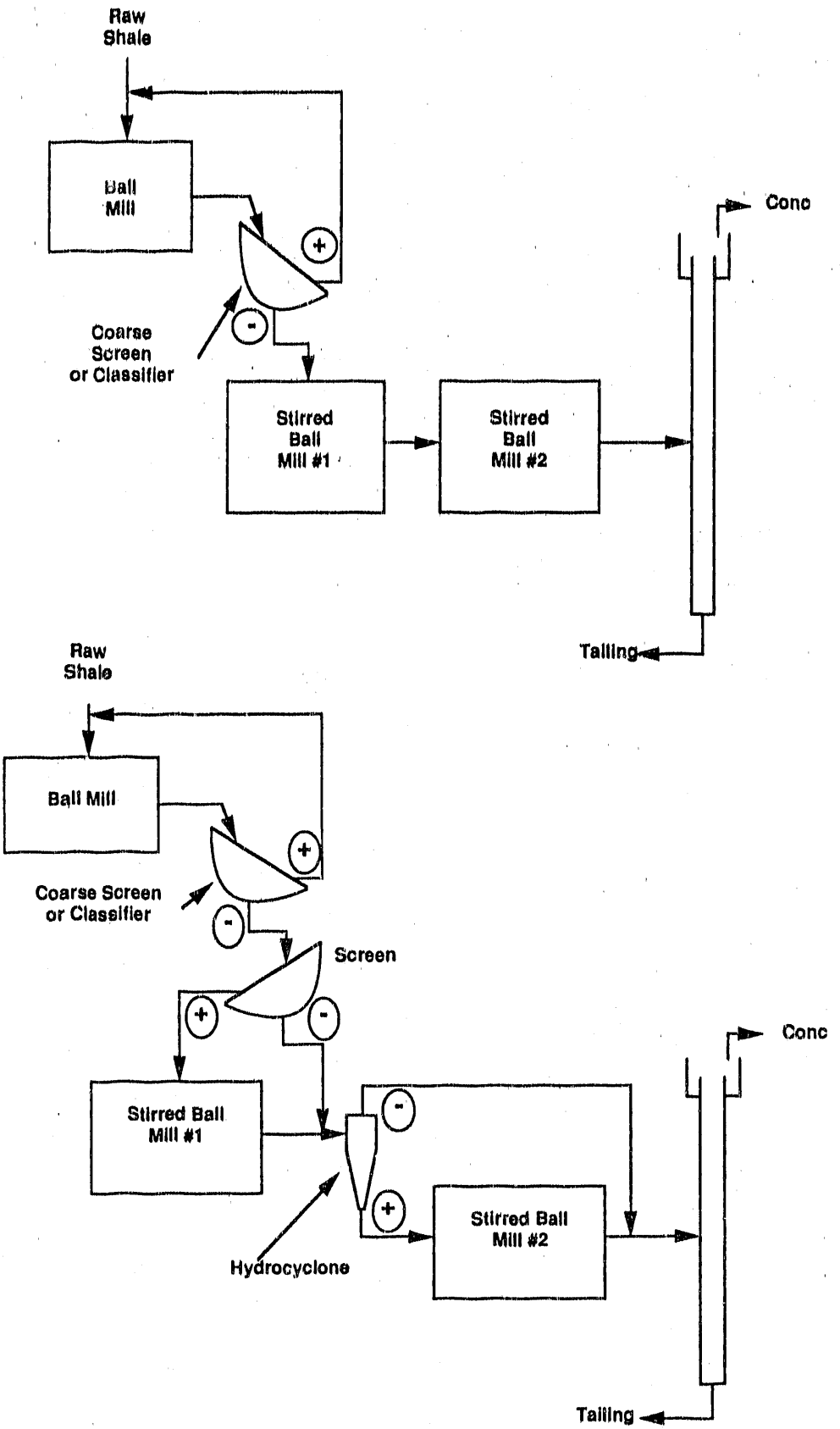

Figure 4-37. BENEFICIATION FLOWSHEET NOS. 1 AND 2

Examination of the -48 mesh product from the primary ball mill revealed that 50% of it was finer than 24 μm. (The size analysis of that product is presented in Tables B-1 through B-4). Screening tests on this product showed that an efficient size separation could be made. This then makes the flow sheet shown in Figure 4-37 (No. 2) a viable option.

In this configuration fully 50% of the total feed stream bypasses the first stage of stirred ball milling and perhaps as much as 25% bypasses the second stage. This flow sheet is, therefore, substantially more energy efficient than the prior one.

Flotation tests were conducted on the -24 μm fraction of the primary ball mill discharge. The tests were conducted in a taller column than had been used previously. The results, shown in Figure 4-38, demonstrate that a satisfactory rougher concentrate can be made at a relatively coarse size.

The favorable flotation results make possible a still further refinement of the beneficiation flow sheet as shown in Figure 4-39 (No. 3). In this arrangement the amount of feed to the secondary stirred ball mill is reduced to about 25% of the total raw shale feed stream. It should be noted that this reduction in grinding cost is achieved by foregoing some of the benefits possible with column flotation.

The net energy required for the three flowsheets discussed above was determined on the basis of Bond Work Indices and stirred ball milling results obtained in this work. The results are shown in Tables 4-26 through 4-28. The assumption made in this calculation is that during cyclone sizing, 50% of the material (raw shale or rougher concentrate) reports to cyclone underflow. Also, the energy balance for secondary stirred mill, as mentioned in Tables 4-26 and 27, are based on the assumption that regrinding characteristics of raw shale is the same as that of rougher shale concentrate.

Based on the total net specific energy values obtained among these 3 flowsheets, it is clear that flowsheet No. 3 is a viable energy efficient integrated circuit.

Conclusions and Recommendations

From the data presented here, it is concluded that:

1. The energy requirements for producing product shale in the size range (d_{90} = 10 μm) from a feed having d_{90} in the range of 200 μm was found to be ~100 kWh/t in a single pass. For an integrated circuit, 50 kWh/t was required for a d_{90} = 10 μm product (see No. 16 below).

2. The operating valuables in the stirred milling of shale that minimized energy requirements were: high percent solids, 53% to 55%; high feed rate, 2100 mL/min; high rotor speed, 1300 rpm.

3. The size reduction efficiency of 2-mm beads was found to be superior than 3-mm beads in terms of energy savings and mill throughput for raw shale.

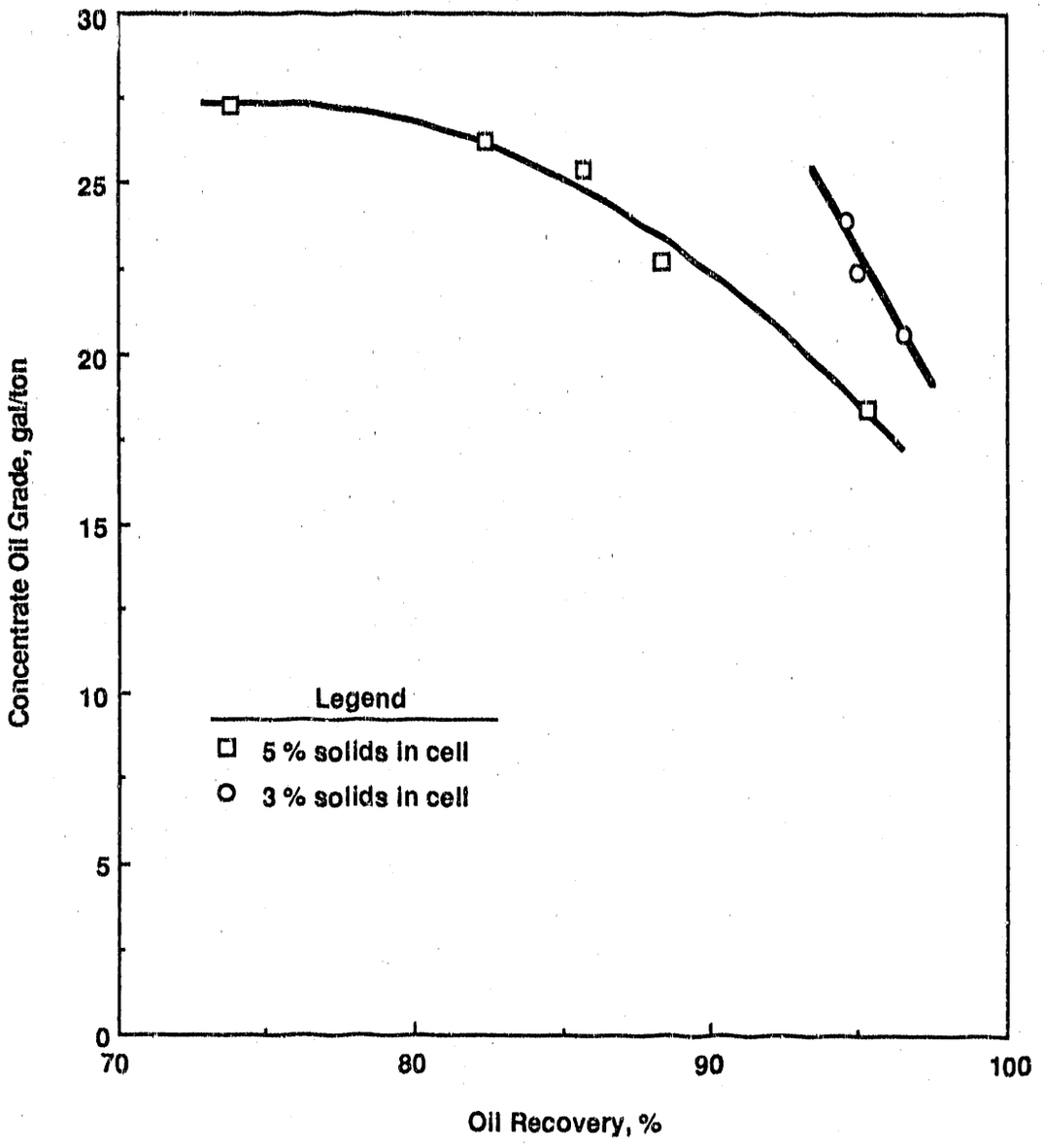

Figure 4-38. GRADE -- RECOVERY RELATIONSHIPS IN COLUMN FLOTATION (Coarse Feed)

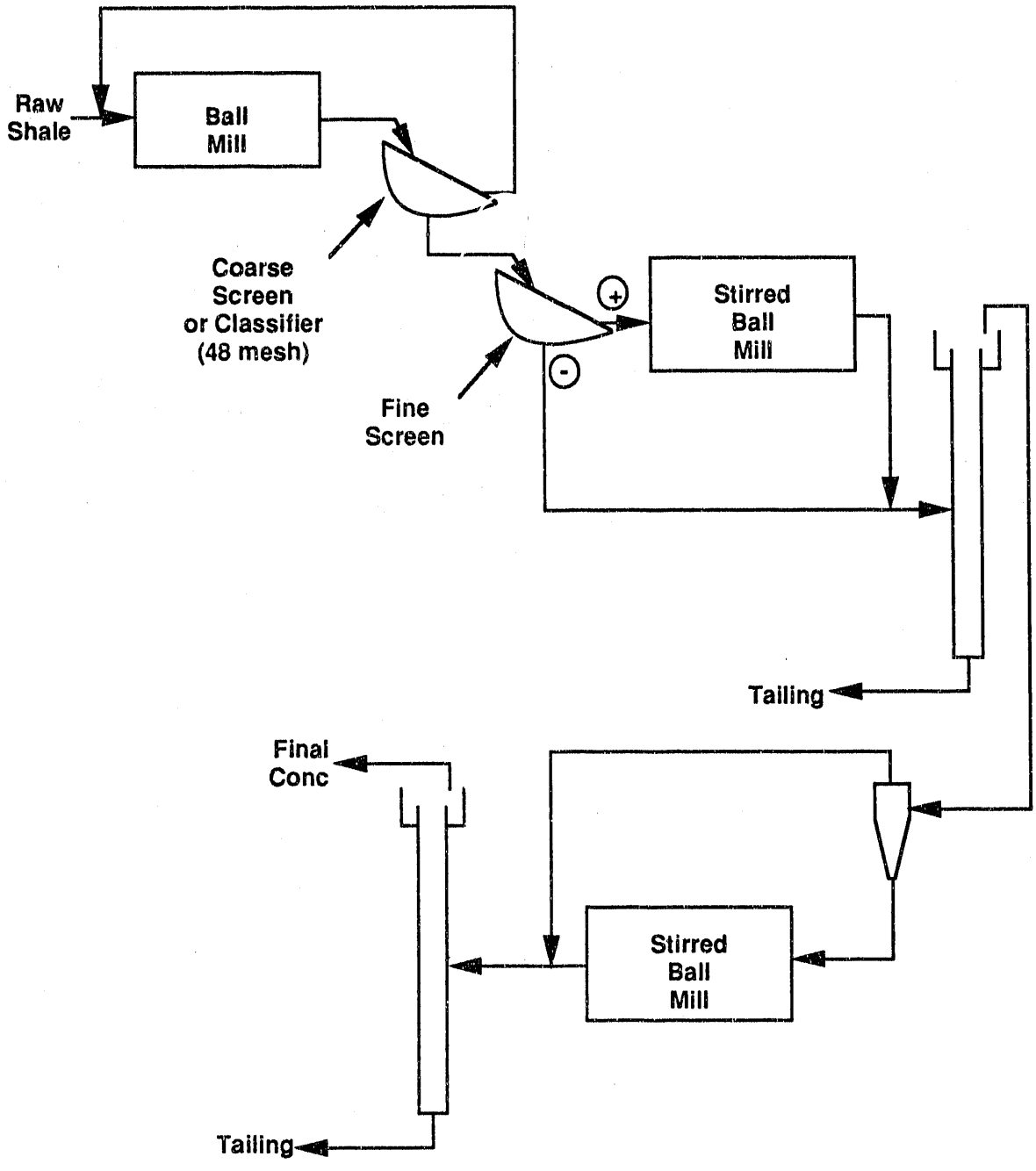

Figure 4-39. BENEFICIATION FLOWSHEET NO. 3

Table 4-26. NET SPECIFIC ENERGY VALUES OF FLOWSHEET NO. 1 FOR ALABAMA SHALE

Unit	Percent of Feed	kWh/t	Net kWh/t
Ball Mill	100	16.48	16.48
Primary Stirred Mill	100	40.00	40.00
Secondary Stirred Mill	100	49.52*	49.52
Total			106.00

* Based on the assumption that regrinding characteristics of raw shale and rougher concentrate are the same as mentioned in Table 4-28.

Table 4-27. NET SPECIFIC ENERGY VALUES OF FLOWSHEET NO. 2 FOR ALABAMA SHALE

Unit	Percent of Feed	kWh/t	Net kWh/t
Ball Mill	100	16.48	16.48
Primary Stirred Mill	50	40.00	20.00
Secondary Stirred Mill	50	49.52*	24.75
Total			61.23

* See footnote of Table 4-26.

Table 4-28. NET SPECIFIC ENERGY VALUES OF FLOWSHEET NO. 3 FOR ALABAMA SHALE

Unit	Percent of Feed	kWh/t	Net kWh/t
Ball Mill	100	16.48	16.48
Primary Stirred Mill	50	40.00	20.00
Secondary Stirred Mill	25	49.52*	12.38
Total			48.86

* Taken from Table 4-16.

4. The size reduction efficiency of 1.1-mm beads was found to be superior than 2-mm beads in terms of energy saving and mill throughput for rougher concentrate.

5. Energy-size reduction behavior of Alabama and Indiana shale was found to follow empirical Charles relationship in the fine size range.

6. In the ultra-fine size range Indiana shale was found to show higher grinding resistance than Alabama shale, whereas, in the coarse size range the opposite was true.

7. The size distributions of ground Alabama and Indiana shale were found to be self-similar.

8. The approach of predicting product particle size distribution using a combination of Charles relationship and self-preserving curve was validated for Indiana shale.

9. The media consumption during stirred milling was found to be about 0.9 kg of media per ton of Indiana shale.

10. The Bond Work Indices of Alabama, Kentucky, Ohio, Michigan, and Tennessee were estimated to be 23.17, 19.56, 15.59, 13.28 and 12.70.

11. Energy-size reduction relationship such as that of Charles was found to be true during coarse grinding of shales.

12. Relative grindability of these shales using Charles approach was as follows:

    Alabama > Indiana > Kentucky > Tennessee > Ohio > Michigan

13. The description of shale grinding behavior in conventional mills was described by population balance approach revealing observations concerning breakage distribution function and selection function.

14. A kinetic approach to mill scale procedure of eastern shales was confirmed using "similar fineness of grind" procedure.

15. Fine screening tests using Derrick Screen resulted in a screening efficiency of 85% at 24 μm size.

16. Three different integrated circuit flowsheets were evaluated on the basis of net energy consumption per ton of raw shale. It was found that intermediate rougher flotation and sizing steps could reduce overall energy consumption to a great extent. An estimate of 50 kWh/t was obtained for the best integrated circuit. The energy consumption for size separation is fairly low (0.25 to 1.00 ¢/ton of screen feed -- Derrick Screen Manual, KB0186, p. 11).

Before advancing the research to a 2 to 5 ton/h process development unit scale, MRI recommends the following:

1. Alternate ways of grinding shale to fine size range should be found. The use of silica sand as a grinding media looks promising as this has been successfully demonstrated for coal (Mehta and Schultz, 1991).

2. Secondary stirred ball milling tests on raw shales should be carried out.

3. Sizing data on raw shales and rougher concentrates should be collected using other devices such as cyclones.

4. Closed-circuit conventional grinding tests should be performed.

5. Optimization of integrated circuit should be carried out on the basis of total overall cost.

61WP/61090top4/RPP

SUBTASK 4.2. KEROGEN/MINERAL MATTER SEPARATION

At the heart of any mineral processing operation is the process by which a separation of the valuable minerals from waste minerals is made. In the case of oil shales it is the separation of kerogen from its associated mineral matter. Prior to the onset of this program all beneficiation research on oil shales was conducted using froth flotation in mechanical flotation cells. The objectives of this subtask have been to evaluate advanced technologies for the separation of kerogen from mineral matter and to determine which technologies might represent an improvement over prior technology.

Three technologies were selected for evaluation: column flotation, the air-sparged hydrocyclone, and the LICADO process. Column flotation and the air sparged cyclone are froth flotation processes. They are new technologies only in terms of the equipment in which the flotation process is conducted. These technologies were evaluated by MRI.

The LICADO process utilizes the property of organic matter, which tends to be wetted by liquid carbon dioxide in preference to water. When finely ground oil shale is agitated in a mixture of liquid CO_2 and water, and the immiscible phases are allowed to separate the kerogen tends to go into the CO_2 layer. Hydrophilic clay particles tend to segregate with the water, thus affecting a separation. The LICADO process was developed by the University of Pittsburgh and evaluated by them in this program.

Subtask 4.2.1. Column Flotation Tests

Column flotation is rapidly gaining wide acceptance in the mineral industries. The increasing popularity is due to the peculiar ability of column flotation cells to make efficient separation at very fine sizes. Typically a single stage of column flotation can replace as many as five consecutive stages of conventional flotation.

The efficiency of column flotation is normally attributed to two factors; effective countercurrent flow of solids relative to air bubbles, and the ability to wash the froth. Figure 4-40 shows the cross section of an idealized column flotation cell. Prepared feed enters the cell as a dilute slurry at a point in the upper portion of the column. Air is directed into the cell at the bottom. The air may be fed under pressure through a porous sparger or as a dispersion of very fine bubbles from an external bubble generator. Feed particles flowing downward are moving countercurrent to the rising bubbles. As a result, each particle is given opportunity to contact and attach to a bubble thereby insuring a high recovery of the kerogen. As the bubbles rise in the column they expand and coalesce to form a froth. The froth consists of kerogen coated air bubbles, water, and clay minerals entrained in the water. A spray of clean water is directed onto the top of the froth. As the spray water drains through the froth it washes out the entrained clay minerals cleaning the kerogen concentrate.

In contrast to column cells, conventional (or mechanical) flotation cells function as perfect mixers offering random opportunity for particles to encounter and adhere to bubbles. Recovery can be controlled by reflotation of the tailings or by increasing the retention time. Effective froth washing is not feasible with conventional cells and as a result cleaning of the concentrate is only achieved by reflotation of the froth product.

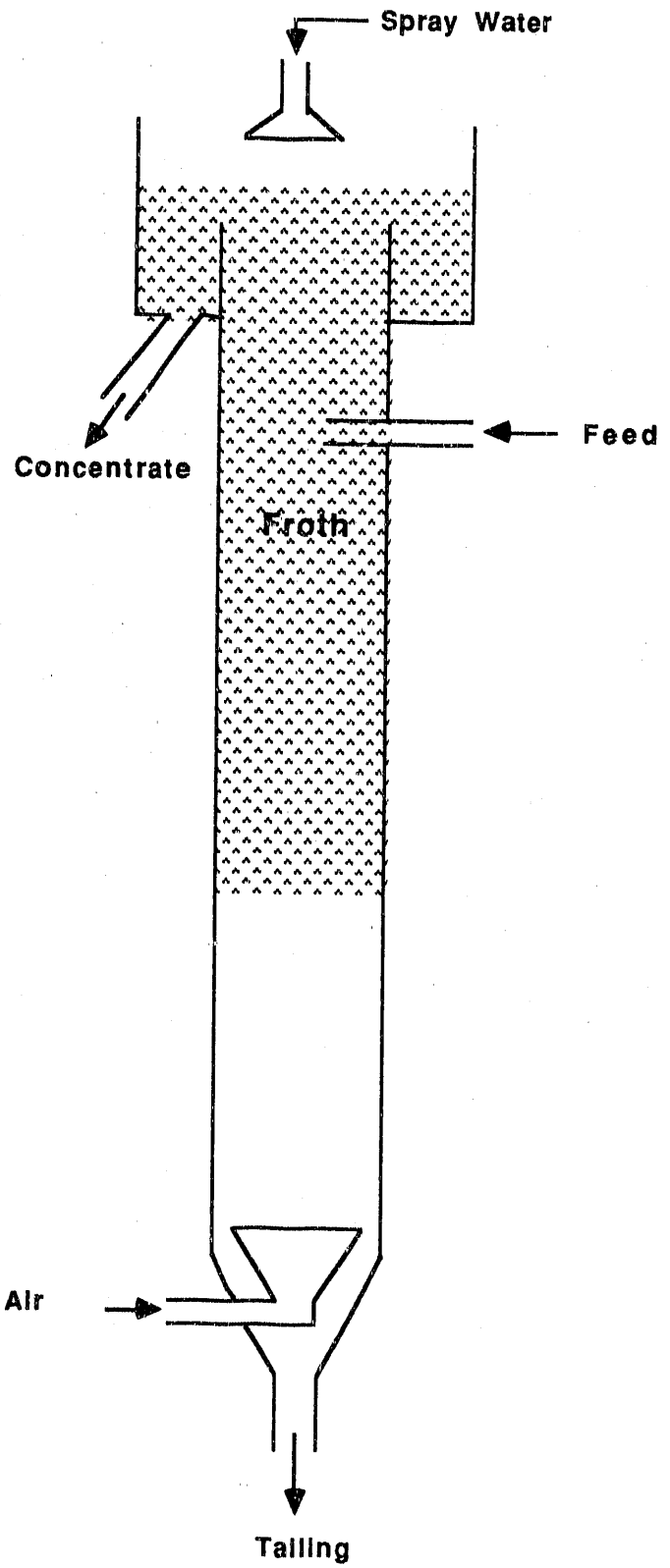

Figure 4-40. COLUMN FLOTATION CELL

Research Plan

The research conducted to evaluate column flotation and to define the preferred conditions for the separation of kerogen from mineral matter was carried out in four distinct phases. The first phase of testing was performed in batch mode for the purpose of screening a number of variables and their effect on oil recovery and concentrate grade. The second and longest phase of the program was performed to gain insight into the effects of several operating variables to compare column flotation with conventional flotation and to compare the behavior of the six oil shale samples used in the program. All tests in phase two were performed in a continuous (equilibrium) mode. The purpose of the third phase of testing was to determine the effect of increased height on column performance. The fourth and final phase of the test program was to define an efficient beneficiation flow scheme. The tests in this phase were interactive with tests being performed in Subtasks 4.1.3 Stirred Ball Mill Grinding and 4.1.4 Grinding Circuit Optimization.

Experimental Equipment and Procedure

Batch column flotation tests were performed using a laboratory column cell which was essentially as illustrated in Figure 4-40. The column was constructed of plexiglass tubing of 7.62 cm ID (3 inch) and was 109.2 cm (43 inch) in height. Air was supplied through a 5.1 cm (2 inch) diameter fritted glass sparger. The air sparger was removable. Three different spargers having average pore diameters of 15, 50 and 85 μm were used in the test program.

When performing tests in batch mode, the column was charged with an initial quantity of slurry at a preselected solids-to-water ratio. After charging the column, air and spray water were supplied at the desired rates of flow. Slurry from the bottom of the column was continuously recycled to a feed entry near the midpoint of the column through an external pump. Froth (concentrate) was collected continuously until it appeared barren of kerogen or until the slurry reached the top of the column. At that point the air and spray water were shut off and everything remaining in the column was taken as tailings.

This is a relatively rapid procedure but tends to obscure the effect of such variables as feed rate, percent solids and froth depth. All were found subsequently to have important effects on column flotation performance.

The arrangement of the column cell and auxiliary equipment for continuous flow testing is shown schematically in Figure 4-41. The feed pump (1) is filled with a sufficient volume of prepared sample to permit a large number of tests to be performed (typically 12). Past experience has shown this is necessary due to high sample variability and variability in the size distribution resulting from ultra fine grinding.

The feed slurry is maintained at abou 20% solids and is constantly recirculated and stirred. Sample is metered from the circulating pipe by a peristaltic pump (2). The feed slurry was diluted with reagentized water (3) by a second peristaltic pump (4). Wash water (5), also reagentized is supplied through a third peristaltic pump (6). While this feed system may seem complex it does permit varying either the wash water rate or the net

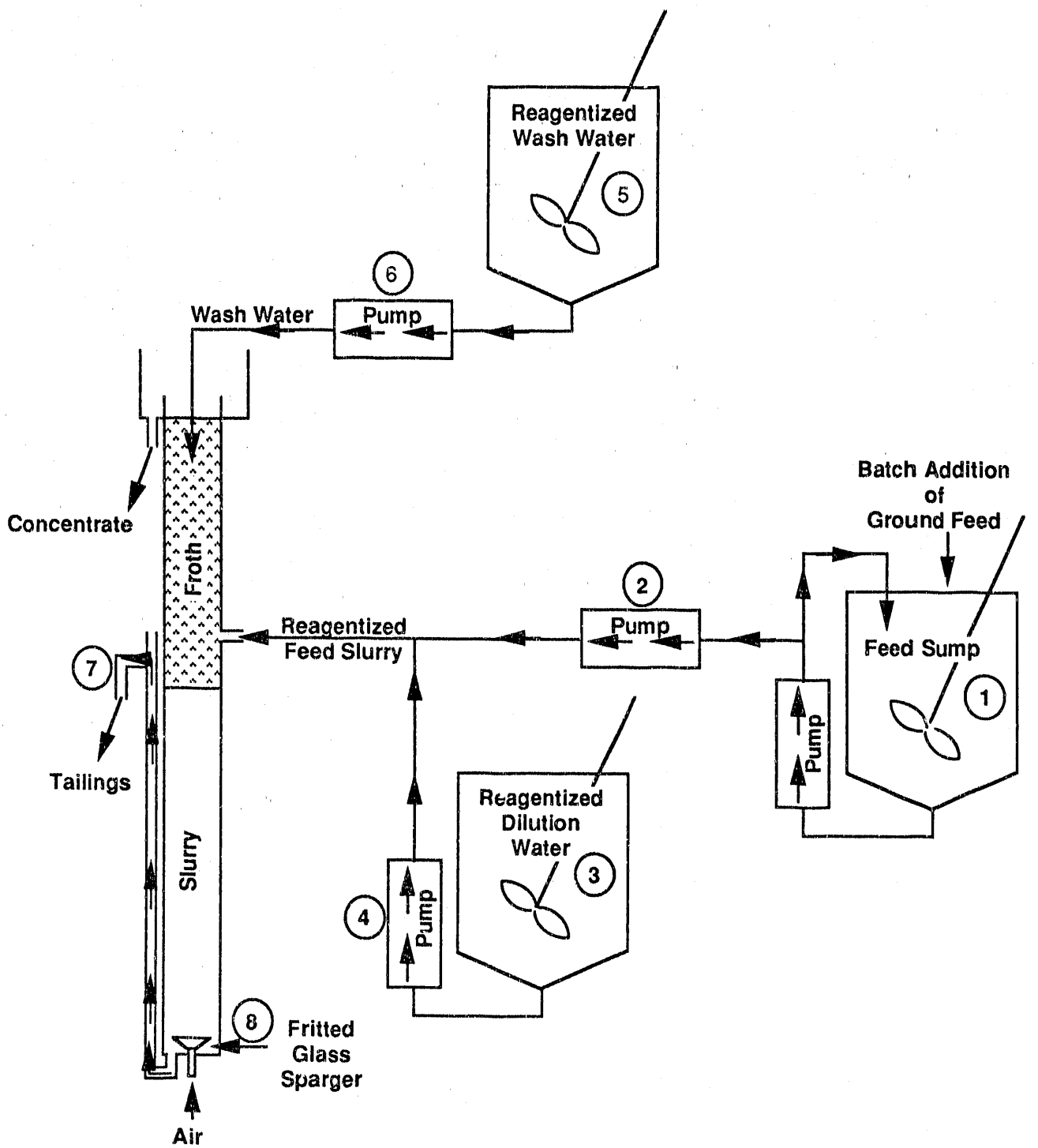

Figure 4-41. CONTINUOUS COLUMN FLOTATION CIRCUIT

solids content of the cell, and to maintain all conditions, including froth depth, constant within the period of each test.

Diluted feed enters the column through 1/4-inch diameter copper tubing and is discharged upwardly at the center of the column. Tailings are discharged through flexible tubing which can be adjusted so as to control the position of the pulp-froth interface.

In performing a series of tests both the concentrate and tailing are allowed to discharge continuously. The system is allowed to equilibrate for a period of 30 minutes after the pulp and froth reach operating levels. Concentrate and tailing samples are taken simultaneously for timed intervals (5 to 15 minutes, depending on the volume of sample desired). After sampling a change in operating conditions is made and the system is again allowed to equilibrate. Operating in this fashion a series of six tests can be performed in a day.

Beyond the first phase of column flotation tests, the results are presented in the form of grade vs. recovery curves. These curves are obtained by repeating each test condition at several air flow rates. The resulting grade-recovery curve represents the range of response possible at that condition. Thus, to judge the effect of frother dosage, for example, two grade-recovery curves would be developed and judgment is made on the relative position of the curves rather than on two single point responses.

Samples are analyzed by measuring their specific gravity with a helium pycnometer. Specific gravity is converted to Fischer Assay oil yield using a experimentally established relationship (Schultz and Bates, 1989). Because the Fischer Assay procedure has a high variability or experimental error the use of the specific gravity relationship has the effect of reducing the experimental error in our flotation tests. The same density to oil relationship was used by other investigators in this program (see Figure 4-70, p. 131).

Experimental Results and Discussion

Phase One

The objective of this phase was to screen a number of variables presumed to be critical to column flotation performance and to quantify their effects on separation, concentrate grade, and organic carbon recovery. Five variables were selected for these screening tests. A factorial experiment was designed in which each variable was tested at two levels plus six replicate centerpoints. The variables tested, together with their coded and absolute levels, are presented in Table 4-29.

The screening tests were performed on a sample of Alabama (Chattanooga) shale which had been ground to d_{90} = 12.6 µm and d_{50} = 4.7 µm. An analysis of the Alabama oil shale used in this experiment is as follows:

Fisher Assay	= 11.7 gal/ton (48.8 L/metric ton)
Carbon	= 15.53%
Hydrogen	= 1.63%
Nitrogen	= 0.41%
Sulfur	= 7.66%

Table 4-29. CODED AND ACTUAL FACTOR LEVELS FOR THE FACTORIAL EXPERIMENTS ON COLUMN FLOTATION OF ALABAMA OIL SHALE

Variable	Units	Coded Values -1	0	+1
Air Sparger Pore Size	μm	15	50	85
Air Flow Rate	SPLM	3	5	7
Frother (MIBC)	ppm	40	60	80
Percent Solids	%	3	5	7
Sodium Silicate	lb/ton	0	5	10

The tests were performed in batch mode as previously described. Both concentrate and tailing products were analyzed for carbon, hydrogen, nitrogen, and sulfur. The coefficient of separation for carbon and the Fischer Assay of the products were calculated from the analyses. The coefficient of separation for carbon is defined as the carbon recovery less the fraction of the non-carbon material recovered in the concentrate. It is a measure of separation efficiency that was used in the factorial experiment as the primary response (Schulz, 1970).

The results of the factorial experiment are presented in total in Table 4-30. A multiple regression analysis on these data yielded the following equation for the coefficient of separation:

$$CS = 0.7761 - 0.04151\ X_1 - 0.002115\ X_2 - 0.01908\ X_3 + 0.003443\ X_4 - 0.000409\ X_1X_2 - 0.000419\ X_1X_4 \quad (26)$$

where --

CS = Coefficient of separation

X_1 = Air flow rate (SLPM)

X_2 = Sparger Pore Size (μm)

X_3 = Feed Pulp Density (percent solids)

X_4 = Frother Concentration (ppm)

As might be expected, air flow rate was found to be the most important variable but appeared to have a negative effect on separation efficiency. Frother level shows a positive effect on separation efficiency but appears to be a much less important variable than might be expected.

The data from the factorial experiment were further evaluated with respect to concentrate grade and carbon recovery. The models derived from this analysis were as follows:

Table 4-30. RESULTS OF FACTORIAL EXPERIMENT ON COLUMN FLOTATION OF ALABAMA SHALE

Air Sparger Pore Size	% Solids	Air Flow Rate	Frother	Sodium Silicate	Separation Coefficient, Carbon	Carbon Grade, wt %	Carbon Recovery, %	Oil Yield, gal/ton
-1	-1	-1	-1	-1	0.58	45.72	73.8	39.0
-1	-1	-1	-1	+1	0.66	42.06	86.9	35.7
-1	-1	-1	+1	-1	0.63	34.68	94.3	29.0
-1	-1	-1	+1	+1	0.65	42.73	83.3	37.2
-1	-1	+1	-1	-1	0.29	19.76	97.1	15.5
-1	-1	+1	-1	+1	0.23	18.55	98.3	14.4
-1	-1	+1	+1	-1	0.34	20.65	97.0	16.3
-1	-1	+1	+1	+1	0.29	19.61	97.1	15.4
-1	+1	-1	-1	-1	0.61	33.49	93.0	27.9
-1	+1	-1	-1	+1	0.35	42.74	46.0	36.0
-1	+1	-1	+1	-1	0.57	31.65	90.3	26.3
-1	+1	-1	+1	+1	0.56	30.32	92.7	25.1
-1	+1	+1	-1	-1	0.28	19.57	97.1	15.4
-1	+1	+1	-1	+1	0.24	18.92	96.1	14.8
-1	+1	+1	+1	-1	0.26	18.85	97.7	14.7
-1	+1	+1	+1	+1	0.21	18.34	96.1	14.3
+1	-1	-1	-1	-1	0.62	38.97	84.7	32.9
+1	-1	-1	-1	+1	0.58	39.67	79.0	33.5
+1	-1	-1	-1	-1	0.60	41.45	82.1	35.1
+1	-1	-1	+1	+1	0.59	42.34	78.5	35.9
+1	-1	+1	-1	-1	0.50	27.35	94.7	22.4
+1	-1	+1	-1	+1	0.45	24.78	94.8	20.1
+1	-1	+1	+1	-1	0.40	23.08	95.7	18.5
+1	-1	+1	+1	+1	0.37	22.08	95.7	17.6
+1	+1	-1	-1	-1	0.48	46.40	60.1	39.6
+1	+1	-1	-1	+1	0.43	38.90	59.6	32.8
+1	+1	-1	+1	-1	0.58	36.93	83.7	31.0
+1	+1	-1	+1	+1	0.58	38.49	81.8	32.5
+1	+1	+1	-1	-1	0.39	22.60	95.8	18.1
+1	+1	+1	-1	+1	0.37	22.13	95.6	17.7
+1	+1	+1	+1	-1	0.32	20.67	96.9	16.4
+1	+1	+1	+1	+1	0.33	20.73	96.4	16.4
0	0	0	0	0	0.45	25.06	95.0	20.3
0	0	0	0	0	0.44	24.49	95.5	19.8
0	0	0	0	0	0.46	25.34	94.7	20.6
0	0	0	0	0	0.45	25.03	94.6	20.3
0	0	0	0	0	0.43	25.66	91.5	20.9
0	0	0	0	0	0.45	25.25	94.3	20.5

For concentrate grade (% carbon)

$$G = 5957 - 3.622\ X_1 + 0.0427X_2 - 0.6836\ X_3 - 0.0594\ X_4 \quad (27)$$

and for carbon recovery %

$$R = 63.786 + 3.4037\ X_1 - 0.0550\ X_2 - 0.8453\ X_3 + 0.1667\ X_4 \quad (28)$$

When considered in total, the models are consistent with expectations. For example, an increase in air flow rate or frother concentration tends to increase carbon recovery and decrease concentrate grade. An increase in sparger pore size accomplishes the opposite effect. Increasing pulp density is detrimental to both grade and recovery. All variables tend to appear more significant with respect to concentrate grade or carbon recovery than with respect to the composite coefficient of separation. Note that in no case does the addition of sodium silicate appear to have an effect and hence does not appear in the model equations.

Phase Two -- Alabama Shales

Beyond the first phase of this test, all column flotation tests were performed in the continuous flow or equilibrium mode described earlier. Initial tests utilized Alabama oil shale as the feedstock. The objectives of the initial testing, in addition to generating "material specific" information on the Alabama shale, were to establish a set of basic operating conditions which would serve as basis for comparing the response characteristics of the various shales, and to establish the reproducibility of individual tests.

Operating conditions for the initial tests were based on experience gained in the variable screening tests. These conditions were:

Feed Rate (dry solids)	=	12.5 g/min
Pulp Density	=	3.3%
Tailing Overflow Height	=	56 cm
Wash Water Rate	=	130 mL/min
Frother (Dowfroth 250)	=	30 ppm

Note that air flow rate, the most important of the variables screened in the factional experiment described previously, is not included in this list. Because air flow is a dominant variable it was decided that it would be used as a variable in each test while all other conditions were held constant.

The response to each test, then, was not a single point but a curve representing the full array of possible outcomes at a single condition. The data plotted in these curves are the grade of the concentrate (i.e., oil yield in gal/ton) versus the recovery of oil on the concentrate.

This type of curve is a common method of characterizing a separation. It is known as a liberation curve in the minerals industry and a washability curve in the coal industry. In the format used in this report, a shift in the curve upward and to the right is indicative of a more efficient separator.

The use of the full grade-recovery curve to judge the response to a single variable avoids the ambiguities and possible errors that might result from a single point comparison.

Figure 4-42 shows the grade-recovery relationship for Alabama oil shale as a function of particle size. Curve A was developed for a feed sample that was ground to d_{90} = 18.6 μm and d_{50} = 6.3 μm. Individual points on the curve represent variations in air flow rate from 4.3 SLPM to 6.0 SLPM. Curve B shows the grade recovery relationship for a feed sample that had a d_{90} = 9.4 and d_{50} = 3.7 particle size and was tested at the same air flow rates. These curves show the expected effect of fine grinding and air flow rate. Curve A also shows that for this material, the fineness of grind limits the grade but not the recovery which is attainable. Note that a 94+ % recovery is achieved at a grade which is approximately twice the feed grade (shown as dashed line).

Figure 4-43 shows that an increase in frother concentration noticeably improves the character of the separation achieved. Curve C was obtained at a frother concentration of 42 ppm (2.5 lb/ton) while Curve B was at the baseline condition of 30 ppm.

An attempt was made to improve the recovery noted in Curve B by increasing the retention time in the cell. In this instance, the retention time was increased by raising the level of the tailing discharge (and with it the pulp froth interface) thereby increasing the pulp volume. The resulting grade-recovery Curve D (Figure 4-44) showed a decrease in recovery rather than the expected increase. It was subsequently noted that the significant difference in the two curves was that in Curve D the feed was introduced into the cell at a point above the pulp-froth interface whereas in Curve B the feed was directed into the pulp phase. This observation indicates that the froth zone in a column flotation cell can have a major role in particle collection (recovery) as well as product cleaning. This observation may be contrary to popular notions concerning column flotation but is consistent with what is being done in froth separators (Young, 1982) and the observations made in a packed column (Yang, 1988).

The effect of increasing wash water rate is illustrated by Figure 4-45. Curve C as described earlier was developed at a frother concentration of 42 ppm and the baseline wash water rate of 130 mL/min. Curve E shows the effect of increasing the wash water rate to 180 mL/min. The grade recovery curve is shifted to generally less favorable results.

Earlier it was stated that one objective of the early continuous flow tests was to establish the reproducibility of tests performed in this manner. This was accomplished by taking consecutive five minute samples immediately following a change in operating conditions. Table 4-31 shows the results of two such experiments. The first set of data show the effect of an increase in air flow while the second set of data were taken after the height of the pulp-froth interface was raised. Note that in both cases the weights of the products equilibrated quite rapidly, (within the first 10 to 15 minutes) while the analyses of the products continued to drift for a longer period of time. These data confirmed the practice of waiting for a period of at least 30 minutes, after making a change in the system, before sampling.

Phase Two -- Indiana Shales

A series of sixteen tests were performed on a sample of Indiana (New Albany) shale. The shale had been ground to 90% finer than 10 μm and had an average particle size of 3.5 μm.

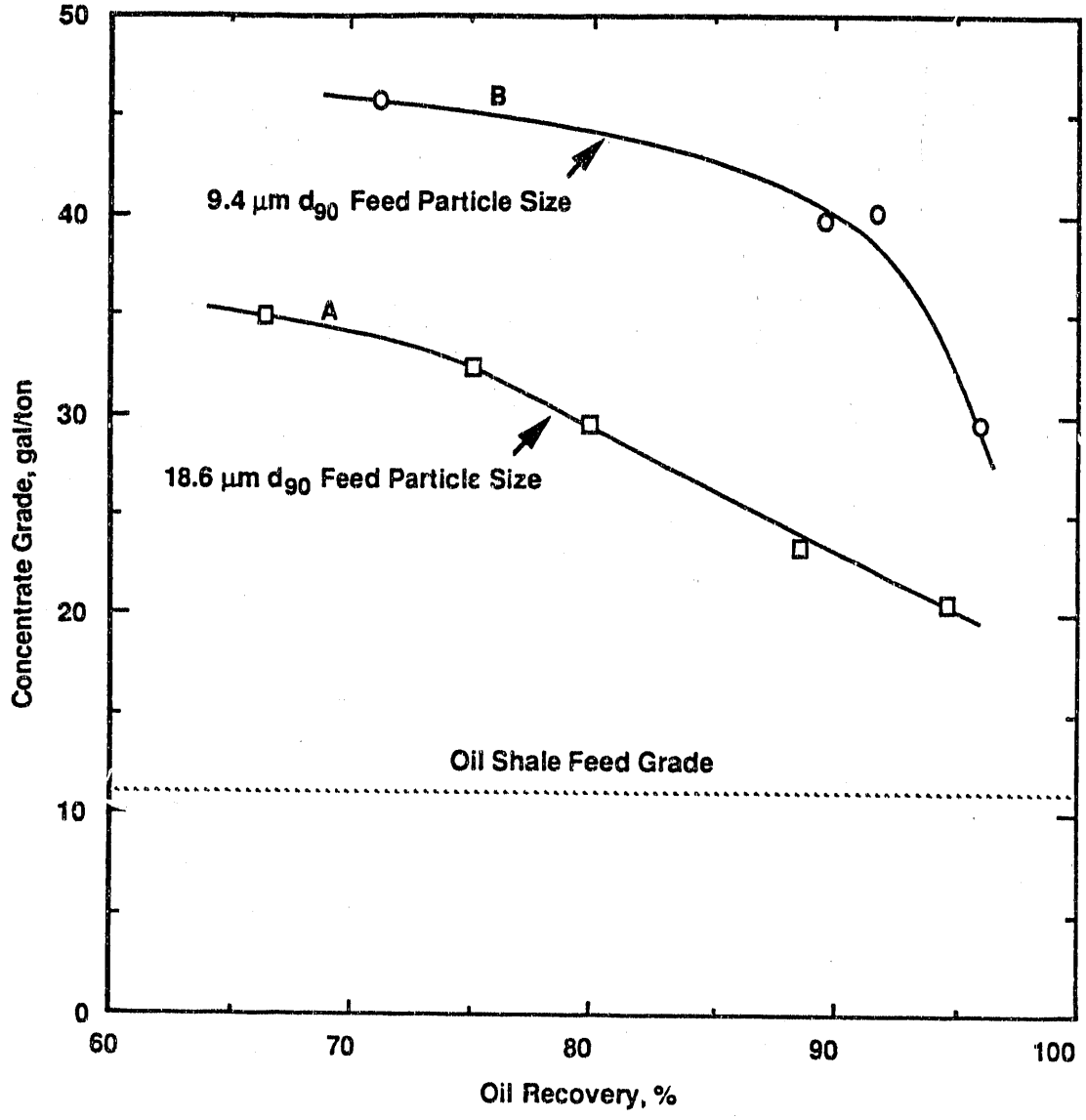

Figure 4-42. THE EFFECT OF FEED PARTICLE SIZE ON GRADE-RECOVERY RELATIONSHIP FOR COLUMN FLOTATION OF ALABAMA OIL SHALE

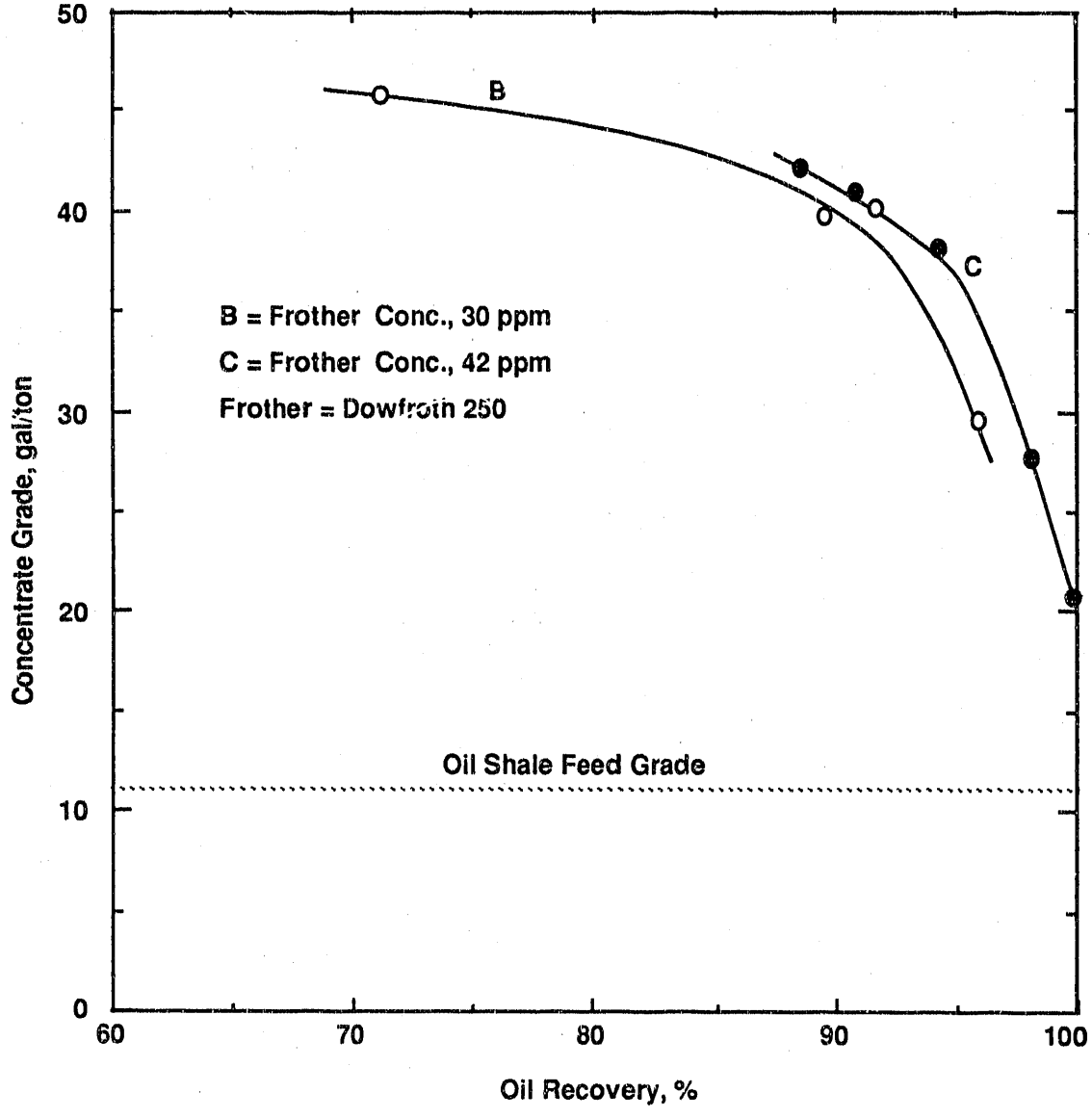

Figure 4-43. EFFECT OF FROTHER CONCENTRATION ON GRADE-RECOVERY RELATIONSHIP FOR ALABAMA OIL SHALE

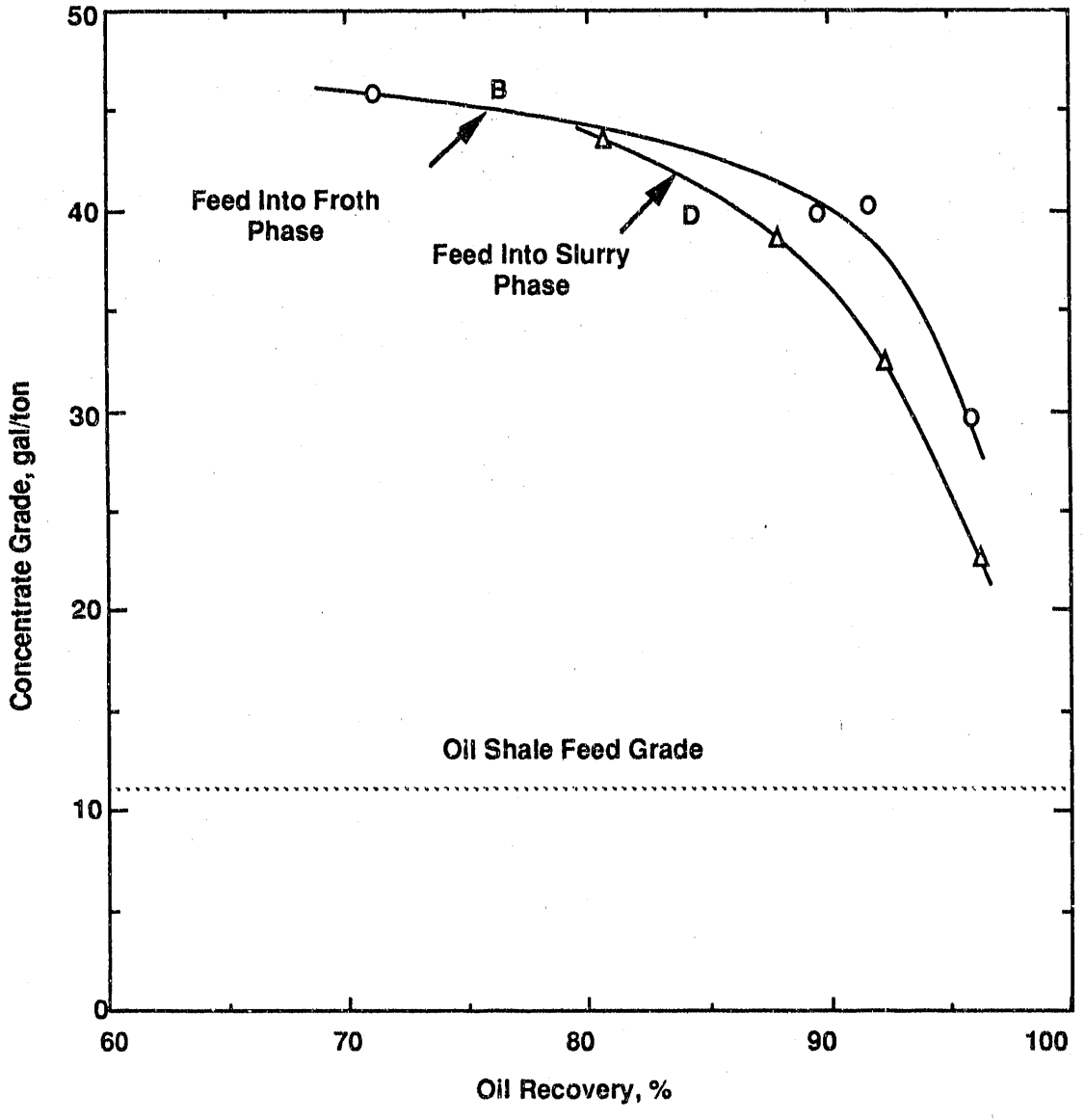

Figure 4-44. EFFECT OF FEED ENTRANCE POSITION ON COLUMN FLOTATION PERFORMANCE

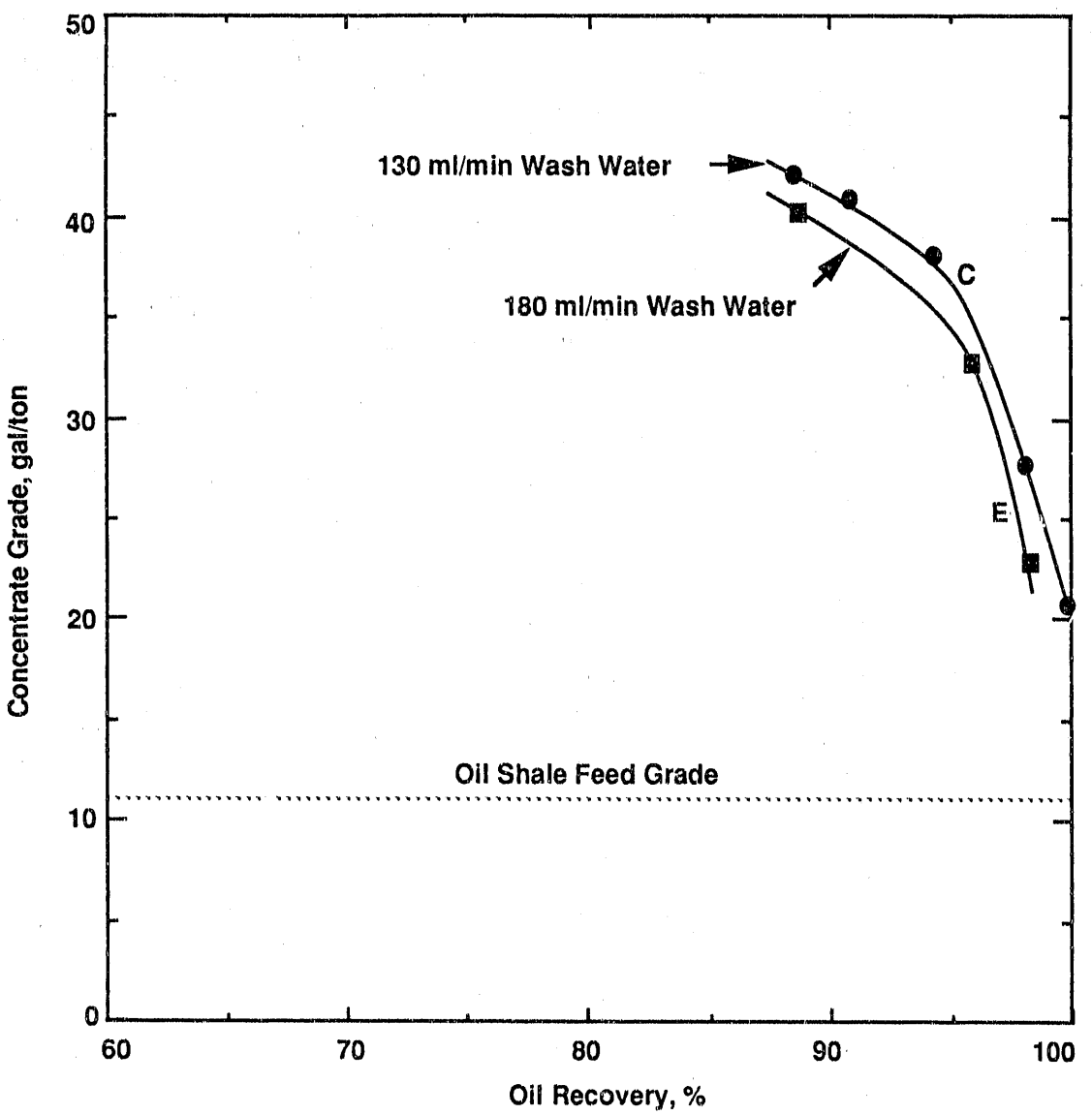

Figure 4-45. EFFECT OF WASH WATER ADDITION ON COLUMN FLOTATION PERFORMANCE

Table 4-31. TIMED SAMPLES OF FLOTATION PRODUCTS

(a) Following an Increase in Air Flow

Sample No.	Concentrate Weight, g	Tailing Weight, g	Carbon Content, % Concentrate	Tailing
1	32.6	41.8	36.26	7.04
2	23.0	47.1	34.73	6.98
3	Lost	--	--	--
4	24.6	47.9	37.14	6.76
5	23.4	48.1	34.98	6.48
6	23.0	47.7	35.02	6.30
7	14.7	49.5	34.71	6.30
8	22.7	46.8	35.05	6.02
9	22.7	48.5	35.55	6.58
10	23.1	46.3	35.01	6.05

(b) Following an Increase in Pulp Height

1	32.2	7.9	29.99	6.56
2	31.3	35.2	28.20	5.80
3	32.3	39.5	28.68	5.88
4	30.3	38.1	28.80	5.47
5	30.8	38.1	28.58	5.46
6	31.7	38.2	28.31	5.23
7	29.7	36.5	28.17	5.19
8	30.9	37.9	28.03	5.12

The purposes of this series of tests were to gain further insight into the effect of column operating parameters and to establish conditions for the production of a bulk concentrate of Indiana shale (Task 7.2). The average analyses of the Indiana shale used in the program are as follows:

Fischer Assay = 14.03 gal/ton (58.5 L/metric ton)
Carbon = 13.45%
Hydrogen = 1.74%
Nitrogen = 0.50%
Sulfur = 3.07%

Figure 4-46 compares the grade-recovery relationships generated at two pulp-froth interface levels. These data show that a more favorable grade-recovery relationship is obtained at lower pulp levels. This observation is an extension of the results reported earlier (Figure 4-45) and further emphasizes the importance of the froth phase in recovery as well as in concentrate grade. The lower grade-recovery curve in Figure 4-46 was obtained at the same conditions as Curve C of Figure 4-43. A comparison of the two curves shows that the Alabama shale yields more favorable results at essentially the same fineness of grind. This difference may be attributed to a difference in the liberation of the two shales or the differences in their surface character.

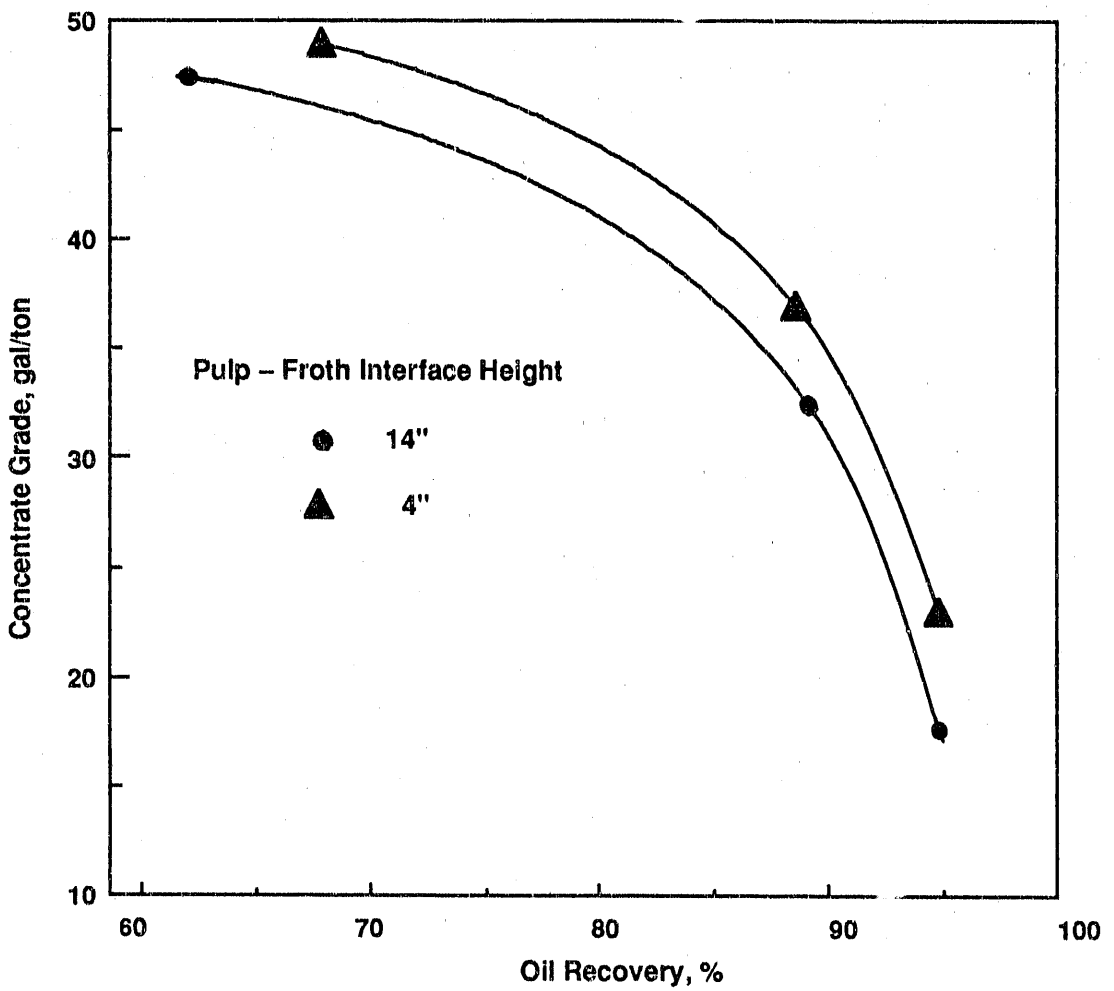

Figure 4-46. EFFECT OF PULP-FROTH INTERFACE POSITION ON FLOTATION OF INDIANA OIL SHALE

Figure 4-47 shows the effects of feed rate and frother concentration on the flotation of Indiana oil shale. The four points shown are all at the same air flow rate. Points A and B were obtained at a feed rate of 6.25 g/min, while Points C and D were obtained at a feed rate of 12.5 g/minute. Clearly, decreasing the feed rate improved the grade of concentrate with virtually no effect on oil recovery. The effect of increased frother concentration is seen by comparing Points A and C (42 ppm) with Points B and D (60 ppm). Oil recovery is increased, but with large decreases in concentrate grade. Note, however, that the effect of increased frother concentration is diminished at lower feed rates (that is, A-B < C-D).

Other tests performed on samples of the Indiana shale indicated that additions of sodium silicate (a dispersant) had no effect on flotation performance.

Phase Two -- Shale Comparisons

The purpose of this series of tests was to determine the relative response of all the shales included in this program to a standard column flotation test. Grade-recovery curves, at 30 and 45 ppm frother, are presented for the Kentucky, Michigan, Ohio, and Tennessee shale in Figures 4-48 through 4-51, respectively. In each case a grade recovery curve representing several stages of conventional cell flotation is also presented.

Note that in all cases the higher frother concentration yields the more favorable results. It is also shown that in most cases the column flotation approaches the results which are achieved in four or five stages of conventional flotation.

Figure 4-52 compares the grade-recovery curves generated for each of the six shales included in this program. The six shales differ widely in their response with the Alabama (Chattanooga) shale being the most readily treatable and the Ohio (Cleveland) the least amenable to beneficiation. The six shales were tested under similar conditions, i.e., feedrate of 12.5 g/min, 3.3 weight percent solids and frother concentration of 45 ppm with the exception of the Michigan and Ohio shales, which are shown at 30 ppm. Note also that the Ohio shale yields a grade-recovery curve of anomalous form. No explanation can be offered at this time.

Phase Three -- Optimization Tests

The objectives of this phase were to optimize the flotation of the Alabama and Indiana shales and to investigate the effects of column design parameters. To achieve these objectives a new flotation column was constructed. The column was of the same diameter as the column described earlier but was built in sections so as to permit variation in column height. The maximum height used in this investigation was 63 inches (1.6 m). The new column was also fitted with multiple access ports to permit changes in the feed entry position.

Figure 4-53 shows the effect of column height and feed inlet position on the flotation of Alabama shale. The sample was somewhat coarser than had been used in previous tests with a d_{90} = 12.2 μm. The data show that at the shorter column height the position of the feed inlet has a marked effect on

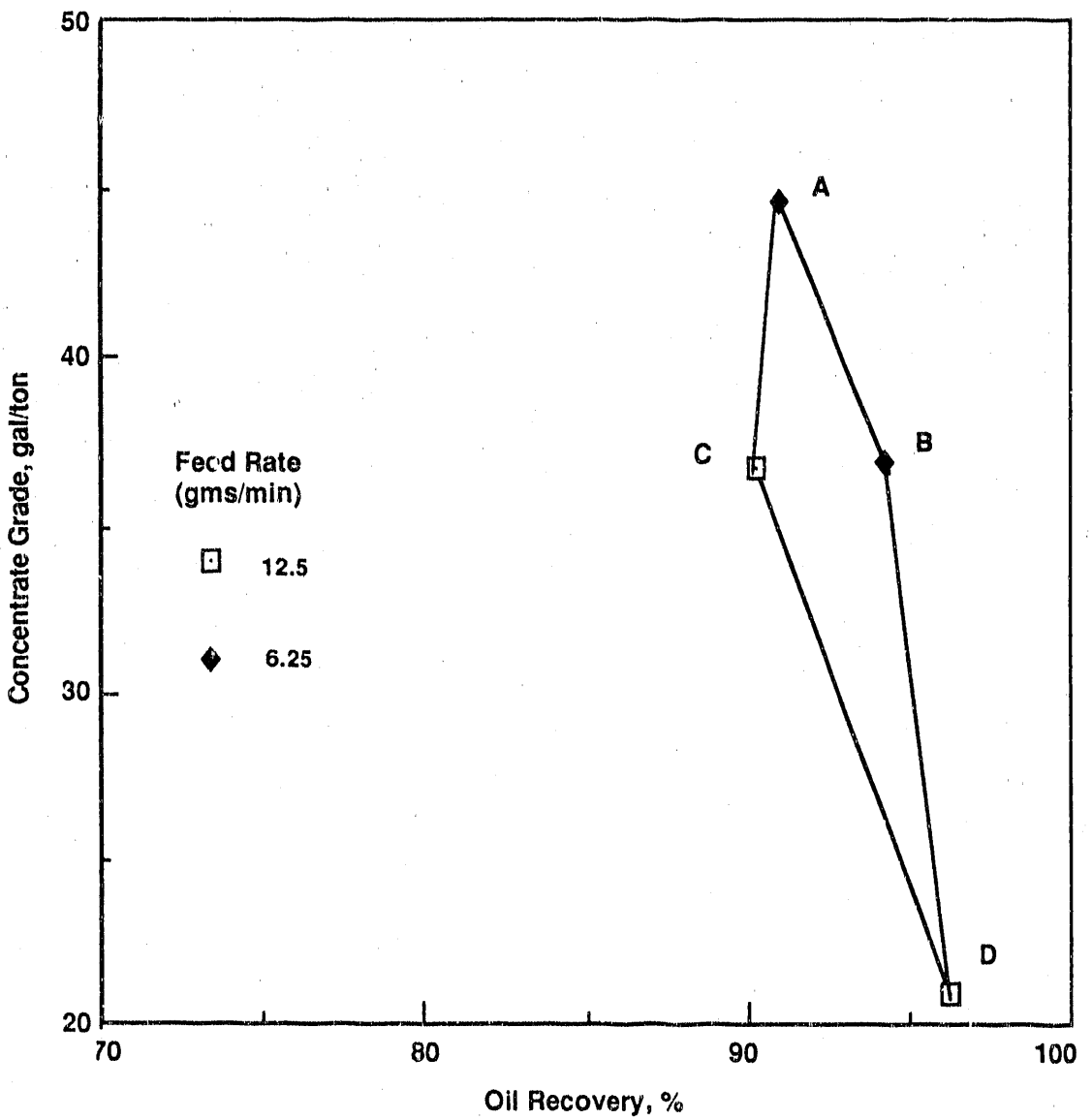

Figure 4-47. THE EFFECT OF FEED RATE AND FROTHER LEVEL ON THE FLOTATION OF INDIANA OIL SHALE

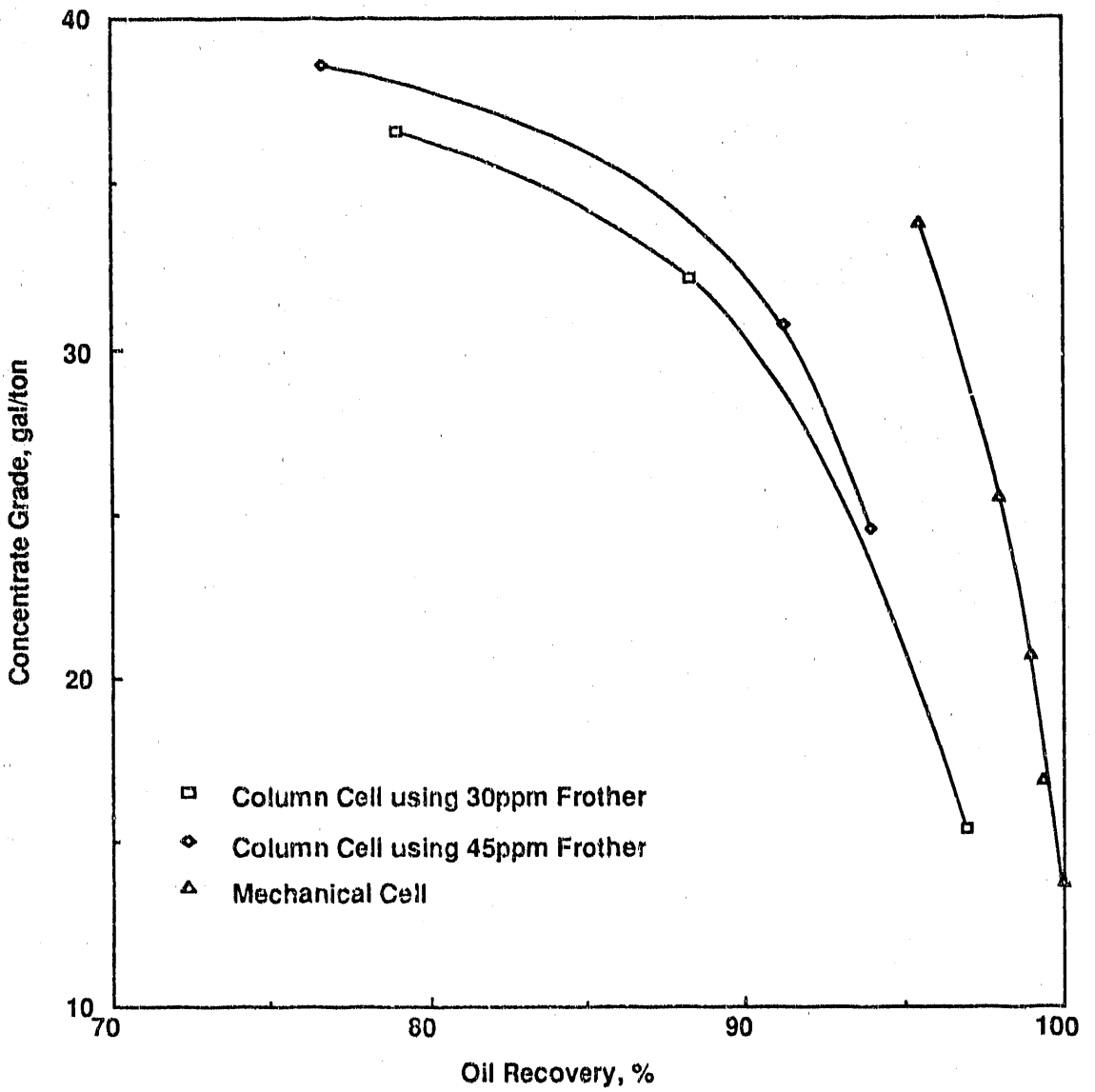

Figure 4-48. KENTUCKY SHALE -- COMPARISON OF MECHANICAL AND COLUMN FLOTATION CELLS

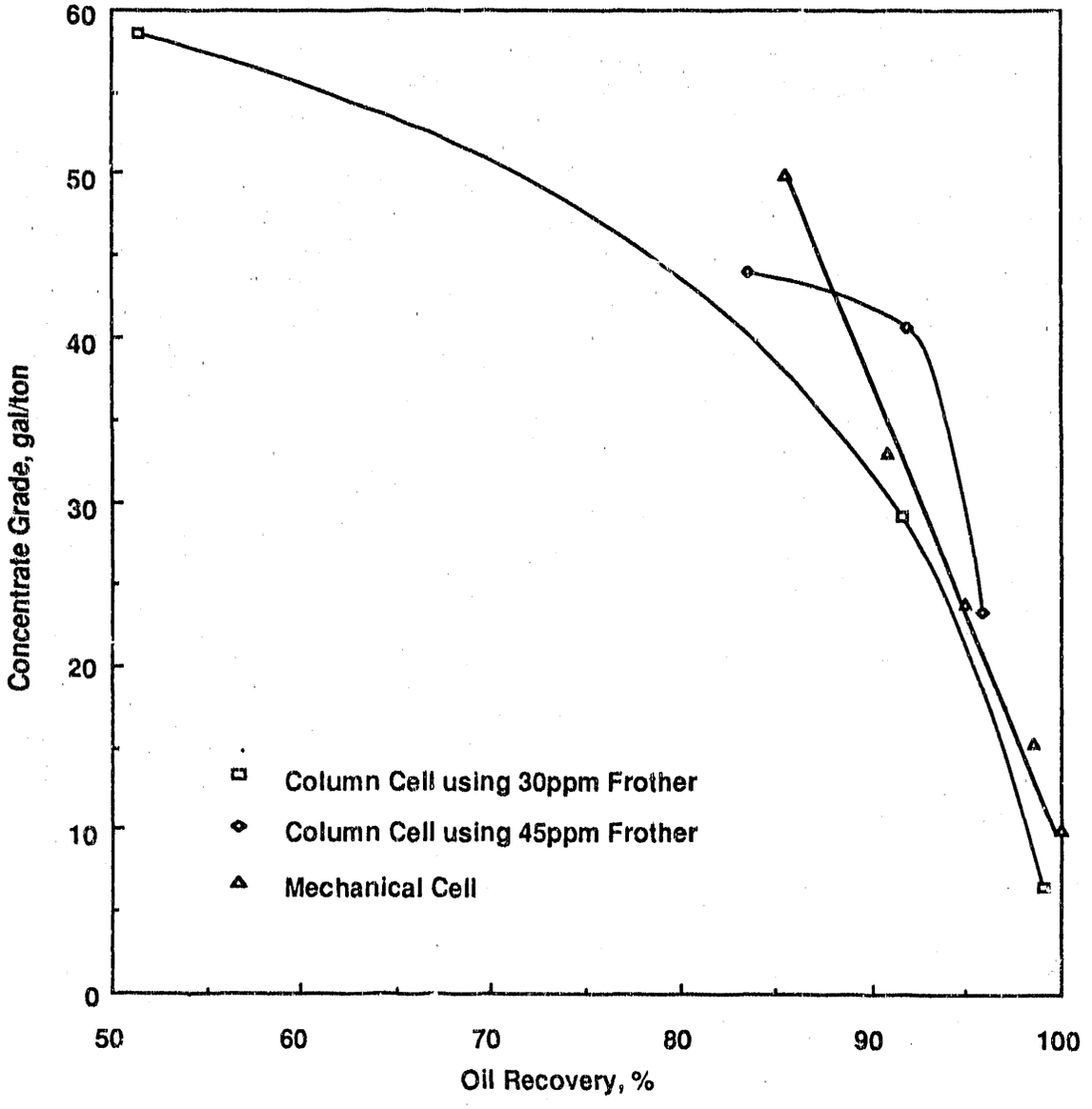

Figure 4-49. MICHIGAN SHALE -- COMPARISON OF MECHANICAL AND COLUMN FLOTATION CELLS

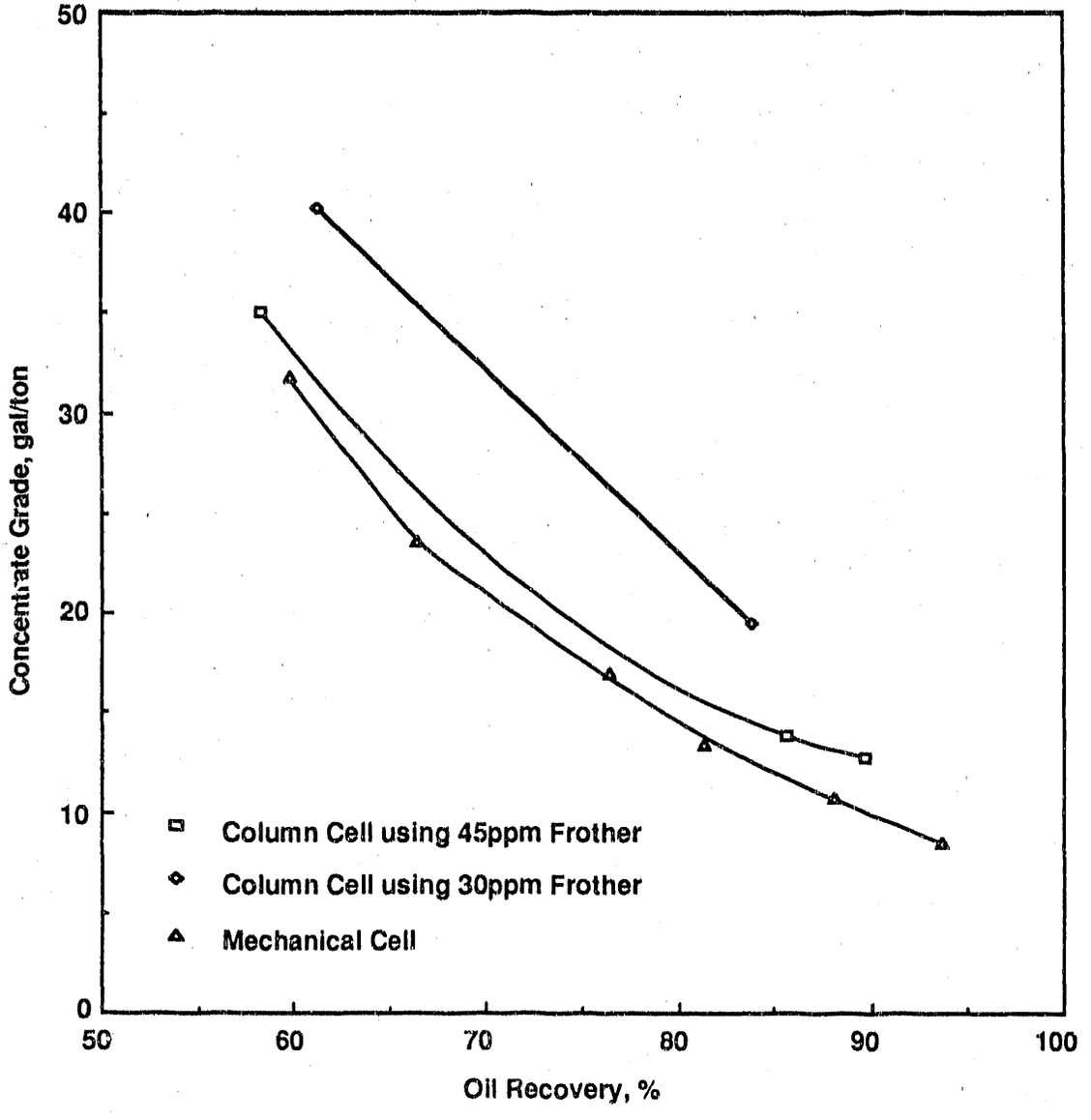

Figure 4-50. OHIO SHALE -- COMPARISON OF MECHANICAL AND COLUMN FLOTATION CELLS

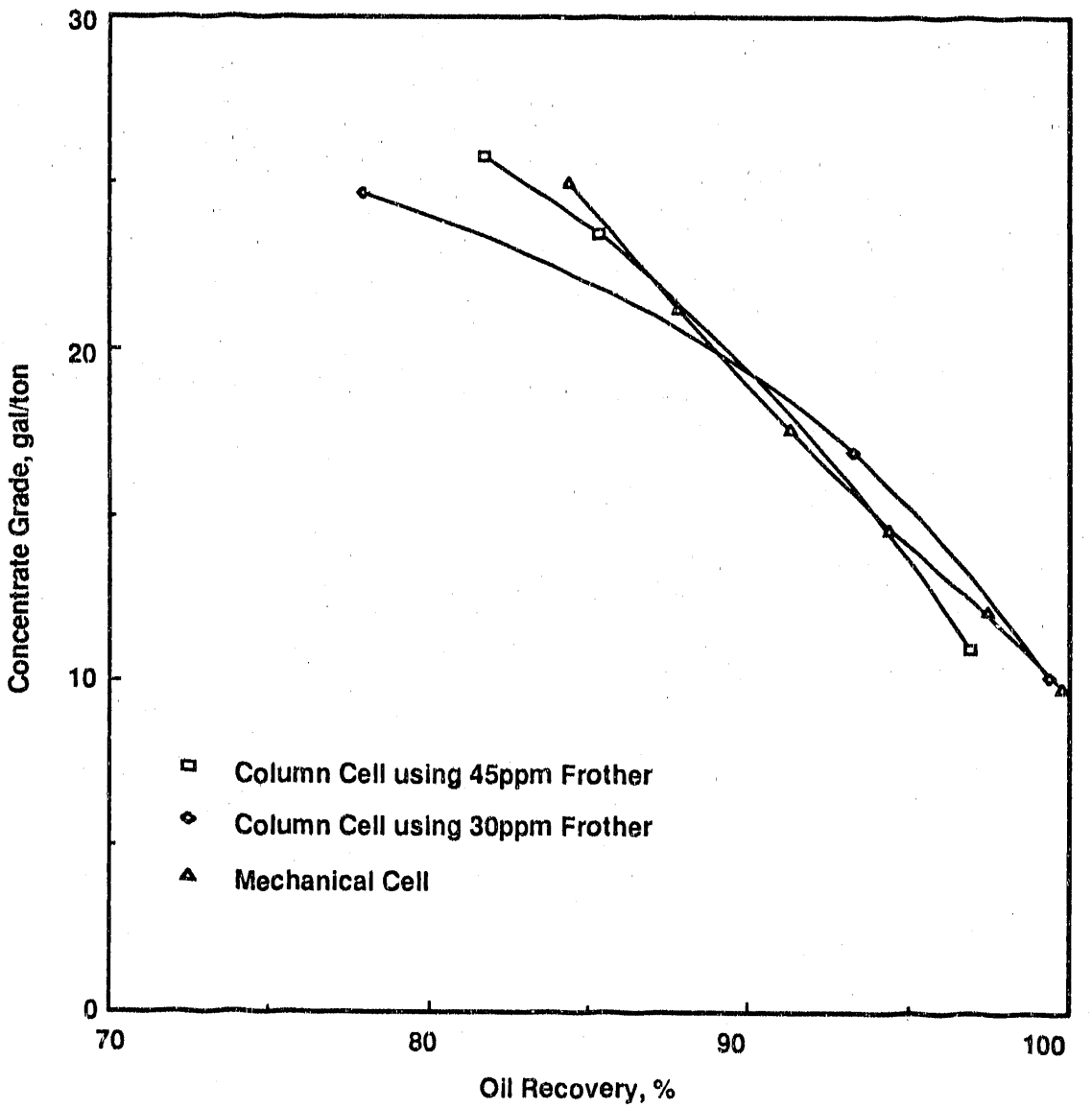

Figure 4-51. TENNESSEE SHALE -- COMPARISON OF MECHANICAL AND COLUMN FLOTATION CELLS

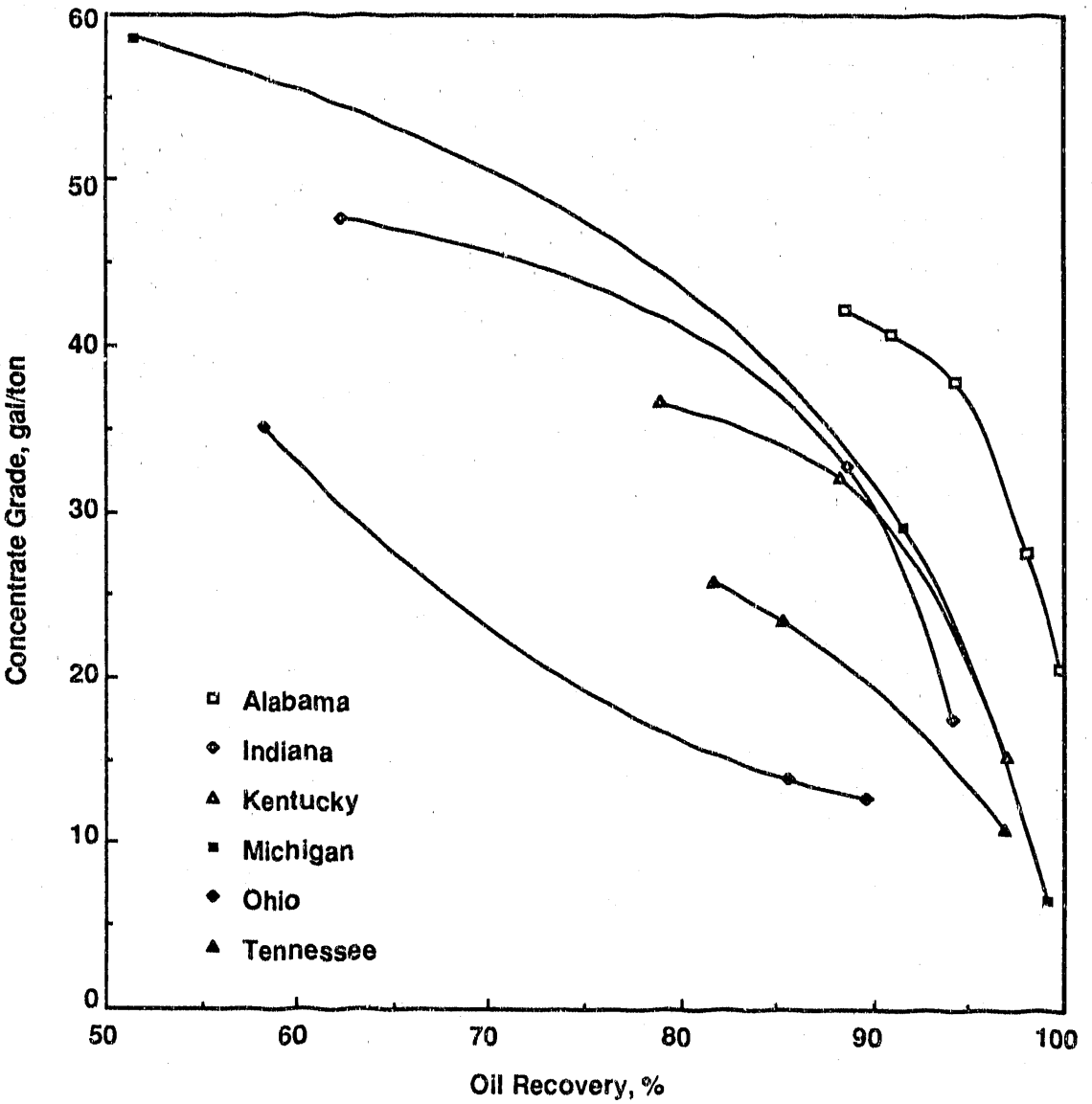

Figure 4-52. FLOTATION CHARACTERISTICS OF SIX EASTERN OIL SHALES

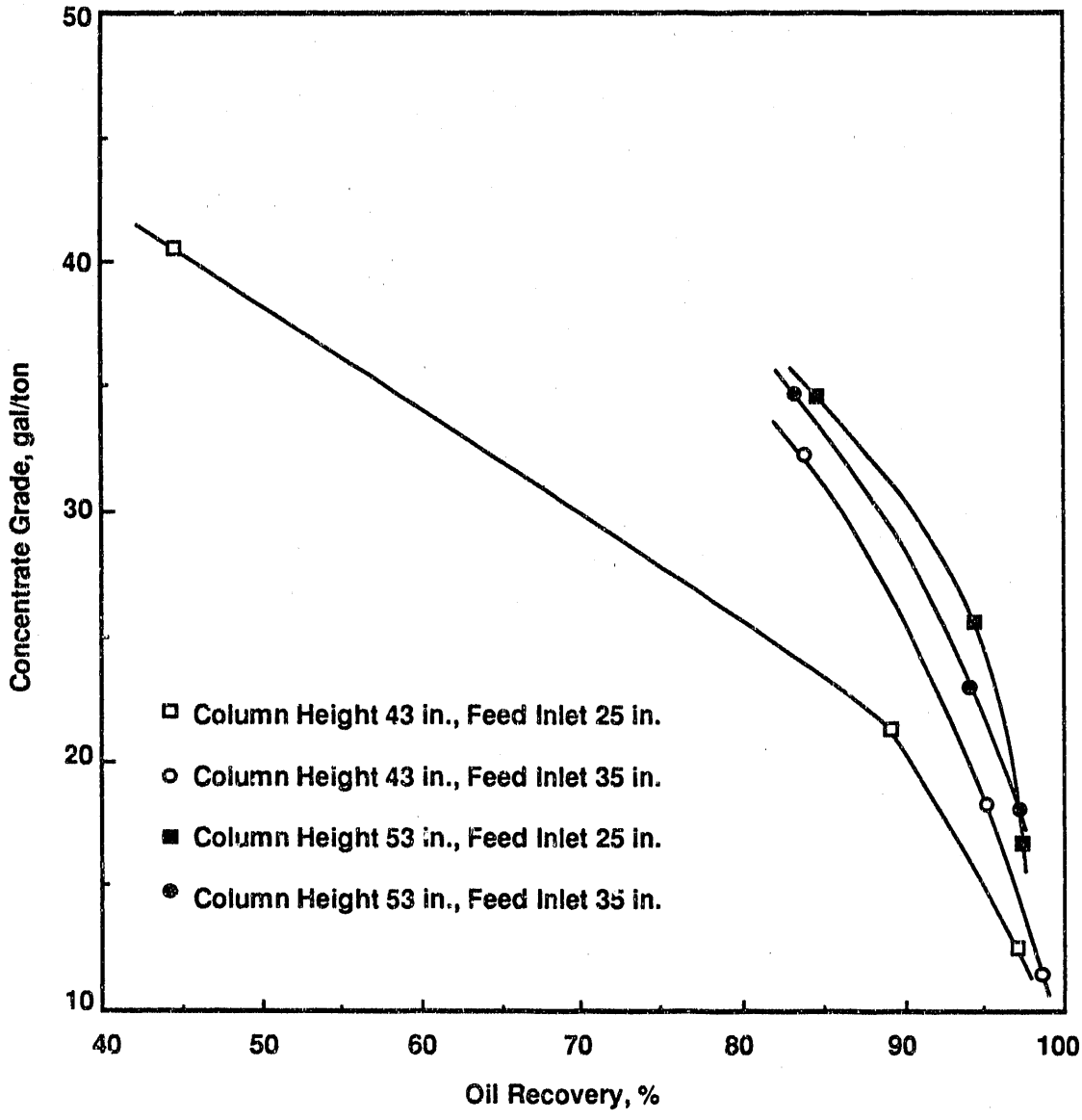

Figure 4-53. THE EFFECT OF COLUMN HEIGHT AND FEED INLET POSITION ON THE FLOTATION OF ALABAMA OIL SHALE

flotation performance. At the greater column height the effect of feed inlet position is greatly diminished. It is difficult to state that a difference exists in the two upper curves. These data further imply an interaction between column height and feed entry position. In all four cases shown the feed was directed into the froth phase, and the pulp-froth interface maintained constant at 14 inches (35.6 cm) above the sparger face.

The effects of air sparger pore size and column height are shown in Figure 4-54. At the 43-inch (109 cm) column height, the finer pore size (and presumably finer bubble size) improves the grade-recovery relationship. At a height of 53-inches (135 cm), the effect of sparger pore size essentially disappears. The data are similar to those shown in Figure 4-53 and also imply an interaction between column height and air sparger pore size.

Figures 4-53 and 4-54, when considered jointly, show that column height is an important design parameter and that increases in column height improve the quality of separation by flotation. On the basis of these observations an experiment was performed to determine whether increased column height could offset the detrimental effects of increased solids concentration which had been observed in phase one. A sample of Indiana shale ground to d_{90} = 11.9 μm was used for this purpose. A baseline grade-recovery curve was established at a column height of 43 inch with a feed rate of 380 mL/min at 3.3% solids. This curve is presented in Figure 4-55 together with grade-recovery curves for operation at 7% solids in 43- and 63-inch columns. The data show that increased solids are detrimental to the quality of separation achieved. However, an increase in column height from 43 to 63 inches more than compensates for the increased solids and yields a grade-recovery relationship superior to the base case. In each of these three cases, the pulp froth interface position was maintained at 14 inches above the sparger face. Thus, with a constant pulp volume and feed rate the residence time in the cell was essentially constant. Therefore, the effects noted can be attributed only to column height and percent solids.

The uppermost curve in Figure 4-55(D) shows that an increase in residence time, brought about by a decrease in slurry feed rate, results in still further improvement in the grade-recovery relationship.

Froth washing is thought to be one of the attributes of column flotation that contributes to its efficiency and its ability to produce clean concentrate. An experiment was undertaken to isolate the effect of wash water additions and to quantify the effect on concentrate grade and oil recovery. A series of twelve tests were performed in the 53-inch column in which four levels of wash water addition including zero were tested, each at three rates of air flow. At each wash water addition rate the dilution water was adjusted so as to maintain the percent solids in the cell constant at 3.3%. The effect of wash water addition was therefore isolated from any effect due to changes in solids concentration.

Figure 4-56 shows the effect of spray water addition rate on oil recovery. As the spray water rate is increased from 0 to 65 mL/min the recovery decreases (at low air flow rates) and increases thereafter. At 130 and 195 mL/min spray water rates, the recovery is higher than at the base level (no spray water). The fact that recovery is improved at the highest spray water rates is contrary to what had been expected.

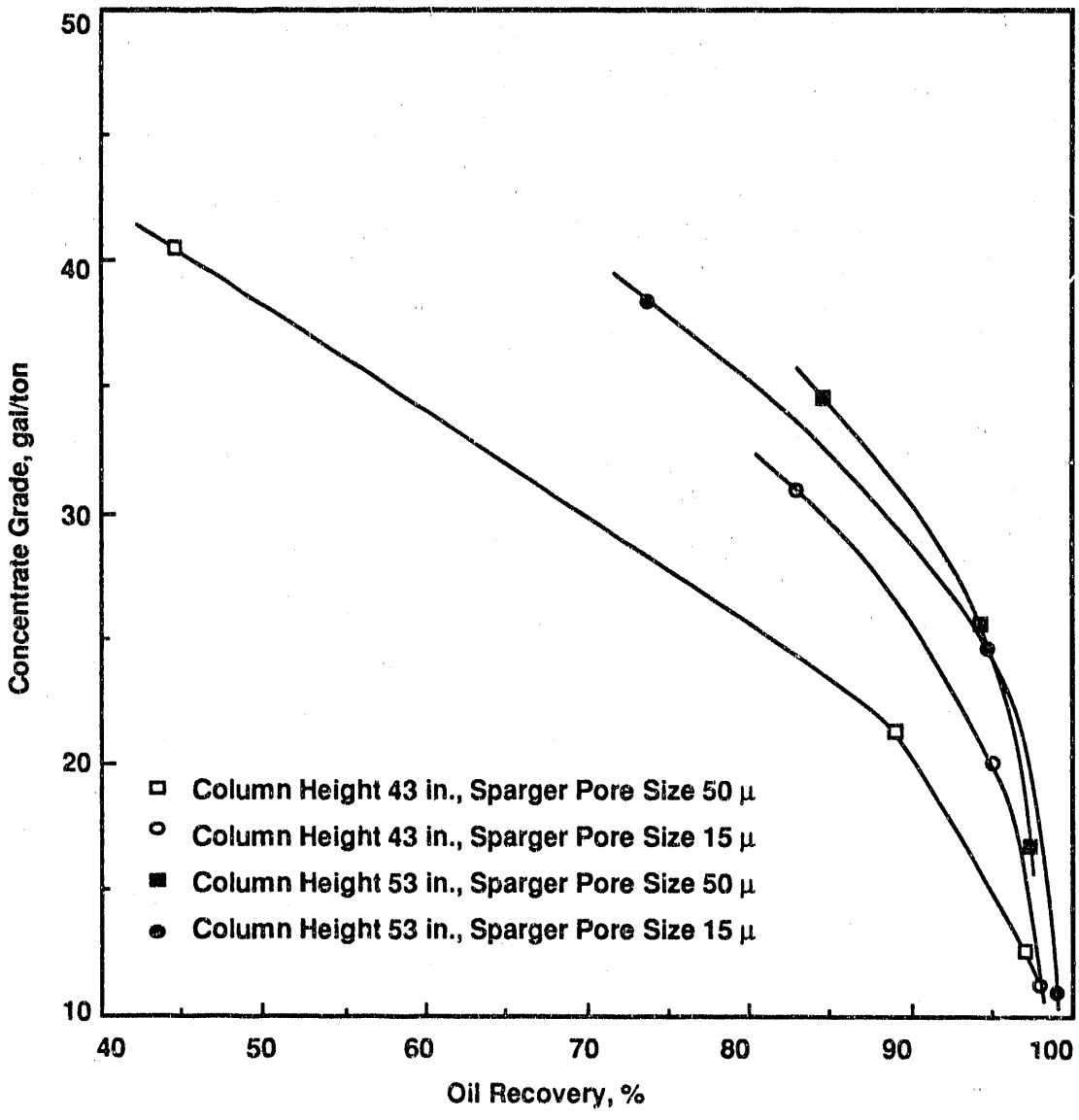

Figure 4-54. EFFECT OF COLUMN HEIGHT AND AIR SPARGER PORE SIZE ON FLOTATION OF ALABAMA OIL SHALES

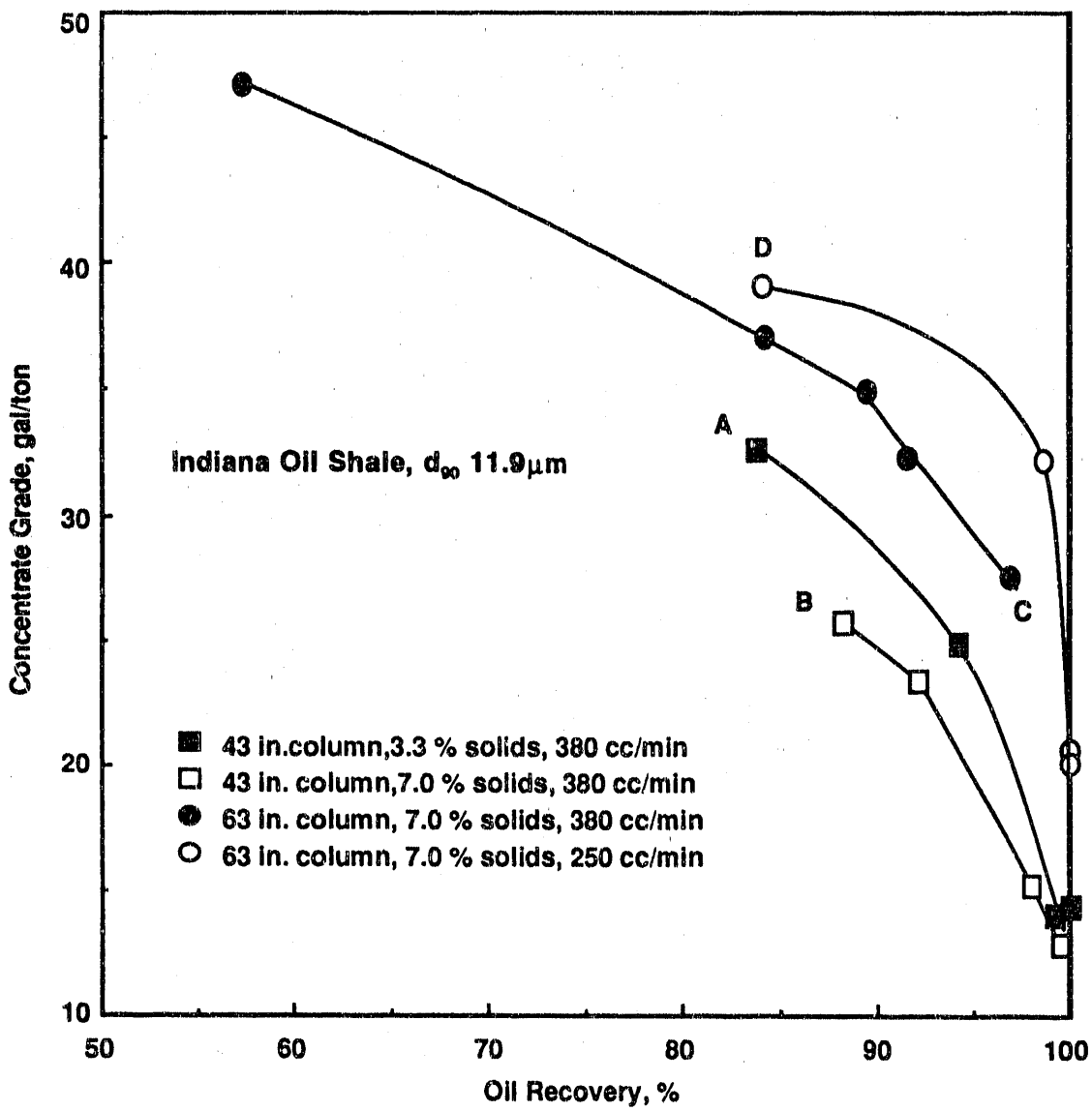

Figure 4-55. THE EFFECT OF COLUMN HEIGHT AND PERCENT SOLIDS ON THE FLOTATION OF INDIANA OIL SHALES

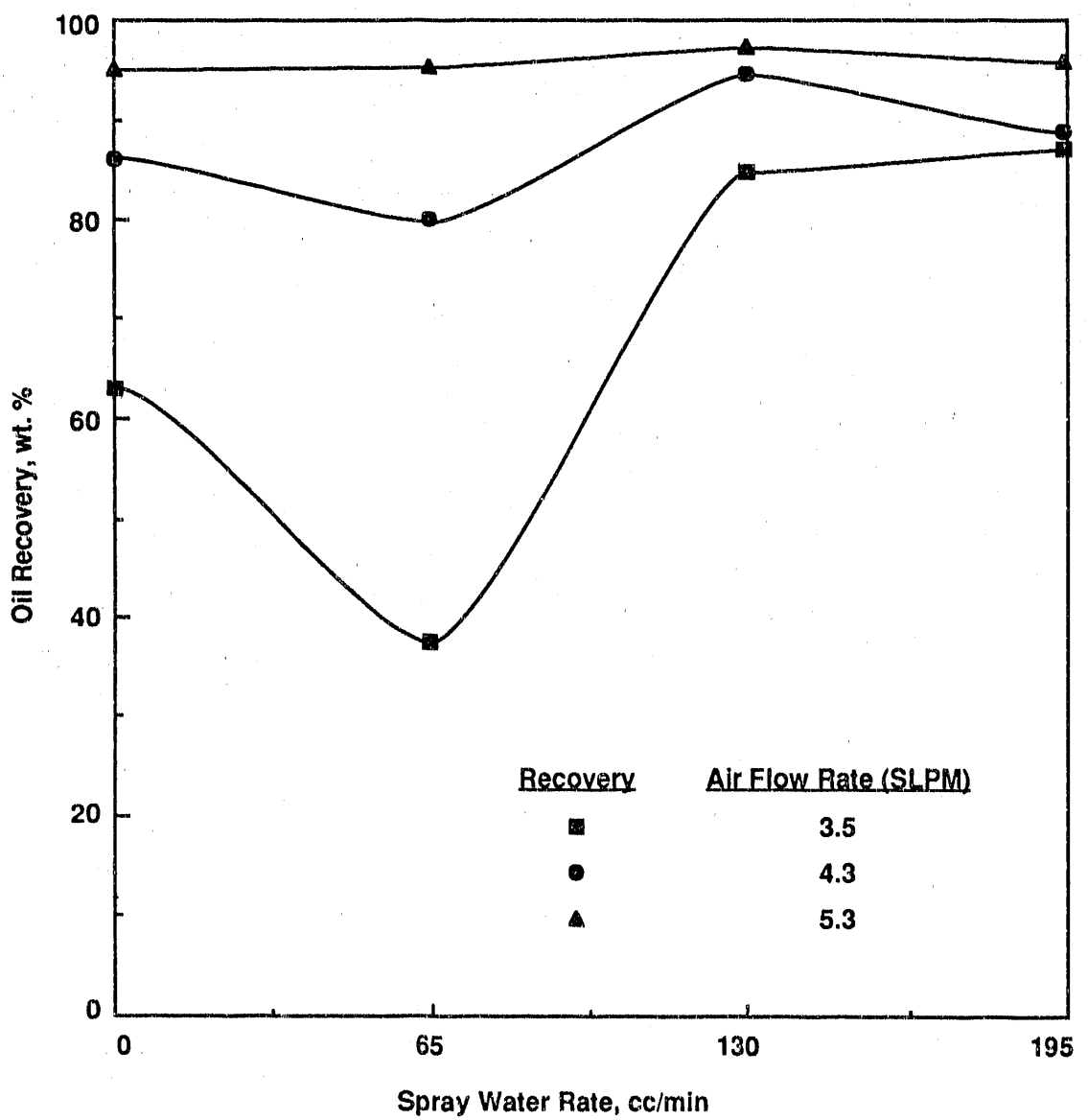

Figure 4-56. EFFECT OF AIR FLOW AND SPRAY WATER RATES ON KEROGEN RECOVERY

The effect of spray water rate on concentrate grade is shown in Figure 4-57. The results are contrary to what had been expected. High spray water rates tend to decrease the grade of concentrate obtained.

An explanation of the effects noted in Figures 4-56 and 4-57 is not readily apparent. It may be, however, that in the operating conditions (that is, low pulp levels and deep froth beds) the spray water tends to stabilize the froth and increase its "carrying capacity". That effect combined with the tendency of wet froths to prevent bubble coalescence may permit greater entrainment of particles not specifically attached to air bubbles which would enhance recovery of gangue and middling particles and in turn dilute the grade of concentrate.

The net effect of spray water addition is shown in Figure 4-58 where the data shown in the previous figures are presented as grade-recovery curves. This figure does show an overall beneficial effect of spray water addition, with the optimum level being 130 mL/min (the curve for 195 mL/min has been omitted for clarity).

Phase Four -- Circuit Development

This final phase of the column flotation testing was the development of an integrated beneficiation flow sheet for Eastern oil shales. A major concern in this effort was to establish a means of reducing overall grinding costs. The most readily apparent means of accomplishing this objectives is to reject material from the circuit at the coarsest possible size. In terms of column flotation testing, the objective was to determine whether a rougher flotation could be conducted to eliminate a substantial fraction of coarse material from the circuit with minimal loss of kerogen.

A sample of Alabama shale having a d_{90} of 23.1 μm was used for this series of tests. The sample was the undersize product from screening a primary ball mill discharge. A secondary objective of the series of tests was to gain further insight into the effect of froth depth and feed entry position. A series of tests were performed in the 63 inch column with varying froth depth and feed entry position. The test conditions are illustrated in Figure 4-59. The effect of froth depth (or pulp froth interface level) is shown in Figure 4-60. The results show that the kerogen recovery improves as the pulp froth interface level is lowered. These data confirm earlier observations that beneficial results are achieved by directing the feed into the froth phase of the column. The data, when compared with those presented in Figure 4-42, further illustrate the beneficial effect of the taller column. These data show that in the best case approximately 50% of the feed weight can be rejected as a tailing product containing only 1.6% of the available oil.

Figure 4-61 shows that the higher feed entry position moderately improves the quality of separation.

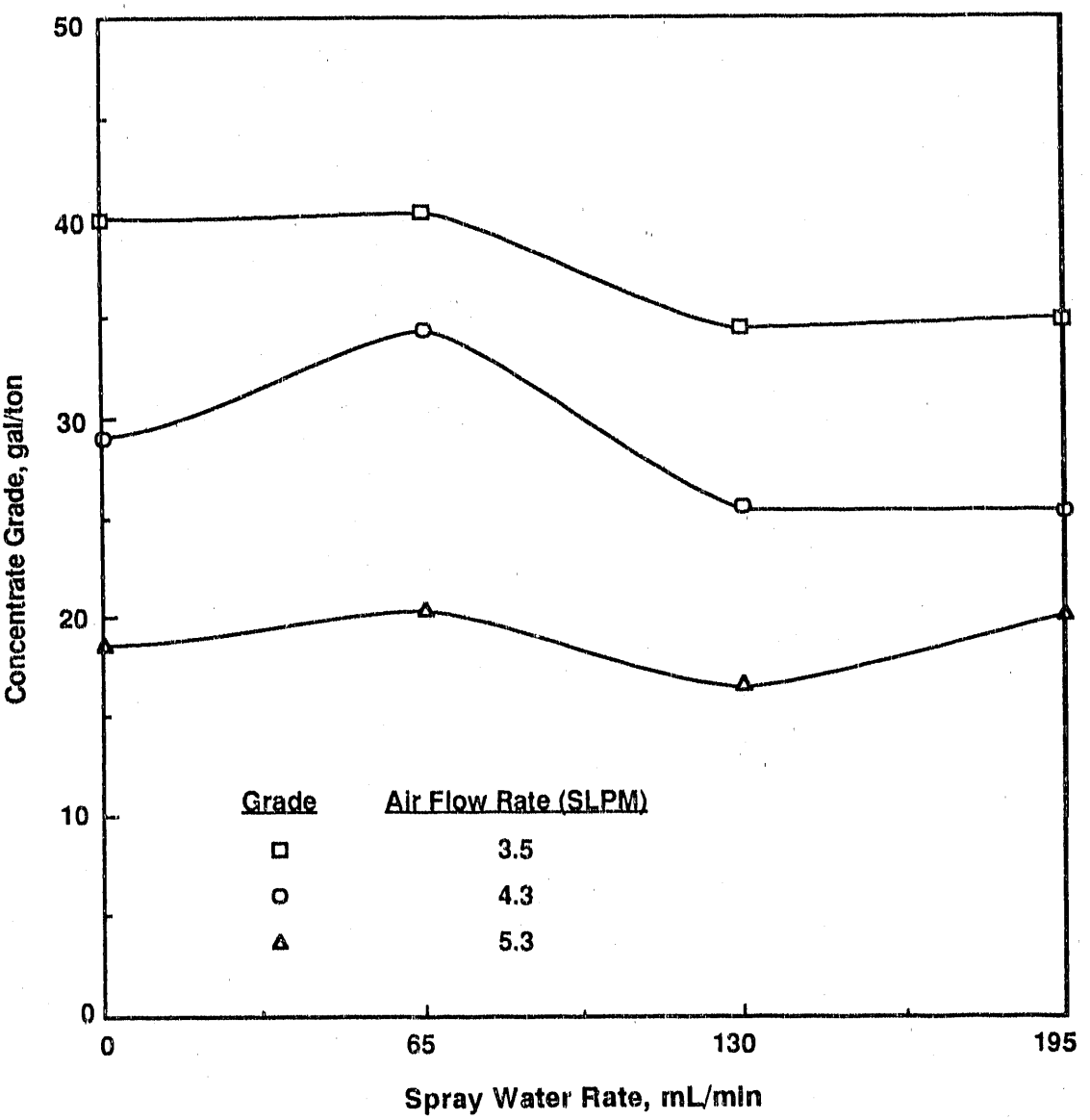

Figure 4-57. EFFECT OF AIR FLOW AND SPRAY WATER RATES ON CONCENTRATE GRADE

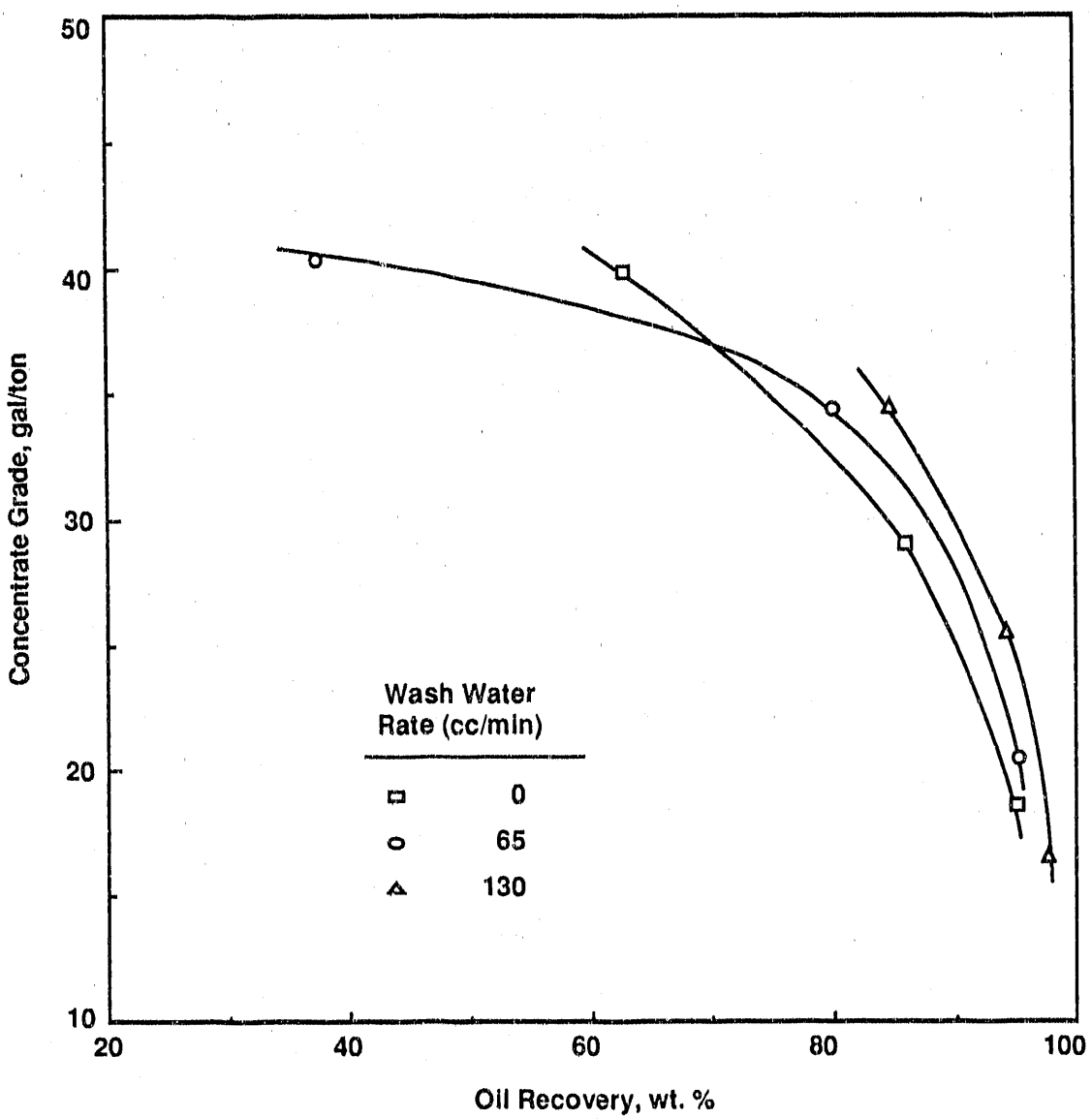

Figure 4-58. EFFECT OF WASH WATER RATE ON GRADE AND RECOVERY OF ALABAMA OIL SHALE

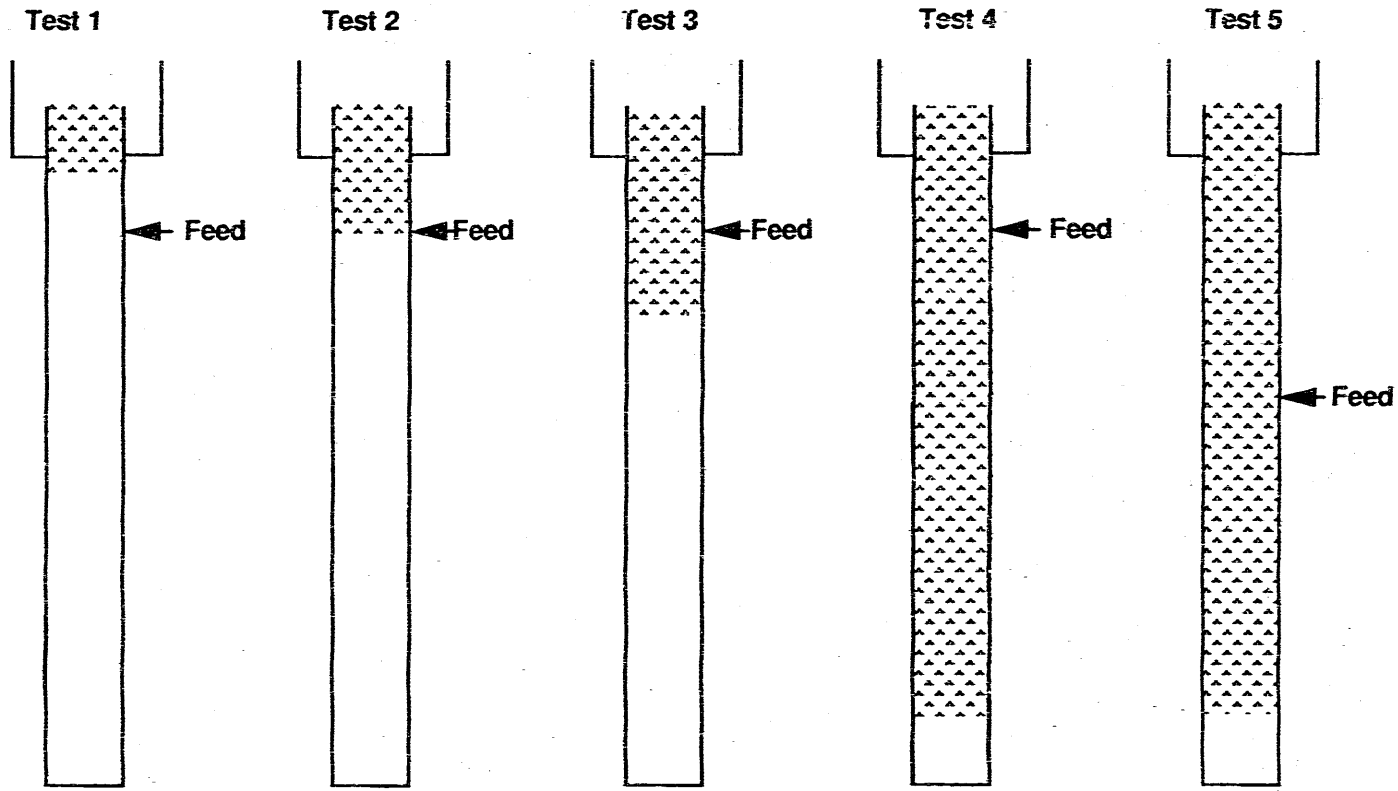

Figure 4-59. TEST CONDITIONS

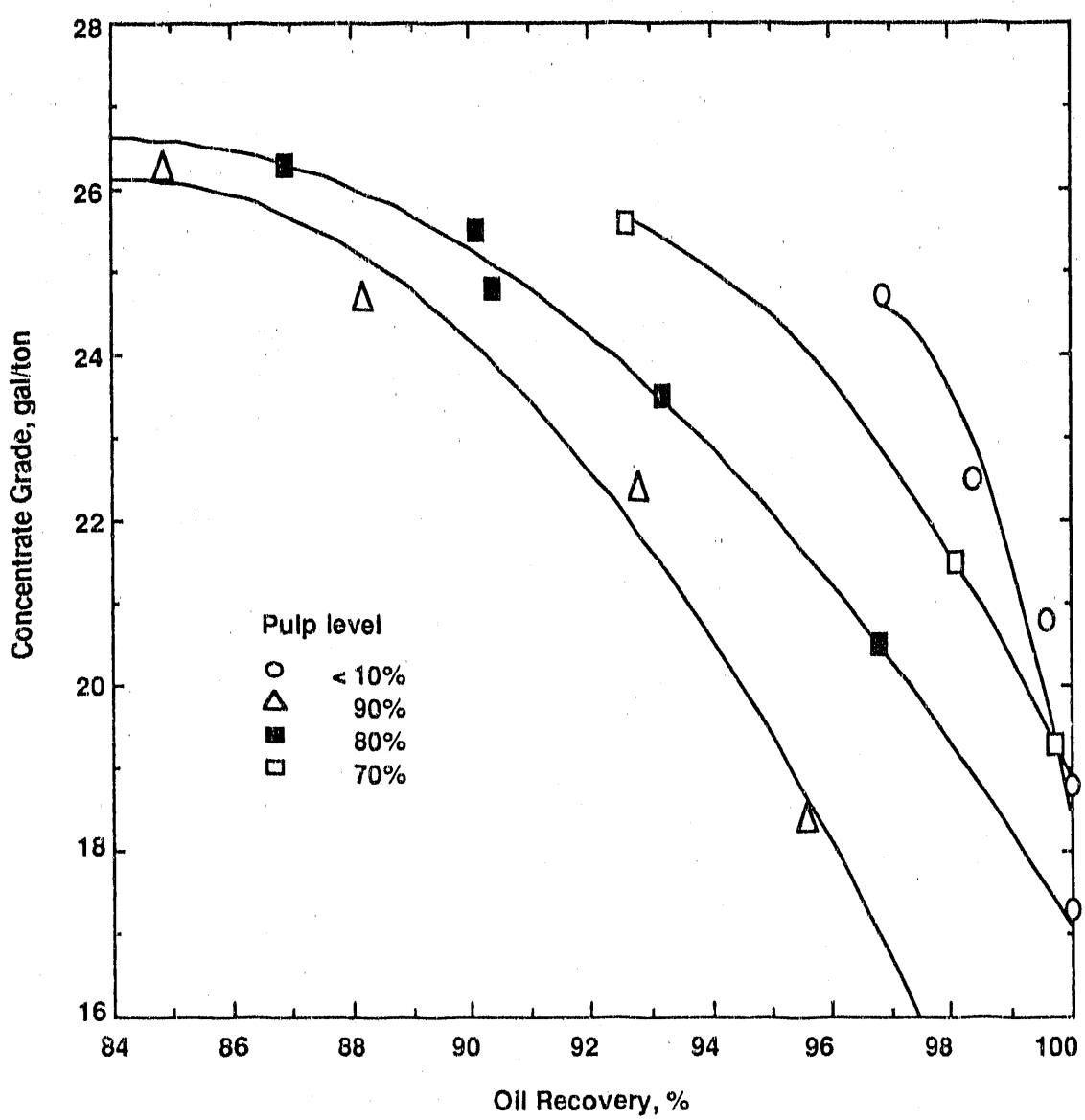

Figure 4-60. GRADE-RECOVERY RELATIONSHIPS AT VARIOUS PULP LEVELS

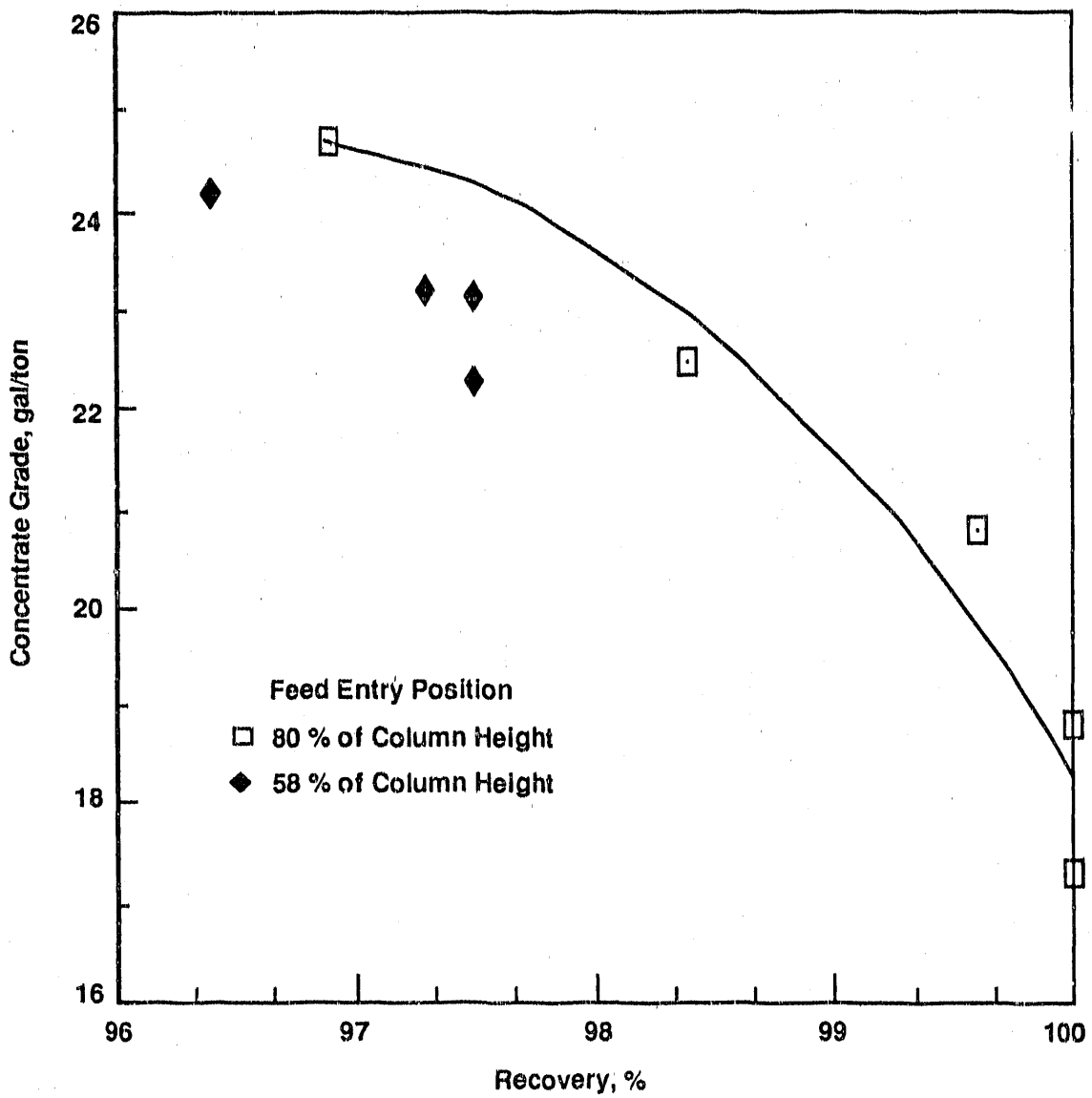

Figure 4-61. THE EFFECT OF FEED ENTRY POSITION ON THE FLOTATION OF ALABAMA OIL SHALE

Conclusions and Recommendations

From the data presented here, it is concluded that:

1. The six oil shales vary considerably in their response to froth flotation with the Alabama sample appearing to be the most readily amenable to separation.

2. Fine grinding, typically in the range of d_{90} = 10 μm, is required to achieve suitable concentrate grades and oil recoveries.

3. A single stage of column flotation is in most cases equal or superior to four or five stages of conventional flotation.

4. Air flow is the most important operating variable in column flotation and can be used to control the grade and recovery of product.

5. Column height appears to be a dominant design parameters. Increased column height enhances the quality of separation which is achieved. No indication of a "maximum" height was seen within the range tested in this investigation.

6. The preferred mode of operation for the flotation of oil shales is to direct the feed into the froth phase at a point near the top of the column with pulp-froth interface maintained at about 10% of column height.

7. Rougher concentrations of coarse shale are possible, producing concentrates in the range of 20 to 25 gal/ton (83.4 to 104.3 L/metric ton) with oil recoveries in excess of 95%.

Before advancing the research to a 2 to 5 ton/h process development unit scale it is recommended that:

1. Long term testing, employing recycled water, be performed to identify any effects due to changes in process water quality.

2. Scaling laws relating operating and performance data to the physical dimensions of the column be developed.

3. Further research be conducted to define limiting effective column height and froth depth.

4. Alternative circuit configurations (flow sheets) be tested in a continuous mode at laboratory scale.

Subtask 4.2.2. Air-Sparged Hydrocyclone

The air-sparged hydrocyclone (ASH) was developed during the early 1980's to achieve fast flotation of fine particles in a centrifugal field (Miller and Van Camp, 1982). A schematic drawing of the ASH and a horizontal cross section showing flow characteristics is presented in Figure 4-62. This device consists of two concentric cylinders, a cyclone header at the top and a froth pedestal at the bottom. The inner cylinder is constructed of porous material

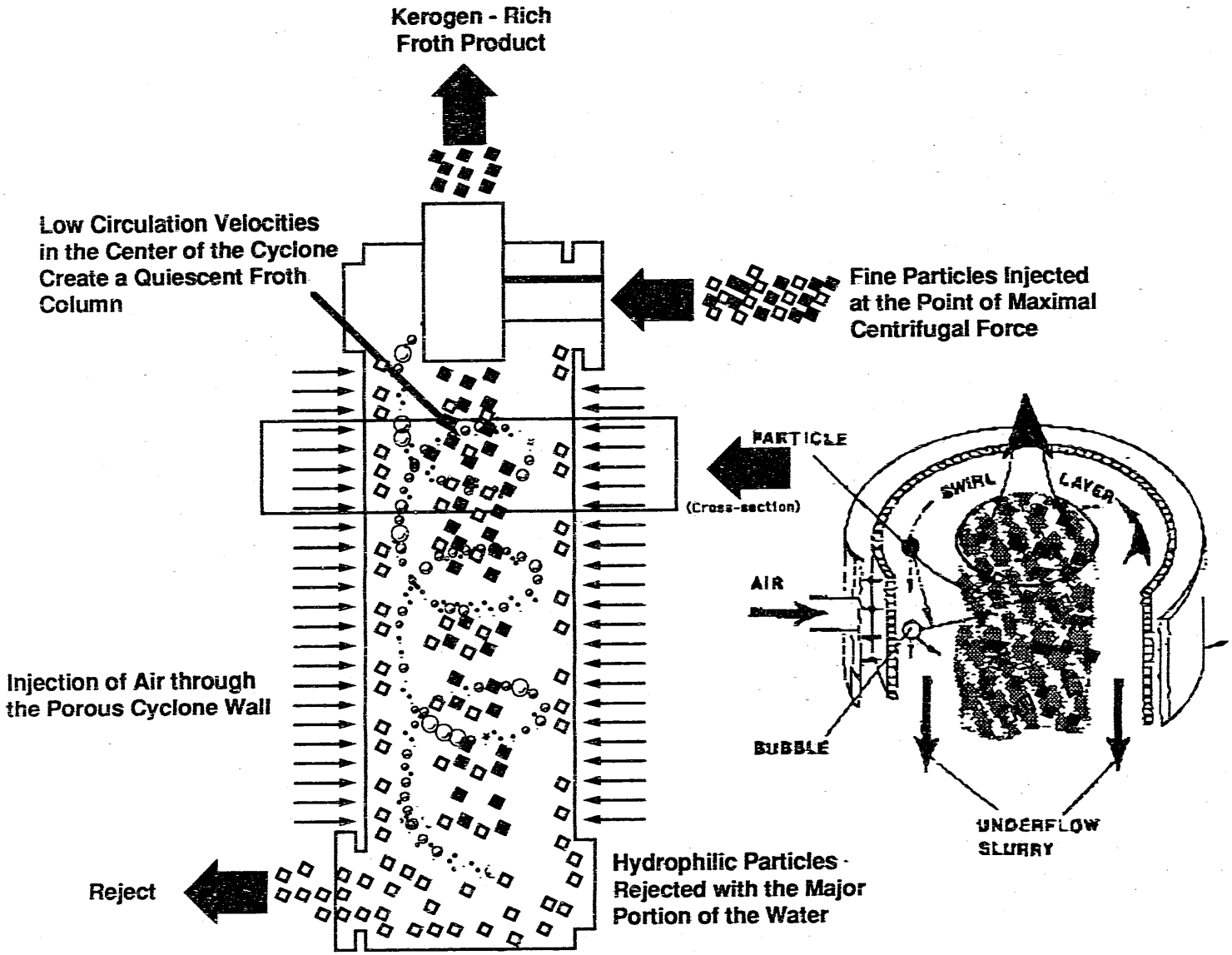

Figure 4-62. SCHEMATIC OF AIR-SPARGED HYDROCYCLONE

through which air is sparged radially. The outer cylinder serves as an air jacket to provide for even distribution of air through the porous inner tube. The slurry is fed tangentially through the header to the inside of the porous cylinder, so as to develop a swirl flow, and is discharged through the annular opening between the inner porous cylinder wall and the froth pedestal. Air is sparged through the jacketed, inner porous wall and is sheared into small bubbles by the swirl flow. Kerogen-rich particles in the slurry collide with these bubbles and after attaching are transported radially into a froth phase. The froth phase is stabilized and constrained by the froth pedestal at the underflow and thus moves towards the vortex finder of the cyclone header and is discharged as an overflow product. Hydrophilic particles (silicious gangue) generally remain in the slurry phase and are discharged as an underflow product through the annulus created by the froth pedestal.

A 5-cm diameter ASH (length, 50 cm; vortex finder, 2.1 cm; and pedestal diameter, 4.4 cm) with a wall pore size of 10 μm was used in the flotation tests. It was reasoned that because residence time in the hydrocyclone is extremely short (less than one second), each kerogen rich particle has very few opportunities (perhaps only one) to collide with an air bubble. Therefore, to increase the probability of attachment in that single collision it would be necessary to increase the hydrophobicity of the kerogen rich particles. Further, it was reasoned that the selectivity of the process might be enhanced if the particles were presented singly rather than as aggregates. The need, therefore, was to develop a system for dispersing finely ground oil shale and selectively coating the kerogen rich particles with oil to enhance their hydrophobicity.

Due to the size and capacity of the equipment involved, air sparged hydrocyclone tests require substantial quantities of prepared sample for a single test. It was decided, therefore, to develop and validate the systems for dispersing and oil coating ground shale in an external system. Oil agglomeration was chosen as the external-pilot system.

Raw Indiana shale ground in the Netzsch mill to a size d_{90} = 10 μm was tested using a Denver scrubber in batch mode. The effects of variables such as scrubbing time, percent solids, oil dosage, agitation intensity and pH were determined in terms of yield and recovery of kerogen. In this series of tests, the agglomeration was found to be very sensitive to pH and agitation intensity. The natural pH of the ground slurry was around 4 and even if agglomeration tests were carried out at the best conditions of other variables such as intensity (3000 rpm), kerosene dosage (40% of the weight of dry shale), percent solids (5% by weight) and scrub time (15 minutes), little agglomeration was observed (that is, concentrate yield was 3%). The yield was determined by screening the slurry at 100 mesh. The +100 mesh material was taken to be agglomerated material. Electrokinetic (zeta potential) measurements indicated that a pH of 10 is required to achieve reasonable repulsive forces (dispersion) between kerogen-kerogen, kerogen-mineral and mineral-mineral aggregates. Based on this finding, experiments were conducted at pH 10 with all other variables held constant, this resulted in a yield of 15% to 20%. Similarly, a positive effect of agitation intensity was also observed. In another series of experiments, the effect of solids loading was observed. Percent solids were varied in the range of 1% to 9% in steps of 2, scrubbing time was kept at 20 minutes and all other variables were the same as

mentioned above. In these experiments, the only experiment that gave yields of 15% to 20% was at percent solids = 5%. Experiments conducted at lower (<5) and higher (>5) percent solids resulted in yields of 9% to 11%. These experiments suggested that optimum ratio of solids and oil was highly desirable. For example, at low solids (~0.5%) not enough shear will be generated to form flocs, and at high solids loading, clustering will inhibit oil coating. Therefore, optimum solids loading of 5% was desired. These tests concluded that concentrate yield should be at least 20% or higher in order to achieve a good kerogen recovery in the concentrate. The conditions for optimum oil agglomeration, in terms of pH and oil coating were subsequently adopted for conditioning micronized oil shale prior to ASH testing.

A conventional ASH test loop has two limitations: 1) A large feedstock of micronized shale was needed and 2) cyclone underflow and overflow are directed into the feed sump. This arrangement reduces the demand for feedstock, but results in a non-homogenized feed for other tests. Hence, an important modification in the ASH circuit was completed so that a small quantity of micronized shale could be used for many tests without altering the feed characteristics. Figure 4-63 shows the schematic diagram of the ASH circuit. Initial tests were conducted using water with and without Dowfroth 250 to find the condition which corresponded to minimum water split to overflow. Two variables were varied, that is, feed inlet pressure (3 to 9 psig) and airflow rate [6 to 14 ft^3/min (170 to 396 L/min)]. In these experiments, a (high) feed inlet pressure of 9 psig and a (low) airflow rate of 6 ft^3/min gave the best response in terms of fractional split (0.5). Table 4-32, 4-33, and 4-34 list the operating conditions for such tests. Using these conditions to be a preliminary optimum, a series of experiments were carried out on Kentucky and an unspecified shale mixture. It is of interest to note that the oil recovery in the overflow product is of the same magnitude as that in the underflow, however, a small but consistent higher grade of overflow was obtained. This may be largely due to a large size (1.75 inch) pedestal being used in these experiments leading to a condition of froth core thickness being larger than swirl layer (1.70 inch) thickness. In subsequent experiments, a smaller size pedestal was used so that fractional overflow water split be maintained in the range of 0.3 to 0.35. Before this change was implemented, alternative ways of reducing the overflow split were tested by replacing the large-size vortex with a middle size vortex. Therefore, a test series using 23 first-order factorial experimental design was conducted using 1.75-inch diameter pedestal and middle-size vortex ($1.6 < d < 2.0$ cm). The manipulated variables were percent solids, slurry inlet pressure, and air flow rate. This test series was repeated for two different levels of kerosene concentration (1 and 3 kg/t). Table 4-35 lists the experimental design along with the results obtained in these experiments.

In another tests series, percent solids was maintained at a fixed value (3%) and the manipulated variables were: kerosene pedestal and vortex were changed to smaller pedestal (1.70-inch diameter) and smaller vortex (1.6 inch diameter). Table 4-36 lists experimental design and results obtained. This change was made in order to check whether a clean concentrate from this device was possible or not. Results similar to those obtained previously (Table 4-35) were achieved except that the oil recovery in the underflow was quite substantial due to the significant weight fraction reporting to the underflow.

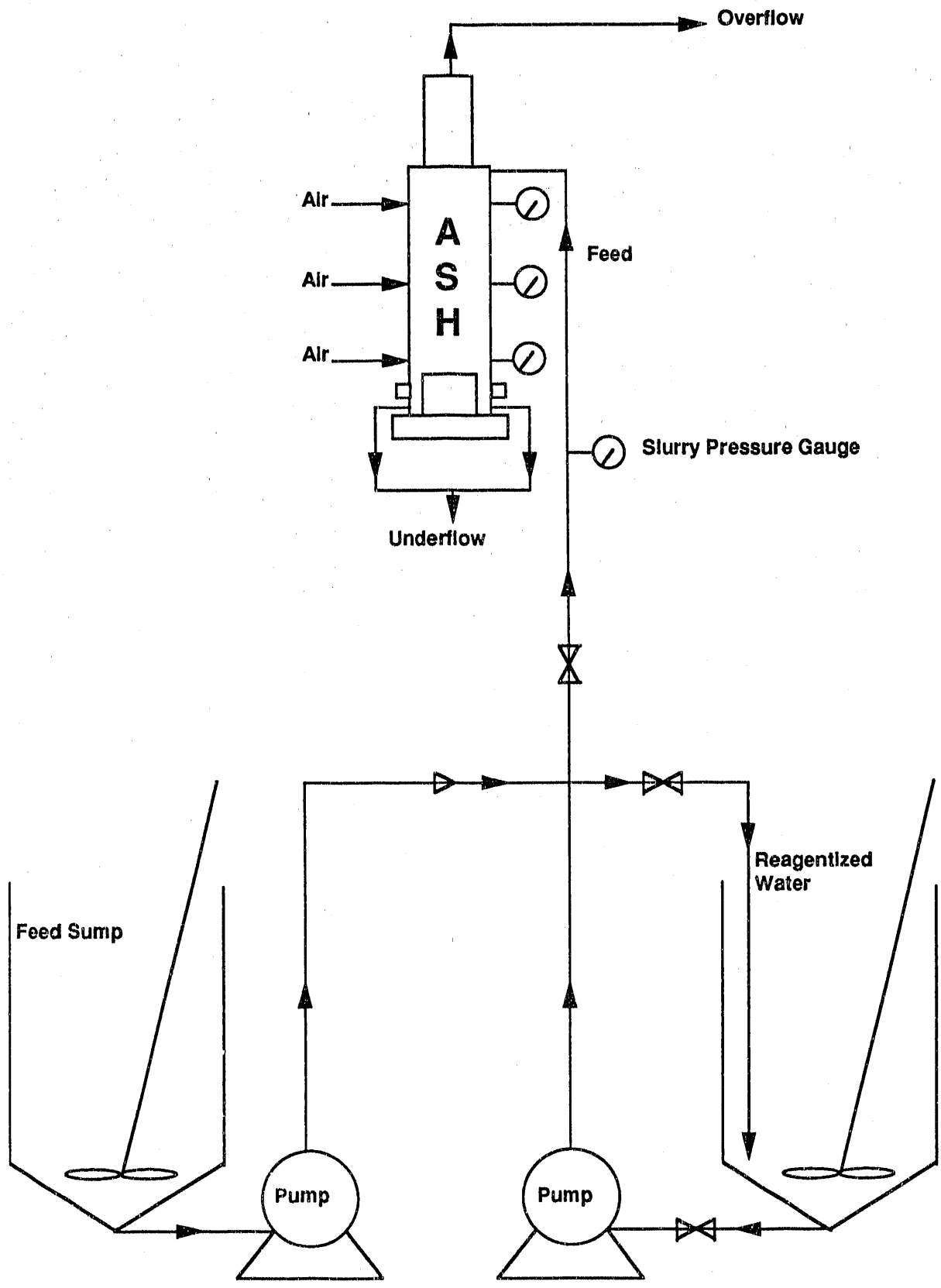

Figure 4-63. SCHEMATIC OF AIR-SPARGED HYDROCYCLONE FLOTATION CIRCUIT

Table 4-32. RESULTS OF AIR-SPARGED HYDROCYCLONE TEST WORK USING WATER WITHOUT FROTHER

psig	Air Flow Rate, SCFM	Slurry Pressure, psig	Slurry Flow Rate, L/min	Fraction of Total Flow Reported in Overflow	Fraction of Total Flow Reported in Underflow
65	6	3	27.93	0.52	0.48
65	6	5	51.56	0.47	0.53
65	6	7	59.84	0.45	0.55
65	6	9	68.34	0.43	0.57
65	10	9	62.87	0.48	0.52
65	10	7	53.90	0.52	0.48
65	10	5	51.56	0.57	0.43
65	10	3	34.60	0.60	0.40
40	14	3	40.62	0.64	0.36
40	14	5	45.31	0.65	0.35
40	14	7	56.71	0.55	0.45
40	14	9	65.62	0.52	0.48

Table 4-33. RESULTS OF AIR-SPARGED HYDROCYCLONE TEST WORK USING WATER WITH 22 ppm DOW FROTH 250

psig	Air Flow Rate, SCFM	Slurry Pressure, psig	Slurry Flow Rate, L/min	Fraction of Total Flow Reported in Overflow	Fraction of Total Flow Reported in Underflow
65	6	3	32.81	0.57	0.43
65	6	5	44.43	0.51	0.49
65	6	7	57.18	0.49	0.51
65	6	9	71.25	0.50	0.50
65	10	9	63.43	0.54	0.45
65	10	7	59.68	0.58	0.42
65	10	5	45.31	0.62	0.38
65	10	3	30.31	0.67	0.38
40	14	3	31.87	0.65	0.35
40	14	5	42.96	0.62	0.38
40	14	7	54.68	0.60	0.40
40	14	9	60.78	0.59	0.41

Table 4-34. RESULTS OF AIR-SPARGED HYDROCYCLONE TEST WORK USING WATER WITH 80 ppm DOW FROTH 250

psig	Air Flow Rate, SCFM	Slurry Pressure, psig	Slurry Flow Rate, L/min	Fraction of Total Flow Reported in Overflow	Fraction of Total Flow Reported in Underflow
65	10	9	54.6	0.60	0.40
65	10	5	39.6	0.69	0.31
65	6	2	30.0	0.50	0.50

Table 4-35. AIR-SPARGED HYDROCYCLONE TEST SERIES USING 2^3 FIRST ORDER FACTORIAL DESIGN WITH PEDESTAL 1.75-INCH-DIAMETER AND MIDDLE VORTEX ON ALABAMA OIL SHALE FOR TWO DIFFERENT LEVELS OF KEROSENE DOSAGE (A1-A8 for 1 kg/t and A9-A16 for 3 kg/t)

Test Number		Pump Setting	Slurry Inlet Pressure, psig	Air Flow Rate, SCFM	Oil gal/ton	Oil Recovery
A-1	OF	50	12	6	9.8	48.6
	UF	50	12	6	8.6	51.4
A-2	OF	50	4	14	10.0	67.1
	UF	50	4	14	9.3	32.9
A-3	OF	35	12	14	11.2	59.6
	UF	35	12	14	8.1	40.4
A-4	OF	35	4	6	11.8	61.8
	UF	35	4	6	10.3	32.2
A-5	OF	35	12	6	12.2	50.1
	UF	35	12	6	10.8	49.9
A-6	OF	35	4	14	11.2	69.1
	UF	35	4	14	10.4	30.9
A-7	OF	50	12	14	11.0	49.8
	UF	50	12	14	9.4	50.2
A-8	OF	50	4	6	9.0	48.9
	UF	50	4	6	9.0	51.1
A-9	OF	50	12	14	10.3	50.7
	UF	50	12	14	9.1	49.3
A-10	OF	50	4	6	8.7	54.7
	UF	50	4	6	9.5	45.3
A-11	OF	35	12	6	11.7	47.7
	UF	35	12	6	10.5	52.3
A-12	OF	35	4	14	10.8	64.5
	UF	35	4	14	10.4	35.5
A-13	OF	35	12	14	10.3	56.3
	UF	35	12	14	9.4	43.7
A-14	OF	35	4	6	10.4	59.3
	UF	35	4	6	9.2	40.7
A-15	OF	50	12	6	10.6	48.0
	UF	50	12	6	9.1	52.0
A-16	OF	50	4	14	11.0	57.2
	UF	5-	4	14	10.9	42.8

* Pump setting 50 gave percent solids in the range of 6 to 13% (average of 9%); a 35 setting yielded a range of 1.5% to 5% (average of 3%).

Table 4-36. AIR-SPARGED HYDROCYCLONE TEST SERIES USING 2^3 FIRST ORDER FACTORIAL DESIGN WITH PEDESTAL 1.70-INCH-DIAMETER AND SMALLER VORTEX, ON ALABAMA OIL SHALE AT FIXED PUMP SETTING AND 4% SOLIDS

Test Number	Kerosene Addition, kg/t	Slurry Inlet Pressure, psig	Air Flow Rate, SCFM	Oil gal/ton	Oil Recovery
A-1 OF	1	4	6	10.36	22.0
UF	1	4	6	9.93	78.0
A-2 OF	1	12	6	10.43	13.3
UF	1	12	6	9.67	86.7
A-3 OF	1	12	14	10.19	16.2
UF	1	12	14	9.52	83.8
A-4 OF	1	4	14	10.10	26.8
UF	1	4	14	9.31	73.2
A-5 OF	2	4	6	9.90	22.0
UF	2	4	6	9.36	78.0
A-6 OF	2	12	6	10.47	15.0
UF	2	12	6	9.04	85.0
A-7 OF	2	4	14	10.07	27.3
UF	2	4	14	9.28	72.7
A-8 OF	2	12	14	10.79	18.4
UF	2	12	14	9.17	81.6

These tests indicated that flotation, through this device, on micronized shale was not feasible. The results were deemed definitive and no further testing of the ASH was performed.

Subtask 4.2.3. LICADO Process

The focus of this subtask was to beneficiate samples of Eastern oil shale using the LICADO high-pressure process, prior to retorting. The objective was to enhance the product quality (Fischer Assay) of the samples and also achieve a high oil recovery.

Background

The LICADO process was originally developed at the University of Pittsburgh as a method to produce premium quality coal by physical beneficiation (Araujo *et al.* 1987; Chi, S.M.B., 1986). The LICADO process can be applied to beneficiate the oil shale by taking advantage of the inherent differences in surface properties of the kerogen-rich materials (hydrophobic) and the mineral matter (hydrophilic). Thus, it is possible to achieve the desired upgrading by contacting an oil-shale water slurry with liquid CO_2. A schematic diagram illustrating the process principles is shown in Figure 4-64. The mechanism of separation is governed by the interaction between the interfacial, shear and body forces present in the oil shale-water-liquid CO_2 system.

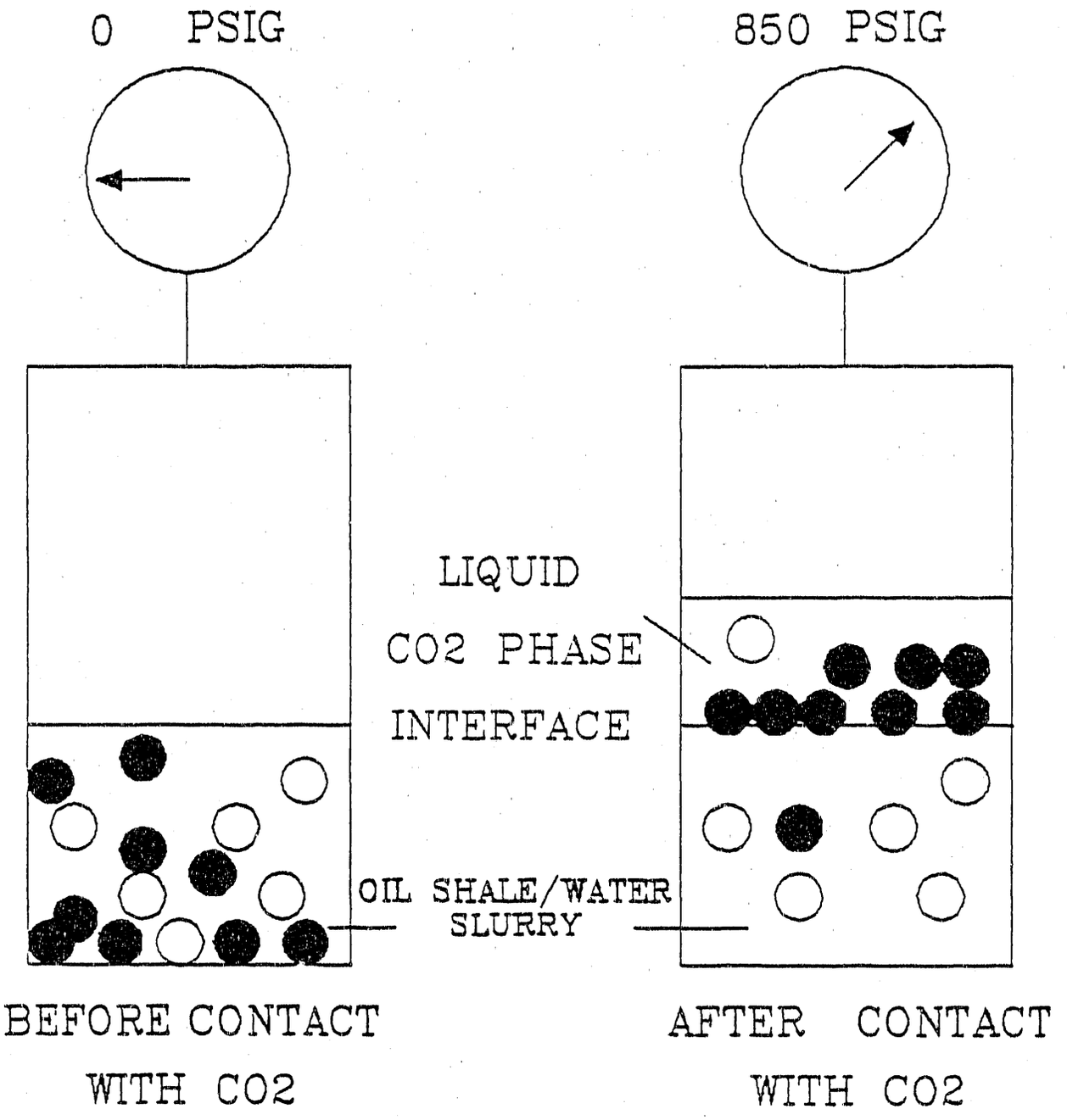

Figure 4-64. MECHANISM OF LICADO PROCESS

The principal advantages of the LICADO process are as follows:

1. Low viscosity and low surface tension of liquid CO_2, permitting easy separation from upgraded product.

2. Low operational cost of the process.

3. Dewatering requirements are minimized since the product is relatively dry.

4. Liquid CO_2 is non-toxic and non-flammable.

Methodology

The principal objective of the experimental work was to increase the Fischer Assay in the product samples and enhance the oil recovery. Four different types of experiments were carried out:

1. Batch experiments in the 2-inch (5.1-cm) Batch Research Unit (BRU).

2. Screen-type agglomeration experiments in the modified BRU.

3. Semi-continuous tests in the 4-inch (10.2-cm) Research Development Unit (RDU) with an internal two-stage device.

4. Surface property measurements to determine wetting characteristics of oil shale samples. These included contact angle measurements in air and CO_2 atmosphere.

The equipment details and operating procedures are provided below.

Batch Research Unit (BRU)

Figure 4-65 shows the 2-inch high pressure Batch Research Unit. It consists of two high pressure cells of 2-inch I.D. connected by a 2-inch ball valve. The system is provided with two variable speed motors. A 900-mL oil shale-water slurry was fed to the lower section of the BRU in each test. Liquid CO_2 was injected from the bottom of the column to effect the upgraded product-refuse separation. At the end of the contact period with liquid CO_2, the upper and lower sections of the BRU were separated by closing the 2-inch ball valve. The system was then de-pressurized to ambient pressure. The contents of the upper cell contained the upgraded product while the refuse fraction was collected in the bottom cell. During these batch tests, the slurry volume is maintained constant and liquid CO_2 does not leave the system.

Figure 4-66 shows the 2-inch BRU modified to perform screen-type agglomeration experiments. An 80-mesh screen was incorporated in the ball valve separating the upper and lower cells. The screen was inserted to retain the agglomerates of the upgraded kerogen-rich material when the mixture of oil shale-water-liquid CO_2 was drained to the bottom cell. A sample of 500 mL slurry was introduced into the top cell with the ball valve in the closed position. The system was then pressurized until 100 mL of liquid CO_2 was observed to collect as a clear layer above the slurry. The ratio of liquid CO_2 to slurry was maintained at about 0.2 in all the experiments conducted at

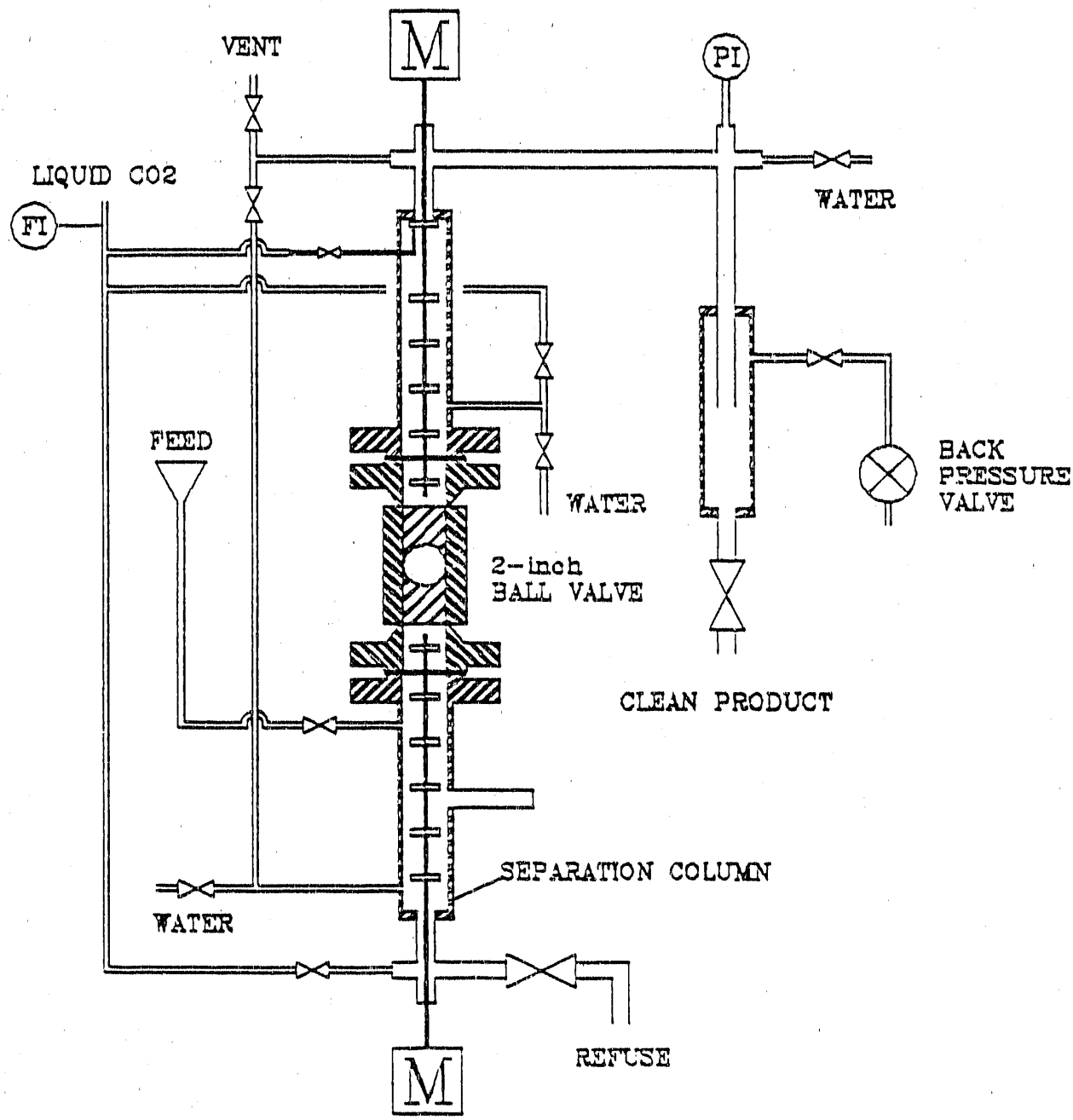

Figure 4-65. BATCH RESEARCH UNIT

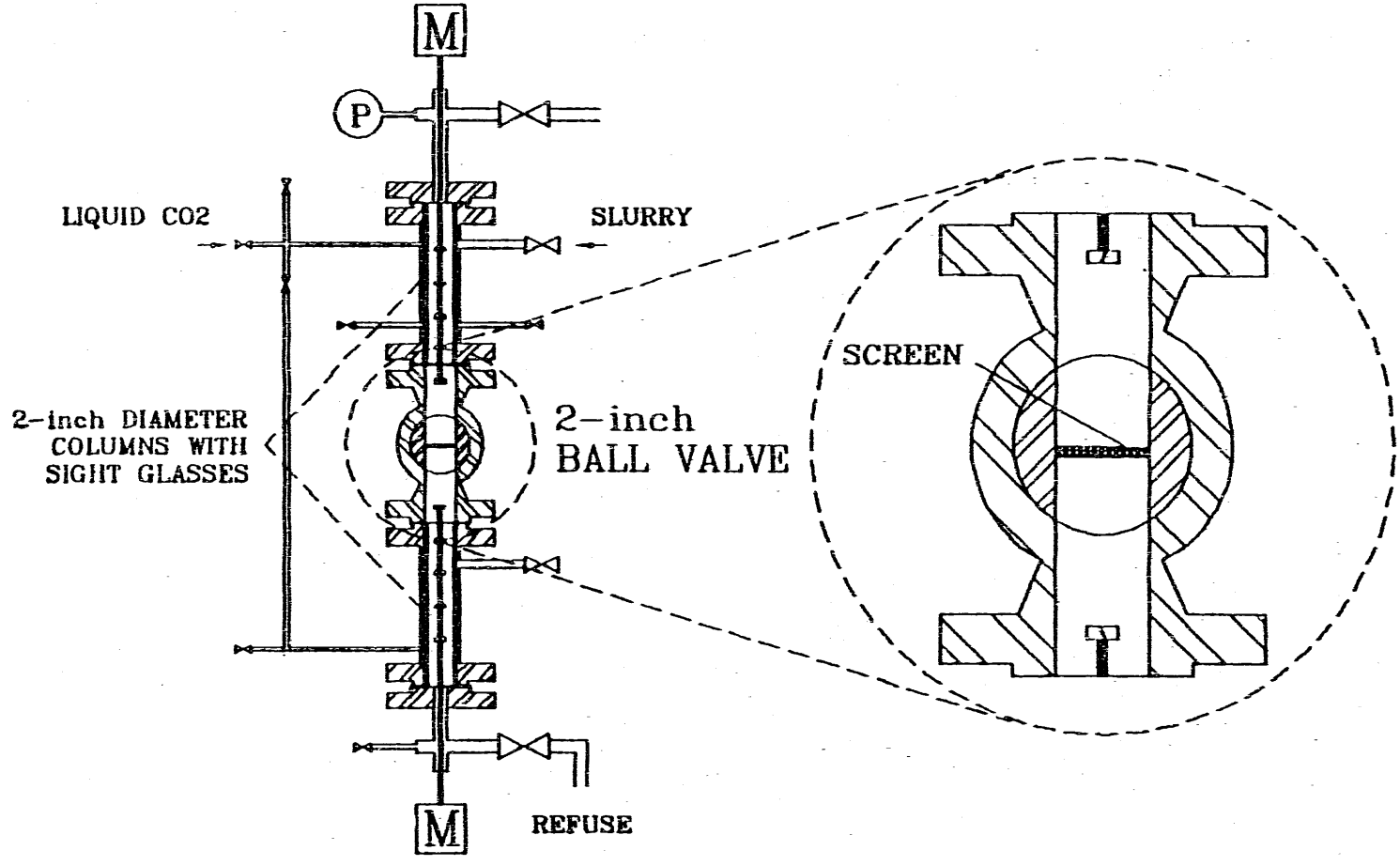

Figure 4-66. SCREEN-TYPE AGGLOMERATION UNIT

a low slurry concentration (2% by weight). The liquid CO_2 was vigorously agitated with the oil shale slurry for 3 minutes at 2500 rpm. The slurry containing the agglomerated product was immediately drained through the screen. The upgraded product, in the form of agglomerates were captured on the screen and samples were collected after de-pressurizing the system.

Research Development Unit

A 4-inch high-pressure unit denoted as the Research Development Unit and shown in Figure 4-67, was utilized in semi-continuous tests. The pressure, temperature and flow rate of liquid CO_2 were monitored from an instrument panel adjacent to the apparatus. Prior to performing the experiment, the slurry was premixed with liquid CO_2 at high speed (3050 rpm) for 7 min. During the experiment, liquid CO_2 was introduced from the bottom of the separation column through a disperser at a constant flow rate for a specified contact time of 30 min. The upgraded product was carried up to a collecting cup at the top of the separation column and into a product sampler where the liquid CO_2 left the system through a back-pressure valve. Refuse samples remained in the separation column and were withdrawn from the bottom of the cell to a sampler at the termination of the experiment.

A two-stage device was fabricated and installed within the separation column of the RDU and this is depicted in Figure 4-68. Two cylindrical draft tubes comprising the two stages were installed with the conical section on top. A vortex-inducing plate was attached at the top of each draft tube with the impeller shaft passing through the draft tubes. In this arrangement, the upgraded product and refuse were ejected tangentially from the vortex plates after being subjected to vigorous agitation of at least 1000 rpm. The denser refuse material sank to the bottom of the separation column after collision with the walls of the column. The lighter agglomerates bearing the kerogen-rich shale were collected on the top after overflowing from the conical section.

Surface Property Measuring Apparatus

Surface property measurements were conducted by measuring the contact angle of water on oil shale pellets in a specially designed high pressure apparatus shown in Figure 4-69. An overhead mixing cell was used to equilibrate the immiscible liquid CO_2 and water phases and to feed either of these two liquids to the measurement cell by gravity. The measurement cell, equipped with 2-inch windows on opposite sides, was mounted on a rotary table capable of a 180 degree rotation. A sessile drop of water was deposited in a CO_2 environment on a 1 X 1/4 inch (2.54 X 0.64 cm) thick polished pellet of an Eastern oil shale, which was contained in a specimen holder. The contact angle of water was measured with an angular protractor inside the eyepiece of the microscope at various liquid CO_2 pressures ranging from zero to saturation pressure at room temperature (about 850 psia).

The contact angle of water was also measured at room temperature and pressure with a conventional goniometer using the sessile-drop method.

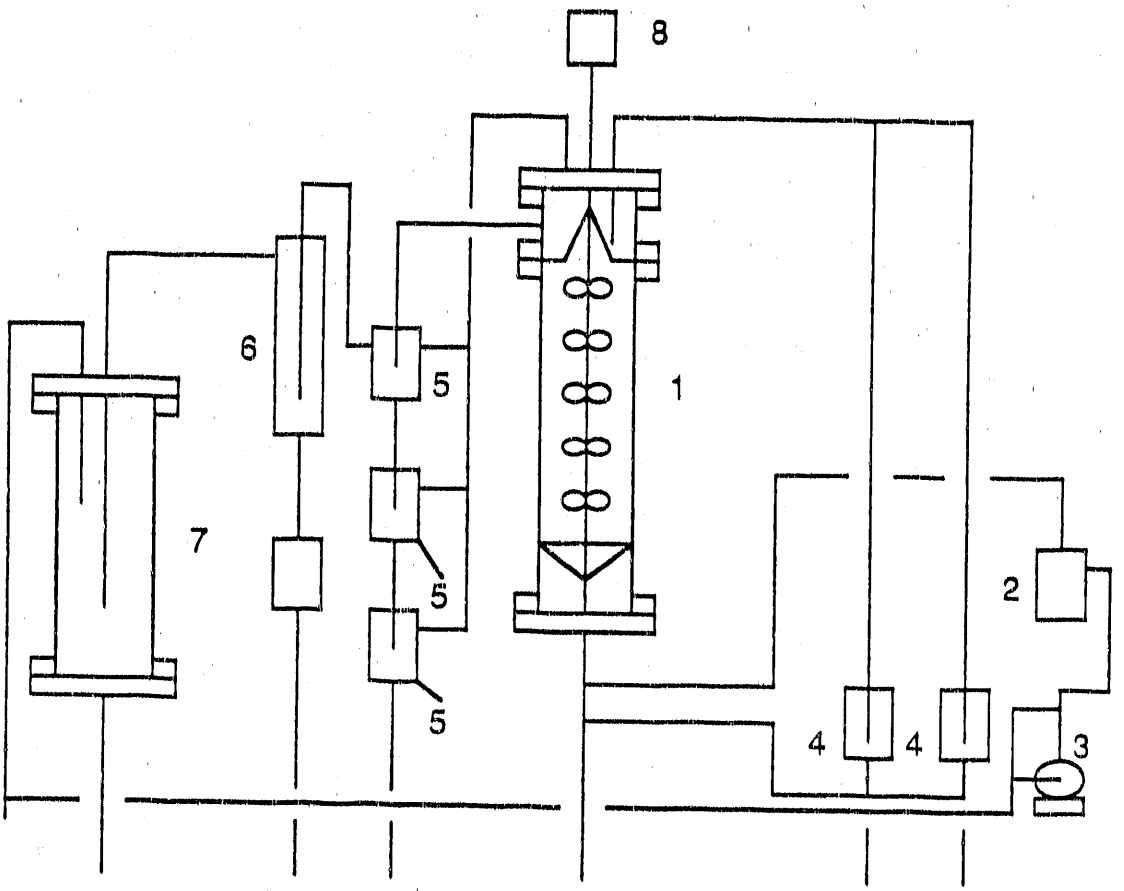

1	column	5	product collector
2	flowmeter	6	settling tank
3	CO2 pump	7	CO2 tank
4	refuse collector	8	motor

Figure 4-67. RESEARCH DEVELOPMENT UNIT

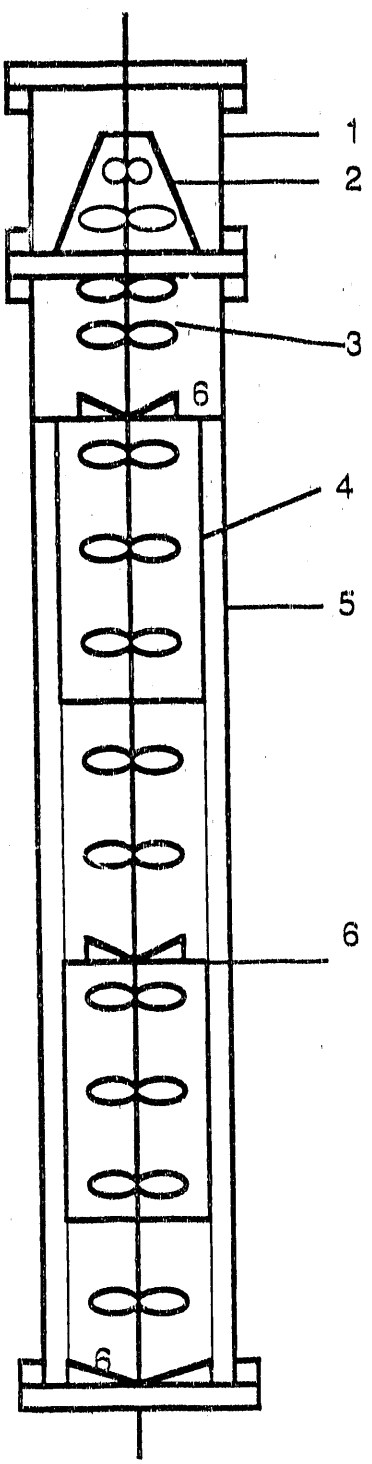

1 - Overflow Section

2 - Overflow Cone

3 - Impeller

4 - Draft Tube

5 - Mixing and Agglomeration Section

6 - Vortex-Induced Plate

Figure 4-68. TWO-STAGE DEVICE

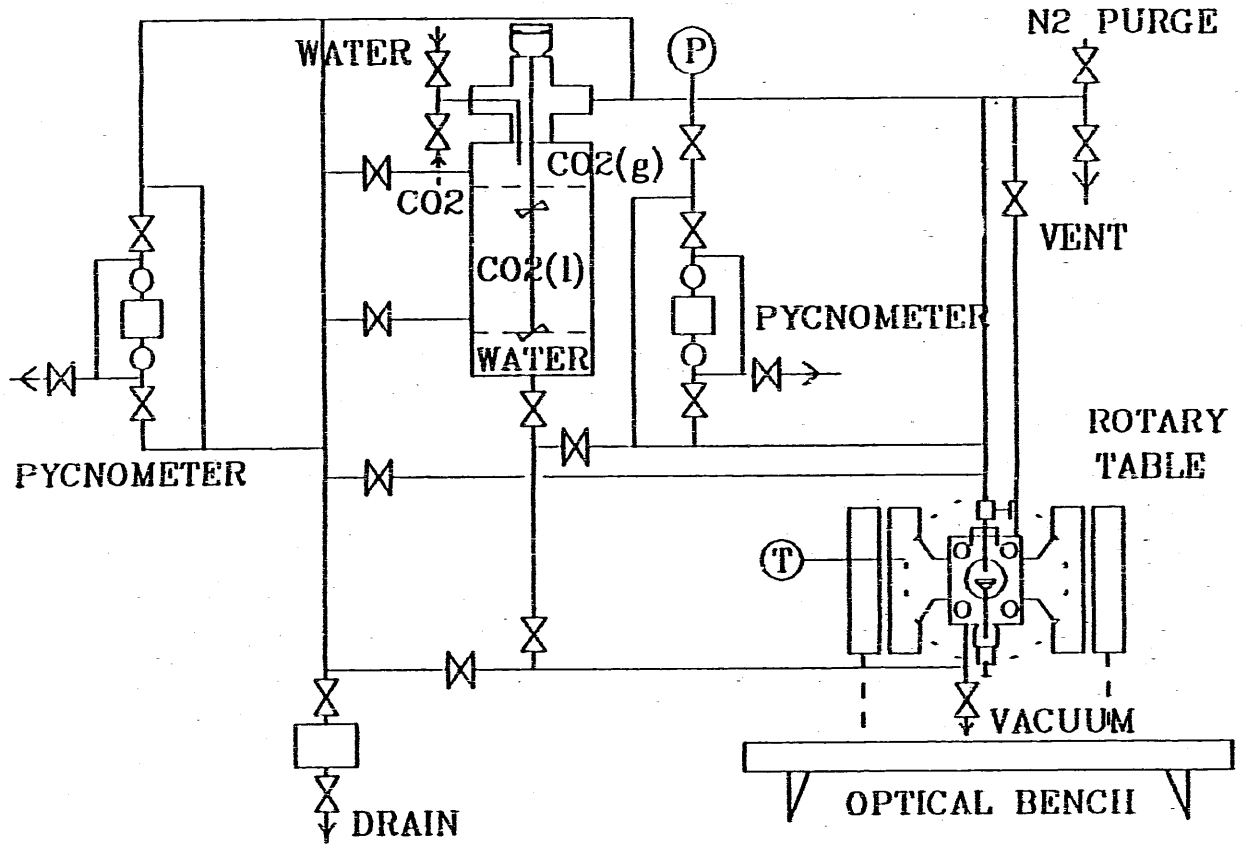

Figure 4-69. INTERFACIAL PROPERTY MEASURING UNIT

Experimental

Three different Eastern oil shale samples were utilized in the experimental work. These samples were supplied by MRI as part of a joint program in beneficiation of Eastern shales. Table 4-37 lists the samples and their principal characteristics.

Table 4-37. KEY PROPERTIES OF OIL SHALE SAMPLES

Oil Shale	Fischer Assay, GPT	Ash Content, %	Carbon Content, %	Particle Size, d_{50}, μm
Michigan	7.5	79.5	7.2	4 and 13
Indiana	12.0	78.0	13.8	7
Alabama	9.0	74.0	14.8	4

Fine grinding of the particles was performed with a rod mill followed by wet grinding in a stirred ball mill to fine particle sizes, usually below 10 μm. The density of the feed and product oil shale samples were measured with a Quantasorb Helium Pycnometer. Ash analysis was also carried out with product samples and the changes in ash content followed the same trend as the changes in product density. Both ash content and density of the product were used as indicators for product quality. Correlations for Fischer Assay and carbon yield were developed by MRI as a function of material bulk density for each of these samples. These were utilized to calculate the Fischer Assay of the upgraded product. A typical correlation for the Fischer Assay of Alabama shale as a function of particle density is shown in Figure 4-70.

The oil recovery was calculated from the following relationship:

$$\text{(Oil Recovery, Wt \%)} = \text{(Product Yield, Wt \%)} \times \frac{\text{(Product Oil Content, gal/ton)}}{\text{(Feed Oil Content, gal/ton)}}$$

An extensive study was also made on the effect of chemical additives on process performance. The chemical reagents included 1-Octanol, 2-Octanol, tall oil and sodium hexametaphosphate. The reagents were introduced at the desired dosage in a slurry of oil shale in water (slurry concentration was varied in the range of 2% to 5% by weight). The slurry was preconditioned by vigorous agitation for at least 45 minutes ensuring that equilibrium adsorption of the reagents occurred on the oil shale samples. Subsequently, beneficiation tests were carried out with the slurry. Duplicate experiments were carried out for each set of conditions. The raw data are presented in Appendix C. The results, discussed below, indicate that the LICADO process holds promise as an efficient method to upgrade Eastern oil shales.

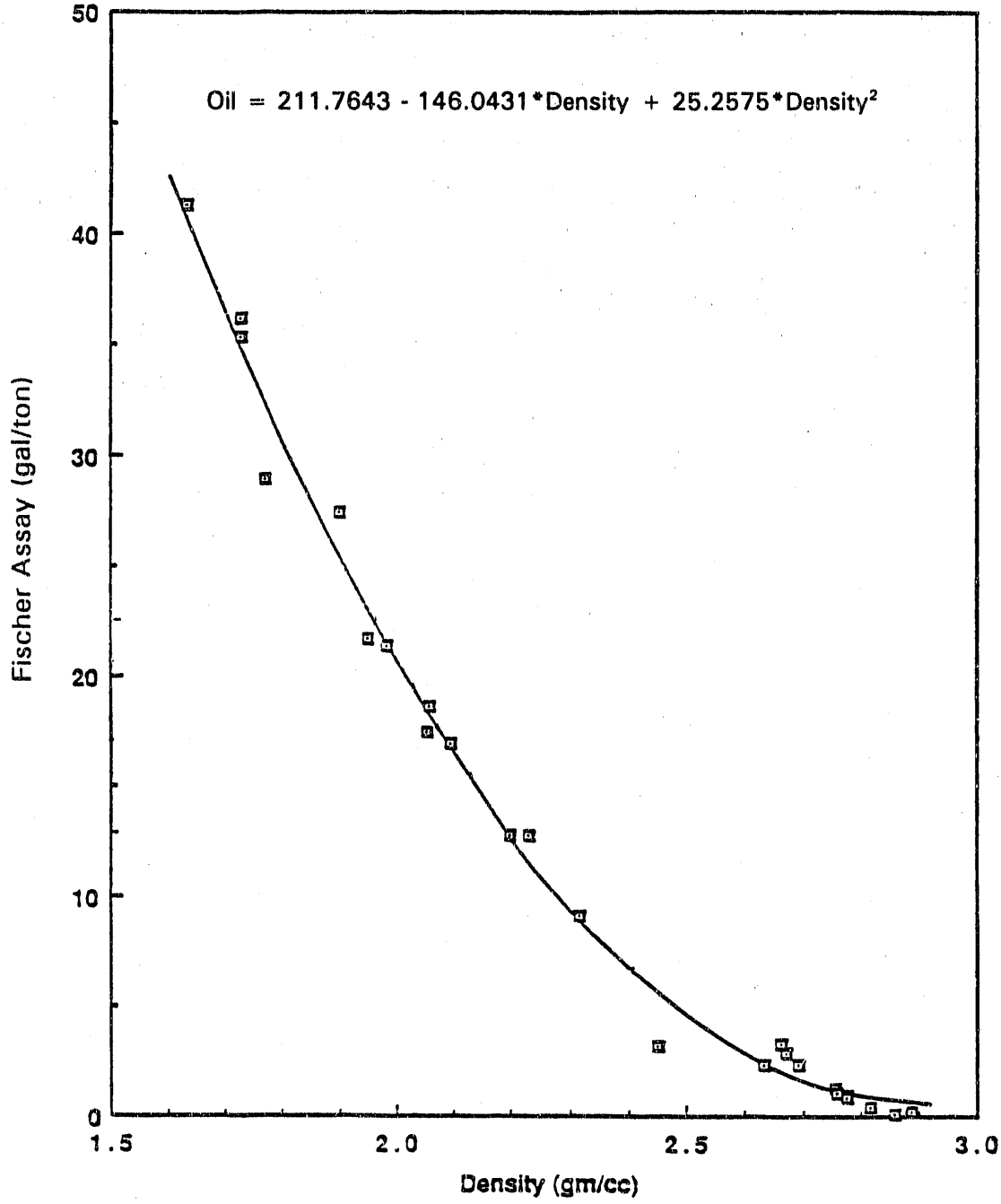

Figure 4-70. CALIBRATION CURVE FOR ALABAMA SHALE

Results and Discussion

Contact Angle Measurements

Measurements of the equilibrium contact angle on polished samples of an Eastern oil shale revealed that the surface of oil shale was being rendered hydrophobic in the presence of liquid CO_2. The results are shown in Figure 4-71. The average value of the contact angle measured in the water phase was 44° at room temperature and atmospheric pressure, but it increased steadily at higher CO_2 partial pressures, reaching 115°F (46°C) at the saturation pressure of 870 psig (6.1 MPa). Based on the enhanced hydrophobicity of oil shale samples (as indicated by large contact angles) in the CO_2 atmosphere, it was concluded that the LICADO process would be effective in upgrading Eastern oil shale samples.

Batch Tests in the BRU Without Additives

Batch tests were conducted in the 2-inch BRU with various samples listed in Table 4-37. In this section, the initial results obtained in parametric studies in the absence of chemical additives will be presented. Table 4-38 lists the experimental parameters and their operating range for these tests. The results obtained in the BRU tests with additives is discussed in detail in the next section.

The effect of contact time of liquid CO_2 on process performance in the batch tests is shown in Figure 4-72 for the finely ground Indiana oil shale. A contact time of 2.5 minutes generated a high yield of 32.6% while the longer contact times resulted in lower yields. When the contact time was increased to 15 min., the yield decreased sharply, to 15.8%. At the same time, the ash content of the product decreased, indicating enrichment of the upgraded shale. It is suspected that particle sedimentation at the longer contact times could be responsible for the observed results.

Settling time (that is, the operating time at which the ball valve was closed in the BRU to effect a physical separation of the refuse and upgraded material) did not improve the results. The data indicated that sedimentation problems in the batch unit could be minimized by maintaining a small contact time of 2.5 minutes and no settling time.

The effect of agitation speed for Indiana shale was also investigated in the parametric tests. A comparison can be made for the results on yield and ash in the product at the same contact time of 5 minutes. Figure 4-73 shows that the ash content of the product shale is dependent on the agitation speed. The lowest ash content of 71.6% was achieved at the lowest impeller speed employed (800 rpm). The yield increases slightly with agitation speed and the increase in product yield is not sufficient to counteract a sharp increase in the product ash content at higher speeds. An increase in the mixing speed in the water phase promotes an increase in the interfacial area available for particle-droplet contact and consequently, a higher product yield is obtained. However, the entrainment of ash particles in the upgraded shale-liquid CO_2 agglomerates at the higher speeds is detrimental to product quality. Subsequently, batch tests were conducted at the lower mixing speed of 800 rpm.

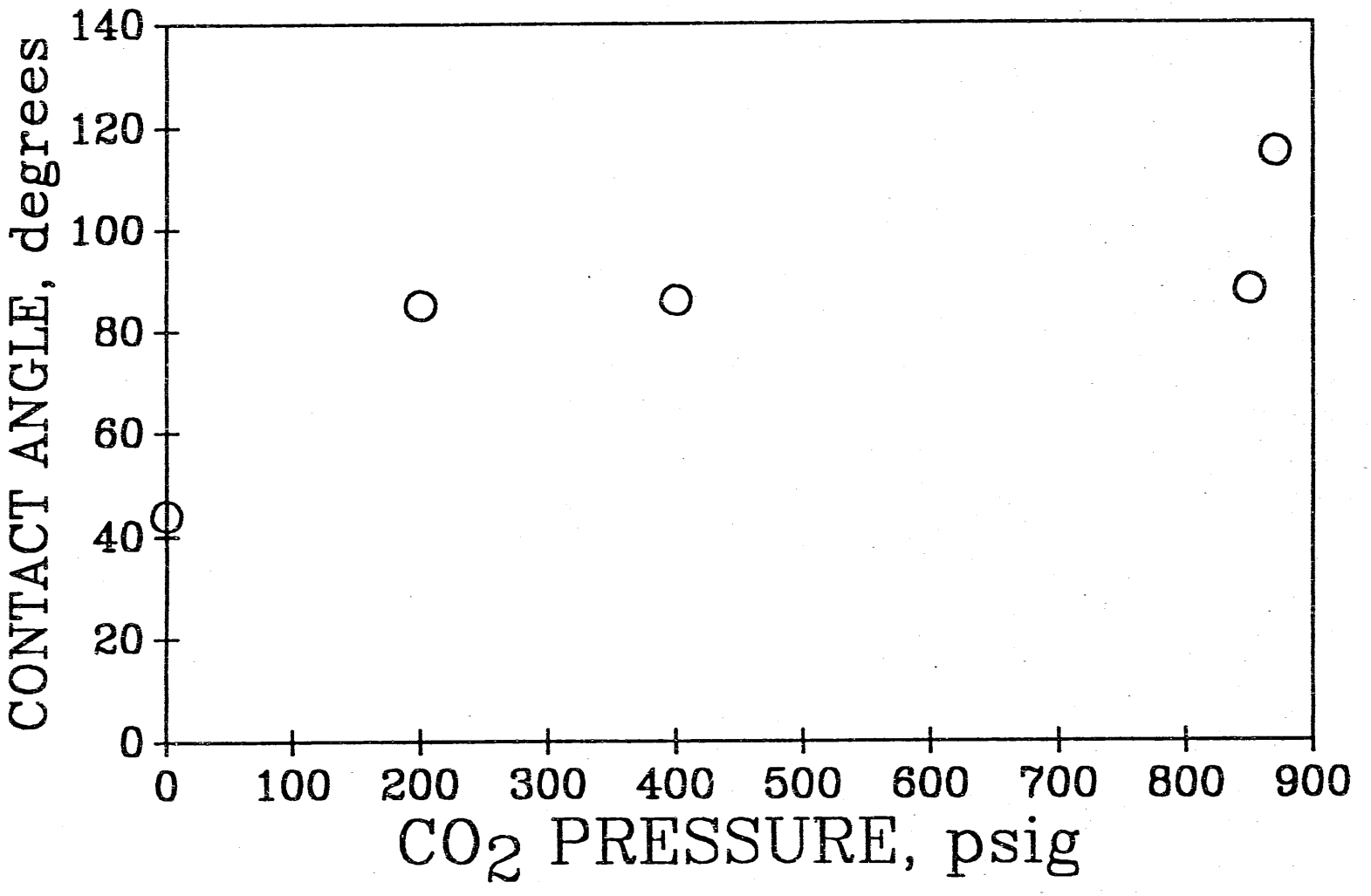

Figure 4-71. CONTACT ANGLE AT VARIOUS CO_2 PRESSURES

Table 4-38. OPERATING VARIABLES IN BRU TESTS

Variables	Range
Pressure, psig	800-870
Temperature, °F	70-80
Particle Size, d_{50}, μm	4-20
Slurry Concentration, wt %	2-10
Agitation Speed, rpm	400-2500
Liquid CO_2 Injection Rate, mL/min	100-350
Contact Time, min	2.5-15
Reagent Dosage, ppm	25-1000

The effect of slurry concentration for the same Indiana shale is demonstrated clearly from the results in Figure 4-74. There is a perceptible increase in yield at the higher slurry concentrations, but it is also accompanied by an increase in the ash content of the upgraded oil shale. While the use of more concentrated slurries translates into a larger operating capacity per unit volume, it is clear that process performance for oil shale slurries would be improved only at lower solid loadings (preferably 2.5%) where the dispersion problem can be minimized.

The effect of injection rate of liquid CO_2 is shown in Figure 4-75 for this sample of Indiana oil shale. An increase in yield as well as product ash content can be observed in Figure 4-75 as the injection rate was increased gradually to 350 mL/min. Higher injection rates would facilitate better contact between the droplets of liquid CO_2 and the oil shale particles and increase the yield. However, the entrapment of fine ash material in the agglomerate at the higher injection rates causes a loss in product quality.

Similar results were achieved with Alabama and Michigan oil shale sample that had been fine ground in a stirred ball mill to an average particle size of 4 μm. The data show a similar trend -- higher injection rates resulted in increased experimental yield. Subsequent batch processing with finely ground Alabama shale was carried out at a injection rate of 150 mL/min. In the case of fine Michigan shale, the trend of the results was similar to that of Alabama shale. Based on this information, it was decided to carry out subsequent tests with fine Michigan shale at a liquid CO_2 injection rate of 200 mL/min.

In one set of experiments with the finely ground Michigan shale, the effects of slurry pretreatment conditions were examined. The slurry was filtered and the filter cake was dried overnight in an oven at 60°C and pulverized prior to processing in the BRU. A 5% slurry was remade with water and the experiments were performed in the BRU. Tests were also carried out by dispersing the filter cake in water directly to form a 5% slurry without drying. Both the yield and product quality are reduced when the sample was subjected to drying. Oxidation of the sample during the drying process and the slime coating on the solid particles during the consolidation of the filter cake are suspected to be the reasons for this behavior.

Figure 4-76 summarizes the results with Alabama and Indiana oil shales in the absence of additives in the BRU tests. The yield appears to increase

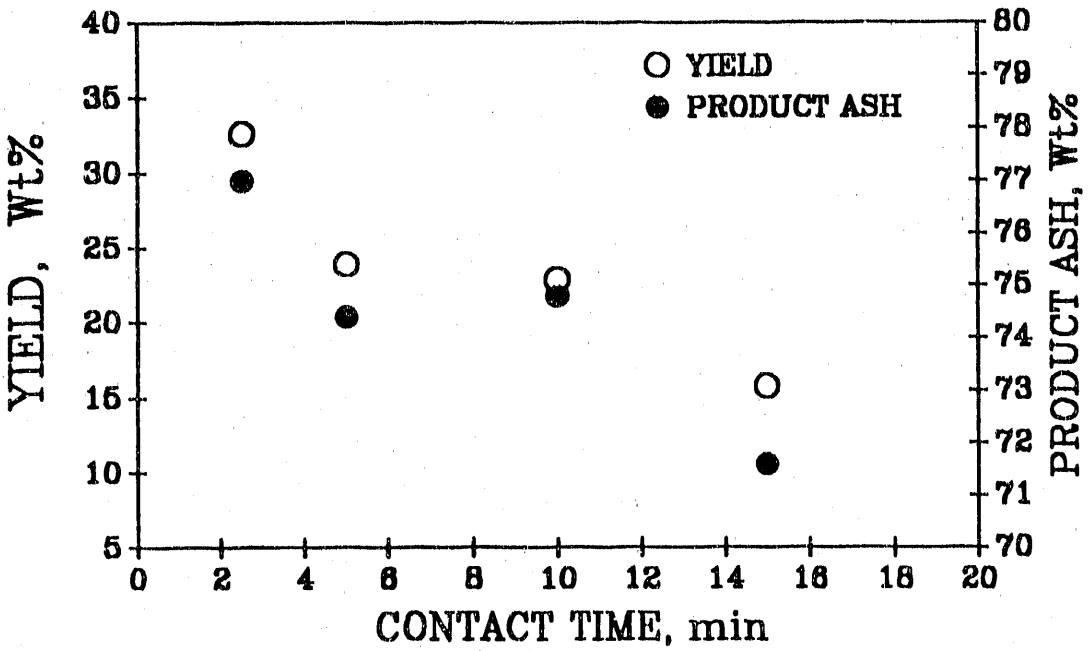

Figure 4-72. EFFECT OF CONTACT TIME FOR INDIANA SHALE

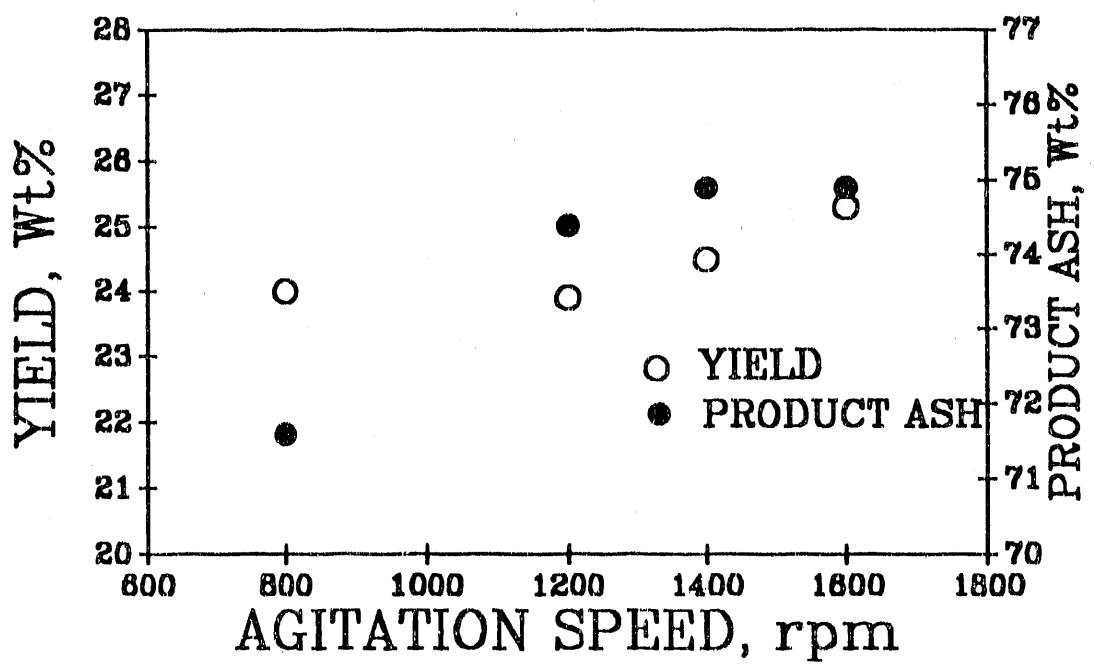

Figure 4-73. EFFECT OF AGITATION SPEED FOR INDIANA SHALE

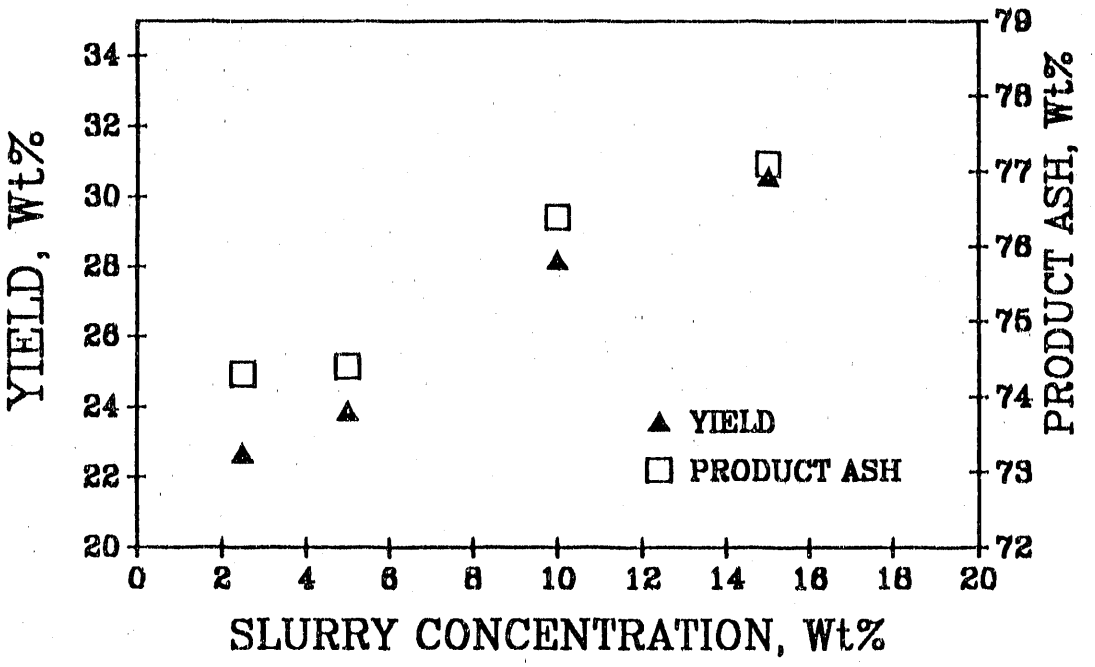

Figure 4-74. EFFECT OF SLURRY CONCENTRATION FOR INDIANA SHALE

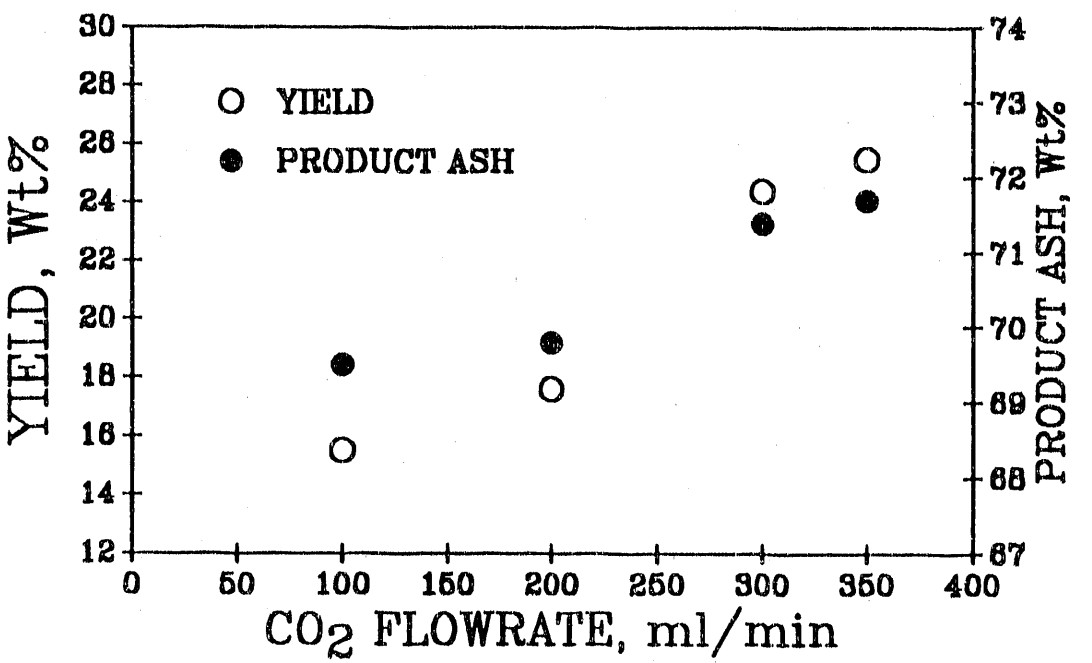

Figure 4-75. EFFECT OF CO_2 INJECTION RATE FOR INDIANA SHALE

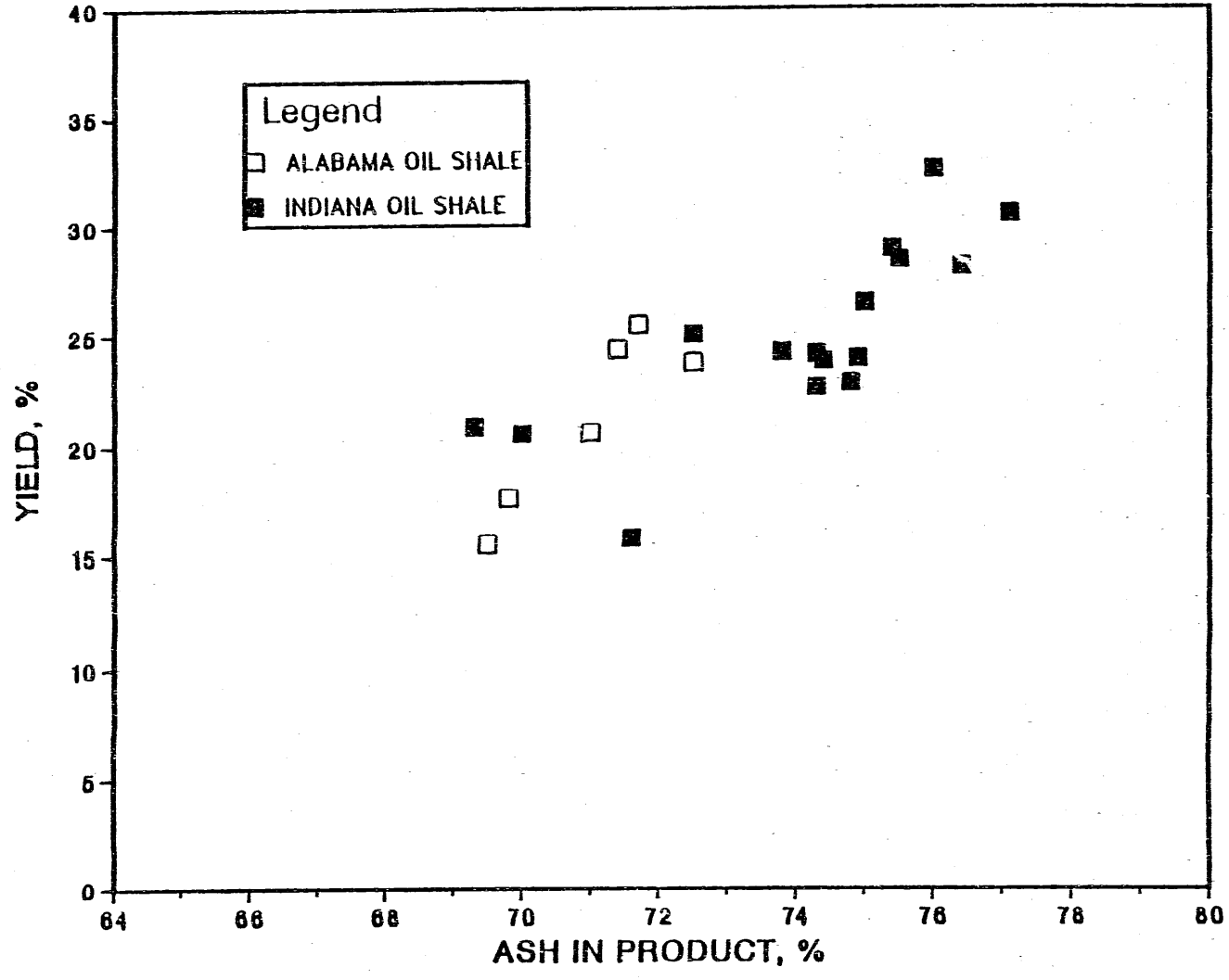

Figure 4-76. SUMMARY OF BRU TEST RESULTS WITHOUT ADDITIVES

correspondingly with ash in the upgraded product shale. This strongly suggests that without the aid of chemical reagents, improved yields could be achieved only at the expense of a decrease in product quality.

The major conclusions from the BRU tests without additives were as follows:

1. Small contact times without a settling period is suitable for obtaining high yields.

2. Higher liquid CO_2 injection rates increased the yield, but only at the expense of a reduction in the product quality. Intermediate injection rates for each shale sample appeared to favor improved product quality and recovery.

3. A low mixing speed of 800 rpm in both phases appeared to generate the best results.

4. Low slurry concentrations were desirable in order to improve the product quality.

5. Sample oxidation must be avoided in order to obtain improved yields and product quality.

Batch Tests in the Presence of Additives

In this section, results of batch tests conducted in the presence of additives, SHMP, 1-Octanol, 2-Octanol, and tall oil are discussed.

SHMP Addition

The first chemical reagent employed in the beneficiation tests in the BRU was a dispersant commonly used in the mineral processing industry: Sodium Hexametaphosphate (SHMP). The dispersant dosage effect was studied at three levels: 100 ppm, 500 ppm and 750 ppm in solution. The batch tests were performed with no settling time allowed.

The results and the earlier parametric tests with Indiana shale show that a decrease in the product yield was registered when the dispersant was employed in the process. However, the decline was not statistically significant. The ash content in the product also appears to be generally lower when the slurry was preconditioned with SHMP. The dosage of the reagent did not influence the results substantially within the range explored. The most encouraging results were achieved at the lower agitation speed of 800 rpm, where the ash content in the product was consistently lower than at the higher agitation speed of 1200 rpm.

The results were analyzed statistically using a statistical software package and are presented in Appendix D. The main conclusions based on the limited number of tests performed are that impeller speed and the presence of dispersant are statistically significant in determining the yield as well as product quality. The higher impeller speed generated higher yields but the lower impeller speed of 800 rpm resulted in improved product quality. The presence of the reagent SHMP at any dosage was detrimental to the product

yield -- that is, it did not selectively disperse the mineral matter. Overall, the process performance in batch tests with SHMP as the additive in upgrading Indiana oil shale was not satisfactory.

Batch Tests in Modified BRU (Screen-Type Agglomeration Experiments)

Beneficiation tests were conducted in the modified BRU by recovering the upgraded agglomerates on a 80 mesh screen, as described earlier. Meaningful and reproducible results were obtained only after eliminating the settling time. The objective in performing screen tests was to obtain a quick qualitative assessment of the reagent addition on process performance and the results are not to be compared to that obtained in the batch tests.

The experimental results obtained in the presence of various dosages of the straight-chain alcohol, 1-Octanol, were analyzed statistically using the Duncan test (Appendix D). The results of the statistical analysis for oil recovery as well as Fischer Assay are shown in Figures 4-77 and 4-78. The error bars represent the 95% probability that experimental data will fall in the indicated range, as obtained in the statistical analysis. Figure 4-77 shows that the higher dosages of 1-Octanol are more conducive for increasing the oil recovery (up to about 70% by weight). From Figure 4-78, it appears that the dosage of 500 ppm is sufficient to cause a significant increase in the Fischer Assay (up to an average value of 27.4 GPT, compared to about 12 GPT in the feed material). It can be concluded that 1-Octanol should be employed at about a dosage of 500 ppm (close to its solubility limit) in order to upgrade Indiana oil shale.

The effect of employing a branched chain alcohol (2-Octanol) on process performance for Indiana shale are similar to that obtained with 1-Octanol. However, the increase in the Fischer Assay was not as pronounced as with 1-Octanol.

Effect of 1-Octanol and Tall Oil in BRU Tests

These experiments were conducted at an impeller speed of 800 rpm with a contact time of 2.5 minutes and no settling period allowed during the test. Except in one series of tests with Alabama shale, the slurry concentration was maintained at 2.5%.

The results of pretreatment of Michigan oil shale with different dosages of 1-Octanol are shown in Figures 4-79 and 4-80. Significantly improved results for oil recovery and Fischer Assay were achieved with the sample that was finely ground to an average particle size of 4 μm. The slurry concentration was maintained at 5% in these tests. At low dosages up to 300 ppm of 1-Octanol, the reagent appeared to disperse the mineral matter effectively, since the Fischer Assay increased from 7.5 GPT in the feed to the range of 24 to 27 GPT in the upgraded product. Unfortunately, it also resulted in a decrease of the product yield, suggesting that the kerogen-rich material was also being partially dispersed. At the higher dosages of 1-Octanol (exceeding 300 ppm), the product yields were much higher at slightly lower values of Fischer Assay, indicating that 1-Octanol was behaving as a co-agglomerating agent. At a dosage of 500 ppm, oil recoveries exceeded 90%. Statistical

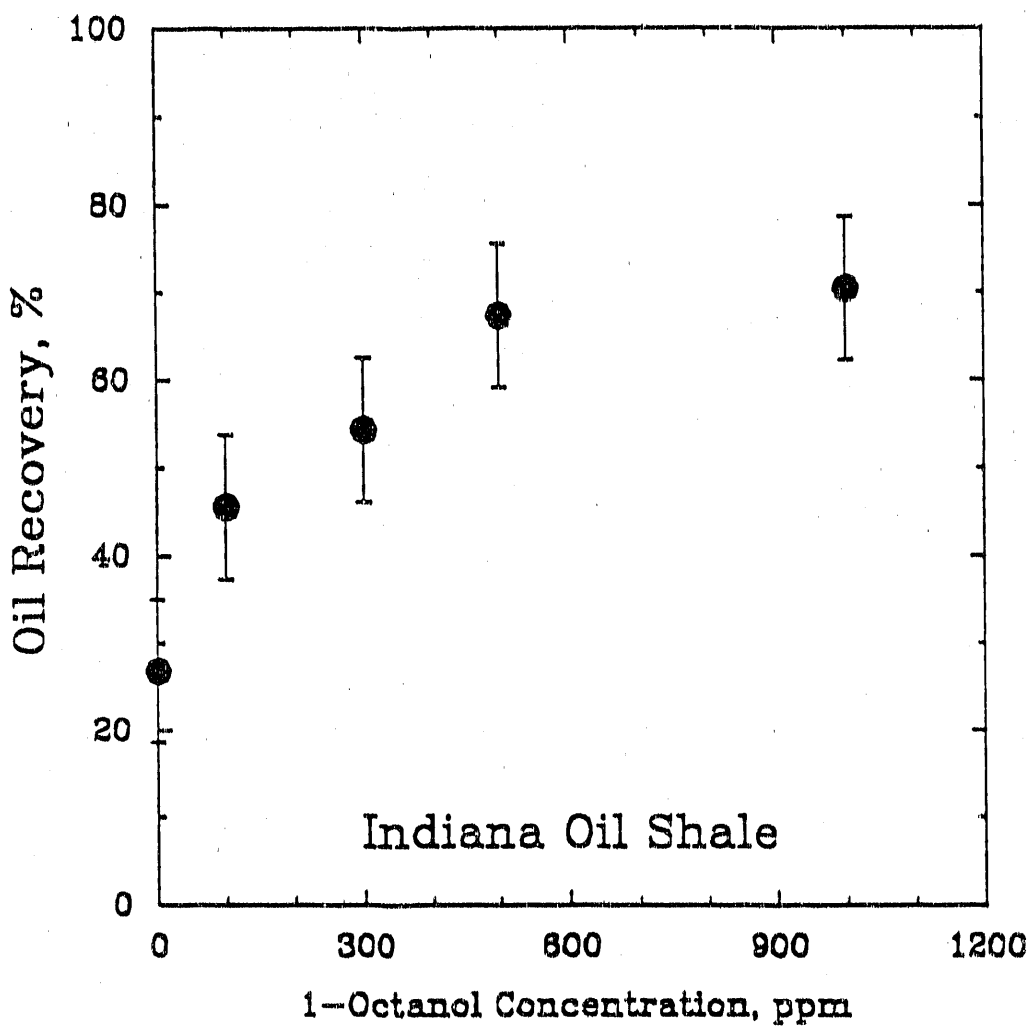

Figure 4-77. OIL RECOVERY AS A FUNCTION OF DOSAGE OF 1-OCTANOL (Screen Tests)

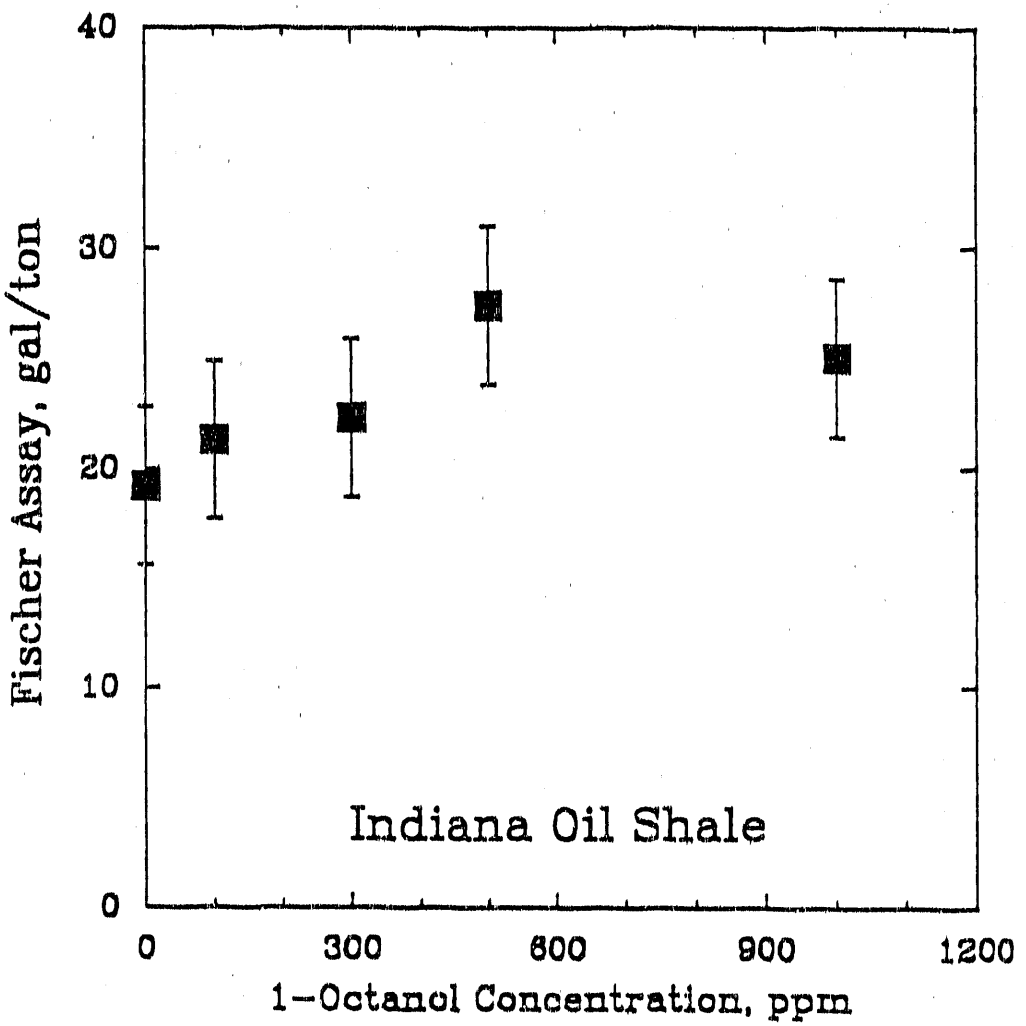

Figure 4-78. FISCHER ASSAY AS A FUNCTION OF DOSAGE OF 1-OCTANOL (Screen Tests)

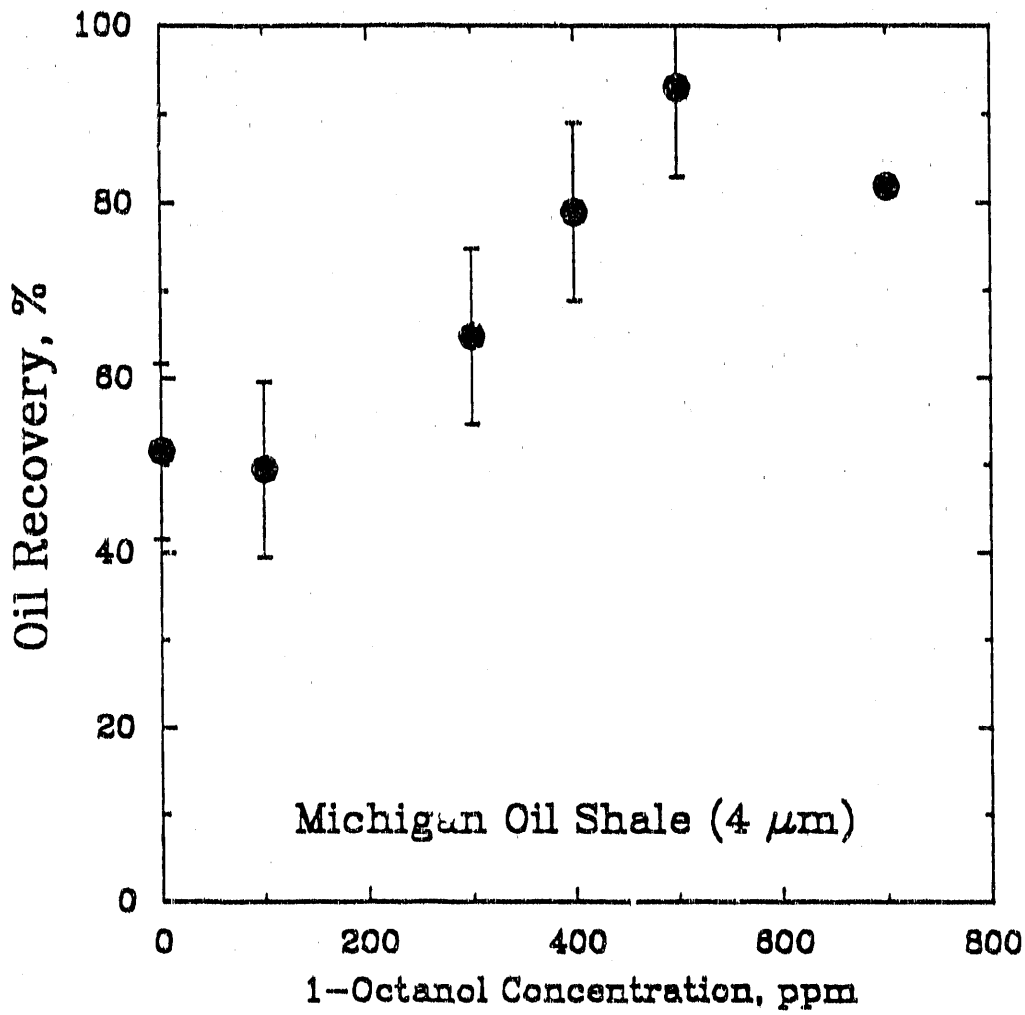

Figure 4-79. VARIATION OF OIL RECOVERY WITH DOSAGE OF 1-OCTANOL FOR 4-μm MICHIGAN OIL SHALE

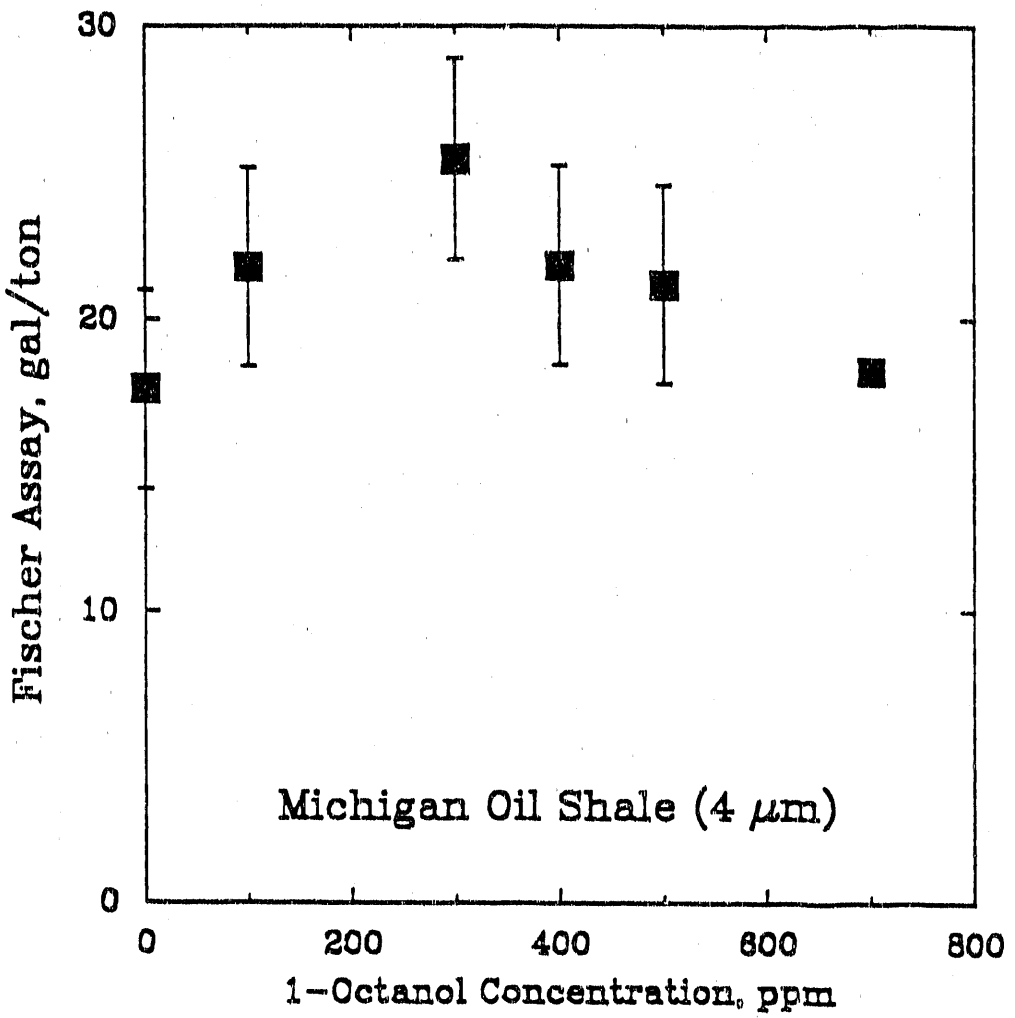

Figure 4-80. VARIATION OF FISCHER ASSAY WITH DOSAGE OF 1-OCTANOL FOR 4-μm MICHIGAN OIL SHALE

analysis using the Duncan test for this case revealed that maintaining the reagent concentration in the range of 500 ppm would be suitable.

It may be speculated that 1-Octanol is essentially acting as a dispersant for Michigan shale at lower dosages owing to its mode of adsorption. At the higher dosages, the orientation of the adsorbed molecule could change, with the formation of multilayers. The configuration of the adsorbed molecule could be such that the hydrophobic tail group might orient toward the bulk phase and accommodate more molecules. This would impart hydrophobicity to the surface and increase the product yields, though not necessarily have a serious detrimental effect on the product quality.

The variation of oil recovery with dosage of 1-Octanol is illustrated in Figure 4-81 for a relatively coarse sample of Michigan shale, ground to a larger particle size of 13 μm. These results may be attributed to poor liberation characteristics of the oil-rich fraction from the mineral-laden matrix for the coarsely ground samples.

Figures 4-82 and 4-83 illustrate the effect of pretreatment of finely ground Michigan oil shale with tall oil at various concentrations, up to 500 ppm. It is apparent from Figure 4-82 that the presence of tall oil considerably enhances the oil recovery, exceeding 95% at dosages greater than 100 ppm. The improvement in Fischer Assay is not so pronounced as in the case of treatment with 1-Octanol, as shown in Figure 4-83. Statistical analysis by the Duncan test for this series of runs revealed essentially no effect of tall oil on the Fischer Assay and a considerable enhancement of oil recovery at a dosage of 300 ppm of tall oil. Figures 4-84 and 4-85 demonstrate the effect of tall oil on Alabama shale, fine ground to an average particle size of 4 μm. The trend of the results was similar to that obtained with Michigan shale.

The effect of preconditioning with 1-Octanol on the process performance was also investigated with Alabama oil shale, finely ground to 4 μm at a slurry concentration of 2.5%. The results are presented in Figures 4-86 and 4-87. It is evident from Figure 4-86 that high oil recoveries (close to 90%) were achieved at dosages of 1-Octanol above 100 ppm. Figure 4-87 reveals that at a dosage of 300 ppm of 1-Octanol, the Fischer Assay of the product increased beyond 25 GPT. Statistical analysis indicated that both high oil recoveries and product quality can be achieved for this case by maintaining a dosage of 300 ppm of 1-Octanol.

In the next series of experiments with finely ground Alabama shale, the slurry concentration was increased to 5% from 2.5% and the tests with 1-Octanol were repeated. Data in Figures 4-88 and 4-89 suggest that though oil recoveries were improved at the higher concentrations of 1-Octanol, there was surprisingly little influence on the Fischer Assay, which varied in the range of 16 to 19 GPT.

Two-Step Processing in the BRU

In this series of tests in the BRU, the product sample from the first step was reprocessed by utilizing it as the feed for the second step. Finely ground Alabama shale was studied in the two-step experiments. The slurry concentration was maintained at 2.5% for both steps. It can be observed that the enrichment of the product is considerably enhanced after pretreatment of

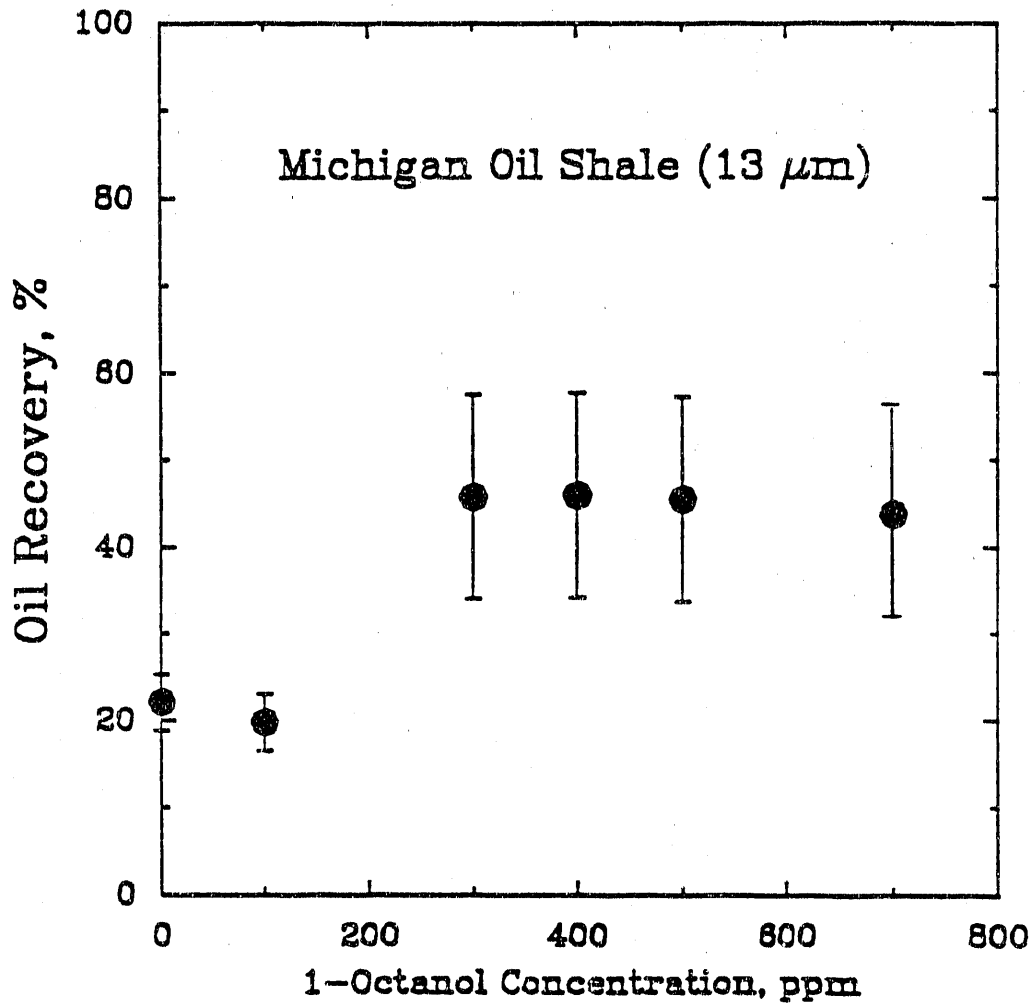

Figure 4-81. VARIATION OF OIL RECOVERY WITH DOSAGE OF 1-OCTANOL FOR 13-μm MICHIGAN OIL SHALE

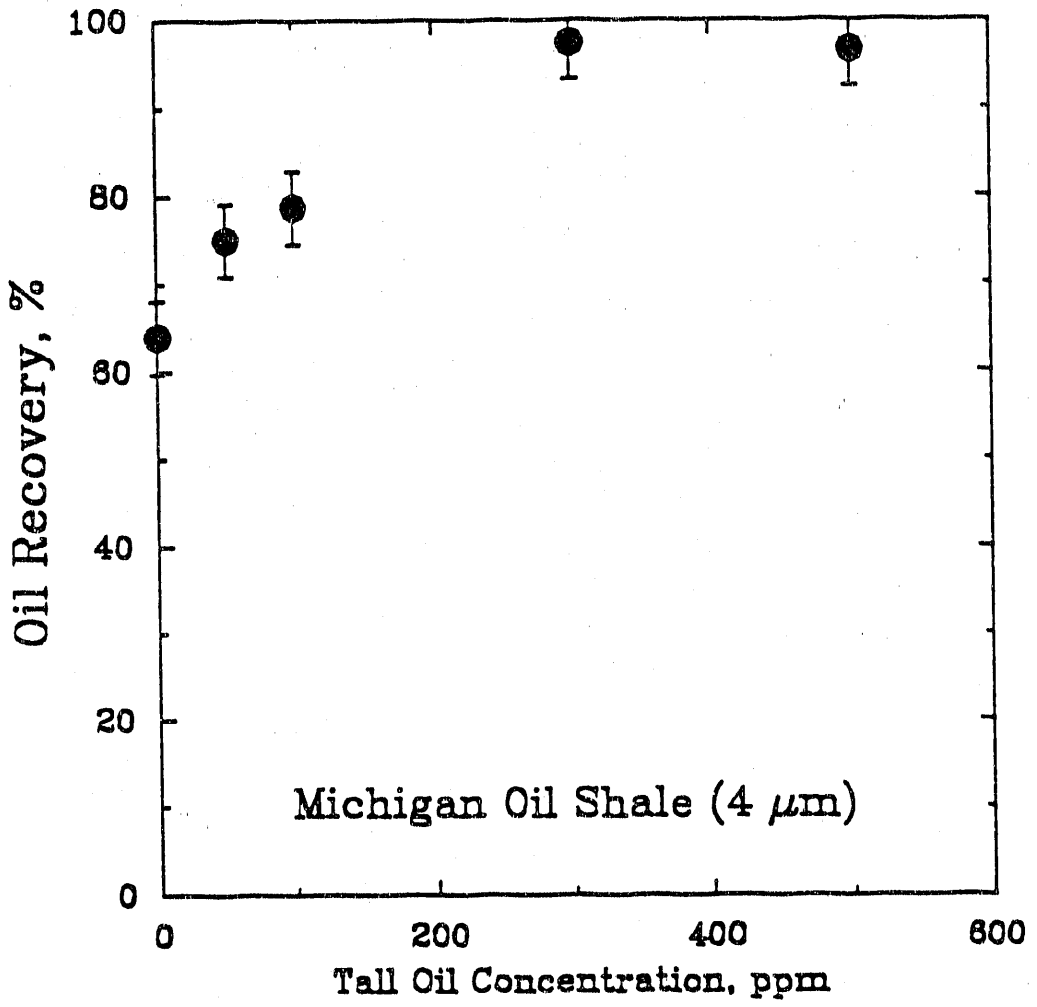

Figure 4-82. VARIATION OF OIL RECOVERY WITH DOSAGE OF TALL OIL FOR 4-μm MICHIGAN OIL SHALE

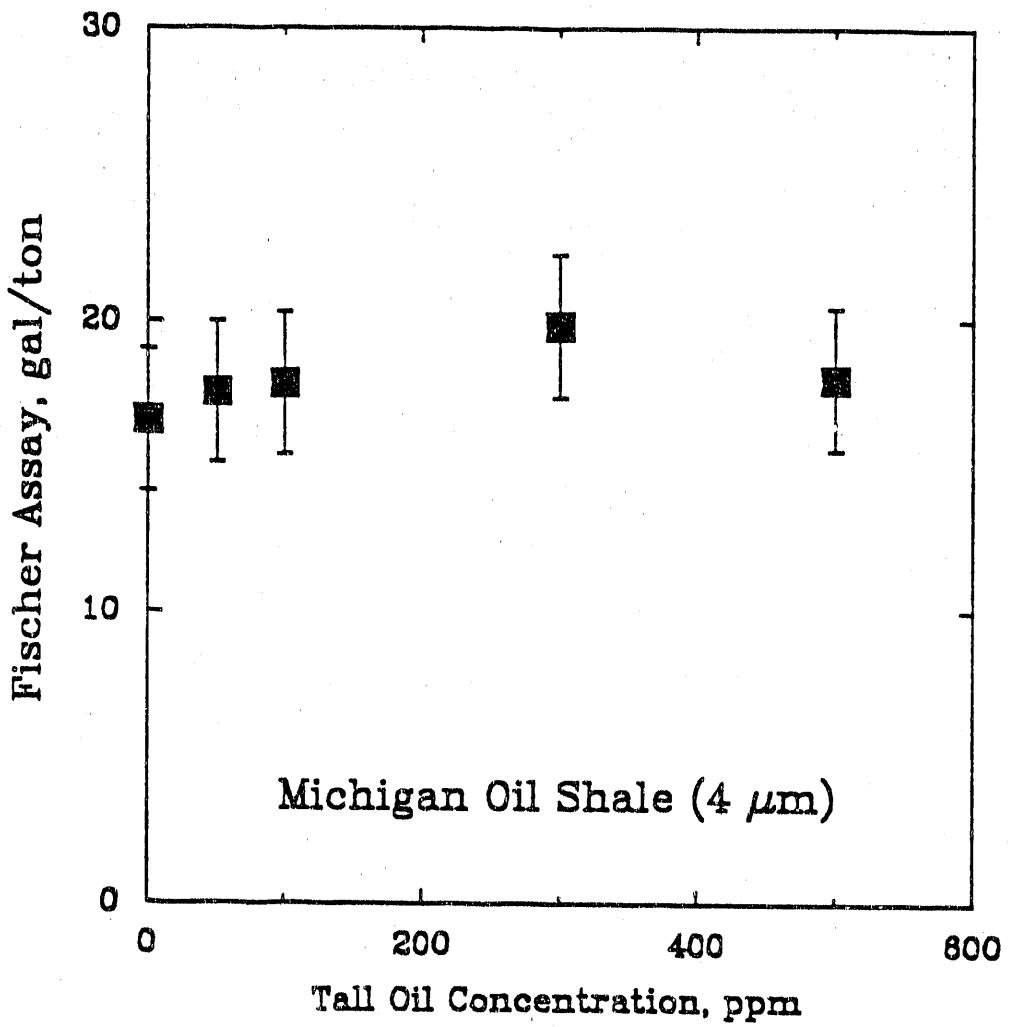

Figure 4-83. VARIATION OF FISCHER ASSAY WITH DOSAGE OF TALL OIL FOR 4-μm MICHIGAN OIL SHALE

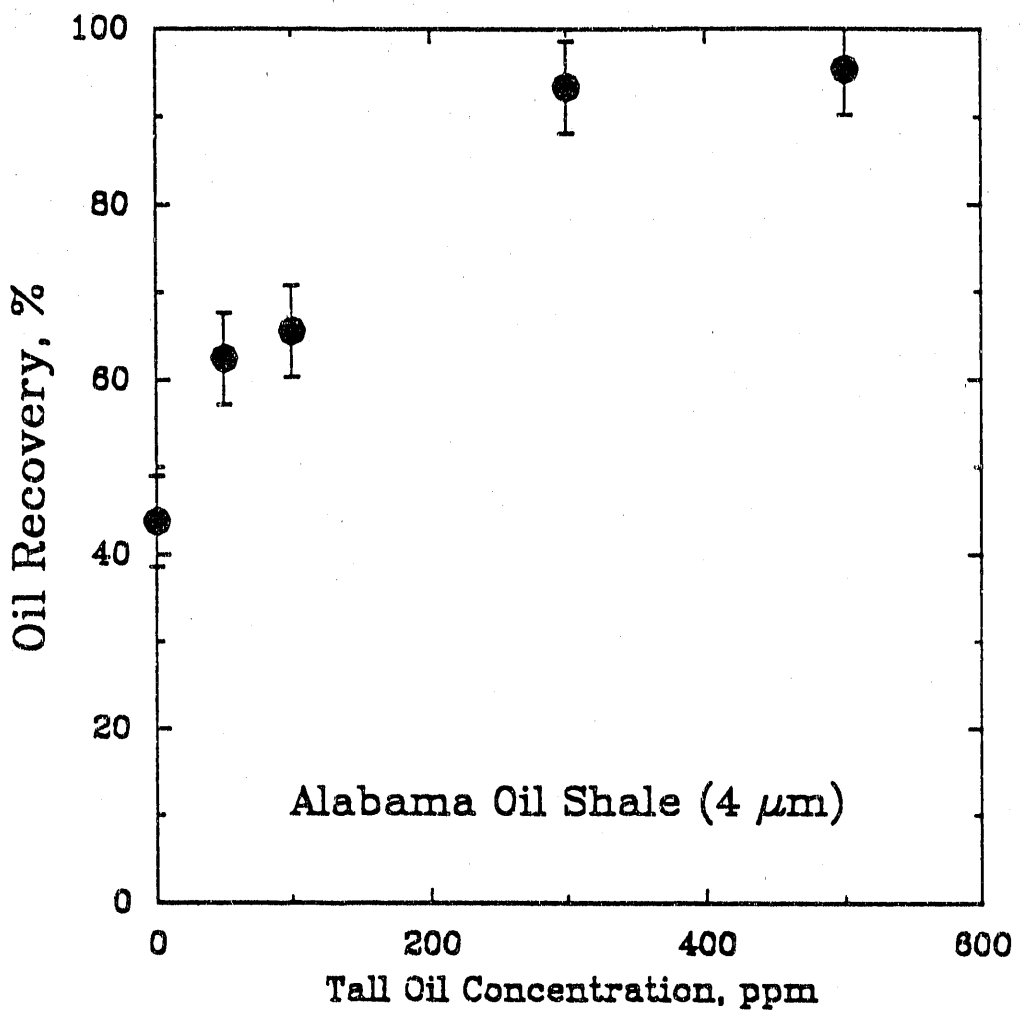

Figure 4-84. VARIATION OF OIL RECOVERY WITH DOSAGE OF TALL OIL FOR 4-μm ALABAMA OIL SHALE

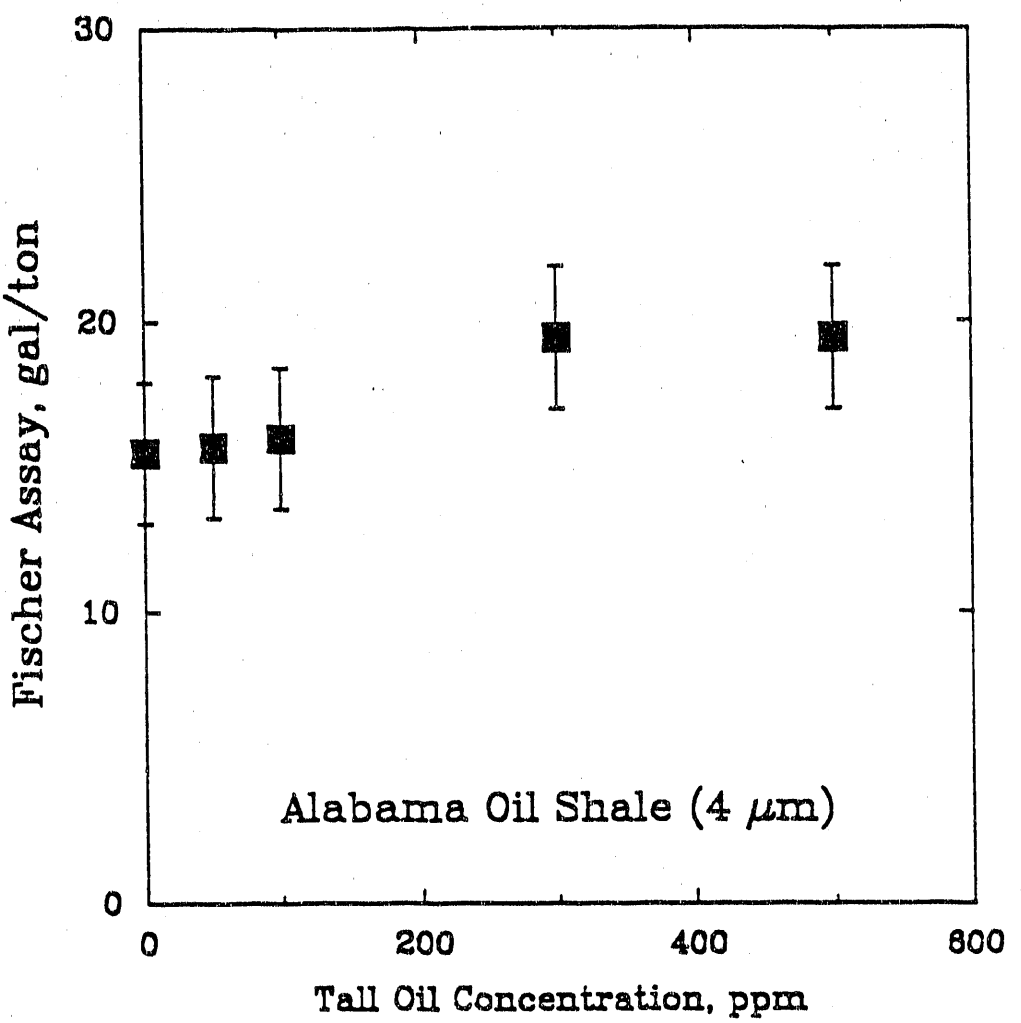

Figure 4-85. VARIATION OF FISCHER ASSAY WITH DOSAGE OF TALL OIL FOR 4-μm ALABAMA OIL SHALE

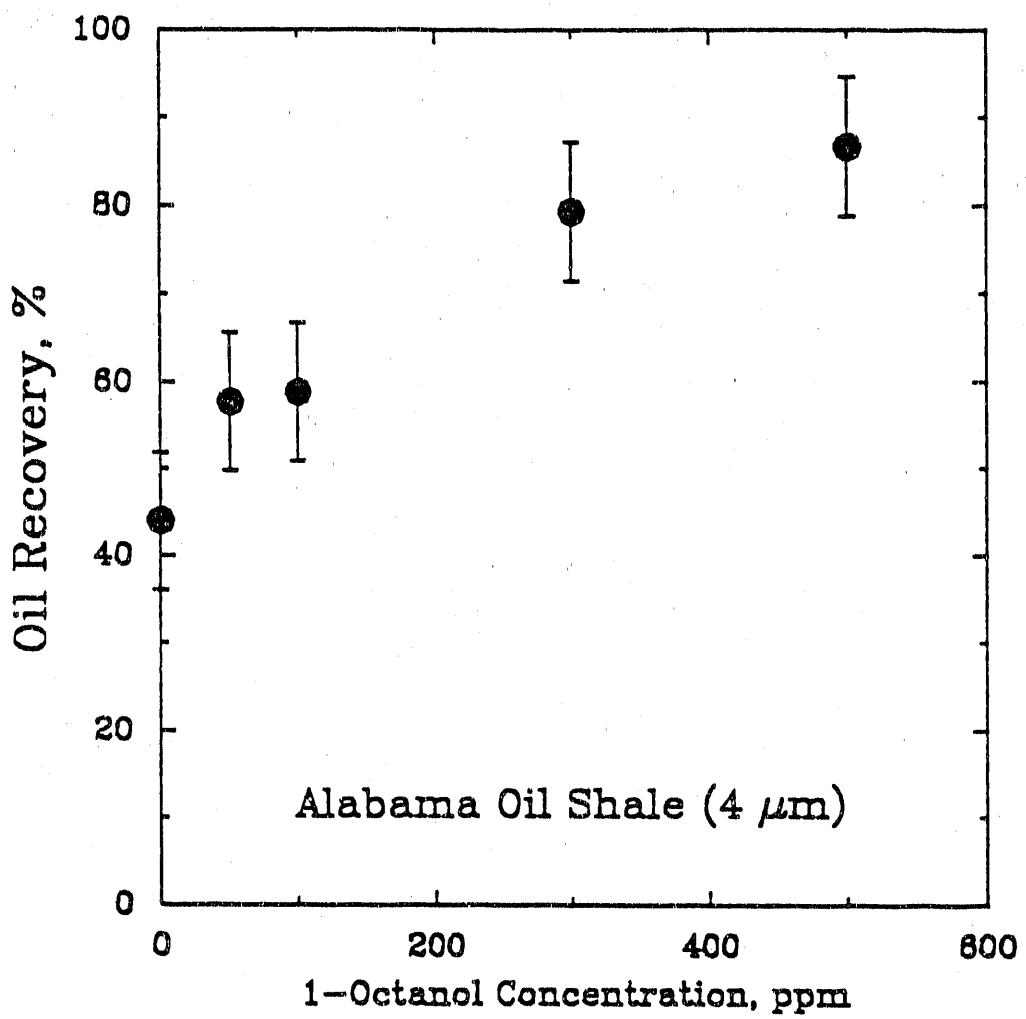

Figure 4-86. EFFECT OF DOSAGE OF 1-OCTANOL ON OIL RECOVERY FOR 2.5% SLURRY CONCENTRATION

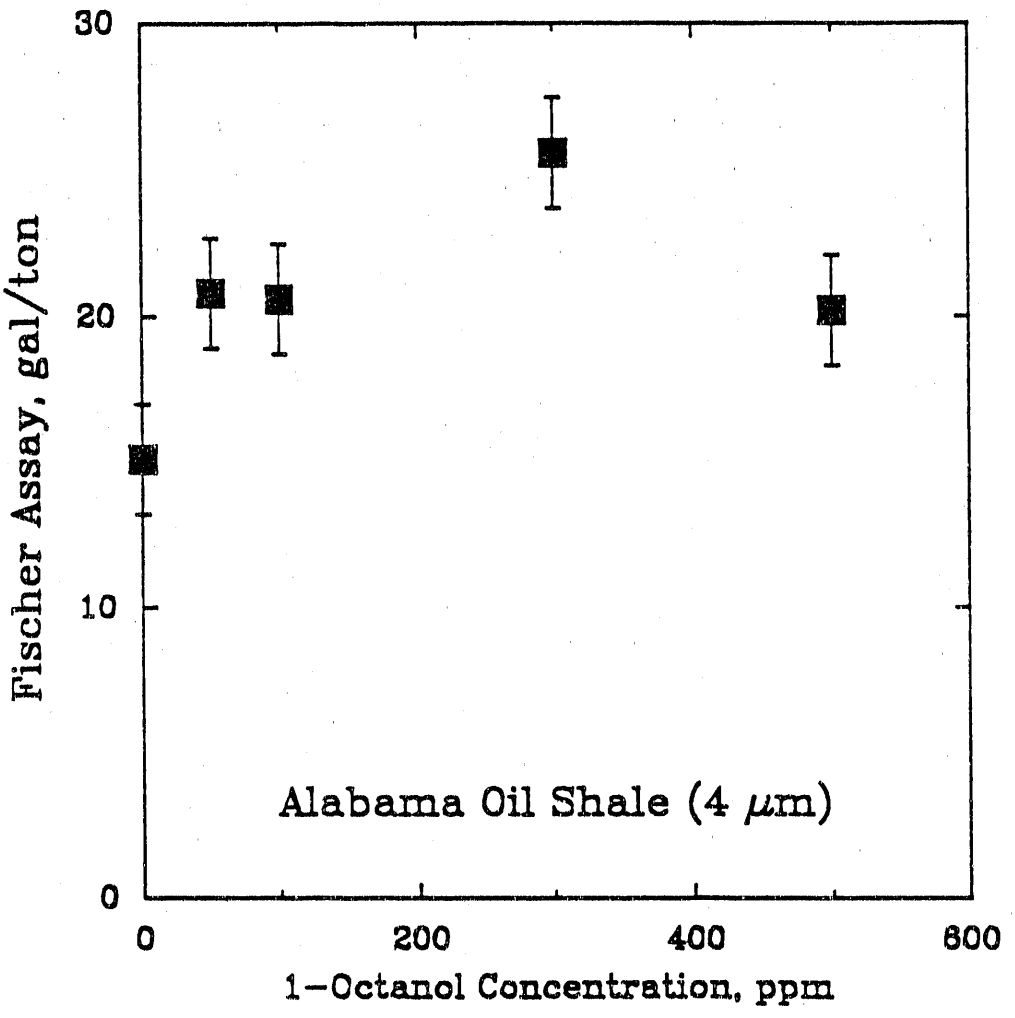

Figure 4-87. EFFECT OF DOSAGE OF 1-OCTANOL ON FISCHER ASSAY FOR 2.5% SLURRY CONCENTRATION

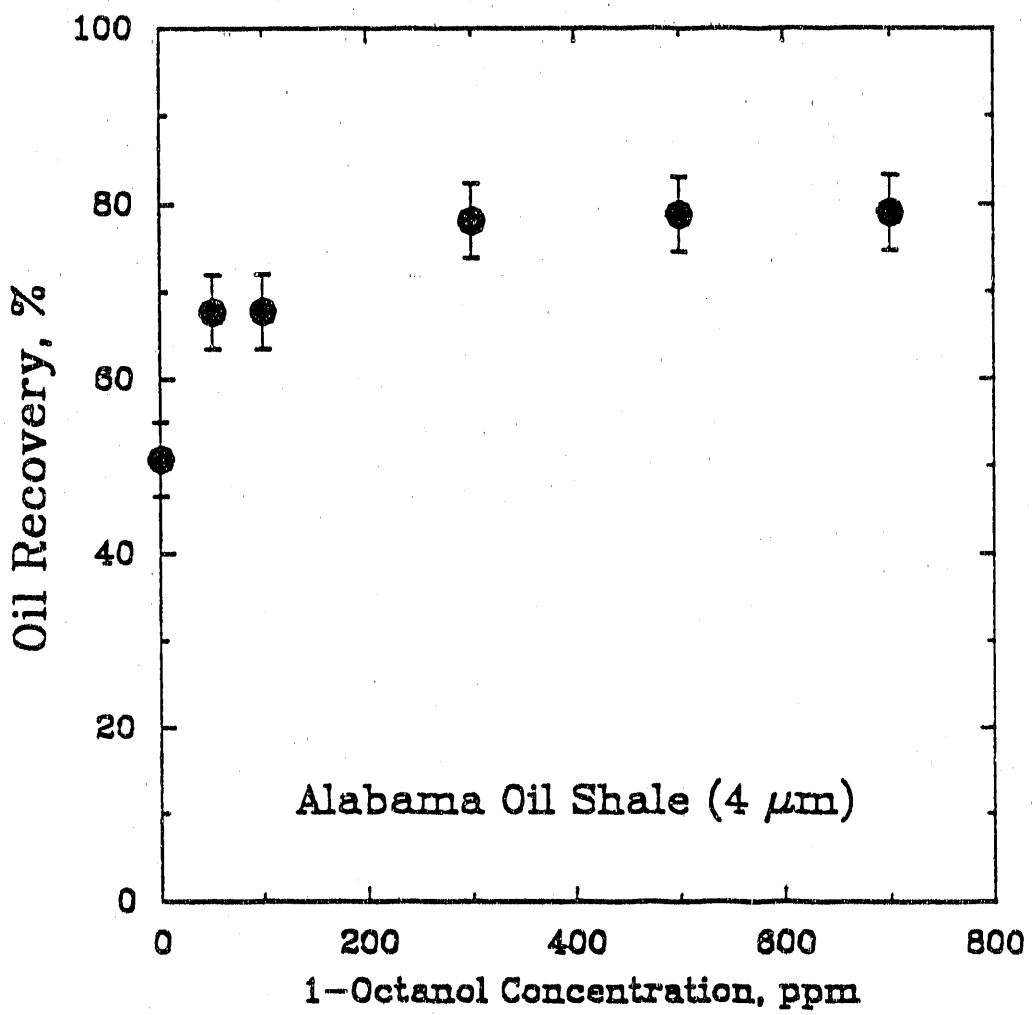

Figure 4-88. EFFECT OF DOSAGE OF 1-OCTANOL ON OIL RECOVERY FOR 5% SLURRY CONCENTRATION

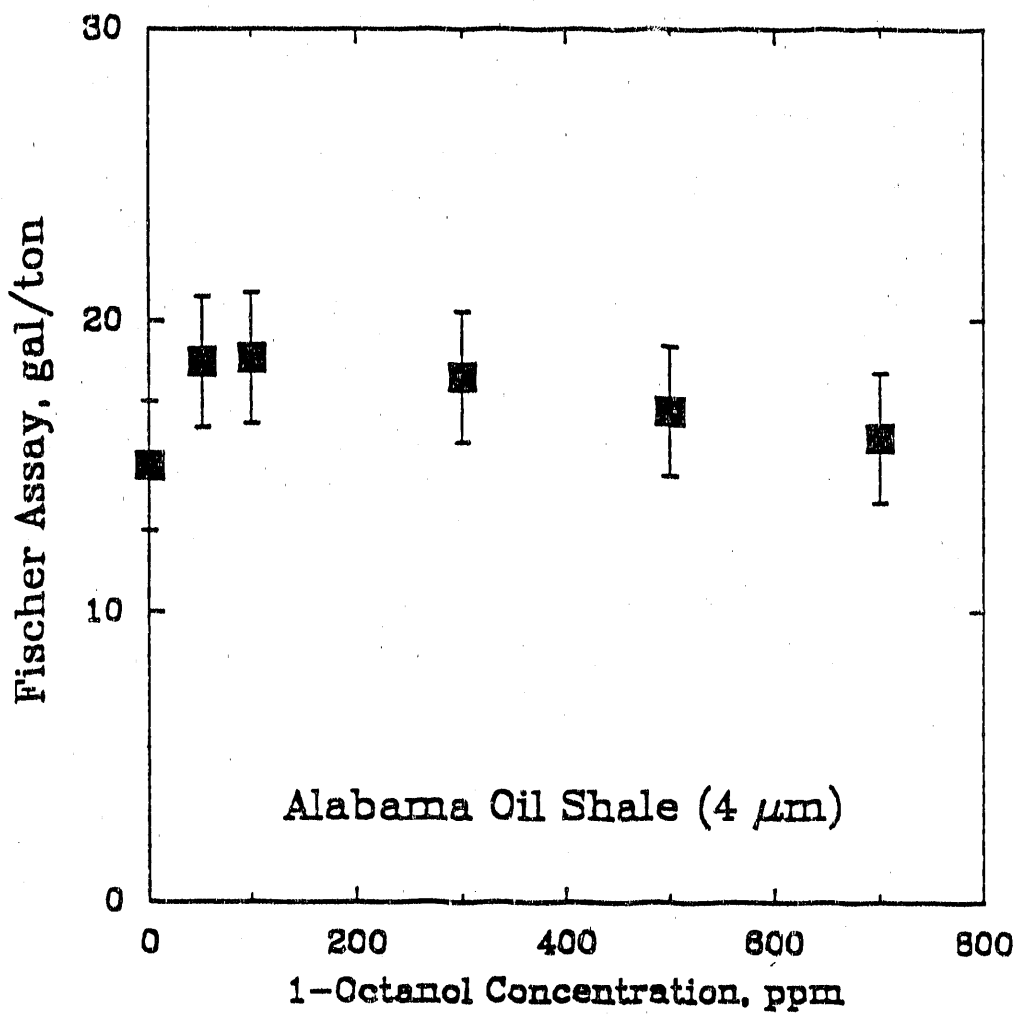

Figure 4-89. EFFECT OF DOSAGE OF 1-OCTANOL ON FISCHER ASSAY FOR 5% SLURRY CONCENTRATION

the feed sample with 1-Octanol. A Fischer Assay of 29 GPT was registered after the second step treatment when the sample was pretreated with 1-Octanol. However, the overall oil recovery is much lower than that obtained after the first step treatment, owing to the sharp decrease in the product yield.

Semi-Continuous Experiments in the RDU

Experiments were conducted in the 4-inch RDU with all three oil shale samples listed in Table 4-37. Alabama and Michigan shale were processed in the RDU after incorporating the internal two-stage device. The product sample was collected in the overflow cell. Some product was also collected in the top of the cone in the separation cell and was recovered independently. The refuse was withdrawn from the bottom of the cell. The product yield was calculated by material balance on the ash of the feed, refuse and product samples for each test.

Single-Stage Processing in the RDU

In the case of Indiana shale, a pre-mixing time of 7 minutes was maintained. The liquid CO_2 flow rate was fixed at 500 mL/min and the contact time at 15 minute. The pre-mixing agitation speed was maintained at 2050 rpm. The results show that higher speeds resulted in increased oil recoveries at the expense of a decrease in Fischer Assay. Significant upgrading of Indiana shale was achieved at an agitation speed of 1700 rpm and a dosage of 500 ppm of 1-Octanol, since the Fischer Assay of the product was nearly 26 GPT.

Two-Stage Processing in the RDU

The internal two-stage device in the RDU was employed for processing Alabama oil shale in the semi-continuous mode of operation. The pre-mixing speed was set at 3050 rpm and the slurry was preconditioned with liquid CO_2 for 7 minutes prior to carrying out the test. A slurry concentration of 2.5% was utilized. During the experiment, liquid CO_2 was injected for 30 minutes at a flow rate ranging from 1000 to 2000 mL/min.

The results of processing Alabama shale with and without 1-Octanol in the system show that the product quality appeared to improve as the agitation speed was decreased. The effect of agitation speed on the product yield was not significant. Lower impeller speed and higher liquid CO_2 flow rates facilitated increases in the oil recovery. A significant improvement in the oil recovery as well as product quality can be achieved with semi-continuous two-stage treatment with no additives. When 1-Octanol was employed to pretreat Alabama shale at a dosage of 300 ppm, the oil recovery increased to 94%, mainly due to an increase in the product yield. There was no significant effect on Fischer Assay. It can be concluded that two-stage treatment in the RDU is beneficial to process performance compared to BRU tests. The improvement is particularly noticeable in the case where no chemical additive is used.

Economic Evaluation of Process

Economic evaluations were carried out to estimate the cost of the LICADO process for upgrading Eastern oil shale samples. A conceptual 200 ton/h plant was used as the basis for these calculations. A process economics model

developed by Westinghouse Electric Corporation for personal computer applications with LOTUS 123 was used for these calculations. The processing cost of the beneficiated shale was estimated from the capital cost of the plant, operating costs, financing costs, maintenance costs etc. (details are in Appendix E). The experimental data obtained in two-stage processing in the RDU without additives was considered as input data for calculation. Sensitivity analyses were made to determine the effect upon the required processing cost of oil shale for a given rate of return on investment.

Results of the analysis for the conceptual 200 ton/h plant show that a processing cost of $3/ton (grinding costs excluded) must be charged in order not to incur losses. To obtain a rate of return of 20%, the processing cost is estimated to be about $4/ton.

Conclusions

1. The LICADO process proved to be effective in upgrading three different samples of Eastern oil shale.

2. Parametric studies established that low impeller speeds, small contact times, no settling time, intermediate injection rates and low slurry concentrations were favorable in upgrading the oil shale samples tested.

3. Sample oxidation appeared to have a detrimental effect on oil recovery and product quality.

4. The dispersant SHMP proved ineffective in upgrading the oil shale samples. Tall oil facilitated an enhancement in oil recovery without degrading the product quality.

5. Significant improvements in oil recovery and product quality were achieved by conditioning all three oil shale samples with 1-Octanol. The desired dosage of reagent was established for each set of experiments. Oil recoveries exceeded 90% and the Fischer Assay was improved three-fold for Michigan and Alabama shale samples.

6. Smaller particle sizes (below 5 μm) and low slurry concentrations (2.5 wt %) were favorable for enrichment of the shale samples.

7. Two-step operation in the batch mode improved the Fischer Assay of the product at the expense of a decrease in overall oil recovery.

8. Two-stage operation in semi-continuous mode improved the process performance in terms of oil recovery and product quality as compared to single-stage operation.

9. An economic analysis of the process indicated that the processing cost for beneficiated oil shale is estimated to be about $4/ton for a rate of return on investment of 20%.

SUBTASK 4.3. WASTE TREATMENT AND DISPOSAL

Processing of Eastern oil shales by flotation to recover upgraded kerogen products requires grinding the shales to particle sizes finer than 10 μm to liberate the inorganic mineral matter from the kerogen network. This results in the release of organic and inorganic constituents into the process waters. These soluble constituents may or may not be hazardous but their control and containment have become a matter of concern.

The tailings remaining after removal of the kerogen represent 65% to 80% by weight of the shale. Generally they contain some soluble ionic species that are not removed during thickening and dewatering and, in any planned commercial operation, would have to be disposed in an environmentally safe and acceptable manner. Also, because of their fineness, the tailings may be susceptible to natural leaching over extended periods of time. Although disposal of tailings continues to be the subject of discussion, little attention has been given to the use of the rejects as a potential raw inorganic mineral resource. The extent to which that may be possible needs to be determined.

In this subtask, the flotation process waters and tailing rejects were considered waste streams in need of treatment to render them innocuous. The tailing solids also were evaluated as a potential raw mineral for recycling. Thus, the overall objectives were to --

- Characterize the type and quantities of soluble organic and inorganic ionic species generated and released to process water during fine grinding and flotation treatment of Eastern oil shales.

- Develop methods for removing or recovering the soluble constituents from the process water to a level acceptable for recycle or discharge to the land, rivers and streams.

- Determine the quantity of soluble salts discharged with the flotation tailing rejects and assess their significance as a potential environmental problem.

- Determine the susceptibility of the flotation tailing rejects to natural leaching over extended periods of time, and suggest methods for their safe impoundment and storage.

- Study the feasibility of using the flotation tailing in selected commercial applications.

Subtask 4.3.1. Waste Water Treatment

The objective of this subtask is to determine the type and quantity of organic and inorganic constituents that are released into the process waters during ultra-fine grinding and flotation, and to develop methods for removing or recovering them as valuable byproducts for return to the domestic mineral and metal resource base.

Environmental Analysis of Simulated Process Water From Alabama and Indiana Shale

Samples of Alabama and Indiana shales were ground to flotation size (<15 μm) using deionized water and filtered to recover the water. The filtrates were diluted with deionized water in the ratio of 9:1 to represent oil shale flotation process water. Assuming that part of the frother/collector used in the flotation process was not all utilized and would remain in the recycle water, 5 drops of Dowfroth 250, representing about 11 ppm, was added to the process waters.

One half of each process water sample was retained for analysis for BOD, COD, TDS, oil and grease and sulfates. The other half of each water sample was passed through a column of activated charcoal at a flow rate of 1.5 to 2 gallon/min/ft^3 (3.34 to 4.46 L/m^3/s) of charcoal to determine the potential for reducing environmental problems associated with oil shale process water. Results of these studies are shown in Table 4-39.

Table 4-39. RESULTS OF STUDIES TO REDUCE BIOLOGICAL OXYGEN DEMAND (BOD) AND CHEMICAL OXYGEN DEMAND (COD) IN ALABAMA AND INDIANA PROCESS WATERS

Parameter	Alabama		Indiana	
	SPW*	ACE**	SPW	ACE
Biological Oxygen Demand (BOD_5 day), mg/L	4.4	1.1	3.5	<1.0
Chemical Oxygen Demand (COD), mg/L	<5.0	<5.0	<5.0	<5.0
Oil and Grease, mg/L	<1.0	<1.0	<1.0	<1.0
Total Dissolved Solids (TDS), mg/L	800	700	1,230	1,150
Sulfate, mg/L as $SO_4^=$	650	560	1,040	889
pH	4.6	4.3	5.4	4.6
Conductivity, μm mhos/cm	930	886	1,364	1,356

* SPW - Simulated process water.

** ACE - Activated charcoal effluent.

Data in Table 4-39 show that the activated charcoal was effective in reducing the BOD of the simulated waste water and that the COD and oil and grease content of the process water were very low despite the addition of the frother/collector used to float the kerogen.

Additional process water studies from each of the six shale samples were conducted by grinding 500 gram samples of -10 mesh shale at 40% solids, using deionized water, in a stainless steel laboratory rod mill for 2 hours. The ground samples were filtered and filtrate samples were taken for analysis. Results of these studies are shown in Table 4-40.

The results show significant differences in the soluble inorganic metal ion species generated by grinding the six Eastern oil shales. Of particular interest is the high cadmium (Cd) content of the water generated in grinding the Ohio shale sample. Otherwise, the data suggest that the indicated

Table 4-40. ANALYSES OF ROD MILL GRIND WATER FILTRATES

Analysis, ppm	Deionized Water	Oil Shale Source					
		Alabama	Tennessee	Kentucky	Indiana	Ohio	Michigan
Cd	<0.10	0.33	0.02	0.02	0.20	7.90	0.12
Cr	<0.10	1.01	0.07	0.09	0.15	2.79	0.11
Cu	<0.10	0.10	0.03	0.03	0.03	0.91	0.04
Pb	<0.50	0.24	0.15	0.13	0.25	0.21	0.20
Ni	<0.10	75.6	26.0	9.4	41.2	73.7	2.9
Zn	<0.50	51.0	3.8	0.34	16.0	3.00	1.00
Fe	<0.10	1,150	4.84	0.30	284.0	760	6.7
Mn	0.10	34.6	16.4	22.2	73.0	22.7	5.0
F^-	NA*	116.1	ND**	ND	ND	267.5	ND
Cl^-	NA	89.0	11.3	12.7	547.4	236.0	27.3
$PO_4^=$	NA	4,929	2,258	1,900	5,082	5,171	2,784
$SO_4^=$	NA	5,208	2,370	2,140	5,338	5,484	2,959
pH	7.0	4.3	6.2	7.0	5.2	4.3	6.8
Conduc. μm mhos/cm	0.4	5,480	3,190	3,240	6,000	5,700	3,990

* NA - not analyzed.

** ND - not detected.

solubility of the metal ions may be a function of solution pH and/or the sulfate content of the solutions. Previous studies of Alabama oil shale grind waters (Davis, G; Misra, M., and Lamont, W.E., 1987) show much lower metal ion specie solubility when the solution pH was 5.5 as opposed to a solution pH of 4.3 shown in the present study. Data in the previous study show the effect of solution pH, when grinding an Alabama shale sample, on the quantity of Fe in solution. At a pH of 2.5 the total Fe concentration was 200 ppm. By increasing the pH to 5.5, the iron concentration decreased to 2 ppm. Results of this study as well as the data shown in Table 4-40 imply that simple pH control in a grinding and/or flotation circuit would yield conditions conducive to metal-ion precipitation, thus obviating the necessity for expensive wastewater treatment facilities.

However, since Subtask 4.3.1 specifically called for studies of methods for removing or recovering the soluble metal ions two methods were studied to determine the potential for reducing and/or recovering the metals in solution, 1) ion exchange and 2) precipitation as sulfides. Limited studies were made to reduce organic contamination in the recycle, or waste, water.

Flotation Plant Process Water

Since the data shown in Table 4-40 reflect the metal ion solubility attributed to grinding only; that is, at 40% solids, and past flotation studies (Schultz, Bates, and Lamont, 1989) have shown that kerogen flotation was most effective in the 4% to 5% solids range, the grind waters were diluted with deionized water at a 9:1 ratio of deionized water to grind water to represent the type of plant process water that might be encountered in a

flotation plant utilizing on-line metal ion removal techniques. Ion exchange studies as well as sulfide precipitation studies were conducted using this diluted process water. Analyses of the diluted process waters are shown in Table 4-41.

Table 4-41. ANALYSIS OF DILUTED PROCESS WATER USED IN ION EXCHANGE AND SULFIDE PRECIPITATION STUDIES

Analysis, ppm	Oil Shale Source					
	Alabama	Tennessee	Kentucky	Indiana	Ohio	Michigan
Cd	0.08	0.01	0.01	0.06	2.00	0.03
Cr	0.20	0.05	0.04	0.04	0.60	0.04
Cu	0.03	0.01	0.01	0.01	0.25	0.02
Pb	0.05	0.05	0.04	0.04	0.05	0.07
Ni	15.35	6.9	2.2	9.9	12.9	0.68
Zn	24.0	1.20	0.10	3.7	58.0	0.29
Fe	650.0	1.21	0.07	64.0	194	1.06
Mn	11.01	4.4	5.8	17.5	5.4	1.39
F^-		ND	ND	ND	4.0	ND
Cl^-	28.4	2.6	6.6	3.2	4.4	6.2
$SO_4^=$	2,421	605	502	1,149	1,141	643
TOC*	<5	<5	9.5	<5	<5	6.9
pH	3.5	6.3	7.1	5.2	4.5	6.8
Conduc., μm mhos/cm	3,530	1,160	1,110	2,020	1,880	1,450

* TOC - total organic carbon.

Comparison of the data in Tables 4-40 and 4-41 show discrepancies in the analytical data when using a 9:1 dilution ratio of deionized water to grind water; however, these discrepancies may be the result of slight changes in solution pH and/or aging. Since both ion exchange and sulfide precipitation techniques would cause significant pH and conductivity changes in the process water, thus altering the analysis of metal ions in solution, studies utilizing either technique would require testing in a continuous operating mode to determine their effectiveness in removing metal ions as well as the affect on kerogen flotation.

Removal of Organic Contaminants

Analysis of each of the process waters to be used in the metal ion removal studies for total organic carbon (TOC) showed that the Alabama, Tennessee, Indiana and Ohio recycle waters contained less than 5 ppm TOC while the Kentucky and Michigan recycle waters contained 9.5 and 6.9 ppm TOC, respectively.

Each of the recycle waters was passed through a column of activated carbon (Darco HD-4000) manufactured by American Norit Co. Inc., Jacksonville, Florida. Analysis of the recycle water effluent from the activated carbon column showed that the TOC in the Michigan sample was reduced from 6.9 to <5 ppm, whereas, the TOC in the Kentucky sample analyzed 9.7 ppm versus 9.5 ppm in the feed water, probably within the range of experimental error of

the analytical procedure. TOC analyses for the other 4 water samples treated with the activated carbon remained below 5 ppm.

No additional organic analysis of these simulated process waters were made because of the low TOC analyses.

Ion Exchange Removal of Metal Ions

Metal ion removal and recovery by ion exchange techniques from waste streams and/or process streams is well documented and has been utilized successfully for many years on a commercial basis. While certain ion exchange resins are capable of selectively removing specific metal ions from process streams which contain valuable metals in relatively high concentration, other resins can be used to strip bulk metal ions from waste streams to prevent subsequent ecological problems. Under the proper conditions the bulk metal ions removed from such waste steams can be stripped from the resins and, depending upon the commercial value of specific ions, can be further processed to yield recyclable metals.

Oil shale flotation process waters have been found to contain a number of metal ions in solution which represent either potentially valuable by-products, or which must be removed to prevent degradation of the environment. In the present study the flotation process stream waters were considered waste streams requiring removal of bulk metal ions to prevent environmental degradation in case of accidental discharge, or to prevent build-up of specific ions which might subsequently affect the flotation process itself.

In order to determine the potential for removing the various metal ions in solution in the simulated process waters, a bench-scale ion exchange system was set up to measure solution pH and conductivity changes when utilizing both cationic and anionic exchange resins. Exchange resin effluents were sampled on a periodic basis and, based on significant changes in both pH and conductivity, the effluent samples were analyzed for metal ion content.

The simulated process water from the Tennessee oil shale sample was not processed through the ion exchange system because this shale sample was a highly weathered, very soft outcrop sample which could not be considered representative of a mineable shale. While the data in Table 4-41 show that the Kentucky, Indiana, and Michigan shale sample process waters were equally low in metal ion content these shale samples represented material taken from active quarries and hence could be considered representative of an active mining operation.

Both resin forms used in the ion exchange studies of the process waters were obtained from Rohm and Haas Company and represented commercially available resins. The cationic resin, Amberlite IR 120, was received in the sodium form and the anionic resin was received in the chloride form. For the purposes of this study a bulk sample of the cationic resin was converted to the hydrogen form using a 10% solution of hydrochloric acid (HCl) and a bulk sample of the anionic resin was converted to the hydroxyl form using a 10% solution of potassium hydroxide (KOH).

The bench-scale ion exchange resin system consisted of two 250-mL glass burets, which contained 25 mL of glass wool above the annulus and 225 mL of either cationic or anionic resin. The burets were superimposed one above the other so that the effluent from the upper buret containing the cationic resin fed the lower buret containing the anionic resin. A funnel was used as a feed reservoir for the upper buret and the stopcocks on each buret were adjusted to yield a constant flow rate of process water; in these studies, a flow rate equivalent to 1.44 gallon/min/ft^3 (3.21 L/s/m^3) of resin. Timed samples of the effluent from the buret containing the anionic resin were taken every 20 minutes for flow rate calculations as well as pH and conductivity measurements. These timed samples were accumulated separately until pH and conductivity measurements showed significant changes indicating metal ion breakthrough in the system. The cumulative volume of water treated up to breakthrough is indicative of the resin capacity. The five process water samples, excluding the Tennessee shale process water, were all treated by this procedure using fresh resin charges for each sample.

Figure 4-90 presents the results of studies of the pH of each of the process waters exiting the sequential resin exchange system as a function of time, and Figure 4-91 shows the results of studies of the conductivity of the solution from the same timed samples. The data clearly show that the Alabama process water sample, having a resin system indicates capacity of about 1.33 hours or 115 gallon/ft^3 (15.37 kL/m^3) of resin, would be the most difficult to treat in terms of cost per unit of metal ions removed. The other four waste water samples appear to be somewhat similar in resin system indicated capacity based on the flow rate equivalent of about 1.44 gal/min/ft^3 of resin.

Of interest at this point is the statement made previously that studies such as this should be conducted in a continuous oil shale flotation operating mode rather than on a bench scale using simulated process waters. Figure 4-90 shows that when utilizing a resin exchange system such as this, a distinct sharp pH break at the resin system indicated capacity point yields solutions having much lower pH values than found in the initial feed solutions. Returning such low pH water to the grinding and flotation system could exacerbate the solubility of the various metal species not in solution in the finely ground slurry. Conversely, the sharp initial increase in pH of the solutions over that pH found in the feed solution, would effectively precipitate most of the metal ions in solution thus negating the necessity for any ion exchange system.

Data in Table 4-42 show the effectiveness of the ion exchange resin system used for removing selected metal ions, as well as sulfate, from solution. This system effectively removed the Ca, Mg, K, Ni, Zn, Fe, Mn, Cd, and $SO_4^=$ from solution up to the point of saturation loading of the resins at the designed flow rate of 1.44 gal/min/ft^3 of resin; however, the data indicate significant differences in the capacity of the resin system based on the metal ion content of the feed to the system.

Additional analyses of feed solutions were made to determine the Al, U, V, and Ba contents. These analyses were conducted by a local certified testing laboratory using inductively coupled argon emission spectroscopy. Results of these studies are presented in Table 4-43.

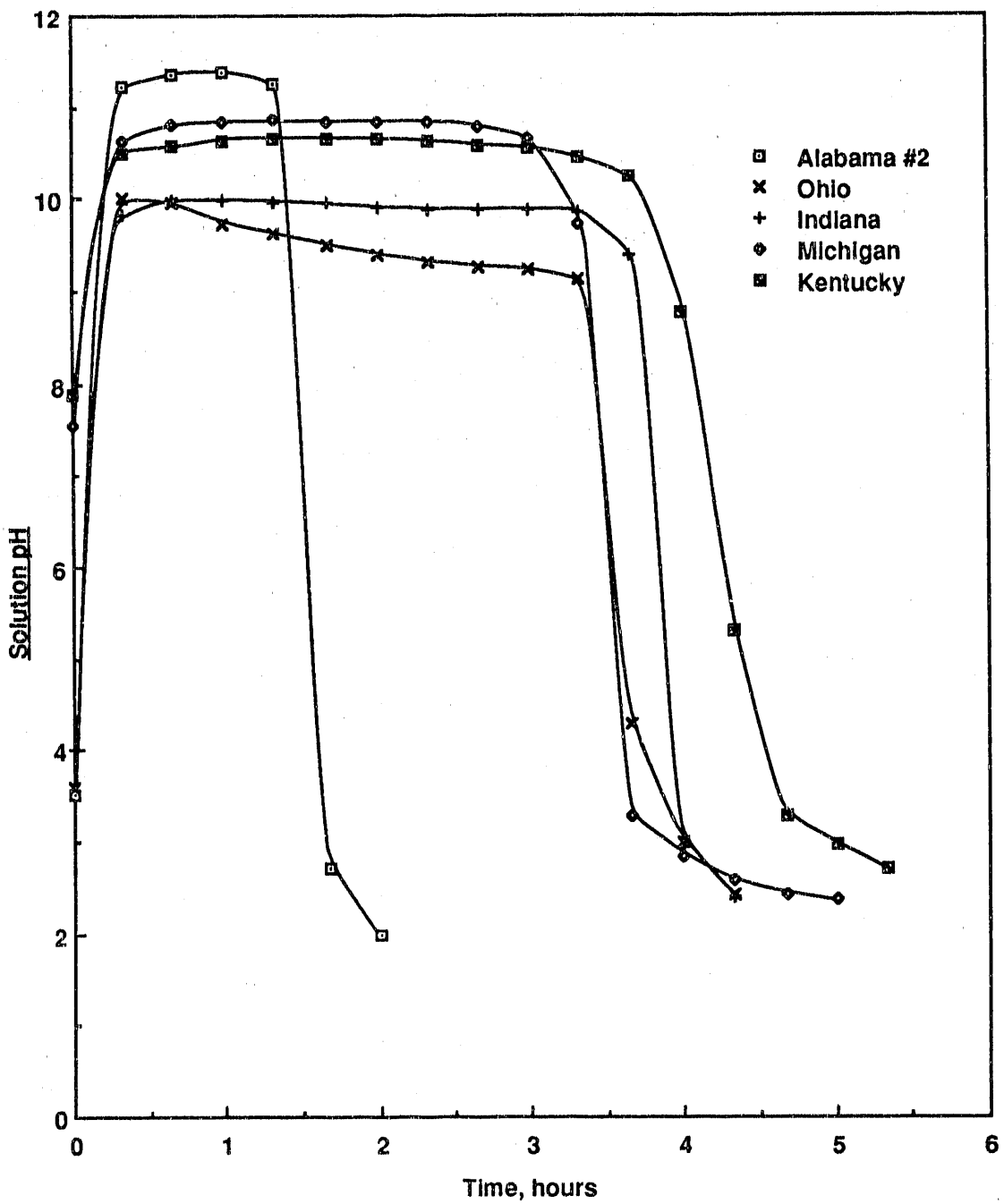

Figure 4-90. EFFECT OF CATIONIC (Hydrogen Form) AND ANIONIC (Hydroxyl Form) RESINS ON pH OF OIL SHALE GRIND WATER FLOW RATE EQUIVALENT: 1.44 (±0.1) gal/min/ft^3

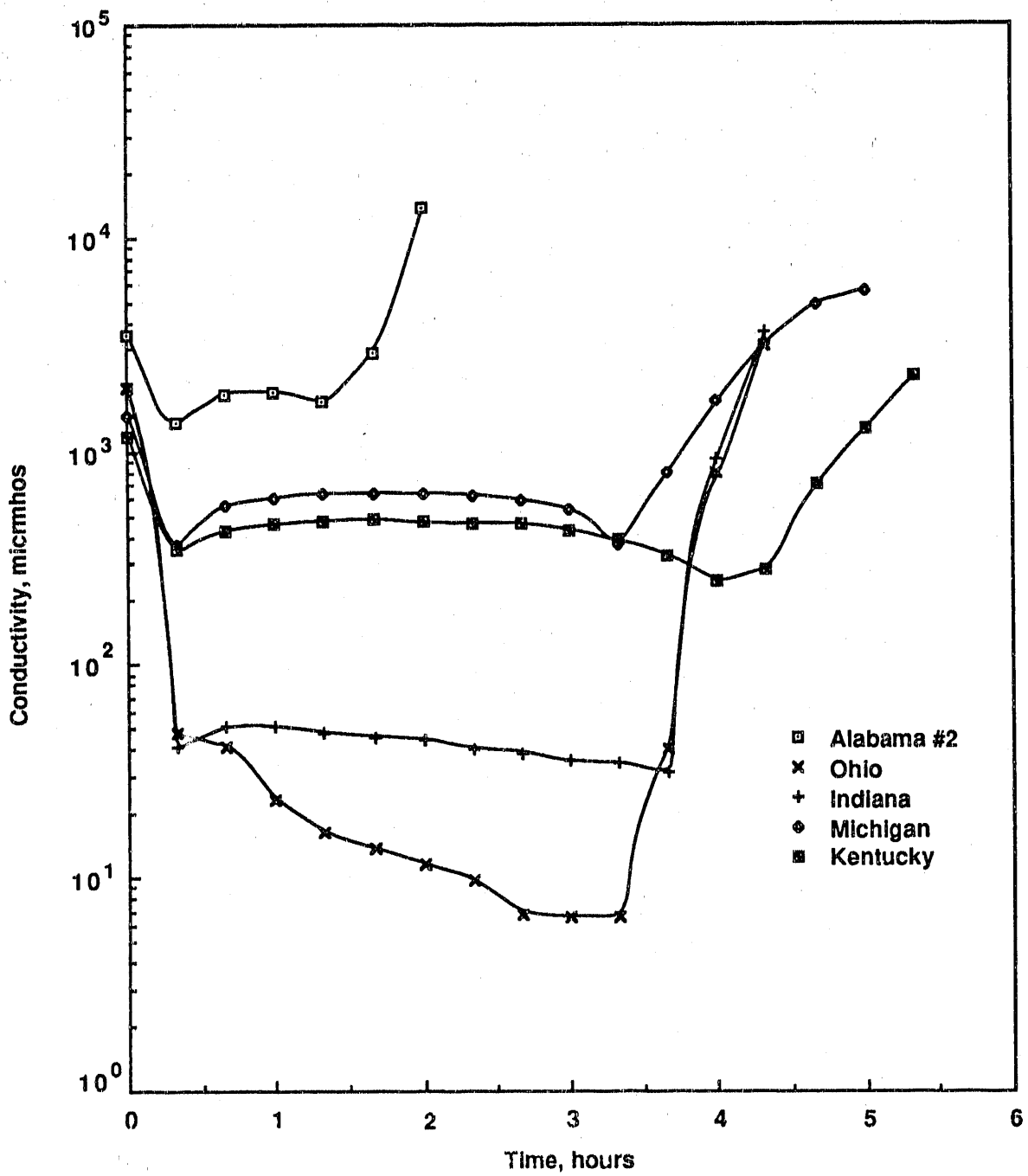

Figure 4-91. EFFECT OF CATIONIC (Hydrogen Form) AND ANIONIC (Hydroxyl Form) RESINS ON CONDUCTIVITY OF OIL SHALE GRIND WATER FLOW RATE EQUIVALENT: 1.44 (±0.1) gal/min/ft^3

Table 4-42. EFFECT OF ION EXCHANGE RESIN SYSTEM ON REMOVING SELECTED METAL IONS AND SULFATE FROM OIL SHALE PROCESS WATER

Shale Water Source	Product	pH	Conductivity*	Ca	Mg	K	Ni	Zn	Fe	Mn	Cd	SO_4
Alabama	Feed Solution	3.51	3,530	92.5	100	11.3	15.35	24.0	650.0	11.1	--	2,421
	RSIC** hrs 1.33	11.25	1,690	0.27	0.02	0.65	ND	0.01	ND	ND	--	ND
	RSIC† (+20 min)	2.71	2,900	1.72	2.00	1.40	0.15	0.25	5.15	0.09	--	ND
Kentucky	Feed Solution	7.8	1,168	166.0	48.5	10.3	2.20	0.10	0.07	5.8	--	502
	RSIC, hrs 3.67	10.28	325	0.62	0.75	0.32	ND	0.01	0.02	0.02	--	NA
	RSIC (+20 min)	8.78	245	0.76	0.50	0.69	ND	0.02	0.02	0.02	--	NA
Indiana	Feed Solution	4.00	2,080	157.0	190.0	17.3	9.9	3.7	64.0	17.5	--	1,149
	RSIC, hrs 3.67	9.38	31.5	0.40	0.52	0.57	ND	ND	0.03	0.01	--	ND
	RSIC (+20 min)	2.96	926	0.68	2.80	1.03	0.20	0.06	0.23	0.05	--	2.0
Ohio	Feed Solution	3.60	1,986	107.0	80.0	16.4	17.90	58.0	194.0	5.4	2.00	1,141
	RSIC, hrs 3.33	9.13	6.6	0.12	0.05	0.32	ND	ND	ND	ND	ND	ND
	RSIC (+20 min)	4.30	39.9	0.47	0.35	0.50	0.10	0.03	ND	ND	ND	ND
Michigan	Feed Solution	7.55	1,489	173.0	110.0	16.9	0.68	0.29	1.06	1.39	--	643
	RSIC, hrs 3.33	9.72	366	0.79	1.45	0.88	ND	0.01	0.02	0.02	--	ND
	RSIC (+20 min)	3.28	801	0.70	1.50	0.87	ND	0.02	0.07	0.03	--	ND

* Conductivity: micromhos/cm.

** RSIC: Resin system indicated capacity.

† RSIC (+20 min): 1st sample after RSIC.

Table 4-43. RESULTS OF ADDITIONAL ANALYSES OF PROCESS WATERS

Oil Shale Sample	Analysis, mg/L			
	Al	U	V	Ba
Alabama	34.00	104.0	0.06	<0.05
Tennessee	0.23	11.6	<0.05	<0.05
Kentucky	0.21	12.4	<0.05	<0.05
Indiana	1.00	21.0	0.05	<0.05
Ohio	52.00	71.3	0.06	<0.05
Michigan	0.28	11.9	<0.05	<0.05

Because of the unexpected high values for uranium in solution, additional samples, representing cationic exchange resin eluates as well as other water samples, were submitted for U analysis. Uranium analyses of these additional samples proved highly inconsistent; hence, samples of other Alabama and Indiana waste waters were submitted to Dr. Paul Bonner of Tennessee Technological University, an authority on uranium analysis. Dr. Bonner's results showed less than 0.05 mg/L U for both samples. The response of the Al in solution in the five samples to the ion exchange resin system was not determined. A copy of Dr. Bonner's report is appended (Appendix F).

Metal Ion Precipitation

Metal ion precipitation using either quick lime (CaO) or hydrated lime ($Ca(OH)_2$) is common practice in industry when metal ion concentration must be reduced in process waste streams or acid-mine drainage streams prior to discharging into the natural environment. Precipitation of metal ions as hydroxides along with flocculation of the solids in most mineral processing streams occurs naturally when using either quick lime or hydrated lime for clarifying process water. Such hydroxide precipitates are generally physically entrapped with the flocculated mass of solids and hence pose little or no problems in water clarification. However, if the metal ions are precipitated from waste streams containing little or no solids, the light, fluffy metal hydroxides generated are extremely difficult to thicken and/or filter.

To determine the potential for precipitating the metal ions contained in oil shale process waters as fast settling, easily filterable sulfide precipitates, as opposed to hydroxide precipitates, the process water from the Alabama shale was titrated incrementally with a 10% solution of sodium sulfide ($Na_2S \cdot 9H_2O$). Upon the first 1-mL addition of the sulfide solution it was determined visually that dense, black, fast settling precipitates were forming. Titration of the Alabama recycle water was continued with pH measurements taken after each 1-mL addition of 10% $Na_2S \cdot 9H_2O$. Subsequently, each of the other 5 recycle process water samples also were titrated in the same manner. Figure 4-92 presents the results of these studies comparing solution pH as a function of grams of Na_2S (converted from $Na_2S \cdot 9H_2O$)/L of recycle solution. Visual observation of the precipitates formed in the titrating studies indicated that only minor precipitates were formed in the Tennessee, Kentucky, and Michigan recycle waters while dense black precipitates were formed in the Indiana, Ohio, and Alabama recycle waters.

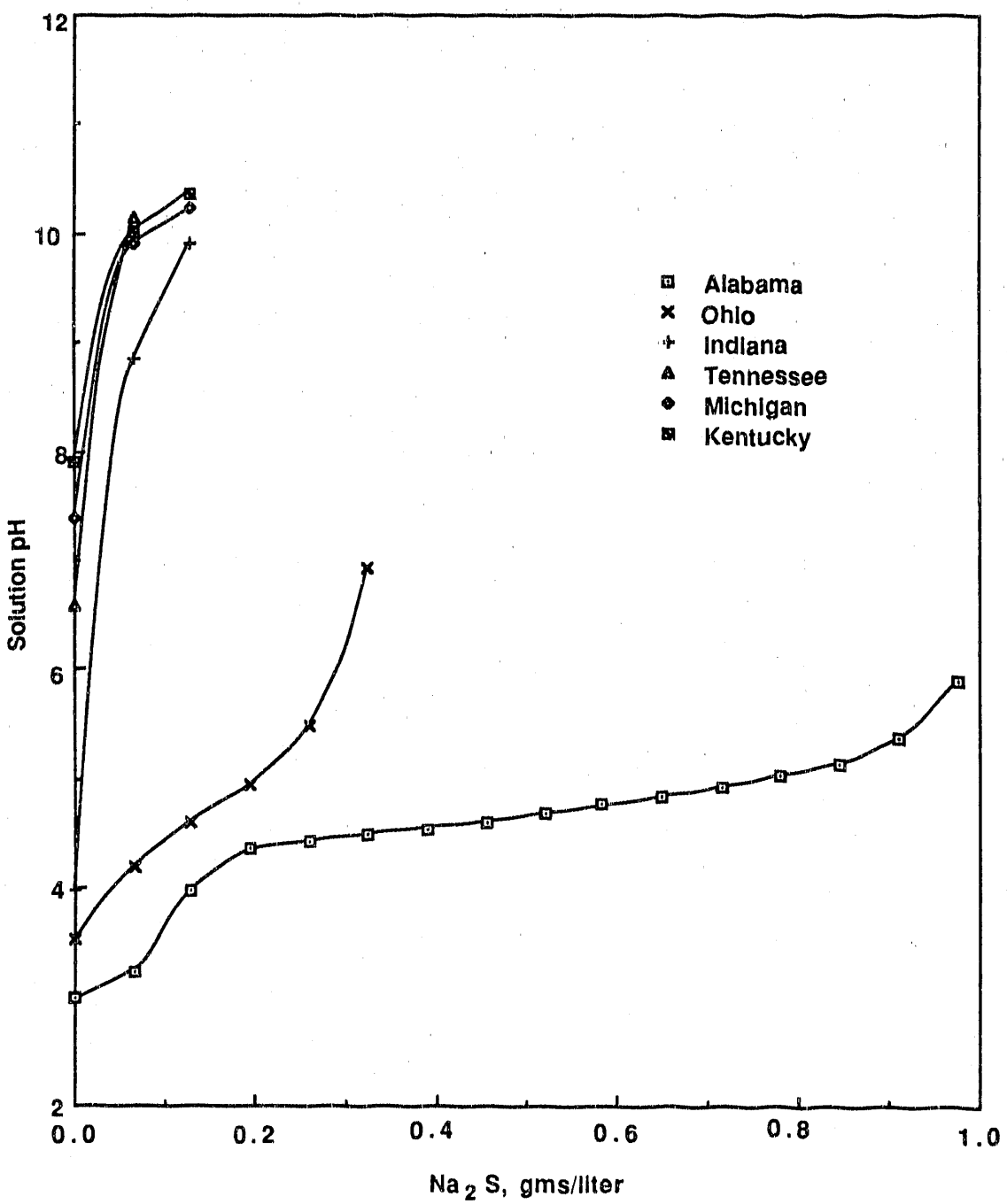

Figure 4-92. EFFECT OF SODIUM SULFIDE ON pH OF OIL SHALE WASTE WATER SOLUTIONS WHEN PRECIPITATING METAL IONS

Upon completion of each of the titration studies shown in Figure 4-92 the titrated waters were filtered and samples of the filtrate were taken for analysis. The filter residues were oven dried; however, only the Alabama and Ohio filter residues yielded sufficient weight of material for subsequent analysis. Data in Table 4-44 present the results of these studies. The data shows that essentially all of the Fe, Ni, Zn, and Mn in solution in the Tennessee, Kentucky, Indiana, and Michigan process waters were precipitated under the conditions of trial. However, incomplete precipitation of the Fe and Mn was indicated for both the Alabama and Ohio process waters. Analyses of the metal precipitates from the Alabama and Ohio process waters indicate the potential for recovering valuable metal species from these process wat by sulfide precipitation.

Sulfide precipitation studies of the Alabama process water, shown in Table 4-44, indicated that there might be a possibility of selective precipitation of the metal ions by incremental addition of Na_2S to the recycle water. One additional study of the Alabama process water was conducted to determine 1) the sequence of metal precipitation and 2) the quantity of Na_2S required for complete precipitation of the Fe, Ni, Zn, and Mn ions. In this study, 4 mL of a 10% solution of $Na_2S \cdot 9H_2O$ was added to 1 L of recycle water and resulting precipitate was filtered from the solution. Conductivity and pH measurements were taken of the filtrate and the filtrate was sampled for analysis. This sequence was repeated until no visible precipitate was formed upon addition of the $Na_2S \cdot 9H_2O$. Results of conductivity and pH measurements are given in Figure 4-93 and analyses of the filtrates for Fe, Ni, Zn, and Mn are presented in Table 4-45.

Data in Table 4-45 show that a total of 1.3 grams of Na_2S/L of recycle process water was required to precipitate essentially all of the Fe, Ni, Zn, and Mn ions. The data also show that the precipitation sequence of these 4 metal ions was Zn > Ni > Fe > Mn thus indicating some potential for controlling the concentration of metal values by sulfide precipitation of the metal ions from oil shale recycle waters.

Subtask 4.3.2. Tailings Disposal Studies

In the beneficiation of Eastern oil shales about 1500 pounds (680 kg) of tailings or waste solids are generated for each ton of raw shale processed. Typically, such tailings are impounded in a closed tailings pond to permit recirculation of process water and to prevent the very finely ground material from being washed into natural waterways (that is, lakes and streams). Three questions relevant to the disposal of tailings are addressed by the research performed in this subtask: 1) What are the thickening and settling characteristics of the tailings?, 2) What are their long-term leaching characteristics?; and, 3) Can the tailings be utilized in ways which do not require impoundment?

Thickener Requirements for Alabama and Indiana Oil Shale Flotation Wastes

Column cell flotation tests were conducted on samples of Alabama and Indiana oil shales, rod mill ground to pass 20 μm, to obtain flotation waste samples for settling tests and thickener calculations.

Table 4-44. EFFECT OF Na_2S ON PRECIPITATION OF SELECTED METAL IONS

Shale Water Source	Na_2S g/L	Product	Solution pH	Analysis, ppm				Analysis, %				
				Fe	Ni	Zn	Mn	Fe	Ni	Zn	Mn	Cd
Alabama		feed	3.00	650.0	15.75	22.50	11.20	--	--	--	--	--
Alabama	0.96	filtrate	5.90	7.50	0.10	0.03	9.50	--	--	--	--	--
Alabama		precipitate	NA*	--	--	--	--	21.98	0.74	0.95	0.03	0.006
Tennessee		feed	6.60	1.21	6.90	1.20	4.40	--	--	--	--	--
Tennessee	0.03	filtrate	10.15	0.03	0.10	0.10	0.01	--	--	--	--	--
Tennessee		precipitate	NA	--	--	--	--	-----	Not enough sample			----
Kentucky		feed	7.91	0.07	2.20	0.10	5.80	--	--	--	--	--
Kentucky	0.06	filtrate	10.37	0.01	ND	0.02	0.02	--	--	--	--	--
Kentucky		precipitate	NA	--	--	--	--	-----	Not enough sample			----
Indiana		feed	3.99	64.0	9.90	3.7	17.50	--	--	--	--	--
Indiana	0.06	filtrate	9.91	0.03	0.10	0.03	0.21	--	--	--	--	--
Indiana		precipitate	NA	--	--	--	--	-----	Not enough sample			----
Ohio		feed	3.53	194.0	17.90	58.0	5.40	--	--	--	--	--
Ohio	0.15	filtrate	6.94	0.03	0.10	0.03	3.02	--	--	--	--	--
Ohio		precipitate	NA**	--	--	--	--	15.50	2.31	8.48	0.18	0.261
Michigan		feed	7.39	1.06	0.68	0.29	1.39	--	--	--	--	--
Michigan	0.06	filtrate	10.24	0.01	0.10	0.01	0.01	--	--	--	--	--
Michigan		precipitate	NA	--	--	--	--	-----	Not enough sample			----

* Alabama shale water precipitate: 1.96 g/L.

** Ohio shale water precipitation: 0.62 g/L.

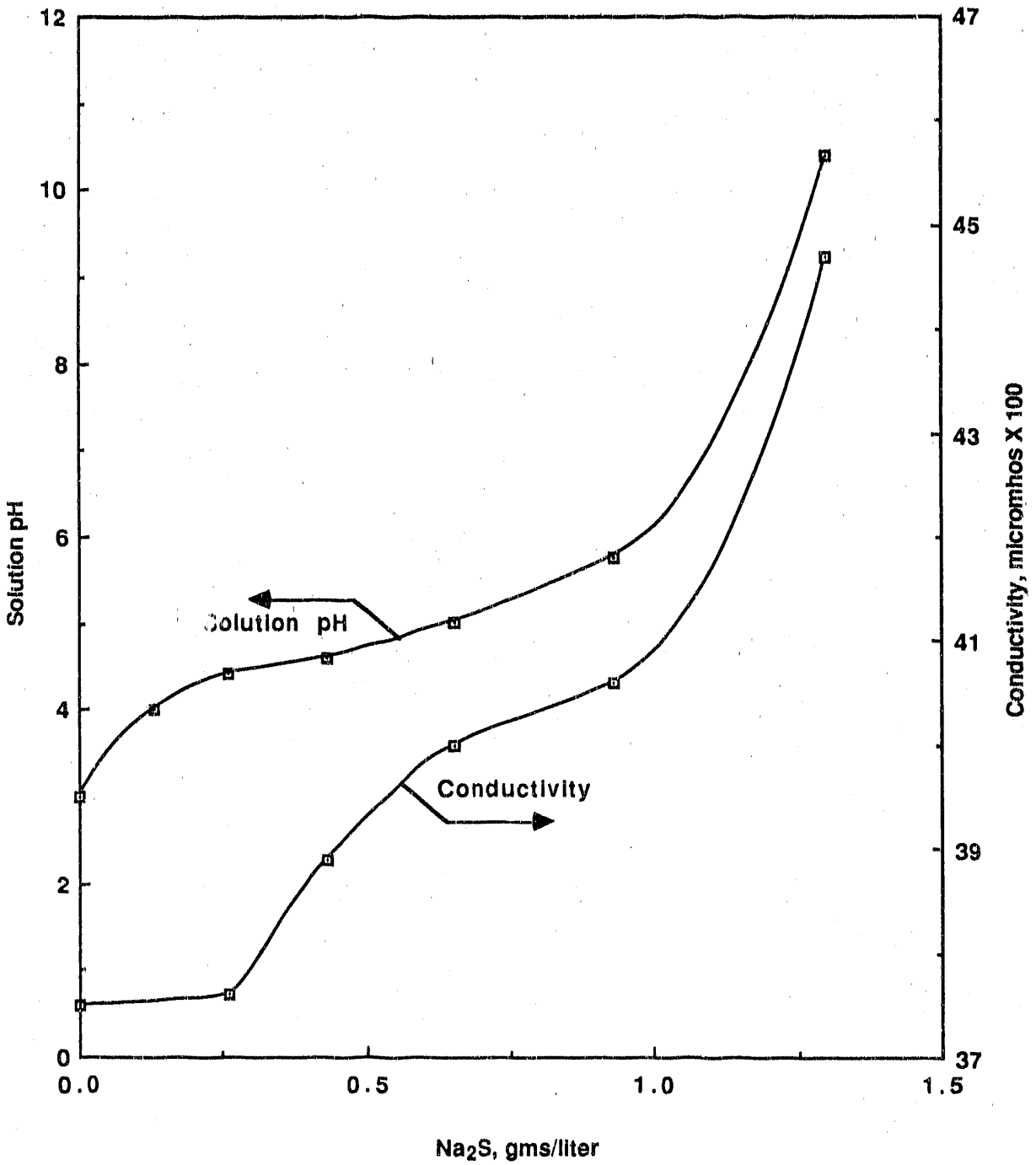

Figure 4-93. EFFECT OF SODIUM SULFIDE ON pH AND CONDUCTIVITY OF ALABAMA OIL SHALE WASTEWATER

Table 4-45. SEQUENTIAL PRECIPITATION STUDIES OF ALABAMA OIL SHALE PROCESS WATER USING Na_2S

Na_2S Added, g/L	Solution, pH	Filtrate Analysis, ppm			
		Fe	Ni	Zn	Mn
0	3.00	650.0	15.75	22.50	11.2
0.26	4.43	420	9.45	0.08	10.6
0.52	4.61	343	4.10	0.03	10.0
0.78	5.03	216	0.10	0.03	9.5
1.04	5.78	28	ND	0.03	8.2
1.30	10.40	0.03	ND	0.01	ND

Size analyses of the flotation tails from the Alabama and Indiana shales are presented in Tables 4-46 and 4-47, respectively. Tailing slurries from both the Alabama and Indiana flotation tests were thoroughly mixed and one 1-L samples were removed from each slurry sample for sedimentation studies. One additional sample was taken from each tailings slurry to determine the density of the solids for subsequent thickener calculations. The density of the slurry solids was found to be 2.8 g/mL for both the Alabama and Indiana samples.

Table 4-46. SIZE ANALYSIS OF ALABAMA FLOTATION TAILS

Size, µm	+16	16/12	12/8	8/6	6/4	4/3	3/2	2/1	-1
Weight, %	11.1	12.0	18.7	13.1	14.2	7.6	7.7	7.9	6.9

Table 4-47. SIZE ANALYSIS OF INDIANA FLOTATION TAILS

Size, µm	+16	16/12	12/8	8/6	6/4	4/3	3/2	2/1	-1
Weight, %	11.2	18.7	17.8	12.9	14.9	8.3	8.9	8.5	6.1

Standard settling tests were conducted on the Alabama and Indiana flotation tailings slurries to determine the natural settling characteristics of the finely ground solids. Upon completion of the studies to determine the natural settling characteristics, the slurries were flocculated with Nalco 8872, a slightly anionic polyacrylamide (molecular weight 10 to 12 million) produced by Nalco Chemical Co. at a dosage rate of 20 ppm.

Settling data from these studies was used to calculate the thickener requirements for both the natural and flocculated slurries based on a standard procedure used to determine the square feet of thickener area required per ton of dry solids per 24 hours.

Results of the calculations for both flotation tailings slurries are presented in Table 4-48.

Table 4-48. CALCULATED THICKENER REQUIREMENTS

	ft^2/ton dry solids/24 hours	
	Alabama	Indiana
Natural Settling	28.72	41.30
Flocculated Settling	2.11	2.37

Data in Table 4-48 show that the use of the slightly anionic polyacrylamide flocculation was highly effective in reducing the square footage of thickener area required.

Long-Term Leaching Studies

Objective

Investigate the natural leaching characteristics of eastern oil shale flotation solid wastes that might occur during long term storage and devise methods for preventing potential ecological problems associated with waste waters from long term storage of the solid wastes.

Procedure

Representative samples of Alabama and Indiana flotation wastes were filtered and thoroughly washed to remove flotation water containing soluble salts. Analyses of the two dry solid waste samples are presented in Table 4-49.

Table 4-49. ANALYSIS OF FLOTATION WASTES

Flotation Waste	Analysis, %							
	C(t)	H	N	S	Vol	Ash	C(f)	Moisture
Alabama	2.78	0.62	0.28	6.18	6.62	90.44	2.05	0.89
Indiana	4.51	0.95	0.28	4.01	8.26	88.02	2.41	1.31

Four 50 gram samples from each of the washed flotation waste samples were taken for long term solubility studies. One 50 gram sample of each waste was mixed with 1 L of deionized water having a pH of 6,5 and conductivity of 1.8 micromhos/cm. Calcium hydroxide ($Ca(OH)_2$ equivalents of 10, 25 and 100 lb/ton of dry solids were added to the other three samples from each waste and each of these samples were mixed with one liter of deionized water to determine the effectiveness of $Ca(OH)_2$ in reducing the metal ion concentration in the pond effluents. Both pH and conductivity measurements were made of each of the samples immediately after mixing with the deionized water. Results of these studies are presented in Table 4-50.

Both pH and conductivity measurements were made of each of the samples every week for a period of 4 months. Water samples were removed from each of the tests after two weeks, one month, two months and four months for soluble metal ion analyses. At each analytical sampling period, 100-mL of effluent was removed for analysis and an additional 100-mL of deionized water was added to the samples to represent potential rain water dilution.

Table 4-50. INITIAL pH AND CONDUCTIVITY OF ALABAMA AND INDIANA SOLID WASTE EFFLUENTS

$Ca(OH)_2$ lbs/ton of dry solids	Alabama		Indiana	
	pH	Conductivity	pH	Conductivity
0	4.4	175	6.4	213
10	6.4	254	8.0	247
25	7.8	282	8.2	288
100	10.8	485	10.5	330

Results

The pH and conductivity of the water sample are presented as a function of time in Figures 4-94 through 4-97.

Figure 4-94 shows that about 25 pounds of $Ca(OH)_2$ per ton of dry solids (12.5 kg/metric ton) was required to keep the pH of the simulated Alabama pond effluent within permissible discharge limits over a four month period; whereas, only 10 pounds of $Ca(OH)_2$ per ton (5 kg/metric ton) was required for the Indiana pond effluents, shown in Figure 4-96. The conductivity of the two wastewater effluents were quite similar in response to the quantity of $Ca(OH)_2$ added to the slurry.

Tables 4-51 and 4-52 present the results of periodic analyses of the pond effluents with no $Ca(OH)_2$ addition and with $Ca(OH)_2$ additions from the Alabama and Indiana flotation solid wastes, respectively.

Analytical data from both simulated pond effluents show continuous solubility of Fe, Ni, Zn, Mn and $SO_4^=$ as a function of time when no $Ca(OH)_2$ was added to the slurry system. The addition of as little as 10 lbs of $Ca(OH)_2$ per ton of dry solids effectively reduced the soluble metal ion concentration of the pond effluents. However, the data also indicate the potential for continued metal ion solubilization, particularly the Zn and Mn, as a function of time when using as much as 100 pounds of $Ca(OH)_2$ per ton of dry solids.

The increase in Ca ion and $SO_4^=$ solubility with both time and quantity of $Ca(OH)_2$ added is reflected in the increase in solution conductivity shown in Figures 4-95 and 4-97. It had been anticipated that the Ca ions present in solution would react with the $SO_4^=$ to yield some form of $CaSO_4 \cdot XH_2O$ which would precipitate out of solution with the metal hydroxides thus yielding a nonhazardous effluent. However, this reaction apparently did not occur under the conditions of trial.

Utilization of Tailings in Cement and Concrete

Objective

The objective of this study was to investigate the potential for utilizing shale tailings as a component in the manufacture of portland cement, and as a replacement or partial replacement for cement in concrete.

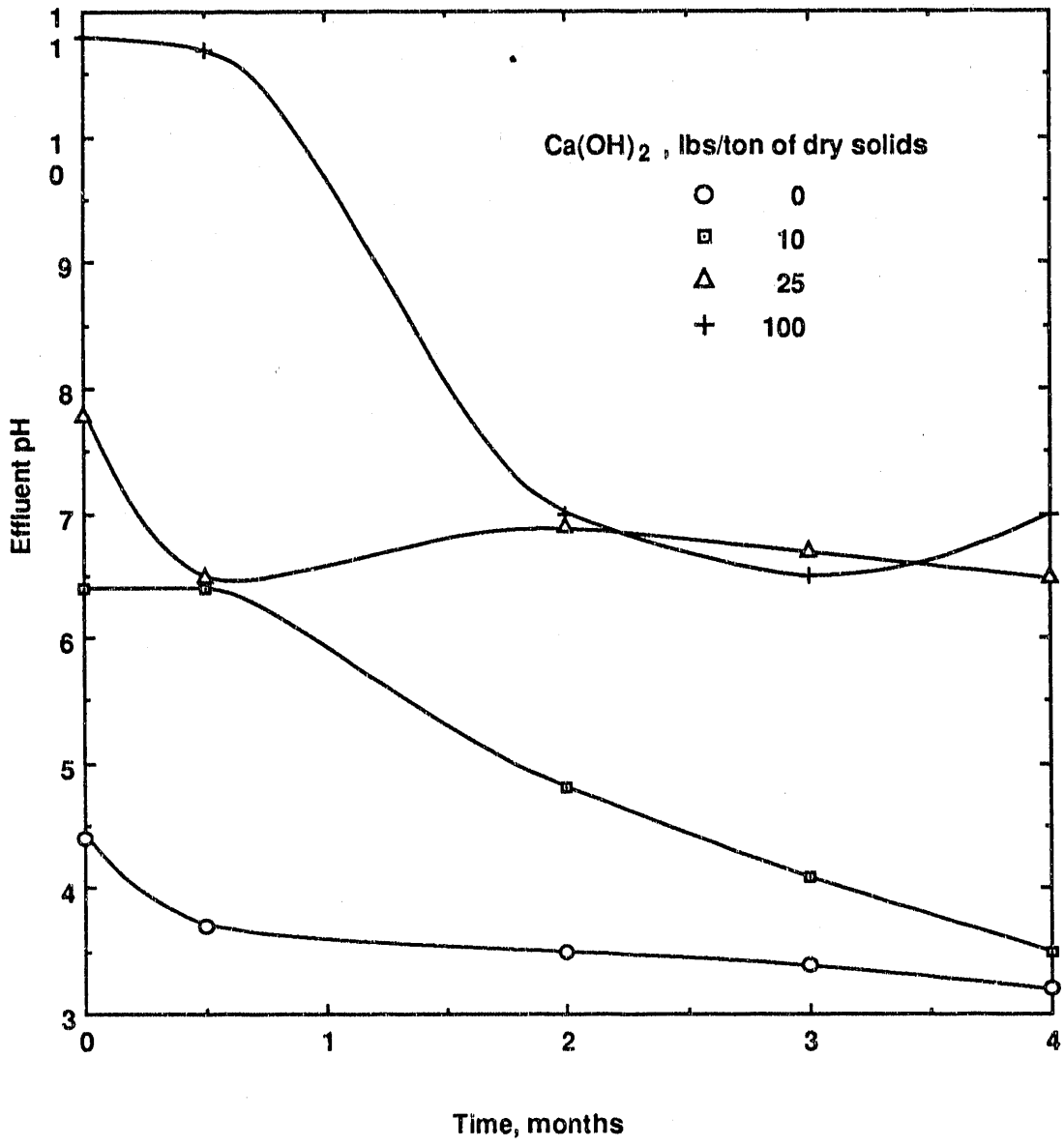

Figure 4-94. EFFECT OF $Ca(OH)_2$ ON THE pH OF ALABAMA OIL SHALE FLOTATION WASTE POND EFFLUENT

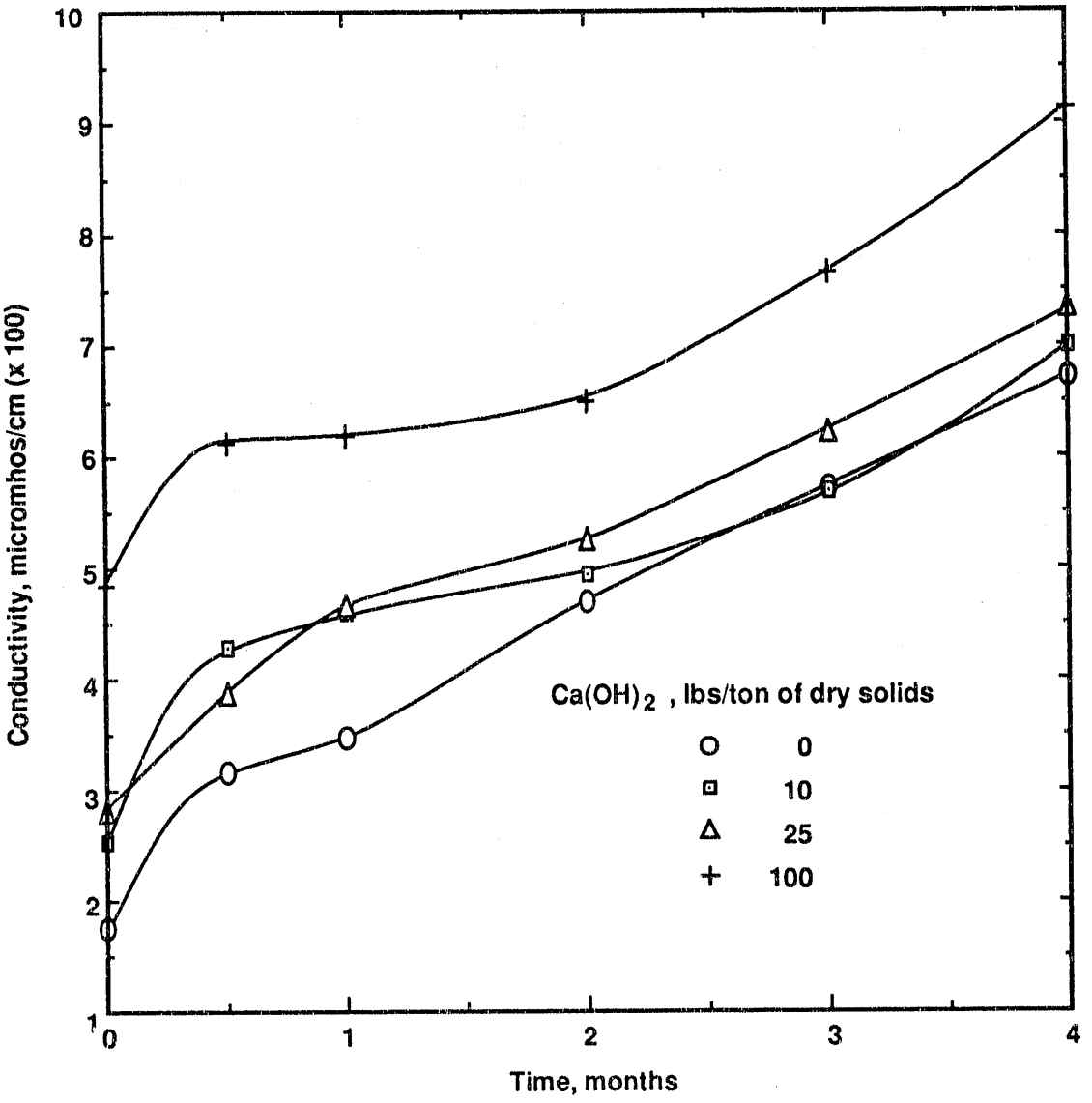

Figure 4-95. EFFECT OF $Ca(OH)_2$ ON THE CONDUCTIVITY OF ALABAMA OIL SHALE FLOTATION WASTE POND EFFLUENT

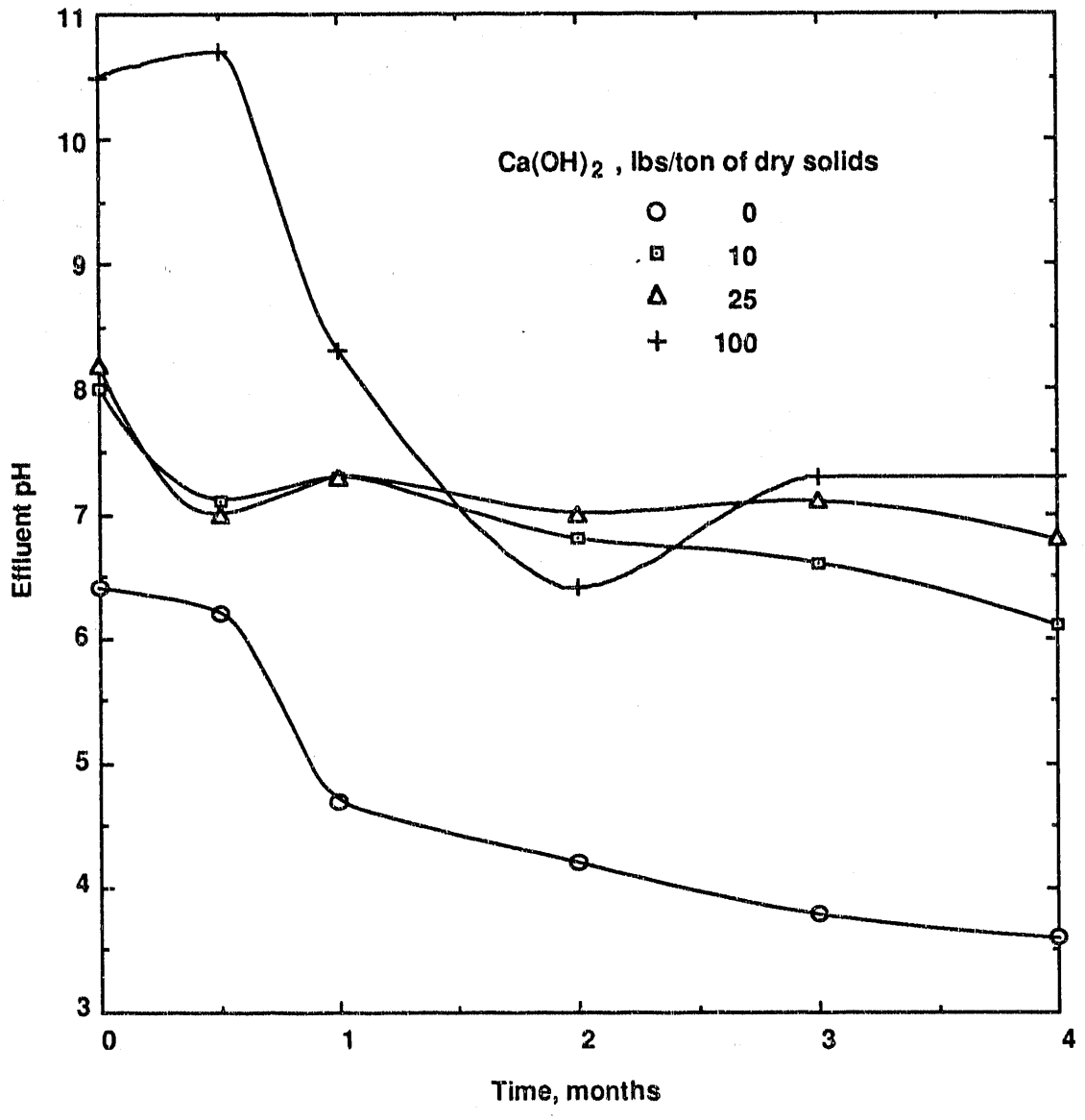

Figure 4-96. EFFECT OF $Ca(OH)_2$ ON THE pH OF INDIANA OIL SHALE FLOTATION WASTE POND EFFLUENT

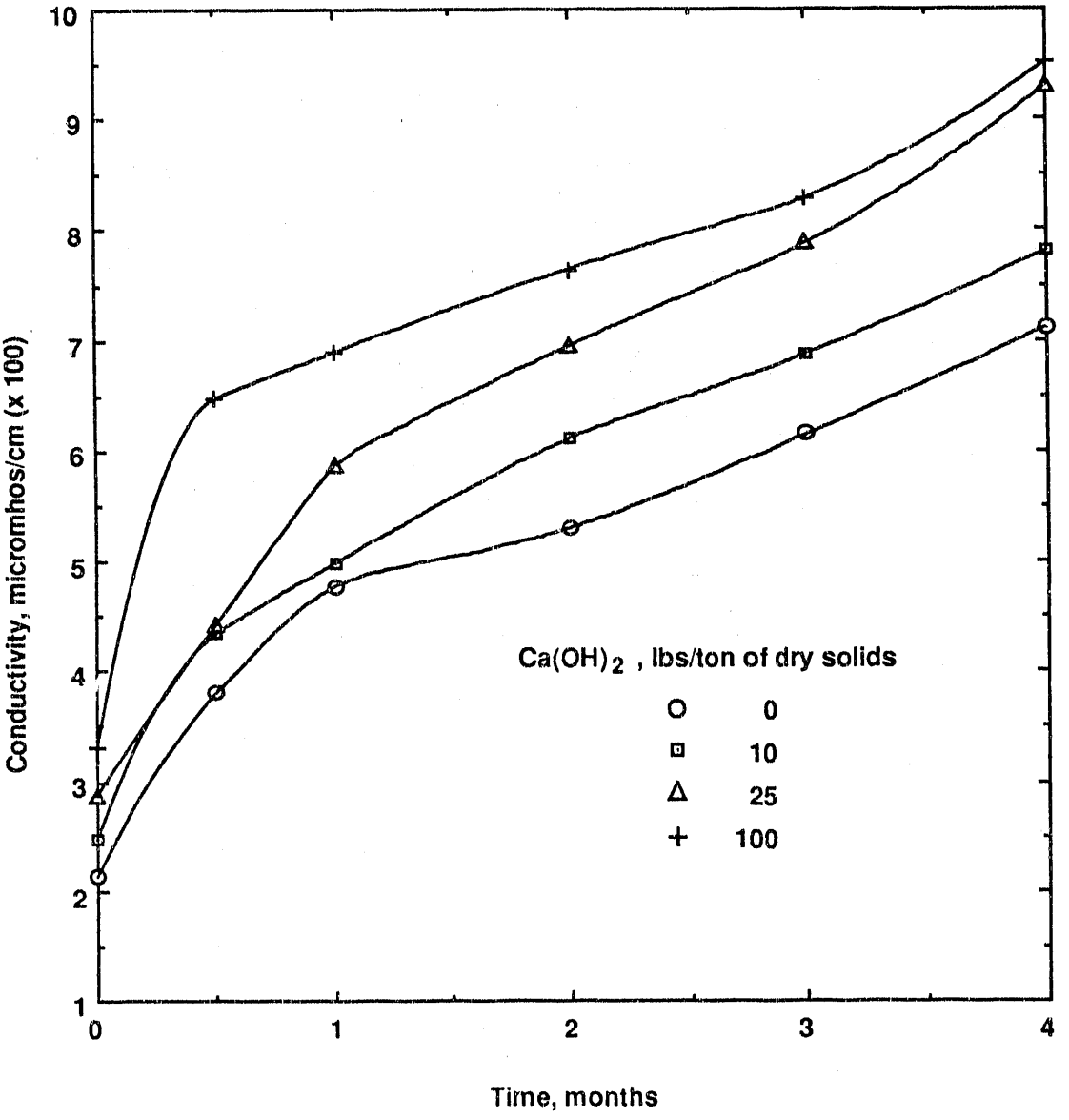

Figure 4-97. EFFECT OF $Ca(OH)_2$ ON THE CONDUCTIVITY OF INDIANA OIL SHALE FLOTATION WASTE POND EFFLUENT

Table 4-51. EFFECT OF $Ca(OH)_2$ ON METAL ION CONCENTRATION IN ALABAMA SOLID WASTE POND EFFLUENTS

Time, months	0.5				1				2				4			
$Ca(OH)_2$, lb/ton	0	10	25	100	0	10	25	100	0	10	25	100	0	10	25	100
Analysis, ppm																
Fe	0.10	0.00	0.00	0.00	0.11	0.00	0.02	0.02	0.71	0.09	0.02	0.02	1.67	2.19	0.04	0.02
Ni	1.10	0.20	0.10	0.10	1.30	0.20	0.00	0.01	1.80	0.30	0.10	0.00	2.35	1.20	0.10	0.00
Zn	0.74	0.04	0.02	0.02	1.02	0.09	0.07	0.01	1.40	0.17	0.03	0.06	2.00	0.90	0.02	0.07
Mn	1.10	0.42	0.07	0.00	1.21	0.44	0.07	0.01	1.38	0.68	0.10	0.02	1.76	1.47	0.28	0.03
Ca	29	80	74	118	26	85	93	125	35	87	109	140	42	106	150	188
$SO_4^=$	114	174	160	209	119	189	172	226	157	224	208	253	246	302	273	444

Table 52. EFFECT OF $Ca(OH)_2$ ON METAL ION CONCENTRATION IN INDIANA SOLID WASTE POND EFFLUENTS

Time, months	0.5				1				2				4			
$Ca(OH)_2$, lb/ton	0	10	25	100	0	10	25	100	0	10	25	100	0	10	25	100
Analysis, ppm																
Fe	0.09	0.04	0.01	0.01	0.32*	0.02	0.02	0.01	0.07*	0.01	0.02	0.02	1.29	0.04	0.02	0.03
Ni	0.50	0.10	0.10	0.10	0.80	0.10	0.00	0.00	1.30	0.10	0.00	0.10	1.75	0.30	0.10	0.00
Zn	0.19	0.03	0.05	0.02	0.20	0.05	0.07	0.11*	0.52	0.03	0.01	0.01	1.20	0.05	0.50	0.01
Mn	0.70	0.15	0.11	0.00	1.21	0.17	0.07	0.00	1.65	0.28	0.10	0.01	2.75	0.86	0.30	0.03
Ca	55	73	77	123	70	98	93	148	71	113	136	151	81	138	184	204
$SO_4^=$	153	191	197	223	197	197	172	283	237	239	287	360	321	356	405	469

* Repeat analyses showed similar results.

Devonian Shales in Cement Manufacturing

The LaFarge Corporation uses Antrim shale in their cement making operation at Alpena, Michigan (Lakin, 1990). Antrim shale is mixed with locally occurring limestone in their clinkering operation. The organic portion of the shale (kerogen) is burned off in the operation and marginally reduces the process energy requirements.

The operation also report that burned shale, the results of spontaneous combustion of the shale during storage, has also been used in the clinkering operation with no ill effects. From this then we can infer that either shale tailings or spent shale would be usable as a raw material in cement manufacturing. Further, the uniformity of the composition of the mineral matter in various Devonian shales means that this inference can be extended to all the shales in the program.

The Use of Tailings in Concrete

A test program was undertaken to determine whether oil shale tailings have pozzolanic properties which would permit them to be used as a replacement, or partial replacement, for portland cement in concrete. Approximately 10 pounds of Alabama oil shale flotation wastes were generated for the pozzolan studies. Fischer Assay, C-H-N, S, and Proximate analyses of the flotation waste are presented in Table 4-53.

Table 4-53. ANALYSIS OF ALABAMA SHALE FLOTATION WASTES

	Analysis, %								
Fischer Assay, GPT	C(t)	H	N	S	Volatiles	Ash	C(f)	Moisture	Specific Gravity, g/mL
0.8	3.42	0.57	0.15	5.82	9.34	87.51	1.77	1.38	2.86

Whole rock analysis of the flotation waste sample gave the results shown in Table 4-54. Particle size analysis of the flotation waste sample is shown in Table 4-55.

Table 4-54. WHOLE ROCK ANALYSES OF ALABAMA FLOTATION WASTES

Compound	Percent	Compound	Percent
SiO_2	58.42	Na_2O	0.53
Al_2O_3	9.80	P_2O_5	0.20
CaO	0.50	TiO	0.51
Fe_2O_3	9.63	MnO	0.02
K_2O	3.71	Ba	0.04
MgO	0.84	Cr	0.03
S	6.01	LOI	12.86

Table 4-55. PARTICLE SIZE ANALYSIS OF ALABAMA FLOTATION WASTES

Size, μm	Plus 24	24/16	16/12	12/8	8/6	6/4	4/3	3/2	2/1	Minus 1
Weight, %	1.7	9.4	12.0	18.7	13.1	14.2	7.6	7.7	7.9	6.9

A standard Type 1 Portland cement and Ottawa sand were used in the pozzolan studies to determine baseline cement parameters. The specific gravity of the Portland cement was 3.26 g/mL and that of the Ottawa sand was 2.67 g/mL. Neither the Portland cement nor the Ottawa sand were chemically analyzed. The Ottawa sand had the size consistency shown in Table 4-56.

Table 4-56. SIZE ANALYSIS OF OTTAWA SAND USED IN POZZOLAN CEMENT STUDIES

Size, mesh	Plus 40	40/50	50/60	60/80	80/100	Minus 100
Weight, %	18.8	33.4	23.0	18.6	4.0	2.2

Tests were conducted by MRI to determine the potential use of oil shale flotation wastes as a pozzolan in cement mixtures. All work was performed according to ASTM specifications.

Table 4-57 summarizes the results of studies conducted under this phase of the oil shale waste program.

Table 4-57. EFFECTS OF ADDITION OF ALABAMA OIL SHALE FLOTATION WASTE TO PORTLAND CEMENT

Mix	Water Required, %	Compressive Strength, psc	Activity Index	Initial Setting Time	Final Setting Time
Control	100.0	2875			
12.5% o.s.*	102.2	1750	60.87	5 hrs 36 min	7 hrs 20 min
25% o.s.	109.5	1640	57.07	5 hrs 55 min	8.0 hrs
37.5% o.s.	115.3	1016	35.33	7 hrs 15 min	9-10 hrs
50% o.s.	116.0	778	27.10	8 hrs	10-11 hrs

* Oil Shale Flotation Waste.

Data in Table 4-57 show that the Alabama oil shale flotation wastes have a negative effect on compressive strength, pozzolanic activity index, and both initial and final setting time.

Conclusions

Studies of the long-term leaching characteristics of flotation solid wastes from the Alabama and Indiana shales show that the effluents from ponded wastes became more acid as a function of time and that Fe, Ni, Zn, Mn, and $SO_4^=$ ions in solution increased as the pH decreased.

The addition of lime, in the form of $Ca(OH)_2$, at a ratio of about 0.0125:1, or 25 pounds of $Ca(OH)_2$ per ton of dry waste solids, effectively reduced the solubilized Fe, Ni, Zn, and Mn to insignificant quantities for a period of four months and also yielded pond effluent pH values falling between 6 and 9, the desired pH range for intentional discharge.

Data derived in these studies over a four-month period indicated that the quantity of Fe and Ni in solution was directly proportional to the quantity of $Ca(OH)_2$ added per ton of dry solid wastes. The quantity of Zn and Mn in solution also was directly proportional to the quantity of $Ca(OH)_2$ added; however, the Zn and Mn was indirectly proportional to time regardless of how much $Ca(OH)_2$ was added.

While the addition of $Ca(OH)_2$ was effective in stabilizing the pH values over a period of four months, the conductivity of the effluents from both oil shale waste solids increased significantly because of the increase in both Ca and $SO_4^=$ ions. The Alabama Department of Environmental Management (ADEM) was contacted to determine the maximum allowable $SO_4^=$ content for industrial waste water discharge; however, ADEM personnel indicated that the $SO_4^=$ content by itself was not a standard parameter used to determine discharge permitting.

Since total dissolved solids is a standard parameter for determining discharge permitting in Alabama and TDS is a function of conductivity (conductivity OX.67 = TDS for both the Alabama and Indiana solid waste effluents), the high TDS content of the effluents indicated potential discharge problems. Upon discussion of this problem with a local certified environmental laboratory it was determined that the maximum permissible TDS content of industrial waste discharges was 250 mg/L, which indicated that both effluents would exceed the permissible limits for TDS. However, it was subsequently determined that the Alabama permissible TDS limits were based on the chloride content of effluents and analyses of the Alabama and Indiana solids waste effluents showed less than 1 mg/L chloride, respectively. On this basis neither of the effluents from the solid wastes should represent potential ecological problems when using sufficient $Ca(OH)_2$ to precipitate out the soluble metal ions and to control the pH of the effluent to meet standard discharge parameters.

Recommendations

Since the data presented in this study represents results obtained under static conditions, and all mineral processing waste ponds operate under dynamic conditions until filled, the most appropriate method for preventing future ecological problems associated with such solid wastes would be to maximize techniques for containing the waste. Such techniques, based on proven technology, would include construction of lined waste ponds, probably with a limestone base, overflow monitoring equipment, as well as a number of monitor wells drilled around the periphery of the waste pond to detect potential future problems.

The existence of an industrial operation utilizing Devonian shale in the manufacture of portland cement precludes any need to conduct laboratory studies toward that end. It would be of interest, however, to determine how much spent shale and shale tailings could be adsorbed into the cement manufacturing market.

61WP/61090to4-3/RPP

CONCLUSIONS AND RECOMMENDATIONS

The objectives of the Oil Shale Beneficiation Research program have been achieved. Investigators from The University of Alabama, The University of Pittsburgh, and The University of Nevada-Reno have conducted definitive evaluations of advanced technologies for oil shale grinding and for kerogen-mineral matter separation. Problems, or potential problems, associated with the disposal of waste materials from beneficiation have been identified and approaches to their solution have been advanced.

With respect to oil shale grinding it can be concluded that:

1. Pressure cycle comminution is not, at its current stage of development, a viable means of grinding oil shale to fine sizes.

2. Stirred ball mill grinding is superior to conventional (tumbling) mills in grinding to the fine sizes required for kerogen-mineral matter separation.

3. The energy efficiency of stirred ball milling is increased as the media size is decreased.

4. Energy efficient circuits can be achieved when appropriate sizing and concentrating devices are used to prevent over-grinding and to reject waste at the earliest possible time.

While considerable progress has been made in reducing the cost grinding still further progress is possible. To that end, it is recommended that further research be conducted in the following areas:

1. The effect of alternative grinding media such as sand.

2. Optimization of operating conditions on the basis of cost rather than energy consumption.

The research conducted in the area of kerogen-mineral matter separation leads to the conclusions that;

1. The air sparged hydrocyclone is not an acceptable means of affecting a kerogen-mineral matter separation.

2. The LICADO process is capable of affecting a separation of kerogen from its associated mineral matter.

3. Column flotation is superior to the other technologies tested for the separation of kerogen from shale and represents an advance over conventional flotation technology.

It is recommended that further research be conducted in preparation for a major PDU program. This research should include:

1. Long-term testing in a closed cycle configuration to determine the effect of recycled water on flotation performance.

2. Evaluation of commercially available column flotation cells.

3. Further research on the effects of cell geometry and the development of scaling laws

4. Further research on specific oil shales other than the Alabama (Chattanooga).

Research on the disposal of waste materials revealed no insurmountable problems. There is, however, a need for continuing research in certain areas. Specifically it is recommended that;

1. Long-term leaching and settling tests in a dynamic mode be conducted in conjunction with long-term, closed-loop column flotation testing.

2. Appropriate market and economic analyses be performed to quantify the potential use of tailings and spent shale in cement manufacturing.

3. The mode of occurrence of certain heavy metals such as Uranium and Vanadium be determined.

4. Means of recovering the potentially valuable Uranium and Vanadium be investigated.

61WP/61090to4co/RPP

REFERENCES CITED

Araujo, G, He, D. X., Chi, S.M.B., Morsi, B. I., Klinzing, G. E., Chiang, S. H., Energy Progress, 7 (1987), pp. 72-76.

Austin, L. G. et al., Process Engineering of Size Reduction-Ball Milling, AIME, 1989.

Austin, L. G., et al., Process Engineering of Size Reduction: Ball Milling, SME, 1984.

Austin, L. G., 1973; "Understanding Ball Mill Sizing," Ind. Eng. Chem. Process Design and Development, Vol. 12, No. 2, p. 121.

Bond, F. C., 1952. "The Third Theory of Comminution," Mining Engineering, Vol. 4, pp. 484-94.

Cardoso, J. B., Rampacek, C., "Developments in Eastern Oil Shale Beneficiation at The University of Alabama," Proceedings, 1985 Eastern Oil Shale Symposium, November 18-20, 1985, p. 149.

Chi, S.M.B. Ph.D. Dissertation, Dept. of Chemical/Petroleum Engineering, University of Pittsburgh (1986).

Committee on Comminution and Energy Consumption, Report of 1981. National Material Advisory Board, Publication NMAB-364, National Academy of Sciences, Washington, D.C., Editor J. A. Herbst.

Cooper, M. H., Private Communications, Westinghouse Electric Corporation Advanced Energy Systems, Pittsburgh, Pa.

Davis, G., Misra, M., and Lamont, W. E. "Environmental Aspects of Beneficiating Eastern Oil Shale". Proceedings Eastern Oil Shale Symposium, Nov. 18-20, 1987, Lexington, Kentucky.

Department of Energy, Energy Data Report, "Power Production Consumption and Capacity", December 1978.

Fahlstrum, P. H., "A Physical Concentration Route in Oil Shale Mining," Proceedings 12th Annual Oil Shale Symposium, Colorado School of Mines, April 1979.

Fox, J. P. and Philips, J. P., "Waste Water Treatment in the Oil Shale Industry, Oil Shale, the Environmental Challenge," Proceedings of an International Symposium, U.S. Department of Energy, April 11-14, 1980.

Gaire, R. J, Hand, T. J. and Mazzella, G., Proc. of 1989 Eastern Oil Shale Symposium, Lexington, Ky (1989), pp. 499-510.

Hanna, H. A. and Carl Rampacek, "Eastern Oil Shale Investigations at The University of Alabama," Proc. 1981 Eastern Oil Shale Symposium, Lexington, Kentucky, November 15-17, 1981.

Hanna, H. S. and Carl Rampacek. "Eastern Oil Shale Investigations of The University of Alabama". Proceedings, 1981 Eastern Oil Shale Symposium, November 1981.

Hanna, H. S. and Lamont, W. E., "Physical Beneficiation Studies of Eastern Oil Shale," Third IGI Synfuels Symposium, IGT Pub., pp. 295-321 (1983).

Hanna, H. S. and Lamont, W. E., "Effect of Soluble Salt on Flotation of Ultra-Fine Coal and Oil Shale," AIME Annual Meeting, 1984.

Herbst, J. A., Editor, "Control 84," AIME 1984.

Herbst, J. A., et al., 1982; Population Balance Approach to Ball Mill Scale-Up: Bench and Pilot Scale Investigations, SME Transactions, Vol. 272-1947.

Herbst, J. A. and Fuerstenau, D. W., 1973, "Mathematical Simulation of Dry Ball Milling Using Specific Power Information," Trans AIME, Vol. 254, p. 343.

Herbst, J. A. and Fuerstenau, D. W., 1980; Scale-Up Procedure for Continuous Grinding Mill Using Population Balance Models," International Journal of Mineral Processing, Vol 7, pp. 1-31.

Herbst, J. A., Lo, Y. C. and Rajamani, K., 1985; Population Balance Model Predictions of the Performance of Large Diameter Mills, Mineral and Metallurgical Processing, pp. 114-120, May.

Himmelblau, D. M. and Bischoff, B. K., 1968; Process Analysis and Simulation, J. Wiley, New York, N.Y.

Hintze, J. L., "Number Cruncher Statistical System, Version 5.3-Power Pack, Reference Manual" (1988).

Johnson, L. R. and Riley, R. H., "Beneficiation -- Hydroretort Processing of U.S. Oil Shales," Part III. Engineering Study of a Conceptual Commerical Facility for Beneficiating Eastern Oil Shale," Final Report of work performed under DOE Grant DE-F621-85LC11066, December 1988.

Kapur, P. C., "Self-Preserving Size Spectra of Comminuted Particles," Chemical Engineering Science, Vol. 27, pp. 425-431, 1972.

Keller, D. V, Burry, W., Colloids and Surfaces, 22 (1987), pp. 37-50.

Klimpel, R. R. and Samuels, R., "Examples of Use of Grinding Aids in Industrial Operations," Proceedings 11th Annual Meeting of Canadian Mineral Processors, Ottawa, 1979.

Lakin, Robert, Private Communication, 1990.

Lamont, W. E., Theodorou, K. and Raymond C. Rex, Jr., Proceedings, 1986 Eastern Oil Shale Symposium, November 1986.

Lamont, W. E., 1990; Private Communication, Mineral Resources Institute.

Lamont, W. E. and Hanna, H. S., "Beneficiation of the Kerogen Content of Eastern Devonian Oil Shales by Flotation," Paper No. 83-621, presented at the SME/AIME Annual Meeting, Atlanta, Georgia, March 6-10, 1983.

Lamont, W. E. and Hanna, H. S., "Beneficiation of the Kerogen Content of Eastern Devonian Shales by Flotation Techniques," AIME Annual Meeting, 1983.

Lawrison, G. C., Crushing and Grinding, CRC Press, Cleveland, Ohio., 1974

Lo, Y. C., et al., 1988; Design Considerations for Large Diameter Ball Mills, International Journal of Mineral Processing, 22, 75-93.

Lynch, A. J. and Rao, T. C., "Modeling and Scale-Up of Hydrocyclone Classifiers," Proceedings 9th International Mineral Processing Congress, Cagliary, Italy, April, 1975.

Malghan, S. G., 1975. The Scale-Up Procedure for Ball Mills Using Population Balance Models. D. Eng. Diss., University of California, Berkeley, California.

McKay, J. D., Foot, D. G., Jr. and Huiatt, J. L., "Column Flotation of Mineral Chromite Ore". Minerals and Metallurgical Processing, August 1986, pp. 170-177.

Mehta, R. K., Adel, G. T. and Yoon, R. H., 1989; Liberation Modeling and Parameter Estimation for Multicomponent Mineral Systems, Powder Technology, 58, pp. 195-209.

Mehta, R. K., Adel G. T. and Yoon, R. H., 1990; Liberation Modeling and Parameter Estimation for Multicomponent Mineral Systems, Minerals and Metallurgical Processing, Vol. 7, No. 3, pp. 156-163.

Mehta, R. K. and Schultz, C. W., "A Novel Energy Efficient Process for Ultrafine Coal Grinding". Preprint No. 91-167, Annual SME/AIME Meeting, Denver, Colorado, 1991.

Miller, J. D. and Misra, M.," Carbon Dioxide Flotation of Fine Coal", International Journal of Coal Preparation, Vol. 2, 1985. p. 69.

Miller, J. D. and Van Camp, M. C., "Fine Coal Flotation in a Centrifugal Field with an Air-Sparged Hydrocyclone," Mining Engineering, November, 1982, p. 1575.

Misra, M., Lin, C. L. and Miller, J. D., "Enhanced Liberation and Flotation of Kerogen from Oil Shale," Presented at the AIME Fall Meeting, 1984, Preprint No. 84-412.

Misra, M., et al.,"Pressure Cycle Comminution of Eastern Oil Shale", Proceedings of 1989 Eastern Oil Shale Symposium, University of Kentucky, Lexington, Kentucky.

Misra, M. and Hilleke, F., "Power Requirements in the Ultrafine Grinding of Oil Shale", Proceedings of 1987 Eastern Oil Shale Symposium, Lexington, Kentucky, 1987.

Misra, M., Lin, C. L. and Miller, J. D., "Concentration of Eastern Oil Shales by Froth Flotation," Proceedings of 1983 Eastern Oil Shale Symposium, Lexington, Kentucky, 1983.

Misra, M. and Davis, G., "Characterization and Recovery of Accessory Trace Elements from Alabama Oil Shale Waste Waters". Presented at the 1986 Eastern Oil Shale Symposium, Lexington, Kentucky, November 19-21, 1986.

Plitt, L. R., "A Mathematical Model of the Hydrocyclone Classifier," CIM Bulletin, Vol. 69, pp. 114, 1976.

Rajaram, V., Mining Engineering, 37 (1985), pp. 1381-1385.

Rampacek, C., Hanna, H. S., Janka, J. and Rex, R. C., "Beneficiation-Hydroretorting of Oil Shale," Engineering Foundation Conference on Processing of Energy Minerals Shale, Tar Sands and Coal," August, 1984.

Rao, M., et al.,"Control and Implementation of Ore Reduction by Hydraulic Pressure Cycle", The International Society for Mini and Microcomputers-ISSM, Editor E. K. Park, page 301, 1990.

Rao, M., et al.,"Computer Based Controller for Pressure Cycle Comminution", Proceedings of 10th International Electromining Conference, West Virginia, July 24-27, 1990.

Rehbinder, P. and Kalinkosvasky, N, Journal of Technology and Physics, Vol. 2, USSR, p. 276, 1937.

Robl, T. L., Cisler, K. and Thomas, K., "Leaching Characteristics of Eastern Oil Shale, First Year Data Summary of the Hope Creek Study," Proceedings, 1985 Eastern Oil Shale Symposium, p. 117 (1985).

Robl, T. L., Rubel, A. M. and Barnhisel, R. I., Proc. of 1989 Eastern Oil Shale Symposium, Lexington, Ky (1989), pp. 212-218.

Schultz, C. W. and Bates, J. B., "Density-Fischer Assay Relationships Among Eastern Oil Shales," Poster presented at the 1989 Eastern Oil Shale Symposium, Lexington, Kentucky, November 15-17, 1989.

Schultz, C. W. and Bates, J. B., "Operating Parameters in the Column Flotation of Alabama Oil Shale," International Symposium on Advances in Fine Particle Processing, Annual Meeting of the Fine Particle Society, Boston, Massachusetts, August 21-25, 1989.

Schultz, C. W., Bates, J. B. and Lamont, W. E., "Operating Parameters in Column Flotation", Proceedings, Eastern Oil Shale Symposium, Lexington, Kentucky, 1990.

Schulz, N. F., "Separation Efficiency" Trans SME/AIME, Vol. 247, pp. 81-87, 1970.

Stehr, N., Mehta, R. K. and Herbst, J. A., "Comparison of Energy Requirements for Conventional and Stirred Ball Milling of Coal-Water Slurries", Coal Preparation, Vol. 2, 1986.

Tanaka, T., 1972; Scale-Up Formula for Grinding Equipment Using Selection Function," Journal of Chemical Engineering of Japan, Vol. 5, No. 3.

Terra Tek, "Energy Efficiency Concept in Fine Size Reduction of Rocks and Ores," Salt Lake City, Utah, TR 89-90, Submitted to National Science Foundation.

Yang, D. C., "A New Packed Column Flotation System," Column Flotation 88 Proceedings of an International Symposium on Column Flotation SME/AIME, 1988.

Yang, D. C., Private Communication, 1988.

Yap, R. F., Sepulveda, J. L. and Jauregui, R., "Determination of the Bond Work Index Using an Ordinary Laboratory Batch Ball Mill," Design Installation of Comminution Circuites, Chapter 12, p. 176-179, 1981.

Yoon, R. H. and Luttrell, G. H., Coal Preparation, 2 (1986), pp. 179-192.

Young, Peter, "Flotation Machines" Mining Magazine, January, 1982.

61WP/61090to4re/RPP

APPENDIX A. Grinding Model Framework

GRINDING MODEL FRAMEWORK

The formulation of population balance models for grinding and relevant discussion have been presented by several authors (Herbst and Fuerstenau, 1980; Austin, 1973). The size-discretized form of the model is especially convenient for application to experimental data. A brief discussion of this follows below.

Consider a mass of material H in a ball mill divided into n narrow size intervals with maximum size x_1, and minimum size x_{x+1}. The ith size interval, bounded by X_i above and X_{i+1} below contains a mass fraction of material $m_i(t)$ at time t. A mass balance for the ith size interval yields the kinetic model:

$$d\left[\frac{Hm_i(t)}{dt}\right] = - S_i Hm_i(t) + \sum_{j=1}^{i-1} b_{ij} S_j Hm_j(t) \qquad (A\text{-}1)$$

Where S_i is the size discretized selection function for the ith size interval that denotes the fractional rate at which the material is broken out of the ith size interval, and b_{ij} is the size discretized breakage function that represents the fraction of primary breakage fragments of material from the jth size interval which appear in the ith size interval. An estimation scheme (Mehta, Adel, and Yoon, 1989, 1990) based on a Modified Levenberg-Marquardt algorithm and a finite difference Jacobian are used in conjunction with this model for the estimation of selection and breakage functions from grinding data.

Mill Scale-Up

The approaches have been explored for finding a relationship between model parameters and mill design and operating variables. The first involves the correlation of selection and breakage functions with mill diameter (Tanaka, 1972; Austin, 1973). The second involves the correlation for the model parameters with the specific power draft of the mill (Herbst and Fuerstenau, 1980, Malghan, 1975). According to findings first reported by Herbst and Fuerstenau (1973), the size discretized selection functions are, to a good approximation, proportional to the specific power input to the mill (P/H), that is,

$$S_i = S_i^E\left(\frac{P}{H}\right) \qquad (A\text{-}2)$$

where S_i^E termed the "specific selection function" for the ith size interval is essentially independent of mill design and operating conditions. Also, the breakage functions, b_{ij}, have been found to be a good approximation invariant with respect to design and operating variables over a wide range of conditions. Incorporating these observations into Equation A-1, yields the energy normalized form of the batch grinding model:

$$\frac{dm_i(\bar{E})}{d\bar{E}} = - S_i^E m_i(\bar{E}) + \sum_{j=1}^{i-1} b_{ij} S_j^E m_j(\bar{E}) \qquad (A\text{-}3)$$

where $\bar{E}$ is the specific energy input to the mill and is equal to the product of specific power (P/H) and grind time t. This "detailed energy-size

reduction relationship" predicts that for a given material and feed-size distribution [$m_i(0)$], a necessary condition for identical product size distributions in different batch mills is identical specific energy input into each mill independent of mill dimensions and mill operating variables in the normal operating range.

A description of continuous tumbling mill requires not only a description of the breakage kinetics, but also a mathematical description of material transport through the mill. Such a description can often be obtained by considering the continuous response, $\underline{m}_p$, to be an average of batch responses, $\underline{m}_{batch}(t)$ weighted according to the amount of material that resides for various times in the mill, $\emptyset(t)$, that is,

$$\underline{m}_{MP} = \int_o^\infty \underline{m}_{batch}(t)\ \emptyset(t)dt \qquad (A-4)$$

where $\emptyset(t)dt$ is the fraction of particles that spend time between t and t+dt within the mill. Since particles spending a time t to t+dt are consuming specific energy input of (P/H)t to (P/H)(T+dt) or $\bar{E}$ to $\bar{E}+d\bar{E}$, Equation A-4 can be transferred to energy normalized form:

$$\underline{m}_{mp} = \int_o^\infty \underline{m}_{batch}(\bar{E})\ \emptyset(\bar{E})d\bar{E} \qquad (A-5)$$

where $\emptyset(\bar{E})$ is an energy density function (or "input energy distribution") that is related to residence time distribution by

$$\emptyset(\bar{E})d\bar{E} = \emptyset(t)dt \qquad (A-6)$$

It has been demonstrated in many research papers that residence time distribution in a mill (t) follows a flexible mixer-in-series model (Himmelblau & Dischoff, 1968).

$$\emptyset(t) = \frac{N^N(t)\tau^{N-1}}{\tau\Gamma(N)}\ e^{-Nt/\tau} \qquad (A-7)$$

where N is the mixing parameter which gives the equivalent number of mixers-in-series and τ is the mean residence time for material in the mill. These values of parameters (N,ν) can be predicted for a given mill design and operating variables using dimensionless correlations (Lo et al., 1988).

To simplify the task of estimating all of these kinetic parameters from experimental data, the following functional forms were used;

$$S_i^E = S_1^E \left[\frac{(X_i X_{i+1})^{0.5}}{(X_i X_2)^{0.5}}\right]^\xi \quad \text{for } n<i<n-1 \qquad (A-8)$$

$$B_{ij} = \frac{1-\exp\left(-\left(\frac{X_i}{X_{j+1}}\right)^{\alpha}\right)}{1-\exp(-1)} \qquad \text{(A-9)}$$

This reduces the parameters to be estimated to: a, ξ, S_i^E.

Finally, the power draft of the mill can be calculated from the following correlation (Bond, 1962):

$$P(kw) = 2.2\ P_{balls}(L/D)D^{3.4}\ M_B^*(3.2 - 3M_B^*)\ N^*\ (1 - .1/2^{9-10N^*}) \qquad \text{(A-10)}$$

APPENDIX B. Stirred-Ball Mill Grinding Results

Table B-1. 460 MESH DERRICK SCREEN SIZE ANALYSIS DATA
(19% Solids, 750 mL/min Feed Rate, No Spray Water)

	Particle Size	Cumulative Percent Passing		
		Screen Undersize	Screen Oversize	Screen Feed
48 mesh	300	100.0	100.0	100.0
270 mesh	53	96.5	63.5	63.2
	48	95.6	30.7	61.3
	32	89.9	21.9	53.9
	24	83.1	16.1	47.7
	16	69.5	11.0	38.6
	12	57.4	8.5	31.5
	8	44.5	6.8	24.6
	6	35.5	5.4	19.6
	4	25.6	4.0	14.2
	3	19.0	2.9	10.5
	2	12.0	1.9	6.7
	1.5	6.5	1.0	3.6
	1	4.8	0.8	2.7
Wt %		47.1	52.9	
% Solids		8.0	6.0	

At 25 µm, the separation efficiency is 82.1%.

Table B-2. 460 MESH DERRICK SCREEN SIZE ANALYSIS DATA
(21% Solids, 750 mL/min Feed Rate, No Spray Water)

	Particle Size	Cumulative Percent Passing		
		Screen Undersize	Screen Oversize	Screen Feed
48 mesh	300	100.0	100.0	100.0
270 mesh	53	99.5	18.0	51.3
	48	99.1	16.9	50.5
	32	94.0	13.3	46.3
	24	88.8	10.8	42.7
	16	74.5	8.2	35.3
	12	62.3	6.5	29.3
	8	47.7	5.1	22.5
	6	38.6	4.1	18.2
	4	27.5	3.0	13.0
	3	20.5	2.2	9.7
	2	12.7	1.4	6.0
	1.5	6.9	0.8	3.3
	1	4.9	0.6	2.4
Wt %		40.9	59.1	
% Solids		12.0	15.0	

At 25 μm, the separation efficiency is 85.1%.

Table B-3. 460 MESH DERRICK SCREEN SIZE ANALYSIS DATA
(21% Solids, 400 mL/min Feed Rate, No Spray Water)

		Cumulative Percent Passing		
	Particle Size	Screen Undersize	Screen Oversize	Screen Feed
48 mesh	300	100.0	100.0	100.0
270 mesh	53	99.6	28.2	62.8
	48	99.3	26.1	61.6
	32	95.0	19.0	55.9
	24	89.6	14.2	50.8
	16	75.4	9.8	41.6
	12	62.8	7.6	34.4
	8	48.3	6.1	26.6
	6	38.9	4.9	21.4
	4	27.9	3.6	15.4
	3	20.8	2.6	11.4
	2	13.1	1.7	7.2
	1.5	7.1	0.9	3.9
	1	5.1	0.7	2.8
Wt %		48.5	51.5	
% Solids		13.0	10.0	

At 24 µm, the separation efficiency is 85.5%.

Table B-4. 460 MESH DERRICK SCREEN SIZE ANALYSIS DATA
(21% Solids, 1400 mL/min Feed Rate With New Feeding System That Uses More of the Screen, No Spray Water)

		Cumulative Percent Passing		
	Particle Size	Screen Undersize	Screen Oversize	Screen Feed
48 mesh	300	100.0	100.0	100.0
270 mesh	53	99.7	23.8	56.7
	48	99.4	22.2	55.6
	32	94.2	15.6	49.6
	24	98.8	11.5	45.0
	16	74.1	7.6	36.4
	12	61.7	5.9	30.1
	8	47.2	4.6	23.0
	6	37.9	3.7	18.5
	4	26.9	2.7	13.2
	3	20.1	2.0	9.8
	2	12.5	1.3	6.1
	1.5	6.8	0.7	3.3
	1	4.9	0.5	2.4
Wt %		43.3	56.7	
% Solids		12.0	18.0	

At 24 μm, the separation efficiency is 85.4%.

APPENDIX C. Data From LICADO Process Testing

Table C-1. CONTACT ANGLE ON POLISHED OIL SHALE PELLETS
(Room Temperature: 22°C)

CO_2 Pressure, psig		Contact Angle, °
14.7		44
200		84
400		86
850		88
870	(liquid CO_2)	115

Table C-2. EFFECT OF CONTACT TIME INDIANA SHALE
(Liquid CO_2 Flowrate: 200 mL/min)

Settling Time, min	Impeller Speed, rpm	Contact Time, secs	Yield, wt %	Product Ash, wt %	Product Ash, wt %
5	1200	5	23.9	74.4	80.4
5	1200	2.5	32.6	75.0	80.2
5	1200	10	22.9	74.8	79.8
5	1200	15	15.8	71.6	79.6
0	1200	5	24.1	76.9	79.5
0	1200	2.5	32.8	74.3	79.8
0	1200	10	23.2	72.8	79.7
0	800	5	26.0	71.8	79.7

Table C-3. PARAMETRIC STUDIES WITH INDIANA SHALE
(Slurry Concentration: 5%)

Impeller Speed, rpm	Injection Rate, mL/min	Contact Time, min	Yield, wt %	Product Ash, wt %	Refuse Ash, wt %
1200	250	5	24.0	74.9	80.6
1200	350	5	26.5	75	80.3
1200	200	2.5	32.6	76	80.2
1200	200	10	22.9	74.8	79.8
800	200	5	27.8	71.6	81.1
1400	200	5	24.5	74.9	80.1
1600	200	5	25.3	74.3	79.8

Table C-4. EFFECT OF SLURRY CONCENTRATION FOR INDIANA SHALE
(Contact Time of Liquid CO_2: 6 min)

Impeller Speed, rpm	Injection Rate, mL/min	Contact Time, min	Yield, wt %	Product Ash, wt %	Refuse Ash, wt %
1200	200	2.5	22.7	74.3	801
1200	200	5	23.9	74.4	80.2
1200	200	10	28.2	76.4	80.1
1200	200	15	30.6	77.1	80.4

Table C-5. EFFECT OF INJECTION RATE FOR INDIANA SHALE
(Slurry Concentration: 5%; Contact Time of Liquid CO_2: 5 min)

Impeller Speed, rpm	Injection Rate, mL/min	Yield, %	Product Ash, %	Refuse Ash, %
1000	100	15.5	69.5	78.6
1000	200	17.6	69.8	80.7
1000	300	24.4	71.4	80.5
1000	350	25.5	71.7	80.7
1200	200	20.6	71.0	80.1
1400	200	23.8	72.5	80.3

Table C-6. EFFECT OF INJECTION RATE FOR ALABAMA SHALE
(Particle Size: 4 Microns; Slurry Concentration: 5%)

Injection Rate, mL/min	Yield, %	Fischer Assay, gal/ton	Oil Recovery, wt %
100	24.0	15.5	41.3
150	30.9	15.1	51.8
200	31.5	15.1	52.8
300	37.0	11.0	45.2

Table C-7. EFFECT OF INJECTION RATE FROM MICHIGAN SHALE
(Particle Size: 4 Microns; Slurry Concentration: 5%)

Injection Rate, mL/min	Yield, %	Fischer Assay, gal/ton	Oil Recovery, wt %
100	22.0	16.9	53.1
150	24.3	16.6	57.6
200	27.0	16.6	64.0
300	27.0	16.0	61.7

Table C-8. PRELIMINARY TESTS WITH MICHIGAN SHALE
(4-Micron Sample)

Filter Cake Treatment	Injection Rate, mL/min	Yield, wt %	Fischer Assay, gal/ton	Oil Recovery, wt %
Dried	250	7.0	11.0	10.3
Dried	350	15.6	15.7	32.5
Not Dried	350	21.8	17.6	51.1

Table C-9. EFFECT OF DISPERSANT SHMP IN BRU TESTS FOR INDIANA SHALE
(Liquid CO_2 Injection Rate: 200 mL/min)

Dispersant Dosage, ppm	Impeller Speed, rpm	Contact Time, min	Yield, wt %	Product Ash, wt %	Refuse Ash, wt %
100	1200	5	29.0	75.4	79.7
100	1200	2.5	24.0	73.8	80.1
100	800	5	25.1	72.5	79.6
500	1200	5	29.2	76.2	79.7
500	1200	2.5	28.5	75.5	80.1
500	800	5	20.9	69.3	79.9
750	1200	5	28.4	74.4	79.9
750	1200	2.5	24.3	73.8	80
750	800	5	20.6	70	80.1

Table C-10. EFFECT OF SETTLING TIME IN SCREEN TESTS FOR INDIANA SHALE
(Slurry Concentration: 2%)

Liquid CO_2 Volume, mL	Settling Time, min	Yield, wt %	Product Ash, wt %
0	3	25.0	782
100	3	58.0	77.4
0	0	1.0	--
100	0	16.0	75.1

Table C-11. SCREEN-TYPE AGGLOMERATION EXPERIMENTS WITH INDIANA SHALE

Dosage of 1-Octanol, ppm	Product Yield wt %	Fischer Assay, gal/ton	Oil Recovery, wt %
0	18.1	15.6	23.5
0	19.2	15.0	24.0
0	14.9	16.9	21.0
100	18.8	27.8	43.5
100	20.4	27.2	46.2
100	25.0	22.3	46.4
300	28.0	23.6	55.1
300	26.2	25.8	56.3
300	26.8	24.0	53.6
500	25.1	33.0	69.0
500	24.8	32.0	66.1
500	27.0	29.2	65.7
1000	30.4	20.9	53.0
1000	29.1	22.4	54.3
1000	30.8	21.7	55.7

Table C-12. SCREEN-TYPE AGGLOMERATION EXPERIMENTS WITH INDIANA SHALE

Dosage of 1-Octanol, ppm	Product Yield wt %	Fischer Assay, gal/ton	Oil Recovery, wt %
0	18.7	17.1	26.6
0	19.2	16.4	26.2
0	14.8	20.0	24.6
100	20.9	25.9	45.1
100	24.3	26.9	54.5
100	21.9	23.2	42.4
300	26.4	22.1	48.6
300	27.2	24.1	54.6
300	25.0	24.8	51.7
500	31.0	22.7	58.7
500	30.2	23.2	58.4
500	28.8	24.5	58.8
1000	30.6	27.3	69.6
1000	30.2	26.4	65.3
1000	31.6	25.9	68.2

Table C-13. BATCH EXPERIMENTS WITH MICHIGAN SHALE
(Slurry Concentration: 2.5%; Particle Size: 4 Microns)

Dosage of 1-Octanol, ppm	Product Yield wt %	Fischer Assay, gal/ton	Oil Recovery, wt %
0	21.8	16.4	47.6
0	24.0	18.4	58.9
0	201	18.0	48.3
100	17.8	20.3	48.2
100	18.8	20.9	52.4
100	14.9	24.2	48.1
300	19.2	25.0	68.6
300	20.9	24.3	67.7
300	16.0	27.2	58.0
400	29.0	20.6	79.7
400	27.0	22.0	79.2
400	25.4	23.0	77.9
500	33.1	20.9	92.2
500	32.2	21.6	92.7
500	33.4	21.1	94.0
700	33.6	18.2	81.8

Table C-14. BATCH EXPERIMENTS WITH MICHIGAN SHALE
(Slurry Concentration: 2.5%; Particle Size: 13 Microns)

Dosage of 1-Octanol, ppm	Product Yield wt %	Fischer Assay, gal/ton	Oil Recovery, wt %
0	17.6	9.1	21.3
0	15.8	11.0	23.1
0	16.0	10.2	21.8
100	9.4	15.1	18.9
100	12.3	12.2	20.0
100	10.6	14.4	20.4
300	23.8	14.5	46.0
300	25.1	13.6	45.5
400	24.1	14.0	45.0
400	25.3	13.9	46.9
500	24.5	13.9	45.4
500	26.0	12.0	41.6

Table C-15. BATCH EXPERIMENTS WITH MICHIGAN SHALE
(Slurry Concentration: 2.5%; Particle Size: 4 Micron)

Dosage of Tall Oil, ppm	Product Yield, wt %	Fischer Assay, gal/ton	Oil Recovery, wt %
0	28.0	16.0	64.0
0	26.0	17.2	63.9
0	27.0	16.6	64.0
50	32.2	16.0	73.6
50	28.6	18.7	76.4
50	29.4	18.0	75.0
100	32.0	17.0	77.7
100	29.1	18.6	77.3
100	31.6	18.0	81.2
300	36.0	19.1	98.2
300	33.0	20.2	95.2
300	34.5	20.1	99.0
500	39.0	17.2	94.9
500	35.7	19.4	98.8
500	38.4	17.4	95.3

Table C-16. BATCH EXPERIMENTS WITH ALABAMA SHALE
(Slurry Concentration: 2.5%; Particle Size: 4 Microns)

Dosage of Tall Oil, ppm	Product Yield, wt %	Fischer Assay, gal/ton	Oil Recovery, wt %
0	26.3	14.8	43.2
0	27.2	14.1	42.6
0	23.3	17.6	45.6
50	36.2	15.6	62.7
50	34.3	16.0	61.0
50	36.9	15.5	63.6
100	38.1	15.0	63.5
100	35.0	16.5	64.2
100	37.6	16.5	69.0
300	42.7	20.0	95.1
300	43.2	19.0	91.3
300	44.1	19.3	94.8
500	44.4	18.9	93.1
500	43.2	20.0	96.0
500	45.1	19.4	97.2

Table C-17. BATCH EXPERIMENTS WITH ALABAMA SHALE
(Slurry Concentration: 2.5%; Particle Size: 4 Microns)

Dosage of 1-Octanol, ppm	Product Yield wt %	Fischer Assay, gal/ton	Oil Recovery, wt %
0	26.8	14.9	41.4
0	25.8	15.3	43.9
50	24.0	21.3	56.8
50	26.0	20.5	59.2
50	25.0	20.6	57.2
100	26.2	20.4	59.4
100	24.9	22.1	61.1
100	26.1	19.3	56.0
300	28.2	25.9	81.2
300	27.5	25.0	76.4
300	27.9	25.9	80.3
500	40.0	20.9	92.9
500	37.0	19.7	81.0
500	38.8	20.0	86.2

Table C-18. BATCH EXPERIMENTS WITH ALABAMA SHALE
(Slurry Concentration: 5%; Particle Size: 4 Microns)

Dosage of 1-Octanol, ppm	Product Yield wt %	Fischer Assay, gal/ton	Oil Recovery, wt %
0	30.9	15.1	51.8
0	32.6	14.0	50.0
0	28.4	16.0	50.5
50	33.0	18.7	68.6
50	31.3	20.2	70.3
50	34.2	16.9	64.2
100	32.2	19.0	68.0
100	35.0	18.0	70.0
100	30.6	19.2	65.3
300	39.3	17.8	77.7
300	40.6	17.5	78.9
300	37.0	18.9	77.7
500	43.1	16.5	79.0
500	42.2	17.0	79.7
500	40.7	17.2	77.8
700	44.6	16.0	79.3
700	45.2	15.7	78.8
700	43.9	16.2	79.0

Table C-19. BATCH TWO-STEP TESTS WITH ALABAMA SHALE
(Particle Size: 4 Microns; Flowrate: 150 mL/min)

Step	Slurry Conc., wt %	1-Octanol Dosage, ppm	Yield, wt %	Fischer Assay, gal/ton	Oil Recovery, wt %
1	2.5	0	28.	16.0	9.7
2	2.5	0	40.0 (11.2)*	24.1	30.1
1	2.5	300	42.8	19.2	91.2
2	2.5	300	60.6 (25.9)*	29.0	82.9

Table C-20. RESULTS OF RDU TESTS FOR INDIANA SHALE

Speed, rpm	Dosage, ppm	Flowrate, mL/min	Product Ash, wt %	Yield, wt %	Fischer Assay, gal/ton	Oil Recovery, wt %
1800	0	500	70.1	17.5	22.8	31.6
1700	500	500	66.5	14.8	25.9	30.4
1700	1000	500	66.5	23.8	24.3	5.8
2050	500	500	73.6	40.5	19.7	63.3

Table C-21. RESULTS OF TWO-STAGE RDU TESTS FOR ALABAMA SHALE

Speed, rpm	Dosage, ppm	Flowrate, mL/min	Product Ash, wt %	Yield, wt %	Fischer Assay, gal/ton	Oil Recovery, wt %
1320	0	1000	67.7	39.1	15.1	65.6
1700	0	1000	69.4	41.8	13.0	60.4
1000	0	2000	64.8	38.9	19.1	82.6
1000	50	2000	65.3	36.1	19.5	78.2
1000	300	2000	65.1	42.5	19.9	94.0

Table C-22. COMPARISON OF PERFORMANCE FOR ALABAMA SHALE IN TWO-STAGE RDU WITH BRU TESTS (No Additives Used)

Mode of Operation	Flowrate, mL/min	Operating Speed, rpm	Product Yield, wt %	Fischer Assay, gal/ton	Oil Recovery, wt %
Batch Single-Stage	150	800	25.6	15.5	44.0
Semi-Continuous Two-Stage	2000	1000	38.9	19.1	82.6

Table C-23. RESULTS OF TWO-STAGE RDU TESTS FOR MICHIGAN SHALE

Speed, rpm	Dosage, ppm	Flowrate, mL/min	Product Ash, wt %	Yield, wt %	Fischer Assay, gal/ton	Oil Recovery, wt %
1000	0	2000	77.8	31.5	19.1	85.9
1000	300	2000	74.6	24.5	22.3	78.1

APPENDIX D. Statistical Analysis of Data From LICADO Process Testing

STATISTICAL ANALYSIS OF THE BATCH TESTS WITH INDIANA OIL SHALE

A brief description of the methodology for statistical analysis is given below. This is followed by the presentation of the results for experiments conducted using the Batch Research Unit. The conclusions are based on yield as well as the ash in the product.

The experiments in the batch mode were designed at four levels for one factor and at two levels for two other factors. These are indicated in Table D-1. Twelve tests (without replication) were considered for analysis of results. The raw data were presented in the preceding section. It must be mentioned that the statistical analysis was carried out to provide an indication of any definitive trends in the results and that more tests are planned in the future based on the initial conclusions.

Table D-1. TEST VARIABLES LEVELS

Factor	Level 1	2	3	4
Dispersant Concentration, ppm	0	100	500	750
Contact Time of Liquid CO_2, ppm	2.5	5	--	--
Impeller Speed, rpm	800	1200	--	--

Two parameters were analyzed:

(a) Yield, defined as:

$$\text{Yield} = \frac{\text{Weight of recovered product}}{\text{Weight of the feed in experiment}}$$

(b) Ash in the final product:

The data are analyzed for each factor as follows:

Total for each level: $t_j = \sum_{i=1}^{n} y_{ij} \qquad j = 1,2,\ldots,m$

Total Number of Tests: $N = nxm = 12$

Sum of Squares: $SS = \sum_{j=1}^{n} t_j^2/n - SS_t$

$$SS_t = \left(\sum_{i=1}^{n}\sum_{j=1}^{m} y_{ij}\right)^2/N$$

Total Sum of Squares: $SS_{TOT} = \sum_{i=1}^{n}\sum_{j=1}^{m} y_{ij}^2 - SS_t$

Each factor has f = m - 1 degrees of freedom and the total number of degrees of freedom is $f_{TOT} = N - 1 = 11$.

The mean square for each factor can be calculated as:

$$s^2 = SS/f$$

The residue is considered an estimation of the experimental error. The same parameters calculated for the factors can be determined for the residue:

$$SS_R = SS_{TOT} - \underset{\text{factors}}{\text{SDUM SS}}$$

$$(s_R)^2 = SS_R/f_R$$

$$f_R = f_{TOT} - \underset{\text{factors}}{\text{SUM f}} = 6$$

The significance of each factor is determined by comparing the ratio $s^2/(s_R)^2$ with F distribution values with (f, f_R) degrees of freedom.

The analysis of variance was performed for the yield and the product ash results of the batch experiments. Table D-1 lists the levels considered for each variable studied for the Indiana oil shale. Several tests were repeated and the reproducibility was within 10%.

A summary of the analysis of variance results for the Indiana oil shale is given in Tables D-2 and D-3.

Table D-2. YIELD (%) ANALYSIS OF VARIANCE

Factor	Level Average 1	2	3	4	SS	s^2	s^2/s_R^2
Concentration of Dispersant	29.4	24.4	24.8	22.8	73.5	24.5	5.6
Contact Time	24.1	26.6			12.5	12.5	2.9
Impeller Speed	22.0	28.7			91.1	91.1	20.9
				Residue	26.1	4.4	

Table D-3. PRODUCT ASH ANALYSIS OF VARIANCE

Factor	Level Average 1	2	3	4	SS	s^2	s^2/s_R^2
Concentration of Dispersant	73.8	72.8	72.6	71.7	4.1	1.4	1.0
Contact Time	71.9	73.3			3.6	3.6	2.7
Impeller Speed	70.2	75.0			46.1	46.1	34.8
				Residue	7.9	1.3	

Table D-2 shows the analysis of variance of the yield results. The analysis of variance indicates that the yields are influenced significantly only by the impeller speed with a speed of 1200 rpm generating higher yields. This conclusion is significant at the 99% confidence level. It is also interesting to note that the presence of any concentration of dispersant proved detrimental to the yield obtained.

Table D-3 depicts the analysis of variance performed to the product ash results. The analysis indicates that impeller speed again influenced the results significantly at the 99.9% confidence level. The lower impeller speed of 800 rpm generated lower ash in the product. Higher concentrations of dispersant resulted in lower ash contents in the product. There appears to be an optimum speed and dispersant concentration where it is possible to obtain higher yields as well as low ash content in the product.

DUNCAN MULTIPLE RANGE TEST

(Excerpt from "Design and Analysis of Experiments,"
Douglas C. Montgomery, John Wiley & Sons, 1976)

To apply Duncan's multiple range test for equal sample sizes, the "a" treatment means are arranged in ascending order, and the standardy error of each mean is determined as

$$S_{\bar{y}_i} = \sqrt{\frac{MS_E}{n}}$$

From Duncan's table of significant ranges, obtain the values $r_\alpha(p,f)$, for $p = 2,3,\ldots,a$, where α is the significance level and f is the number of degrees of freedom for error. Convert these ranes into a set of (a - 1) least significant ranges (e.g., R_p) for $p = 2,3,\ldots,a$, by calculating

$$R_p = r_\alpha(p,f)\ S_{\bar{y}_i}, \qquad \text{for } p = 2,3,\ldots,a$$

Then the observed ranges between means are tested, beginning with largest versus smallest, which would be compared with the least significant range R_a. Then the range of the largest and the second smallest is computed and compared with the least significant range R_{a-1}. These comparisons are continued until all means have been compared with the largest mean. Then the range of the second largest mean and the smallest is computed and compared against the least significant range R_{a-1}. This process is continued until the ranes of all possible a(a - 1)/2 pairs of means have been considered. If an observed range is greater than the corresponding least significant range, then we conclude that the pair of means in question are significantly different. To prevent contradictions, no differences between a pair of means is considered significant if the two means involved fall between two other means that do not differ significantly.

Analysis of Variance Report
Indiana Oil Shale
Reagent: 1-Octanol

FISCHER ASSAY

Mean of Squares	Standard Deviation	95% C. L.
2.09	1.45	3.59

1-Octanol Concentration, ppm	Number of Tests	Average Fischer Assay, gal/ton (L/metric, ton)
0	3	19.23 (80.2)
100	3	21.33 (89.0)
300	3	22.33 (93.2)
500	3	27.40 (114.3)
1000	3	25.03 (104.4)

Duncan's Range Test
$\alpha = 0.05$
Response Variable: FISCHER ASSAY
Independent Variable: 1-Octanol Concentration

```
19.23                                                    27.40
A.....................B........C.....................E.............D
XXXXXXXXXXXXXXXXXXXXX.....................................
.....................XXXXXXXXXX.....................................
.....................................................XXXXXXXXXXXXXXX
A = 0          B = 100          C = 300          E = 1000          D = 500
```

OIL RECOVERY

Mean of Squares	Standard Deviation	95% C. L.
10.94	3.31	8.31

1-Octanol Concentration, ppm	Number of Tests	Average Oil Recovery, %
0	3	26.83
100	3	45.57
300	3	54.37
500	3	67.43
1000	3	70.47

Duncan's Range Test
$\alpha = 0.05$
Response Variable: OIL RECOVERY
Independent Variables: 1-Octanol Concentration

```
26.83                                                        70.47
A.................................B.............C.....................D....E
.....................................................................XXXXXX
A = 0          B = 100          C = 300          D = 500          E = 1000
```

Analysis of Variance Report
Michigan Oil Shale (4 μm)
Reagent: 1-Octanol

FISCHER ASSAY

Mean of Squares	Standard Deviation	95% C. L.
1.88	1.37	3.41

1-Octanol Concentration, ppm	Number of Tests	Average Fischer Assay, gal/ton (L/metric, ton)
0	3	17.60 (73.4)
100	3	21.80 (91.0)
300	3	25.50 (106.4)
400	3	21.87 (91.2)
500	3	21.20 (88.5)
700	1	18.20 (75.9)

Duncan's Range Test
α = 0.05
Response Variable: FISCHER ASSAY
Independent Variable: 1-Octanol Concentration

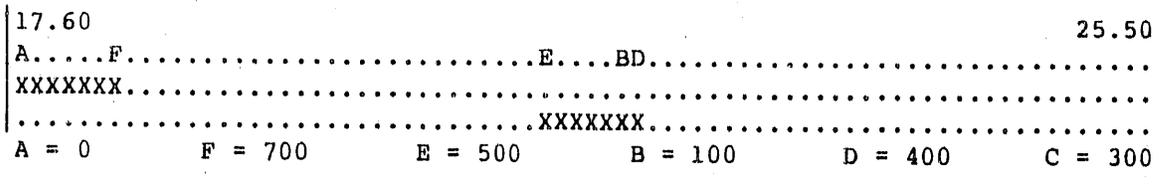

OIL RECOVERY

Mean of Squares	Standard Deviation	95% C. L.
16.48	4.06	10.08

1-Octanol Concentration, ppm	Number of Tests	Average Oil Recovery, %
0	3	51.60
100	3	59.57
300	3	64.77
400	3	78.93
500	3	92.97
700	1	81.97

Duncan's Range Test
α = 0.05
Response Variable: OIL RECOVERY
Independent Variables: 1-Octanol Concentration

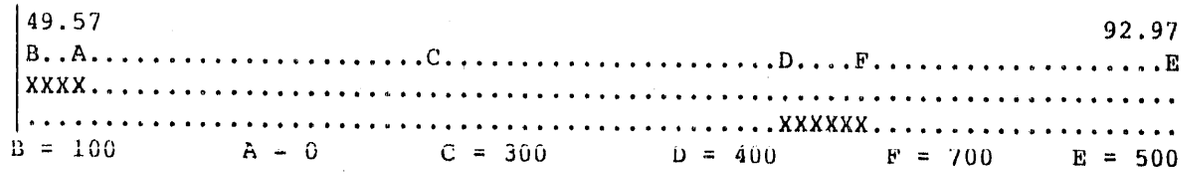

Analysis of Variance Report
Michigan Oil Shale (13 μm)
Reagent: 1-Octanol

FISCHER ASSAY

Mean of Squares	Standard Deviation	95% C. L.
1.23	1.11	2.75

1-Octanol Concentration, ppm	Number of Tests	Average Fischer Assay, gal/ton (L/metric, ton)
0	3	10.10 (42.1)
100	3	13.90 (58.0)
300	3	14.05 (58.6)
400	3	13.95 (58.2)
500	3	12.95 (54.0)
700	1	13.80 (57.6)

Duncan's Range Test
α = 0.05
Response Variable: FISCHER ASSAY
Independent Variable: 1-Octanol Concentration

```
|10.10                                                                14.05|
|A.....................................................E.................F.BD.C|
|......................................................XXXXXXXXXXXXXXXXXXXXXXX|
A = 0        E = 500        F = 700        B = 100        D = 400     C = 300
```

OIL RECOVERY

Mean of Squares	Standard Deviation	95% C. L.
1.73	1.31	3.24

1-Octanol Concentration, ppm	Number of Tests	Average Oil Recovery, %
0	3	22.07
100	3	19.77
300	2	45.75
400	2	45.95
500	2	43.50
700	1	43.80

Duncan's Range Test
α = 0.05
Response Variable: OIL RECOVERY
Independent Variables: 1-Octanol Concentration

```
|19.77                                                                45.95|
|B.......A.....................................................EF....CD|
|XXXXXXXX.....................................................XXXXXX|
B = 100        A = 0        E = 500        F = 700        C = 300      D = 400
```

Analysis of Variance Report
Michigan Oil Shale (4 μm)
Reagent: Tall Oil

FISCHER ASSAY

Mean of Squares	Standard Deviation	95% C. L.
0.97	0.98	2.44

1-Octanol Concentration, ppm	Number of Tests	Average Fischer Assay, gal/ton (L/metric, ton)	
0	3	16.60	(69.3)
50	3	17.57	(65.0)
100	3	17.87	(74.6)
300	3	19.80	(82.6)
500	3	18.00	(75.1)

Duncan's Range Test
α = 0.05
Response Variable: FISCHER ASSAY
Independent Variable: Tall Oil Concentration

```
16.60                                                              19.80
A.....................B......C..E.....................................E
XXXXXXXXXXXXXXXXXXXXXXXXXXXXXXXXXX.....................................
A = 0          B = 50          C = 100          E = 500          D = 300
```

OIL RECOVERY

Mean of Squares	Standard Deviation	95% C. L.
2.82	1.68	4.17

1-Octanol Concentration, ppm	Number of Tests	Average Oil Recovery, %
0	3	63.97
50	3	75.03
100	3	78.73
300	3	97.47
500	3	96.67

Duncan's Range Test
α = 0.05
Response Variable: OIL RECOVERY
Independent Variables: Tall Oil Concentration

```
63.97                                                              97.47
A.....................B........C.....................................E.D
.....................................................................XXX
A = 0          B = 50          C = 100          E = 500          E = 500
```

Analysis of Variance Report
Alabama Oil Shale (4 μm)
Reagent: Tall Oil

FISCHER ASSAY

Mean of Squares	Standard Deviation	95% C. L.
0.96	0.98	2.44

1-Octanol Concentration, ppm	Number of Tests	Average Fischer Assay, gal/ton (L/metric, ton)	
0	3	15.50	(64.7)
50	3	15.70	(65.5)
100	3	16.00	(66.8)
300	3	19.43	(81.1)
500	3	19.43	(81.1)

Duncan's Range Test
α = 0.05
Response Variable: FISCHER ASSAY
Independent Variable: Tall Oil Concentration

```
15.50                                                          19.43
A...B....C.....................................................D
XXXXXXXXXX.....................................................
...............................................................X
A = 0        B = 50        C = 100        D = 300        E = 500   Note: D~E
```

OIL RECOVERY

Mean of Squares	Standard Deviation	95% C. L.
4.43	2.10	5.23

1-Octanol Concentration, ppm	Number of Tests	Average Oil Recovery, %
0	3	43.80
50	3	62.43
100	3	65.57
300	3	93.73
500	3	95.43

Duncan's Range Test
α = 0.05
Response Variable: OIL RECOVERY
Independent Variables: Tall Oil Concentration

```
43.80                                                          95.43
A.........................B...C.....................................D.E
.........................XXXXX.....................................
A = 0          B = 50          C = 100          D = 300          E = 500
```

Analysis of Variance Report
Alabama Oil Shale (4 μm)
Reagent: 1-Octanol

FISCHER ASSAY

Mean of Squares	Standard Deviation	95% C. L.
0.58	0.76	1.89

1-Octanol Concentration, ppm	Number of Tests	Average Fischer Assay, gal/ton (L/metric, ton)	
0	3	15.10	(63.0)
50	3	20.80	(86.9)
100	3	20.60	(85.9)
300	3	25.60	(106.8)
500	3	20.20	(84.3)

Duncan's Range Test
α = 0.05
Response Variable: FISCHER ASSAY
Independent Variable: 1-Octanol Concentration

```
15.10                                    5                                25.60
A.....................................E..CB.....................................D
.....................................XXXXX.....................................
A = 0          E = 500          C = 100          B = 50          D = 300
```

OIL RECOVERY

Mean of Squares	Standard Deviation	95% C. L.
10.11	3.18	7.90

1-Octanol Concentration, ppm	Number of Tests	Average Oil Recovery, %
0	3	43.97
50	3	57.73
100	3	58.83
300	3	79.28
500	3	86.70

Duncan's Range Test
α = 0.05
Response Variable: OIL RECOVERY
Independent Variables: 1-Octanol Concentration

```
43.97                                                                    86.70
A.......................B.C.....................C..............D.............E
.......................XXX.....................................................
A = 0          B = 50          C = 100          D = 300          E = 500
```

Analysis of Variance Report
Alabama Oil Shale (4 μm)
Reagent: 1-Octanol

FISCHER ASSAY

Mean of Squares	Standard Deviation	95% C. L.
0.82	0.90	2.23

1-Octanol Concentration, ppm	Number of Tests	Average Fischer Assay, gal/ton (L/metric, ton)
0	3	15.03 (62.7)
50	3	18.60 (77.6)
100	3	18.73 (78.1)
300	3	18.07 (75.4)
500	3	16.90 (70.1)
700	3	15.97 (66.6)

Duncan's Range Test
α = 0.05
Response Variable: FISCHER ASSAY
Independent Variable: 1-Octanol Concentration

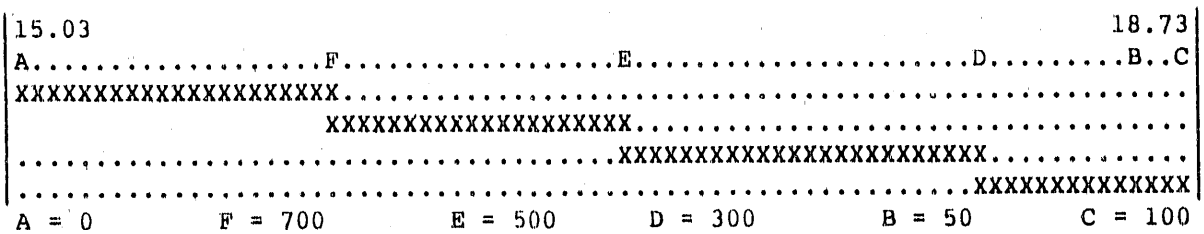

OIL RECOVERY

Mean of Squares	Standard Deviation	95% C. L.
2.97	1.72	4.26

1-Octanol Concentration, ppm	Number of Tests	Average Oil Recovery, %
0	3	50.77
50	3	67.70
100	3	67.77
300	3	78.10
500	3	78.83
700	3	79.03

Duncan's Range Test
α = 0.05
Response Variable: OIL RECOVERY
Independent Variables: 1-Octanol Concentration

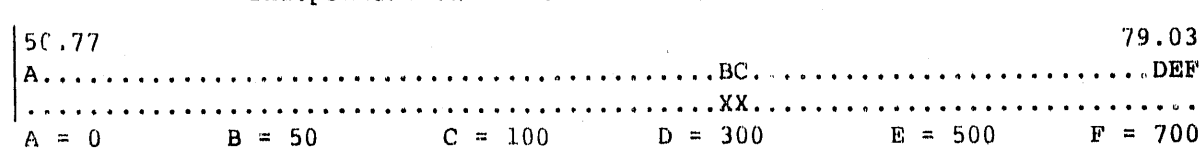

APPENDIX E. Economic Analysis of the LICADO Process

Table E-1. CALCULATION OF FIXED CAPITAL COST
BASED ON PROCESSING 200 TONS/H OF BENEFICIATED SHALE

DIRECT COSTS

No.	Item/Components	No. of Units	Power, hp	Total Cost in $1000
1.	Raw Shale Storage (*)	3	0	500
2.	Filters for Product	6	100	1309
3.	Slurry Feed Pump	2	400	450
4.	CO_2 Circulating Pump	2	300	325
5.	Slurry Tanks	3	90	2520
6.	Hydraulic Mixer	3	--	30
7.	Separator	3	--	1190
8.	Product Shale Column	2	--	1175
9.	Pressurizer	1	--	152
10.	CO_2 Accumulator	1	--	140
11.	CO_2 Recycle Compressor	1	350	275
12.	Cyclone	4	--	125
13.	Coolers	2	--	60
14.	Gas CO_2 Filter	3	--	24
A.	Total for Components			8275
B.	Installation (0.39 [A-*])			3227
C.	Instrumentation (0.13A)			1153
D.	Piping Installation (0.31A)			2751
E.	Electrical System (0.1A)			887
F.	Site Preparation (0.1A)			887
G.	General Services			100
	Total Direct Costs			17919

INDIRECT COSTS

H.	Engineering and Supervision (0.20A)	1775
I.	Construction (0.45 [A-*])	3768
J.	Contractors Fee (0.09A)	753
L.	Contingency (0.25A)	2093
	Total Indirect Costs	8389

Hence, Total Capital Cost = Direct Cost + Indirect Cost
= 17919 + 8389 $26308 X 1000
i.e., Total Capital Cost = 26.3 Million Dollars

Calculation of Total Operating Cost/yr:

Total Operating Hours, assuming 75% time operation (18 hrs daily) = 24 X 365 X 0.75 = 6570 hours.
This is split into 3 shifts of 6 hours each daily.
Assume 4 people/shift, i.e., 12 people/day.

Assume average salary/person = $40,000/yr.
Overhead = 50% of salary
Total Operating labor cost = 60,000 X 12 = $720,000/yr
Hence, labor cost/yr = 0.72 Millions Dollars.

Utility Costs/yr are estimated as = $1.44 M
CO_2/yr Costs = $0.70 M

Hence total operating cost/yr = 0.72 + 1.44 + 0.70 = $2.86 M.

Table E-2. PARAMETERS USED IN ECONOMIC MODEL
CAPACITY: 200 TONS/HR OF BENEFICIATED SHALE

Plant Capacity, tons/h	200
Capital Cost, $M	26.3
CO_2 Usage, wt % of Product	0.5
Return on Investment (after taxes), %	20
Taxes, %	37
Plant Capacity Factor, dimensionless	0.80
Operation and Maintenance, $M/yr	2.86
Plant Life, years	20
Escalation, % per year	5
Interest During Construction, %	10
Debt, %	75
Long Term Interest, %	12

Table E-3. PROCESSING COSTS VERSUS RATE OF RETURN

Oil Shale Selling Price, $/ton	Rate of Return, %
3.00	1.1
4.00	18.5
4.25	23.3
4.50	28.4
5.00	40.3

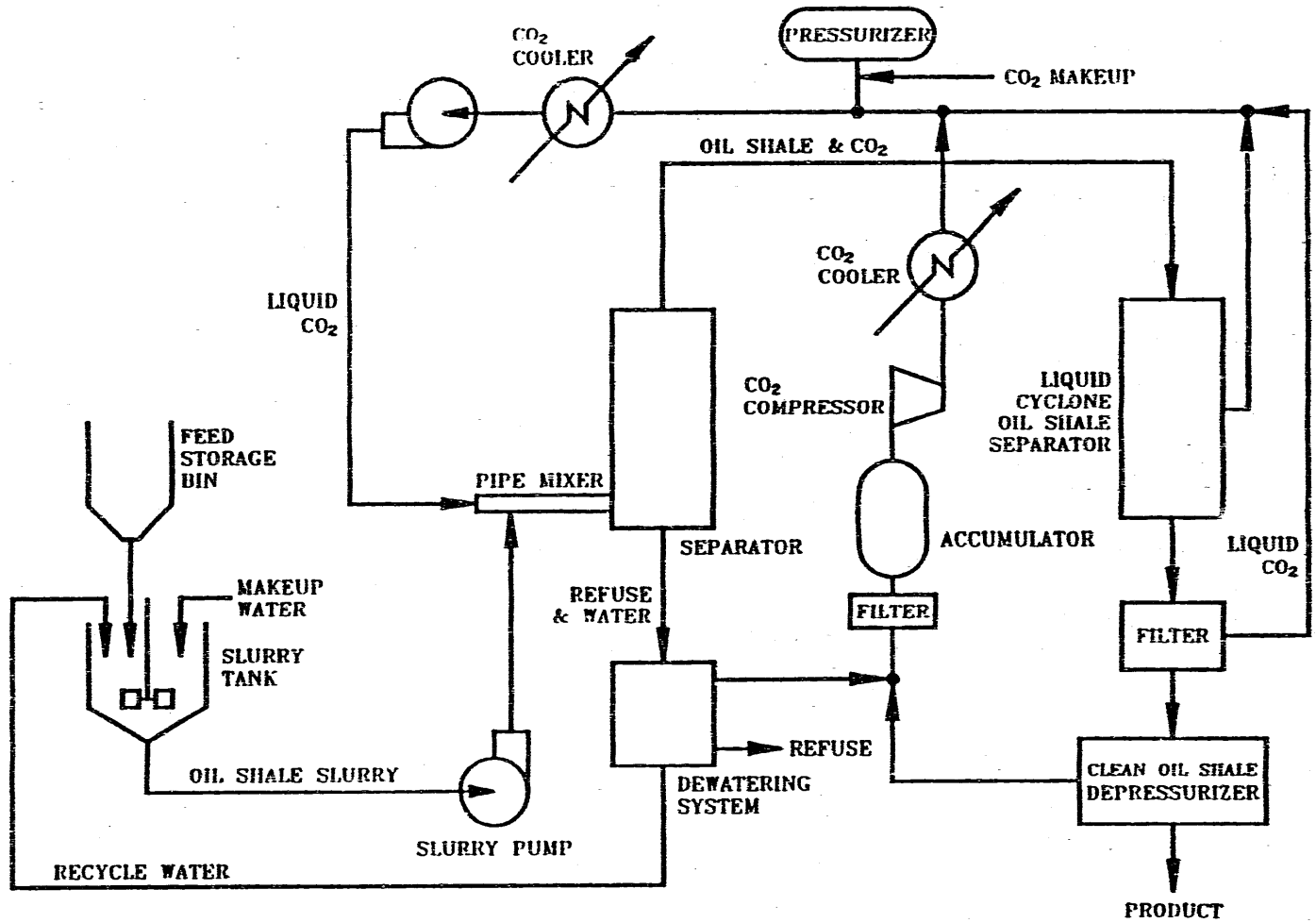

Figure E-1. FLOWSHEET OF THE LICADO PROCESS

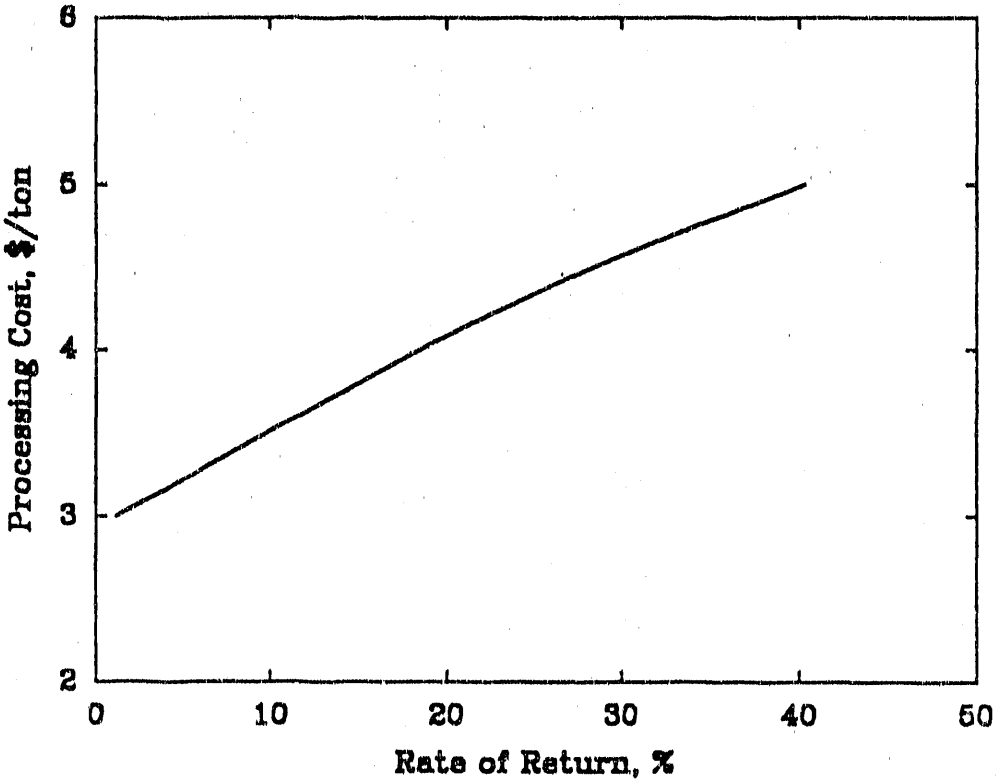

Figure E-2. PROCESSING COST VERSUS RATE OF RETURN

APPENDIX F. Uranium Analysis From TTU

NOV 2 1 1990

"building the future on past achievements"

Tennessee Technological University
Department of Civil Engineering
Box 5015 . Cookeville, TN 38505 . 615-372-3454
FAX Number: 615-372-6172

November 19, 1990

Dr. W. E. Lamont
Assistant Research Engineer
The University of Alabama
Mineral Resources Institute
Box 870204
Tuscaloosa, AL 35487-0204

Dear Dr. Lamont:

Results from the analysis of two samples for uranium are enclosed. The two samples were identified as:

(A) IGT Alabama, Net 2C5H Mill, Feed water, from 48 M grind, and

(I) IGT Indiana, Feed water, 3/30/90, pH 3.0.

Solids were present in each sample. Thus, the samples were pretreated by adding two drops of distilled HCl to 25 ml of the homogeneous sample and gently heating. The result was a clear sample.

The samples submitted to the lab for analysis were designated as I, A, and A_o. The A_o sample was clear supernatant from the IGT Alabama sample. I simply wanted to determine if uranium was in the solids. Samples I and A were pretreated as above.

Analyses were performed by inductively coupled plasma. The instrument was standardized with a uranium standard certified by Fisher Scientific.

Quality control parameters are as follows:

Parameter	Outcome
1.0 mg/L standard	92.9% recovery
Spiked sample	94.6% recovery
Duplicate samples	0% relative error

I hope the results are helpful. Please let me know if I can be of additional assistance.

Sincerely,

William P. Bonner
Professor

WPB:jb

TENNESSEE TECH UNIVERSITY

Tennessee Technological University
Center for the Management, Utilization and Protection of Water Resources
Box 5082 • Cookeville, TN 38505 • 615-372-3507

MEMORANDUM

TO: Dr. Paul Bonner, TTU Civil Engineering

FROM: Mr. Jeff Curtis, TTU Water Center

DATE: October 30, 1990

SUBJECT: Results, samples received 10/23/90: 2893

Sample	mg Uranium/L
I	<0.05
A_o	<0.05
A	<0.05

END

DATE FILMED

11/20/92